VOLUME 11 AUGUST, 1934 NUMBER 2

NATIONAL
RESEARCH COUNCIL
of CANADA

CANADIAN JOURNAL OF RESEARCH

CANADA

Published under the authority
of the
Chairman of the Committee of the
Privy Council on Scientific and Industrial Research

OTTAWA - CANADA

CONTENTS

Original Papers

PAGE

The Relative Rigidity of Welded and Riveted Connections—*C. R. Young* and *K. B. Jackson* 101

On the Acoustic Radiation Field of the Piezo-electric Oscillator and the Effect of Viscosity on Transmission—*Louis V. King* 135

On the Theory of the X-ray Determination of Elastic Scattering of Cathode Rays—*Darol K. Froman* 156

Reflections from the Ionosphere—*Sydney Sillitoe* 163

Tetraphenylcyclopentadienone in the Diene Synthesis—*C. F. H. Allen* and *L. J. Sheps* 171

Studies on Homogeneous First Order Gas Reactions. V. The Decomposition of Paracetaldehyde at High Pressures—*A. L. Geddes* and *C. C. Coffin* 180

Studies on the Overwintering of Certain Fungi Parasitic and Saprophytic on Fruit Trees—*L. W. Koch* 190

The Relation between Awns and Yield in Spring Wheat—*O. S. Aamodt* and *J. H. Torrie* 207

A Karyosystematic Investigation in the Gramineae—*A. W. S. Hunter* 213

A New *Ophiobolus* on Eelgrass—*Irene Mounce* and *Wm. W. Diehl* 242

Reviews and Notes

Note sur les Emulsions de la Triéthanolamine avec le Kérosène et des Huiles Lubrifiantes Minérales—*J. Risi* et *H. Bernard* 247

Publications and Subscriptions

The Canadian Journal of Research is published monthly by the National Research Council of Canada, Ottawa, to which address all correspondence should be directed.

The subscription rate is $3.00 per year to any part of the world. Single copies are thirty-five cents each.

Canadian Journal *of* Research

Issued by THE NATIONAL RESEARCH COUNCIL OF CANADA

VOLUME 11 AUGUST, 1934 NUMBER 2

THE RELATIVE RIGIDITY OF WELDED AND RIVETED CONNECTIONS[1]

BY C. R. YOUNG AND K. B. JACKSON

IV. Analysis of Experimental Results

25. *General*

The specimens of the first series were designed to develop beam continuity only, and tested to determine the relation between load and coefficient of restraint in the simulated beam. The results obtained are given in Figs. 26 to 30 and discussed, together with similar results for the second series, in Arts. 28 and 29, on Coefficient of Restraint.

The specimens of the second series were designed to develop beam continuity and to resist wind load moments. They were tested, not only to determine their over-all capacity in these respects, but also to allocate the particular causes of strength or weakness.

The results for the second series therefore include:

(a) The deformation of the test specimens;

(b) The coefficient of restraint and moment distribution in the simulated beam;

(c) The story-drift angle in the building of which the simulated beam would constitute a part.

Finally, a table of ultimate strengths and factors of safety, etc., is given for the specimens of each series.

26. *Deformation of the Test Specimens, Second Series—Flexural Slope by Flanges and Regions*

For purposes of analysis the connections have been divided longitudinally into three regions, I, II and III, and transversely into two halves termed the top and bottom flanges, as indicated in Fig. 14. Regions IV and V extend beyond the connection and Region VI comprises I, II and III.

The flexural slopes developed in each flange and region have been computed for the two significant loads, XY and Z, as described in Sections II and III, and are presented in Figs. 17 to 23. Figs. 17 and 18 give, in statistical form

[1] *Concluded from July issue.*

for each and both flanges and for each and all regions wholly comprised within the limits of the connection, the total slopes developed by the XY and Z loads, respectively. Figs. 19 and 20 indicate by curves the development of flexural slope during the application of the two loads, for each flange and

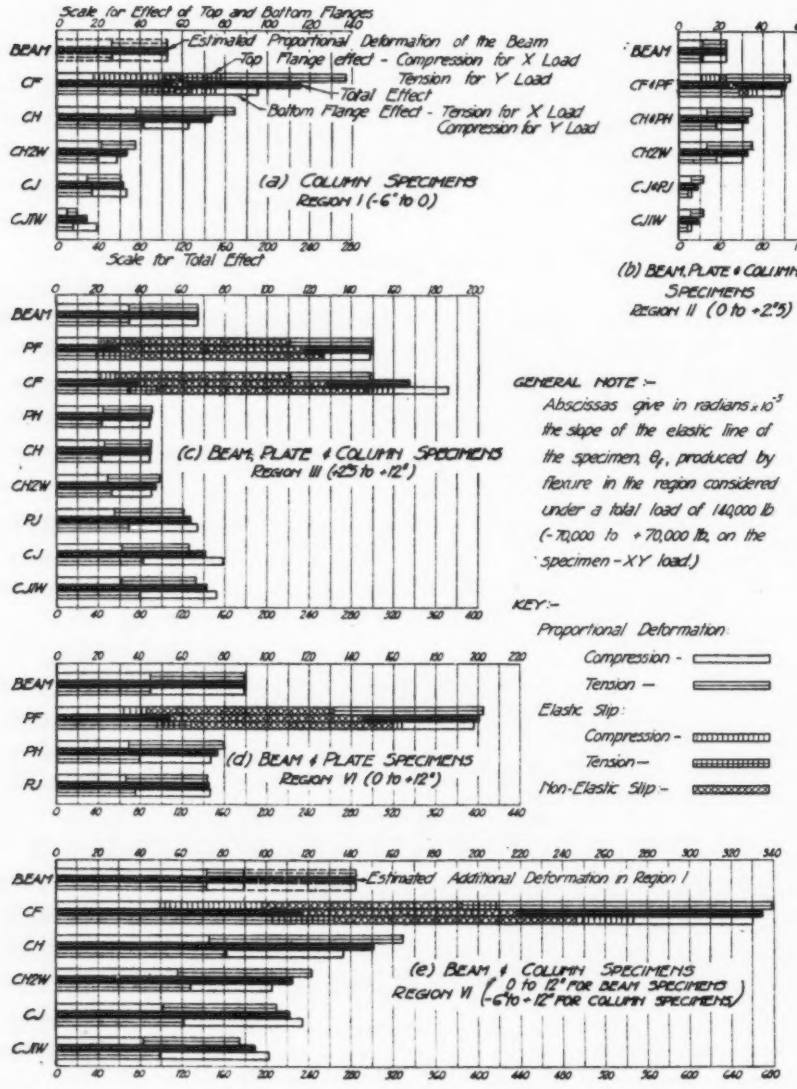

FIG. 17. *Flexural slope produced in Regions I, II, III and VI of specimens by total load change of 140,000 lb. (−70,000 to +70,000 lb.).*

region, and Figs. 21, 22, and 23 give the sum of these regional developments for each flange and for both flanges.

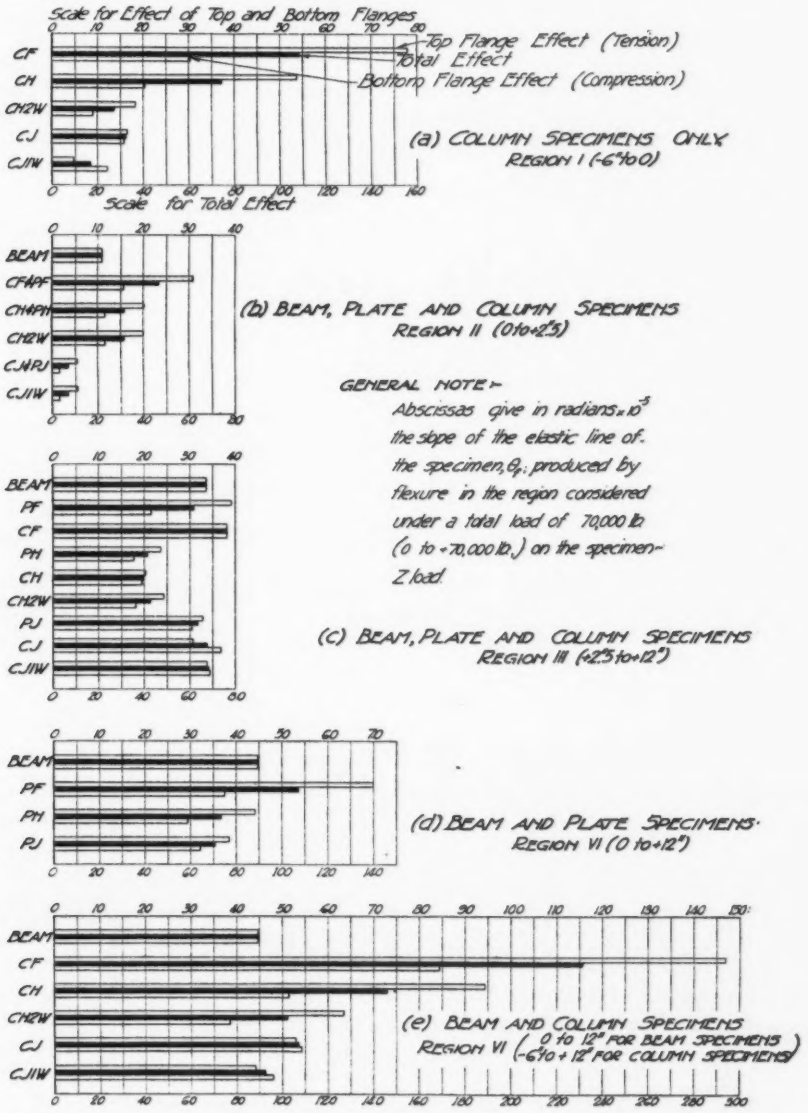

FIG. 18. *Flexural slope produced in Regions I, II, III and VI of specimens by total load change of 0 to +70,000 lb.*

The flexural slope developed in a given flange and region is determined by:
(1) The type of connection—*PF*, *CH2W*, etc.;

(2) The flange included—top or bottom;

(3) The stress involved—tension or compression;

(4) The loading sequence—including or excluding non-elastic slip.

In some types of connections the effect of a change in (2), (3) or (4) is small, while in others it is considerable. A comprehensive test, therefore, of any type of connection must involve both flanges in both kinds of stress and the loading sequence must be such as to include any non-elastic slip that may

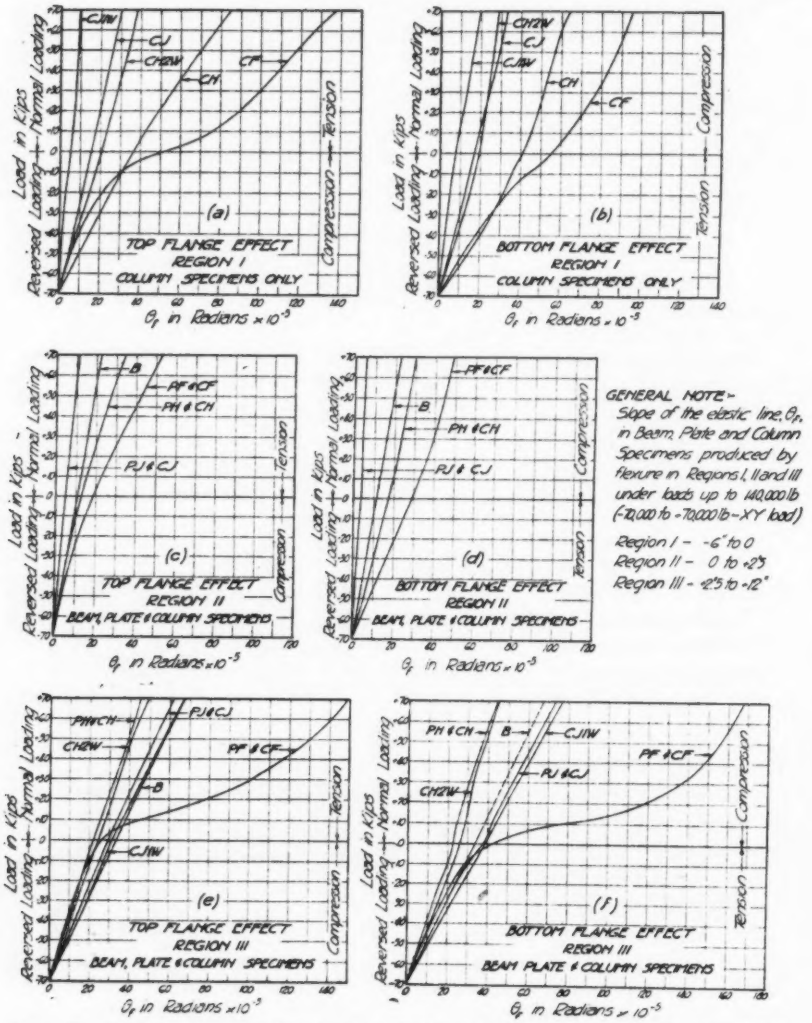

FIG. 19. *Load-slope relation for specimens produced by flexure in Regions I, II and III under load varying from −70,000 to +70,000 lb.*

occur. This is provided by the XY load, and the corresponding flexural slopes developed under it in all regions by all types are indicated by the solid black lines in Fig. 17. The relative values of these slopes are given in Table II, which provides the simplest means of comparing the regional and over-all flexural performance of the connections and the plain beam. The

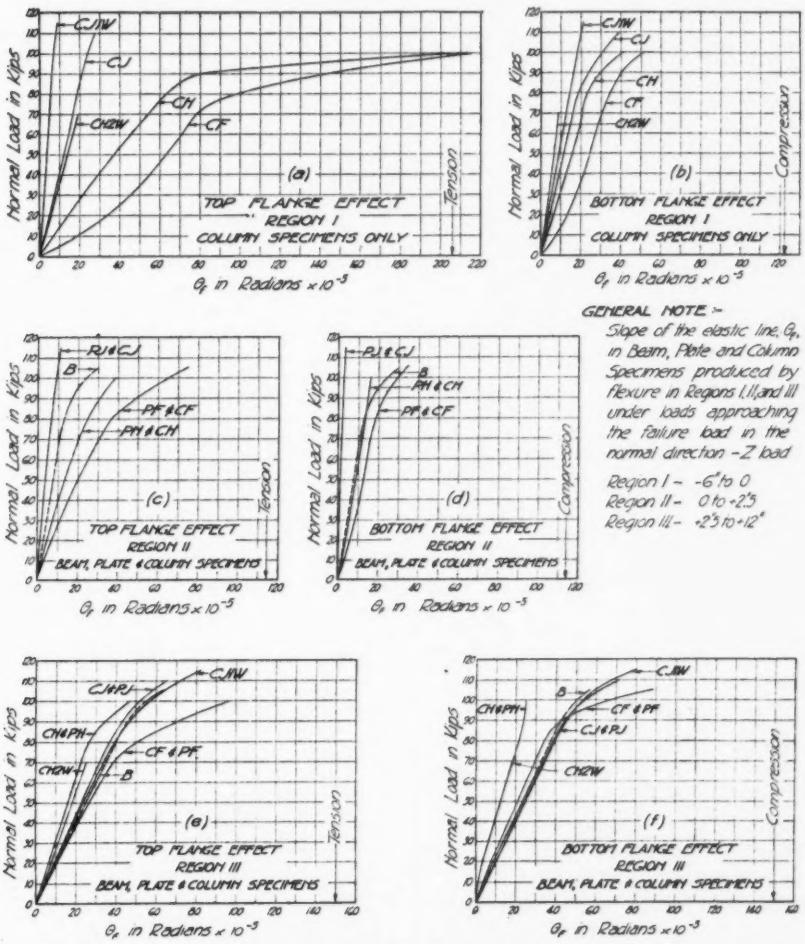

FIG. 20. *Load-slope relation for specimens produced by flexure in Regions I, II and III under load varying from 0 to + approximate failure load.*

relative slopes developed in the connections are given in three forms in the table:

(a) In terms of the slope developed in the plain beam in the same region—to compare the types in each region;

TABLE II

RELATIVE FLEXURAL SLOPES DEVELOPED BY TWO FLANGES IN EACH REGION FOR EACH TYPE OF CONNECTION OF THE SECOND SERIES DURING A COMPLETE REVERSAL OF LOAD*

Connection				Relative flexural slope											
				(a) Beam slope in each region = 1.00				(b) Total beam slope = 1.00				(c) Total slope in each specimen = 1.00			
				Region No.				Region No.				Region No.			
Type	Attached to column web or flange	With or without column stiffeners	Specimen	I	II	III	Total VI	I	II	III	Total VI	I	II	III	Total VI
Plain beam	—	—	*B*	—	1.00	1.00	1.00	—	0.25	0.75	1.00	—	0.25	0.75	1.00
	Assumed as extended into Region No. 1			1.00	1.00	1.00	1.00	0.59	0.25	0.75	1.59	0.37	0.16	0.47	1.00
Riveted T	Web	—	*PF*	—	2.27	2.22	2.24	—	0.57	1.67	2.24	—	0.25	0.75	1.00
	Flange	Without	*CF*	2.19	2.27	2.50	2.34	1.30	0.57	1.87	3.74	0.35	0.15	0.50	1.00
Welded T	Web	—	*PH*	—	1.42	0.67	0.86	—	0.36	0.50	0.86	—	0.42	0.58	1.00
	Flange	Without	*CH*	1.38	1.42	0.67	1.05	0.83	0.36	0.50	1.69	0.49	0.21	0.30	1.00
		With	*CH2W*	0.62	1.42	0.70	0.79	0.38	0.36	0.52	1.26	0.30	0.29	0.41	1.00
Welded gusset	Web	—	*PJ*	—	0.38	0.95	0.81	—	0.10	0.71	0.81	—	0.12	0.88	1.00
	Flange	Without	*CJ*	0.60	0.38	1.05	0.78	0.36	0.10	0.79	1.25	0.29	0.08	0.63	1.00
		With	*CJ1W*	0.28	0.38	1.06	0.66	0.17	0.10	0.80	1.07	0.16	0.09	0.75	1.00

* *See "Total effects", Fig. 17.*

(*b*) In terms of the *total* slope developed in the plain beam—to compare all types in all regions on a common basis;

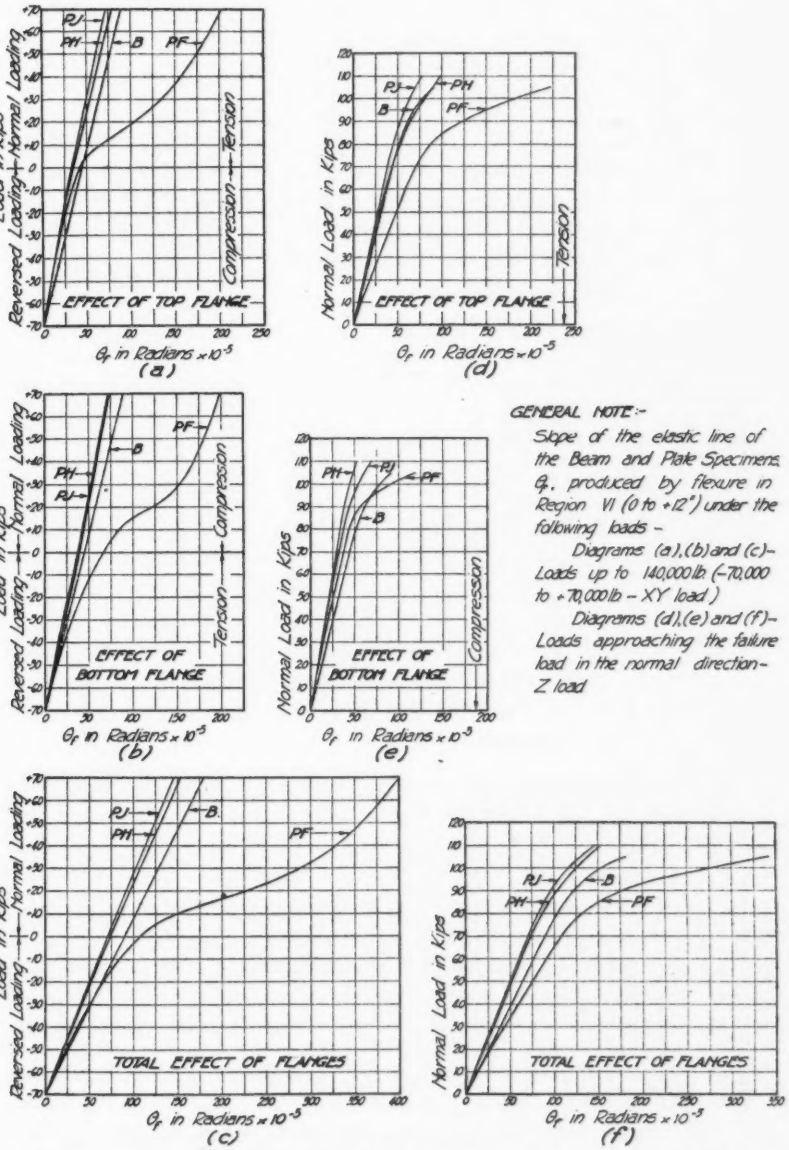

GENERAL NOTE:-
Slope of the elastic line of the Beam and Plate Specimens θ_f, produced by flexure in Region VI (0 to +12") under the following loads –

Diagrams (a), (b) and (c)– Loads up to 140,000 lb (–70,000 to +70,000 lb – XY load)

Diagrams (d), (e) and (f)– Loads approaching the failure load in the normal direction– Z load

FIG. 21. *Load-slope relation for beam and plate specimens produced by flexure in Region VI under loads varying from −70,000 to +70,000 lb. and from 0 to + approximate failure load.*

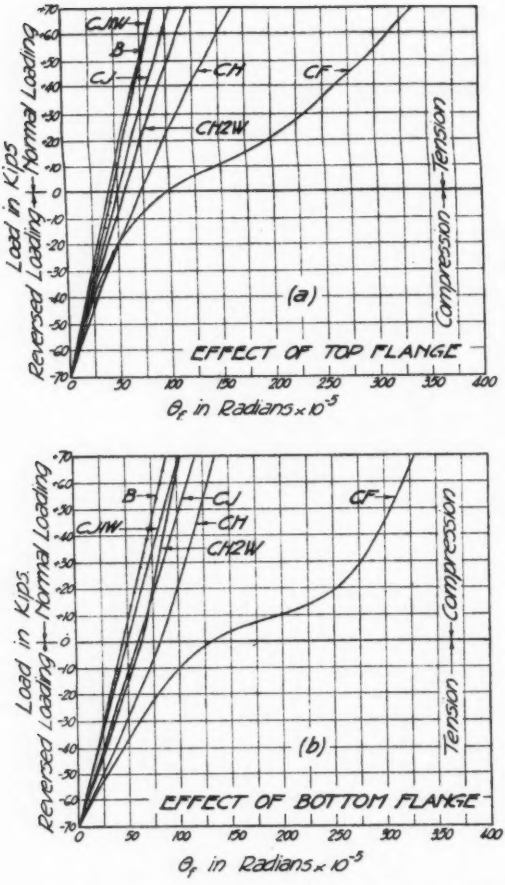

GENERAL NOTE:-
Slope of the elastic line of the Beam and Column Specimens, θ_f, produced by flexure in Region VI (0 to +12" for Beam Specimens B and -6" to +12" for Column Specimens CF, CH, CH2W, CJ and CJIW) under loads up to 140,000 lb (-70,000 to +70,000 lb. -XY load.)

FIG. 22. *Load-slope relation for beam and column specimens produced by flexure in Region VI under load varying from −70,000 to +70,000 lb.*

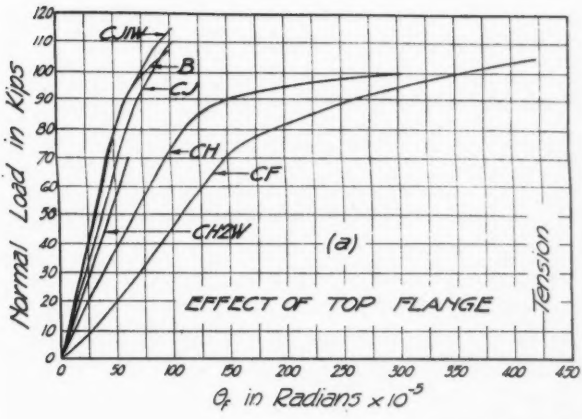

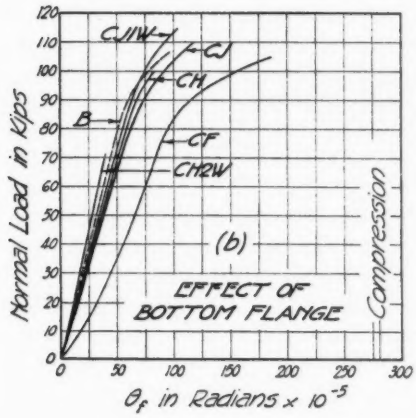

GENERAL NOTE:-
Slope of the elastic line of the Beam and Column Specimens, θ_f produced by flexure in Region VI (0 to 12" for Beam Specimens B and -6" to +12" for Column Specimens CF, CH, CH2W, CJ and CJ1W) under loads approaching the failure load in the normal direction – Z load.

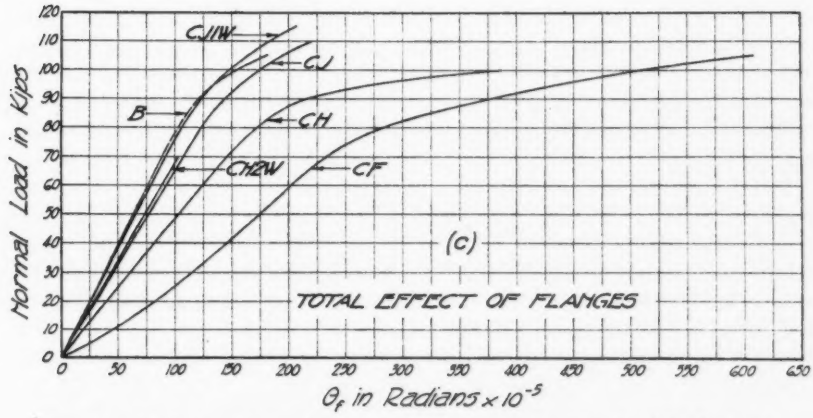

FIG. 23. *Load-slope relation for beam and column specimens produced by flexure in Region VI under loads varying from 0 to + approximate failure load.*

(c) In terms of the total slope in each type—to compare the regions in each type.

To make the comparison complete it is necessary to estimate the slope that would be developed in the plain beam if it were to extend through Region I. The relative values of this slope as required in *(a)*, *(b)* and *(c)* are indicated in the second line of the table.

The slope developed in the top and bottom flanges respectively, is shown above and below the solid black lines in Fig. 17, and these flange deformations are further analyzed, by reference to the load-slope curves in Figs. 19 to 23, to determine the relative significance of tension, compression and elastic and non-elastic slip. That portion occurring during the *X* load may consist of proportional deformation only, indicated by a straight load-slope curve, or it may include elastic slip indicated by a more or less distinct "toe" in the curve. This characteristic is most prominent in *F* specimens in Regions I and III, as is evident from Fig. 19.

The deformation during the *Y* load includes non-elastic slip, if any occurs, the value of which is estimated by the difference between the deformation occurring during the *Y* and *Z* loads (within the same load range), allowance being made for any excessive "subsequent set" during the *Z* load. Elastic slip during the *Y* load is assumed to be the same as in the *Z* load, which is indicated by a toe in the *Z* load curve. The method of estimating these components of the deformation in a single flange is illustrated in Fig. 11 *(b)* and the results are indicated by a subdivision of the flange deformations shown in Fig. 17.

This analysis of the flexural deformation occurring in each flange and region of the specimens under design load (Fig. 17), combined with the evidence obtained during failure loads, forms the basis of the following observations which attempt to explain the deformations indicated in terms of the structural details involved.

Region I. Region I consists nominally of half the column width but, as the deformation indicated is derived from the differences in short-extensometer readings on plate and column specimens, it includes any difference in the deformation in Region II caused by the column, and, as pointed out in Art. 16, any difference in the behavior of the rivet group utilized for attaching the connections to a column or connections to one another through a plate.

(1) General

(a) The two connections utilizing T's and no column flange stiffeners, *CF* and *CH*, produce deformations in the column 3.6 and 2.3 times as great respectively as that produced by the gusset plate connection, *CJ*. Fig. 17 *(a)*.

(b) The tension attachment to the column is the critical element in the *CF* and *CH* connections. See Fig. 20 *(a)*.

(c) The column flange stiffeners used in *CH2W* and *CJ1W* reduced the deformation in the column to 45% of its previous value, being more effective in tension than in compression.

(2) The Riveted T, or *CF*, Specimens

(a) Elastic slip is slightly greater in compression than in tension, but is about twice as great in the top flange as in the bottom. Elastic slip here is assumed to be caused by progressive seating, that is by the bending of the column flanges, inward in compression until the centres of the column and T flanges are in contact, and outwards in tension until the edges of the T flanges bear against the column flanges and greatly restrain further bending in both column and T flanges. If this is true the amount of elastic slip would depend upon the distances between the surfaces at zero load, which might well be affected by the sequence in riveting. Otherwise, the greater elastic slip in the top flange can be explained only by accidental variations in the curvature of the bearing surfaces after riveting.

(b) Proportional deformation is 2.6 times as great in tension as in compression but only slightly greater in the top flange than in the bottom. This excessive deformation in tension is due to the outward bending of the column flanges and the elongation of the connecting rivets.

(c) By comparing the deformations at 100,000 lb. during the *Z* load, Fig. 20, it will be seen that the tension-half of this region is the critical element in this type of connection.

(3) The Welded T, or *CH*, Specimens

(a) A negligible amount of elastic slip occurs in compression during the seating of the T and column flanges.

(b) The greater concentration of the connecting material about the column flange in this type, compared with the previous one, produces less proportional deformation in tension on account of the decrease in column flange bending, but greater deformation in compression.

(c) The outward bending of the column flanges in line with the tension connection causes excessive concentration of stress in the centre of the horizontal welds between T and column flanges. Progressive failure began here within the design load and as a result complete failure occurred at an early stage. The column flange stiffeners, obviously, improved this defect by reducing the bending of the column flanges, but similar though less serious concentration of stress occurs in the vertical welds due to the bending of the T flanges, and it is this inevitable, uneven distribution of stress in the welds connecting the T to the column that is responsible for the low failure loads obtained for this type of connection.

(4) The Welded Gusset Plate, or *CJ*, Specimens

(a) Slip does not occur.

(b) Proportional deformation is practically the same in tension and compression but slightly greater in the bottom flange than in the top, owing to the altered distribution of stress caused by the shelf plate required in the bottom connection. The column flange stiffeners reduced top flange deformation to one-third its previous value and bottom flange to nearly one-half.

Region II. The deformations in this region are assumed to be the same in plate and column specimens and are derived from the short-extensometer readings on the plate specimens: they include; longitudinal deformation of the attachment within $2\frac{1}{2}$ in. of the column face, bending of the T flanges if any, and deformation of the connecting welds or rivets.

(a) The mean cross-sectional areas of the two attachments in this region do not vary by as much as 8% in the three types of connections, and consequently the wide variations in deformation ($F : H : J = 6 : 4 : 1$) must be attributed to the bending of the T flanges in *CF* and *CH* and the deformation of the rivets in *CF*. This assumption is supported by the facts that the deformation in tension is much greater than in compression, (60 : 40), and that elastic slip occurs in compression in these two types.

(b) The deformations of top and bottom flanges are very similar in the *F* specimen, for which the top and bottom attachments are the same, but the greater differences in the *H* and *J* specimens are to be expected, on account of the bottom attachments being heavier than the top ones. Another reason for the small deformations indicated in the bottom flange, involving stress distribution and the position of the gauge points, will be discussed later.

Region III. The deformations indicated for this region are derived from the differences in readings of the short and long extensometers, and include the longitudinal deformation of the attachment and beam, and the shear deformation of the connecting rivets or welds with any slip that may occur.

(a) As might be expected, the deformations in this region are similar in plate and column specimens of the welded types, and are not affected by the addition of column flange stiffeners. In the riveted specimens, where slip and elastic deformation are greatly affected by details in the process of riveting, slight variations of no significance occur.

(b) Non-elastic slip produces more than half the deformation that occurs in the riveted specimens in this region and constitutes nearly one-third of the total deformation of this type of connection.

(c) Elastic slip is negligible.

(d) Proportional deformation is similar to that of the plain beam, except in the welded T specimens where it is reduced by the stiffening effect of webs of the T's on the beam flanges.

Region VI. The regional analysis given above is based on the assumption that the cross-sectional planes through the gauge points of the extensometers remain plane during loading and therefore the movement of the gauge points accurately represents the inclination of the planes. Owing to the uneven distribution of stress in the vicinity of the gauge points of the short extensometers the assumption here is only approximately true, and there are obvious reasons for believing that some of the deformation charged to one region actually occurs in another. It is thought, however, that the gauge points of the long extensometers are removed sufficiently far from the causes of uneven stress distribution to be unaffected by them, and consequently the deform-

ation indicated for Region VI, based solely upon the long-extensometer readings and the adopted value of the deformation of the plain beam between the end of the region and the extensometer gauge points, is thoroughly reliable. The deformations indicated in Regions I, II and III are less accurate subdivisions of this deformation.

The analysis of the deformation is indicated in Fig. 17 *(d)* and *(e)* and agrees with the corresponding curves in Figs. 21, 22 and 23 and the regional analysis given above.

Table III indicates the total flexural deformation that occurs in each type during the *XY* load and the relative effect of tension and compression, top and bottom flanges, and normal and reversed loads in producing it.

From these results it is apparent that:

(1) About 30–45% of the deformation of the riveted types consists of non-elastic slip.

(2) The aggregate elastic deformation in tension is from 4–33% greater than that in compression for welded specimens, and from 56–70% greater for the riveted specimens.

TABLE III

ANALYSIS OF FLEXURAL DEFORMATION THAT OCCURS IN REGION NO. VI DURING THE *XY* LOAD

Type of connection	Total flexural deformation in radians $\times 10^{-5}$	Percentages of total deformation							
		(a) Stress			*(b)* Flange		*(c)* Load		
		Tension	Compression	Non-elastic slip	Top	Bottom	Normal	Reversed	Non-elastic slip
PF	400	34	20	46	50	50	27	27	46
PH	154	55	45	—	52	48	51	49	—
PJ	146	53	47	—	50	50	51	49	—
CF	669	42	27	31	51	49	34.5	34.5	31
CH	301	57	43	—	55	45	49	51	—
CH2W	224	57	43	—	54	46	46	54	—
CJ	222	52	48	—	47	53	50	50	—
CJ1W	189	51	49	—	47	53	52	48	—

(3) Opposite flanges deform equally in the riveted specimens, while the bottom attachment is the stiffer in the welded T and the top the stiffer in welded gusset plate specimens.

(4) Except in the case of *CH2W*, which had to be subjected to a modified loading program on account of previous partial failure, the deformations under normal and reversed loads are almost identical.

(5) The welded column flange stiffeners reduced the deformation of the *H* and *J* connection to 75 and 85% of their previous values, respectively.

All comparisons, heretofore, have been based on the deformation of the specimens during a complete reversal of load involving both flanges in tension

and compression and any intermediate slip that may occur. In Fig. 18 an analysis is given of the deformation that occurs during a repeated application of a normal load, within the design load limit of 70,000 lb., involving the top flange in tension and the bottom in compression and excluding non-elastic slip. As has been shown, the difference in deformation of the two flanges is due to the difference in effect of tension and compression rather than to structural difference.

27. *Deformation of the Test Specimens, Second Series—Flexural and Shear Deflection*

The deflections produced at 36 in. from the cantilever support by flexure and shear in individual regions during the *XY* load are given in Fig. 24. The total deflections are derived from the deflectometer readings and the flexural deflections from the extensometer readings according to Equations given in Art. 17. The resulting difference in deflection is assumed to be caused by shear. It is therefore obvious that, while the total deflections indicated are reliable, the component values of flexure and shear deflection are subject to the accuracy of the assumptions involved in the derivation of the former.

For example, compare the distribution of stress in Region II of the bottom attachment of the *PH* and *CH* specimens with relation to the short-extensometer gauge points, and it will be obvious that while the deformation indicated by the extensometer on the *PH* specimen will be less than the average for the cross section, owing to the concentration of stress in line with the beam welds, the extensometers on the *CH* specimens will indicate values more nearly equal to, or even greater than, the average, owing to the convergence of stress on the column web.

These errors, which occur also in the *J* specimens, will yield too great a value of $\delta\theta_{f_I}$ (the flexural slope developed in Region I), and similarly too small a value of $\delta\theta_{f_{II+III}}$, which in turn will yield too great a value of $\delta\Delta_{f_I}$ (the deflection produced by flexure in Region I) and too small a value of $\delta\Delta_{f_{II+III}}$.

The extent of such errors in flexural deflection is indeterminate and depends on the variation in the distribution of stress in Region II in the plate and column specimens. If, however, the vertical shear deformation in the column is negligible, as has been assumed, it is reasonable to explain the negative value of shear deformation obtained in Region I by the positive errors in flexural deflection recognized above. The positive values of shear deformation obtained for *CF* in Region I may be correct on account of the connection being made by rivets. An error in the flexural deflection for this region is also less probable.

Corrections to the deflections indicated, based on these assumptions, are shown as adjusted values in Fig. 24. They involve a slight decrease in the values of flexural deflection assigned to Region I and an almost identical increase in the values in Region (II + III). They do not affect the values

indicated for Region VI which therefore afford a dependable comparison of the total deformation of the connections tested during a reversal of load within the design load limits.

Similar regional values of flexural and shear deflection for a repeated normal load, up to 70,000 lb., as well as the development of these deflections during the application of the loads, were determined and plotted.

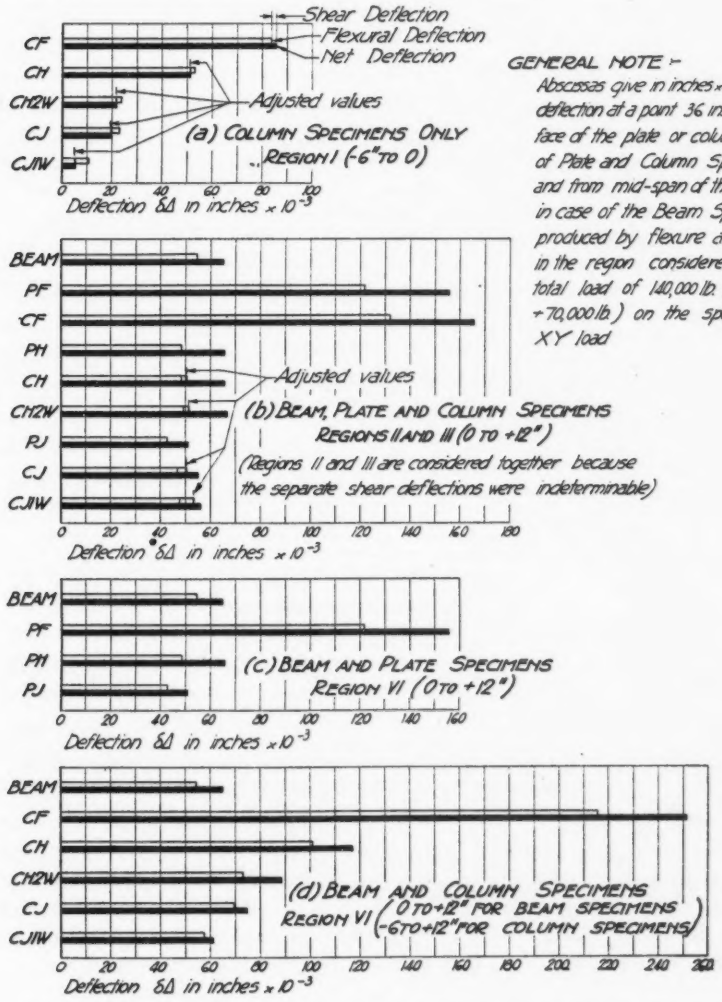
Shear Deflection
Flexural Deflection
Net Deflection
CF
CH
CH2W
CJ
CJIW
Adjusted values
(a) COLUMN SPECIMENS ONLY
REGION I (-6" TO 0)
Deflection δΔ in inches × 10⁻³
GENERAL NOTE:-
Abscissas give in inches ×10⁻³ the total deflection at a point 36 in. from the face of the plate or column in case of Plate and Column Specimens, and from mid-span of the specimen in case of the Beam Specimens produced by flexure and shear in the region considered under a total load of 140,000 lb. (-70,000 to +70,000 lb.) on the specimen-XY load
BEAM
PF
CF
PH
CH
CH2W
PJ
CJ
CJIW
Adjusted values
(b) BEAM, PLATE AND COLUMN SPECIMENS
REGIONS II AND III (0 TO +12")
(Regions II and III are considered together because the separate shear deflections were indeterminable)
Deflection δΔ in inches × 10⁻³
BEAM
PF
PH
PJ
(c) BEAM AND PLATE SPECIMENS
REGION VI (0 TO +12")
Deflection δΔ in inches × 10⁻³
BEAM
CF
CH
CH2W
CJ
CJIW
(d) BEAM AND COLUMN SPECIMENS
REGION VI (0 TO +12" FOR BEAM SPECIMENS
-6 TO +12" FOR COLUMN SPECIMENS)
Deflection δΔ in inches × 10⁻³

FIG. 24. *Total deflection produced at 36 in. from cantilever support by flexure and shear in individual regions due to total load change of 140,000 lb. (−70,000 to +70,000 lb.).*

A complete comparison of the performance of the specimens, including deformation during reversal within the design load and during a normal load approaching failure, as well as the value of the failure load, is given in Fig. 25.

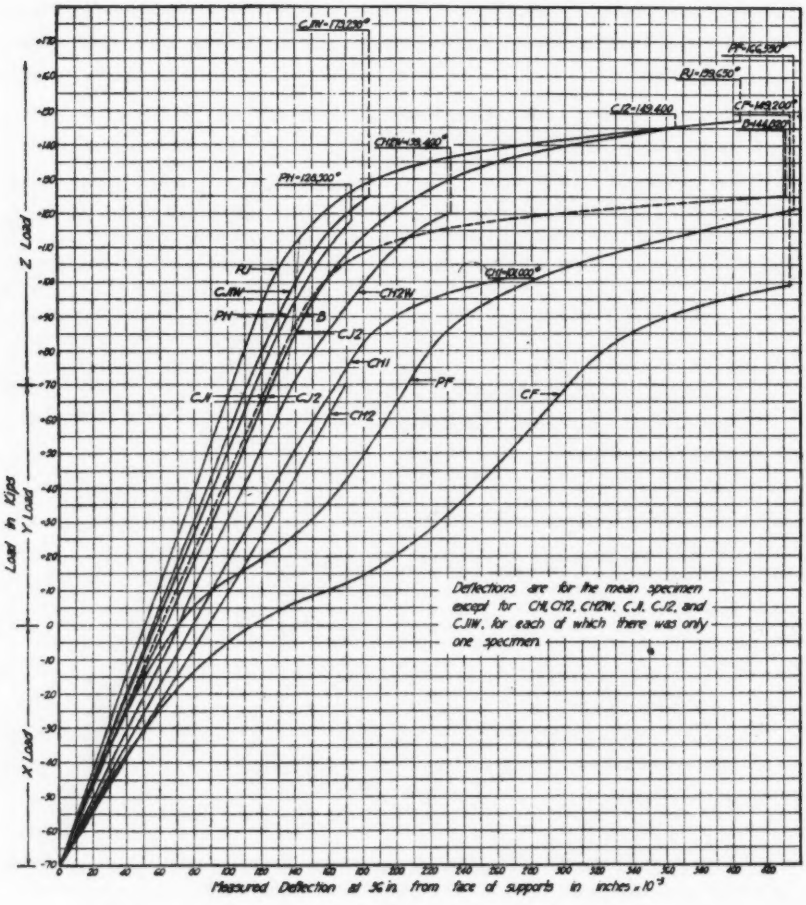

FIG. 25. *Deflection at 36 in. from cantilever support, and failure loads.*

From these results it is obvious that while both the welded types are much more rigid than the riveted, one of them, the welded T, is much weaker. The other, the gusset plate type, is somewhat stronger. The column flange stiffeners greatly increase the strength and rigidity of the connections.

28. *Coefficients of Restraint—First Series*

The coefficients of restraint that would be developed in the uniformly loaded, simulated beam were computed from the observed deformations of

the test specimens by the method outlined in Art. 23, Section III. Determinations were made for a series of loads corresponding to loads on the double-cantilever specimens from 4,000 lb. to failure, at intervals of 4,000 lb.

Proceeding on the theoretical basis of the article mentioned, the attachments to the top and bottom flanges were compared in so far as their relative effect on the coefficient of restraint was concerned. For this purpose the slope angles θ_t and θ_b attributable to these flanges were calculated and the coefficients of restraint determined for the following three cases:

(1) Assuming that the bottom attachment developed complete restraint, or $\theta_b = 0$.

(2) Assuming that the top attachment developed complete restraint, or $\theta_t = 0$.

(3) For the combined result of the two attachments using $\theta = \theta_t + \theta_b$.

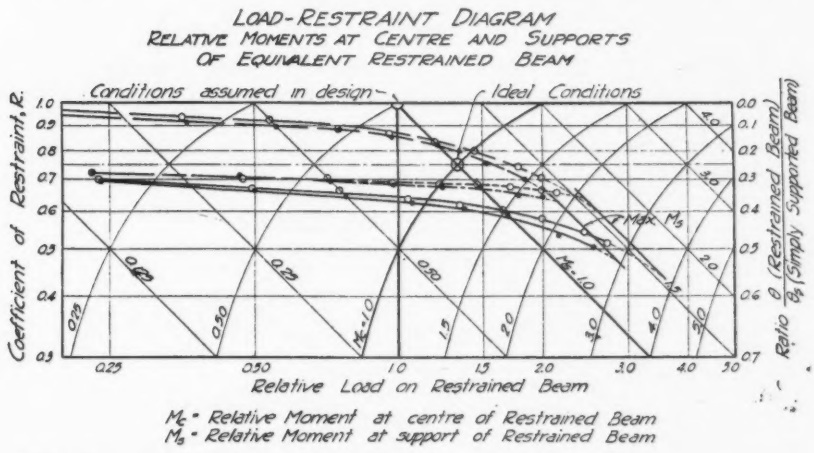
LOAD-RESTRAINT DIAGRAM
RELATIVE MOMENTS AT CENTRE AND SUPPORTS OF EQUIVALENT RESTRAINED BEAM
Conditions assumed in design
Ideal Conditions
Coefficient of Restraint, R
Ratio θ (Restrained Beam) / θ (Simply Supported Beam)
Max Ms
Relative Load on Restrained Beam
Mc = Relative Moment at centre of Restrained Beam
Ms = Relative Moment at support of Restrained Beam

Specimen		PA1	PA2
Curves	Tension	———	———
	Compression	- - -	- - -
	Tension & Compn	———	———
Total length of ⅜" weld in two tension connections (See diagram) - in		29	28.8
Welding time - mins		185	145
Rate of welding - ft per hr		7.6	9.9
Wire used (⅜" Roebling) - in		78	77
Maximum stress - lb per lin in		7,340	8,340

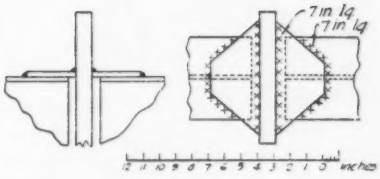

FIG. 26. *Coefficient of restraint, Connection A, first series.*

The relation of these coefficients of restraint to relative load on the simulated beam was plotted logarithmically as in Figs. 26 to 30 assuming the design load of 24,000 lb. on the beam as unity.

For each of the two specimens to which the figure pertains the coefficient of restraint that would arise if the attachment to one flange or the other

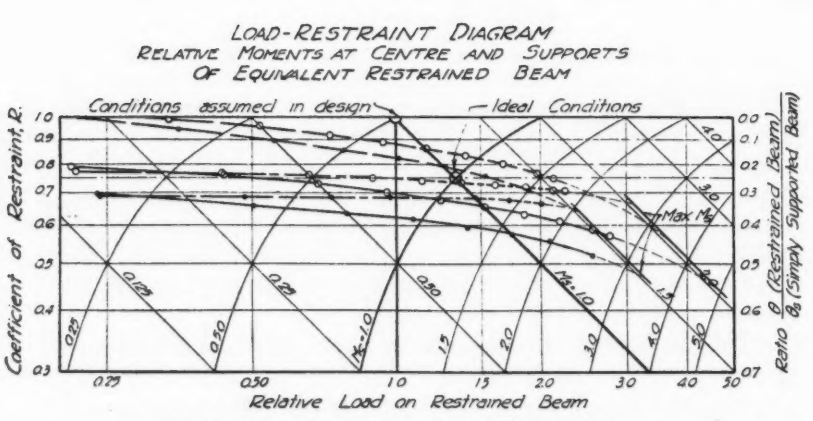

M_c = Relative Moment at centre of Restrained Beam
M_s = Relative Moment at support of Restrained Beam

Specimen		PB1	PB2
Curves	Tension	———	———
	Compression	- - -	- - -
	Tension & Compn	———	———
Total length of 1/8" weld in two tension connections (See diagram) - in.		28	28
Welding time - mins		15	15
Rate of welding - ft per hr		9.3	9.3
Wire used (7/16" Roebling) - in.		83	84
Maximum stress - lb per lin in		9,200	11,060

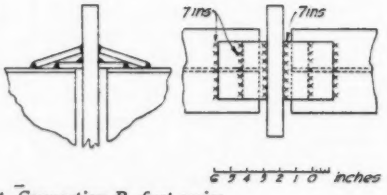

FIG. 27. Coefficient of restraint, Connection B, first series.

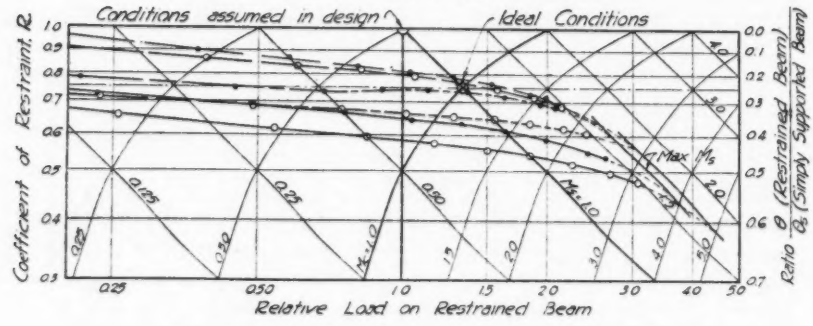

M_c = Relative Moment at centre of Restrained Beam
M_s = Relative Moment at support of Restrained Beam

Specimen		PC1	PC2
Curves	Tension	———	———
	Compression	- - -	- - -
	Tension & Compn	———	———
Total length of 1/8" weld in two tension connections (See diagram) - in		28	28
Welding time - mins		18	18
Rate of welding - ft per hr		7.8	7.8
Wire used (7/16" Roebling) - in		79	78
Maximum stress - lb per lin in		8720	3160

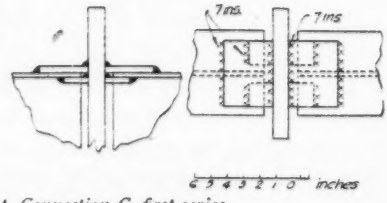

FIG. 28. Coefficient of restraint, Connection C, first series.

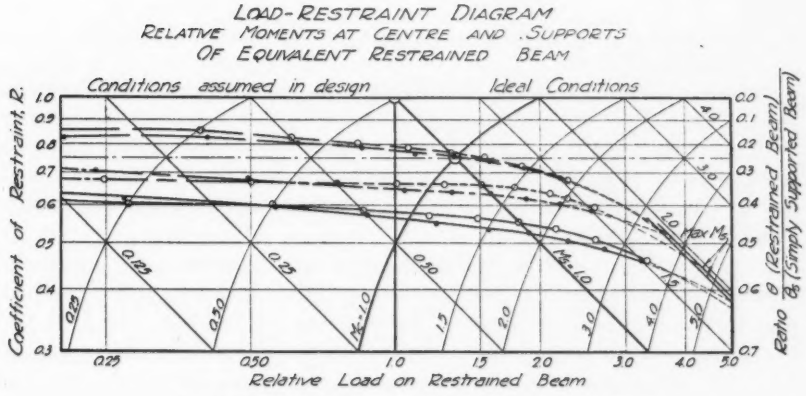

M_c = Relative Moment at centre of Restrained Beam
M_s = Relative Moment at support of Restrained Beam

Specimen	PD1	PD2
Curves — Tension	←—→	○—○
Curves — Compression	←- -→	○- -○
Curves — Tension & Comp^n	←—→	○—○
Total length of 3/16" weld in two tension connections (see diagram) in	38	38
Welding time - mins.	22	27
Rate of welding - ft. per hr.	8.6	7.0
Wire used (7/16" Roebling) - in	89	110
Maximum stress - lb. per lin. in	7,480	7,660

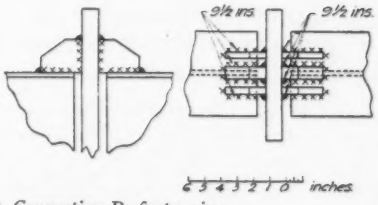

FIG. 29. *Coefficient of restraint, Connection D, first series.*

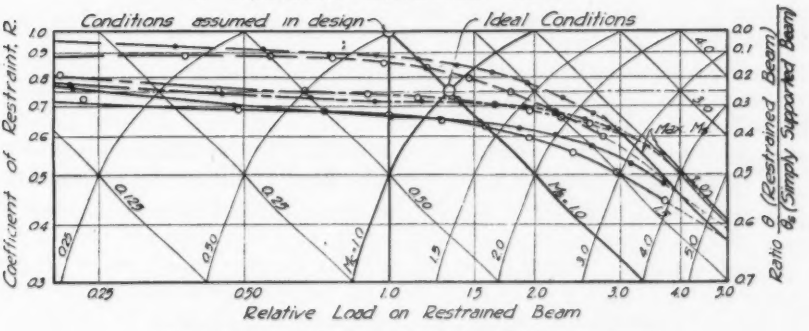

M_c = Relative Moment at centre of Restrained Beam
M_s = Relative Moment at support of Restrained Beam

Specimen	PE1	PE2
Curves — Tension	←—→	○—○
Curves — Compression	←- -→	○- -○
Curves — Tension & Comp^n	←—→	○—○
Total length of 3/16" weld in two tension connections (see diagram) - in	47	47
Welding time - mins.	28	21
Rate of welding - ft. per hr.	8.4	11.2
Wire used (7/16" Roebling) - in	124	104
Maximum stress - lb. per lin. in	6,500	5,850

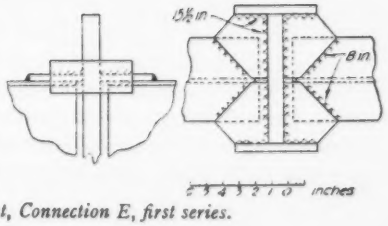

FIG. 30. *Coefficient of restraint, Connection E, first series.*

developed complete restraint is indicated in broken lines. The resulting curves show that the tension flange attachment is the more satisfactory of the two so far as restraint is concerned, since, if the compression attachment were perfectly rigid, the coefficient of restraint would be much higher than if the tension attachment were assumed perfectly rigid and the compression one alone deformed.

The connection as a whole failed, for this type, to develop ideal restraint, even at loads less than one-quarter of the design load. As the failure load was approached, the coefficient of restraint fell off to little more than 0.5.

For the purpose of determining the existing moment at centre or support corresponding to any combination of coefficient of restraint and beam load, one series of straight lines of equal moments at the centre and another of equal moments at the support were superimposed on the diagram. The simulated beam having been designed for perfect end restraint, the support moment for a design load of unity was itself considered to be unity. With a reduction of the coefficient of restraint to 0.5, the relative load would consequently need to be 2.0, if the support moment were to remain 1.0.

Utilizing this superimposed grid it is found by interpolation that, for example, the specimen *PA*1 developed a coefficient of restraint of 0.6 at a load 1.5 times the design load, that the support moment was about 0.9 and the centre moment about 1.4 times the design moment at the support.

While the extensometers had to be removed before failure, it is useful to consider the relation of the plotted curves of load-coefficient of restraint to the maximum moment developed in the connection. Curves of these observed moments, on the relative basis, are interpolated in Figs. 26 to 30. It is impossible to determine the coefficients of restraint at failure exactly, or the relative load on the simulated beam, which depends on coefficient of restraint, but by extending the observational curves to join the maximum moment curves at the support, an estimate may be made of them by considering the position of the intersection. If, owing to low coefficient of restraint, this point should approach the lower right hand corner of the diagram, the simulated beam would have failed at the centre before failing at the ends, as is evident from the high values indicated by the centre moment curves.

Examination of these diagrams shows that for the connections of all five types the top flange attachment is the one that promotes most the development of a relatively high coefficient of restraint. The bottom flange attachment, being more yielding, operates to offset in some measure the restraining merits of the other. For all specimens the coefficient decreases slowly as the load is increased and falls off rapidly as the load nears the failure load.

The pronounced influence of the top flange attachment in furthering a high coefficient of restraint suggests that by stiffening up the bottom flange attachment the ideal coefficient of restraint for the connection as a whole should not be difficult of attainment. Longitudinal shear deformation in the thin bottom flanges of the beams employed is believed to have been an important source of yield in the bottom attachment.

29. *Coefficients of Restraint—Second Series*

Proceeding as for the first series, the coefficients of restraint developed in the large specimens of the second series were determined for three loadings. In finding the difference between the slope angle developed in the cut-and-connected specimens and that developed in the mean plain beam, the readings of the extensometers with gauge points 18 in. from the back of the connection, or, in the case of the plain beam, 18 in. from the middle, were utilized.

Fig. 31 shows the coefficients of restraint, R, developed in the specimens of the second series under the AZ load. This loading is the initial load up to the safe design limit extended by connecting with the Z load, as described in

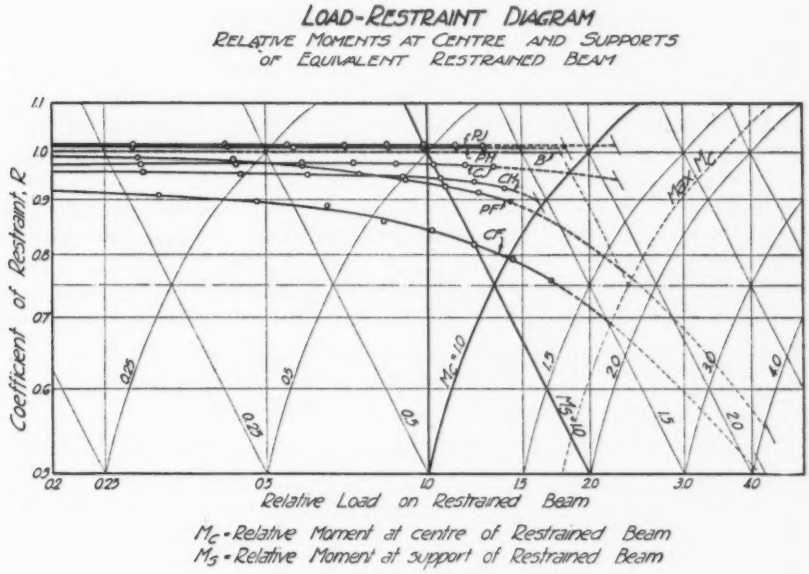
LOAD-RESTRAINT DIAGRAM
RELATIVE MOMENTS AT CENTRE AND SUPPORTS
OF EQUIVALENT RESTRAINED BEAM
Coefficient of Restraint, R
Relative Load on Restrained Beam
Mc = Relative Moment at centre of Restrained Beam
Ms = Relative Moment at support of Restrained Beam

FIG. 31. *Coefficient of restraint, second series, AZ load.*

Art. 7, thus representing the probable behavior of the specimens if the initial load had been carried directly to failure. Account is thus taken of initial set, or slip, or both. Obviously, for total moment calculations, this is the correct loading to employ, as unrecoverable deformation in the connections permanently lessens their participation in the total moment developed in the span.

Coefficients of restraint greater than unity are found for PH and PJ. The riveted T specimen CF shows the smallest restraint, but even it, for the design load, gives a value of about 0.84.

Design of a connection for large wind moment may thus cause it to absorb an amount of gravity load moment in excess of the ideal. As illustrated in Fig. 16, restraint beyond this limit is a disadvantage and hence beams with riveted connections of the type employed in this investigation are better than those with welded connections, so far as the economical distribution of moments due to gravity loads is concerned.

A more typical situation with respect to end restraint arises when any one of the innumerable loadings following the initial load is applied. The connections have then suffered permanent deformation and permanent impairment of their restraining value. A specimen load representative of such typical loading on the simulated beam would be the Z load, but calculations of the coefficient of restraint should include a constant amount for the permanent deformation resulting between the beginning of the initial load, A, and the beginning of the Z load. Deformations due to the combined effect will be considered as arising from what has been designated the Z' load.

In the case of the riveted specimens the question arises as to how much of the non-elastic slip should be included in this combination. It is conceivable that all or none might actually occur during the application of the Z load to the simulated beam, depending on the accuracy in punching and conditions at the time of erection. For uniformity, however, the net deformation of the specimen up to the time of application of the Z load, has been used with all specimens.

Coefficients of restraint, R, for the Z' load are shown in Fig. 32. As is to be expected, the recognition of a large permanent deformation at the beginning

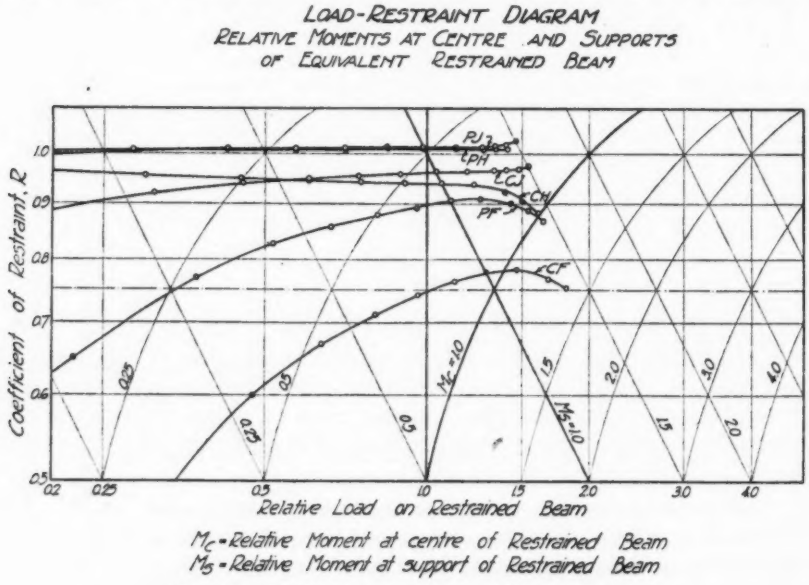

FIG. 32. *Coefficient of restraint, second series, Z' load.*

TABLE IV

LENGTHS OF WELDS, FAILURE LOADS, STRESSES DEVELOPED AND FACTORS OF SAFETY FOR SPECIMENS OF THE FIRST SERIES

Specimen		Total nominal length of welds in complete connection, in.	Nominal length of welds that failed, in.	Effective depth, in.	Load, lb.		Estimated average ultimate stress, lb. per lin. in. of welds that failed	Factor of safety		Ratio $\frac{F_T}{F_D}$	Manner of failure
Mark	Type				Design	Ultimate		Design, F_D	Test, F_T		
*BA*1	Plain beam	—	—	—	24,000	63,080	—	2.50	2.63	1.05	
*BA*2	Plain beam	—	—	—	24,000	60,900	—	2.50	2.54	1.02	
*PA*1	See Fig. 1	60	7	9.7	24,000	32,550	6,700	2.02	1.36	0.67	
*PA*2	See Fig. 1	60	7	9.7	24,000	37,680	7,800	2.02	1.57	0.78	
*PB*1	See Fig. 1	60	7	10.2	24,000	36,900	7,200	2.13	1.54	0.72	
*PB*2	See Fig. 1	60	7	10.2	24,000	49,800	9,700	2.13	2.07	0.97	In tension welds between connecting plates, and Plate *P*.
*PC*1	See Fig. 1	60	7	9.5	24,000	39,230	8,300	1.98	1.63	0.82	
*PC*2	See Fig. 1	60	7	9.5	24,000	41,200	8,700	1.98	1.72	0.87	
*PD*1	See Fig. 1	70	9.5	10.4	24,000	45,700	6,500	2.94	1.90	0.65	
*PD*2	See Fig. 1	70	9.5	10.4	24,000	46,800	6,600	2.94	1.95	0.66	
*PE*1	See Fig. 1	79	8	9.4	24,000	49,180	9,200	2.24	2.05	0.92	In welds between connecting plates *X* and beam *B*, and partially in welds between plates *X* and plate *P*.
*PE*2	See Fig. 1	79	8	9.4	24,000	44,200	8,300	2.24	1.84	0.82	

of loading reduces the coefficients for small loads on the riveted specimens to values much below those for the *AZ* load. For the higher loads, the relative importance of the initial deformation is lessened and the coefficients become larger, even reaching the ideal value for *CF* at the design load. It is important to note that the values for *PH* and *PJ* are everywhere greater than unity, as was the case for the initial *AZ* load, while for *CH* and *CJ* they are not very much less than for the initial load.

30. *Ultimate Strength and Factors of Safety—First Series*

Ultimate strengths and factors of safety for the specimens of the first series are shown in detail in Table IV.

The design factor of safety is the estimated failure load on the specimen, based on an assumed ultimate strength in $\frac{3}{8}$-in. welds of 10,000 lb. per lineal inch, divided by the design load. The test factor of safety is, of course, the actual failure load divided by the design load, or the actual ultimate strength of welds in pounds per lineal inch divided by the working stress expressed in the same unit.

Although the design factor of safety was nominally about 2.0, it was increased in certain cases, notably for specimens *PD*1 and *PD*2, in order to compensate for anticipated uncertain behavior.

The relation of test factors of safety to design factors of safety was not so close as had been expected, since the ultimate strength of welds on test was less than the 10,000 lb. per lineal inch assumed for $\frac{3}{8}$-in. fillets. The actual realized values of the weld strength set forth in the eighth column of the table show the extent of the deficiency.

31. *Ultimate Strength and Factors of Safety—Second Series*

A general comparison of the performance of the specimens of the second series, so far as ultimate strength and factors of safety are concerned, is possible from an examination of Table V. The nature of the failures of three typical specimens *CF*1, *CH*1 and *CJ*2 is evident from Figs. 33, 34 and 35. Factors of safety were computed in the same manner as for the first series.

The relatively low design factor of safety for the plain beams, that is, 2.03, is due to the fact that the maximum flexural stress in the beam sections employed for making up the welded and riveted specimens, was assumed as occurring at 10 in. out from the face of the cantilever support. At that point, in either the plain or the cut-and-connected specimens, the factor of safety would be 2.50, but at the middle of the plain beams, which may be considered as two 54-in. cantilevers, it would be only 2.03.

While the design factor of safety originally planned for cut-and-connected specimens was from about 2.25 to 2.50, it actually varied from 1.84 for *PJ*2 to 3.15 for *PH*2. This arose either from inability to provide the exact length

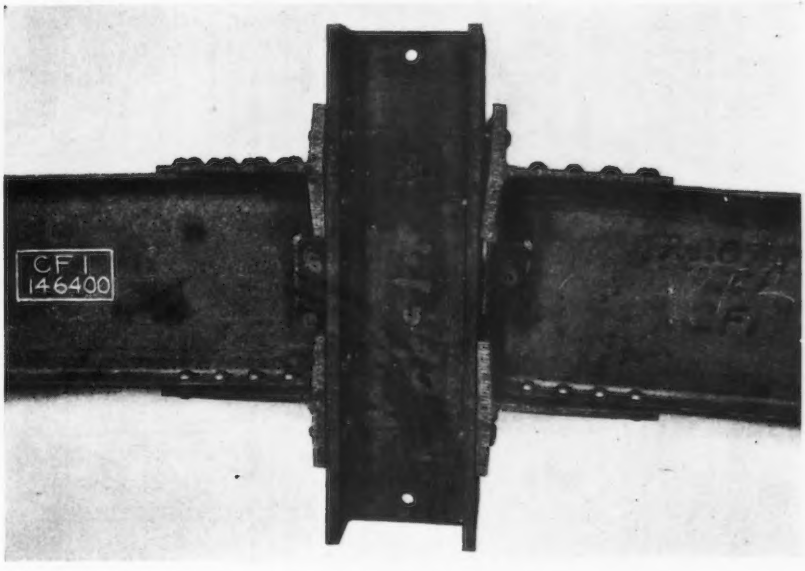

FIG. 33. *Riveted column specimen CF1 after failure at 146,000 lb.*

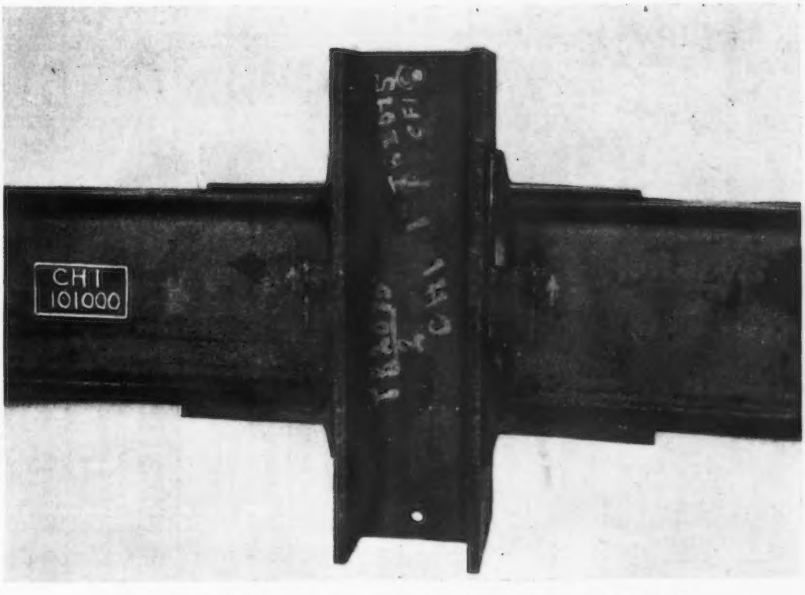

FIG. 34. *Welded column specimen CH1 after failure at 101 000 lb.*

TABLE V

LENGTHS OF WELDS, FAILURE LOADS, STRESSES DEVELOPED AND FACTORS OF SAFETY FOR SPECIMENS OF THE SECOND SERIES[1]

Specimen		Number of rivets or total nominal length of welds in complete connection[2]	Number of rivets or adjusted length of welds that failed	Effective depth, in.	Load, lb.		Estimated average ultimate stress in lb. per rivet or in lb. per lin. in., of adjusted length of welds that failed	Factor of safety		Ratio $\frac{F_T}{F_D}$	Manner of failure
Mark	Type				Design	Ultimate		Design, F_D	Test, F_T		
*BF*1	Plain beam	—	—	—	70,000	140,000	—	2.03[3]	2.00	0.99	Compression flange buckled locally
*BF*2	Plain beam	—	—	—	70,000	144,870	—	2.03[3]	2.07	1.02	Compression flange buckled locally
*BH*1	Plain beam	—	—	—	70,000	147,500	—	2.03[3]	2.11	1.04	Compression flange buckled locally
*BH*2	Plain beam	—	—	—	70,000	—	—	—	—	—	Not loaded to failure
*BJ*1	Plain beam	—	—	—	70,000	146,900	—	2.03[3]	2.10	1.04	Compression flange buckled locally
*BJ*2	Plain beam	—	—	—	70,000	—	—	—	—	—	Not loaded to failure
*PF*1	Plate specimen, riveted T's	48, ¾-in. rivets	8, ¾-in. rivets	18.7	70,000	165,100	29,800 lb. per rivet	2.45[4]	2.36	0.96	Rivets did not fail. Beam flanges and web buckled. Shear plate welds began to fail at 150,000 lb.
*PF*2	Plate specimens, riveted T's	48, ¾-in. rivets	8, ¾-in. rivets	18.7	70,000	168,000	30,100 lb. per rivet	2.45[4]	2.40	0.98	Rivets did not fail. Beam flanges buckled at end of connection
*PH*1	Plate specimen, welded T's	197 in.	30.1	18.9	70,000	139,000	6,600 lb. per in.	3.01[5]	1.99	0.66	Welds of tension T and of shear plates failed at plate face
*PH*2	Plate specimen, welded T's	197 in.	31.5	18.9	70,000	118,000	5,400 lb. per in.	3.15[5]	1.69	0.54	Welds of tension T failed at plate face

PJ1	Plate specimen, welded gussets	222 in.	17.3	21.6	70,000	153,300	11,100 lb. per in.	1.98[5]	2.19	1.11	Welds of tension gusset and of shear plates failed at plate face
PJ2	Plate specimen, welded gussets	222 in.	16.1	21.6	70,000	166,000	12,900 lb. per in.	1.84[5]	2.37	1.29	Beam flanges and web buckled. One shear plate weld failed at 100,000 lb.
CF1	Column specimen, riveted T's	32, $\frac{7}{8}$-in. rivets 32, $\frac{3}{4}$-in. rivets	8, $\frac{3}{4}$-in. rivets	18.7	70,000	146,400	26,400 lb. per rivet	2.38[4]	2.09	0.88	Extreme tension rivets failed
CF2	Column specimen, riveted T's	32, $\frac{7}{8}$-in. rivets 32, $\frac{3}{4}$-in. rivets	8, $\frac{3}{4}$-in. rivets	18.7	70,000	152,000	27,400 lb. per rivet	2.38[4]	2.17	0.91	Extreme tension rivets failed
CH1	Column specimen, welded T's	197 in.	29.4	18.9	70,000	101,000	4,900 lb. per in.	2.94[5]	1.44	0.49	Welds of tension T failed at column face
CH2W	Column specimen, welded T's, stayed flanges	326 in.	23.9	18.9	70,000	139,400	8,300 lb. per in.	2.39[5]	1.99	0.83	Final load on specimen in reversed position. Welds of tension T failed at column face[6]
CJ1W	Column specimen, welded gussets, stayed flanges	351 in.	17.6	21.6	70,000	173,230	12,300 lb. per in.	2.01[5]	2.47	1.23	Beam flanges and web buckled. Column stiffener weld failed at 159,760 lb. No failure in other welds
CJ2	Column specimen, welded gussets	222 in.	17.5	21.6	70,000	149,400	10,700 lb. per in.	2.00[5]	2.13	1.06	Welds of a tension gusset failed at column face

[1] *Allowance is made in the length of welds that failed for the variation of the fillet size from the desired $\frac{3}{8}$ in. by adjusting the lengths of the fillets.*

[2] *This excludes the welds for shear plates and web stiffeners, which were common to all specimens.*

[3] *Based on assumed ultimate strength of 45,000 lb. per sq. in. in compression flange, at mid-span. At 10 in. from centre of span, the design factor of safety was 2.50.*

[4] *Based on tension rivets.*

[5] *Based on tension welds to face of support.*

[6] *Centre of extreme tension horizontal weld between T and column face began to fail at 73,000 lb., as did weld of one shear plate. Column stiffener welds failed at 120,000 lb.*

of welds, or number of rivets, required to satisfy the working stresses of the established specification, or from a deliberate increase in weld lengths to guard against too early failure, as in the cases of *PH*1 and *PH*2.

Test factors of safety bear a satisfactory relation to the design factors of safety in the case of *PF*1, *PF*2, *PJ*1, *PJ*2, *CJ*1*W* and *CJ*2.

On the other hand, the welded T-connections *PH*1, *PH*2, *CH*1 and *CH*2*W* gave poor results, by reason of the lack of uniformity of stress in the welds. For the plate specimens *PH*1 and *PH*2 early failure occurred at about the

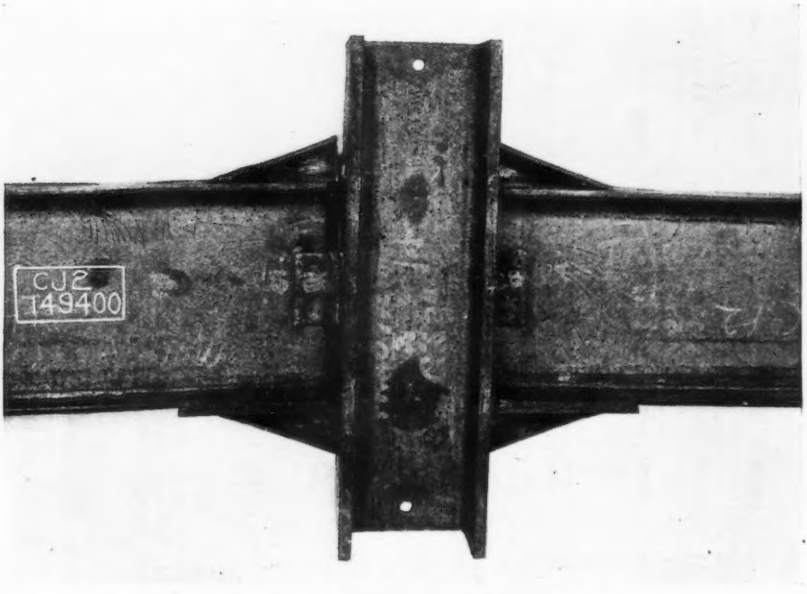

FIG. 35. *Welded column specimen CJ2 after failure at 149,000 lb.*

centre of length of the vertical welds connecting the T to the plate, while for the column specimens *CH*1 and *CH*2*W* it occurred at about the centre of the horizontal welds connecting the T to the column flange, that is, opposite the column web. The great variation in resistance to horizontal deformation afforded by the various portions of a welded connection of this type make it relatively inefficient.

The column specimens of the riveted T-type gave smaller relative factors of safety than the plate specimens of this type. This was due no doubt to a lesser uniformity of stress distribution amongst the tension rivets connecting the T to the column flange, and to the failure of the shorter grip for the $\frac{3}{4}$-in. rivets in the column flange to compensate for the use of smaller tension rivets in the column specimens.

TABLE VI

DRIFT ANGLES IN RADIANS DUE TO DEFORMATION OF CONNECTED BEAM IN 19-FT. CLEAR PANEL, AND DUE TO THE CONNECTIONS ALONE, THE END MOMENT VARYING FROM CAPACITY POSITIVE MOMENT TO CAPACITY NEGATIVE MOMENT

Case	Beam with connections indicated below								
	Plain beam integral with column	*PF*	*PH*	*PJ*	*CF*	*CH*	*CH2W*	*CJ*	*CJ1W*
Connected beam	0.00676	0.00898	0.00653	0.00641	0.01168	0.00799	0.00727	0.00717	0.00682
Plain beam integral with column	0.00676	0.00676	0.00676	0.00676	0.00676	0.00676	0.00676	0.00676	0.00676
Connections only	0	0.00222	−0.00023	−0.00035	0.00492	0.00123	0.00051	0.00041	0.00006
Drift per 12-ft. story due to connections only, in.	0	0.319	0.0331	0.0504	0.709	0.177	0.0735	0.0591	0.00864

32. *Story Drift Angle*

On the assumption that the point of inflection of the beam in the simulated panel is at mid-span, the reasonableness of which has been justified in Art. 24, the story drift angles attributable to the various connections were readily computed from the test results.

For the reversing load, XY, the total drift angle due to the cut-and-connected beam in the simulated panel is the total computed movement of the point of inflection of the beam at right angles to a normal to the column at the end of the beam, divided by the half span. The values of this deflection having been determined, the drift angles that would arise from the deformation of the 18-in., 47-lb. C.B. with its connections in the simulated bay, assuming the connections to be stressed from capacity positive moment to capacity negative moment, and the drift angles attributable to the connections alone, would be as indicated in Table VI.

Examination of the table indicates that the drift angles chargeable to the connections varied only from -0.00035 radian for PJ to $+0.00492$ for CF. The negative sign for PH and PJ shows that, owing to the reinforcement of the ends of the beam by the details, the resulting construction was stiffer than for a plain beam integrally connected to the column.

The significance of these angles is indicated in the table by the corresponding drift in inches that would occur in a 12-ft. story. The excessive drifts for the riveted T-connections are to a considerable extent due to non-elastic slip in the shear rivets connecting the stem of the T's to the beam flange.

On the assumption that a capacity wind force in one direction is applied to the building standing in a vertical position after previous loadings had brought it to seasoned or steady elastic state, the drift angles would be one-half of those listed in Table VI for capacity reversing load.

V. Summary and Conclusions

The principal findings of the investigation are briefly summarized below. Based upon the observed behavior of the specimens tested the indicated conclusions appear to be warranted for the types of connections studied.

A. *Coefficient of Restraint*

(1) At the design load the coefficient of restraint developed by the connections of the first series, designed for beam continuity only, varied from 0.57 to 0.67, as compared with an ideal value of 0.75. The coefficient increases slowly as the load decreases from the design value and decreases rapidly as the load increases therefrom. The lowest value was shown by the D connection, in which three parallel vertical plates were used for the tension attachment, and the highest by the E connection, in which both horizontal and vertical plates were utilized for the tension attachment (see Figs. 26 to 30, inclusive). Attainment of the ideal coefficient of restraint would, therefore, apparently necessitate somewhat heavier details than those adopted for this series.

(2) At the design load the coefficient of restraint developed by the connections of the second series, designed primarily for wind moment, was always equal to, or greater than, the ideal value for beam continuity, 0.75, this high value being partly due to the incidental reinforcing of the beam flanges by connection material. The smallest values were given by the riveted specimens. Whether they were riveted or welded, connections to a column flange gave smaller restraint than the corresponding connections to a column web. For any capacity gravity loading subsequent to the first one, the coefficient of restraint for connections to a column flange varied from 0.75, for a riveted T, to 0.96 for the welded gusset type; for connections to a column web, it varied from 0.90 for a riveted T to 1.01 for the two types of welded connection. Wind connections of the kind tested will develop, therefore, a higher coefficient of restraint than the most economical value required to resist gravity loads only (Fig. 32).

B. *Story Drift Due to Connections*

(3) Due to the incidental reinforcement of the flanges near its ends, the beam, when welded to a plate simulating a column web, developed less drift angle than would have been developed by a plain beam integral with the column. The drift angle for such connections was, therefore, negative. Loss of rigidity due to connections may, consequently, be entirely obviated where welded connections are made to a column web. On the other hand, T's riveted to a column web gave, for a 19-ft. clear panel, and for an end moment varying from capacity positive moment to capacity negative moment, a total, or extreme, drift angle of 0.0022 radian, or a drift of 0.32 in. for a 12-ft. story (see Table VI).

(4) T's riveted to a column flange gave, for the same panel and the same loading, a total drift angle of 0.0049 radian, or a linear drift of 0.71 in. per story. Welded T's gave 0.0012 radian and 0.18 in., while welded gusset connections gave 0.0004 radian, and 0.06 in. Supporting the column flanges by welded stays between them reduced these quantities to 0.0005 radian and 0.07 in. for the welded T's and to 0.00006 radian and 0.009 in. for the welded gusset type (see Table VI). Marked improvement in stiffness of a frame is consequently made possible by the substitution of welded for riveted connections.

(5) For a capacity wind load in one direction only the drift angles and linear drifts due to the connections tested would, if the building were plumb at the beginning of the lateral loading, be one-half of the above amounts for capacity reversing load.

C. *Sources of the Deformation*

(6) In the connections designed for beam continuity only, and subjected to load in one direction only, the top (tension) attachment was in all cases stiffer than the bottom (compression) attachment (see Figs. 26 to 30, inclusive). Transfer of the axial compression from the bottom flange by longitudinal welds at the thin edges of the flange was accompanied by considerable

yield due to horizontal shear in the flanges, which was responsible for approximately two-thirds of the loss of restraint in these specimens. The use of sections with heavier flanges would have reduced this loss and increased the values of restraint almost to those given for the tension connection alone.

(7) In the wind connections to a column web, the top and bottom attachments, under capacity reversing load, gave practically equal longitudinal deformations for all three types. In the connections to a column flange, the riveted T's gave nearly equal deformations in the two attachments; in the welded T's the top attachment gave, on an average, 20% more deformation than the bottom one; in the welded gusset type the bottom attachment gave 13% more deformation than the top one (see Table III). The influence of the half-width of the column on the end slope angle may, therefore, make itself felt to a substantially greater extent in one attachment than in the other, the more yielding attachment depending on the type of connection.

(8) In wind connections to the simulated web of a column the ratios of the flexural slope, under capacity reversing load, developed in the first $2\frac{1}{2}$ in. of the connection to that developed in 12 in., the nominal length of the connection, were as follows: riveted T, 0.25; welded T, 0.42; welded gusset, 0.12 (see Table II). The flexure in the flanges of the welded T apparently contributes a considerable part of the total yield of this type of connection.

(9) In wind connections to the flange of a column, the flexural slope attributable to the half-column width under capacity reversing load bore to the total flexural slope in the nominal length of the connection plus the half-width of the column, the following ratios: riveted T, 0.35; welded T, 0.49; welded gusset, 0.29. When stiffeners were welded to the column flanges, the ratio was reduced to 0.30 and 0.16 for the welded T and the welded gusset, respectively. From a third to a half of the flexural slope in a connection to a column flange may, therefore, be charged to the deformation in the column. This may be reduced by as much as a third by the introduction of flange stiffeners (see Table II).

(10) In the wind connections to a column flange, the half-column width gave, for the welded T, 63%, and for the welded gusset, 27% of the flexural slope developed by the riveted T. When welded stiffeners were added to the column flanges, the welded T gave only 28% and the welded gusset 13%. In the first $2\frac{1}{2}$ in. of the connection the welded T gave 62% and the welded gusset 17% of the flexural slope given by the riveted T. In the next $9\frac{1}{2}$ in. the percentages were 27 and 42, respectively. Consequently, so far as flexural slope is concerned, and this is responsible for most of the angular deformation at a joint, the welded connections were definitely superior to the riveted ones in all regions (see Table II).

(11) The aggregate longitudinal elastic deformation in tension during the application of the reversing load was greater than the aggregate deformation in compression. For the welded specimens the excess varied from 4% for the welded gusset type with column stiffeners to 33% for the welded T-type without column stiffeners. For the riveted T's the excess was much greater,

being 56% for the connection to a column flange and 70% for the connection to a column web (see Table III).

(12) For the riveted T's a large part of the longitudinal deformation was non-elastic slip, being 31% for the connection to a column web and 46% for a connection to a column flange (see Table III).

(13) Except in the case of the welded T-connection to a column flange, which had to be subjected to a modified loading program on account of previous partial failure, the deformations under normal and reversed loads were almost identical (see Table III).

(14) The welded stiffeners to the column flanges reduced the longitudinal deformation of the welded T and the welded gusset connections to 75 and 85% of their previous values, respectively (see Table III).

D. *Ultimate Stresses and Factors of Safety*

(15) In the specimens of the first series, designed for beam continuity only, failures occurred in the welds and generally between the connecting plates and the plate simulating the web of the girder or column to which the beam would be connected. The ultimate strength of the $\frac{3}{8}$-in. fillet welds in transverse shear varied from 6500 to 9700 lb. per lineal inch, as compared with an estimated ultimate strength of 10,000 lb. per lineal inch on the basis of uniform distribution of stress (see Table IV).

(16) For the first series, the ratios of the test factor of safety to the design factor of safety, based on assumed uniform distribution of stress, was in every case below unity, varying from 0.65 to 0.97. Lack of uniformity of stress distribution was no doubt responsible for a part of the deficiency (see Table IV).

(17) In the specimens of the second series, designed primarily as wind connections, the average load on each of the $\frac{7}{8}$-in. rivets of the tension attachment to the simulated column web at the moment of failure of the compression flange of the beam was 29,950 lb., and on each of the $\frac{3}{4}$-in. rivets of the tension attachment to the column flange at the failure of these rivets it was 26,900 lb., as compared with estimated ultimate loads of 31,000 lb. and 30,000 lb., respectively, on the basis of uniform distribution of loads amongst the rivets. In the welded specimens, the stress in the adjusted length of the $\frac{3}{8}$-in. tension welds to the face of the support at failure of the specimen, which usually occurred by rupture of these welds, varied from 4900 lb. per lineal inch for one of the T-specimens to 12,900 lb. per lineal inch for one of the gusset plate specimens, as compared with an estimated ultimate strength of 10,000 lb. per lineal inch on the basis of uniform distribution of stress (see Table V).

(18) For the riveted specimens, the ratio of the test factor of safety to the design factor of safety varied from 0.88 to 0.98, while for welded T-specimens it varied from 0.49 to 0.83, and for welded gusset plate specimens, from 1.06 to 1.29. It is thus evident that non-uniformity of stress may cause the capacity of certain types of connections to fall considerably below that estim-

ated on the basis of uniform distribution. While for the welded T-type the deficiency may be as much as 50%, nevertheless, for a carefully designed gusset plate type the desired factor of safety may be readily obtained (see Table V).

Acknowledgments

The late Professor Peter Gillespie had given some thought to the problem of continuity of restraint of ordinary steel beams carrying gravity loads and, in a preliminary way, had outlined certain experimental and theoretical work. The present authors, in continuing the investigation, extended its scope and, in addition, included a study of a series of heavy wind connections. Acknowledgment is here made (in alphabetical order) of the able and conscientious services of P. A. Ballachey, H. St. Paul Butler, A. H. Corbett, W. B. Dunbar, C. E. Helwig, G. V. Helwig, E. A. Phillips and E. A. Sudden.

Reference

1. YOUNG, C. R. and DUNBAR, W. B. Permissible stresses on rivets in tension. Bull. No. 8. Section No. 16. School of Engineering Research, University of Toronto. 1928.

ON THE ACOUSTIC RADIATION FIELD OF THE PIEZO-ELECTRIC OSCILLATOR AND THE EFFECT OF VISCOSITY ON TRANSMISSION[1]

By Louis V. King[2]

Abstract

The radiation field due to a circular disc oscillating with uniform amplitude in a closely fitting circular aperture surrounded by an infinite rigid flange has been studied in detail, the velocity potential being expressed as an infinite integral involving cylindrical co-ordinates. The procedure adopted may be used to study the effect of viscosity on the characteristics of the radiation field. While having little effect on the field in the neighborhood of an oscillator generating waves in water, the viscosity has a marked effect on the range of distant transmission, which in consequence is appreciably affected by temperature. Of considerable practical importance is the existence of an optimum wave-length for constant output and a given distance of transmission. By means of a simple chart, it is possible to determine the optimum wave-length for a given transmitter when the level of reception for a given range is stated.

Section 1. Introduction

The piezo-electric oscillator originally due to Langevin (9) for the production of beams of sound at supersonic frequencies in water or air is now well known, and is described in easily accessible textbooks and numerous scientific papers (17, p. 147). A few features of the radiation field are well known, having been worked out in terms of polar co-ordinates by Lord Rayleigh (12, v. II, §302, p. 162).

In view of the interesting experiments by R. W. Boyle and his coworkers (5), on the exploration of the radiation field in the immediate neighborhood of the oscillating disc, the writer has developed the complete theory in terms of cylindrical wave-functions when the disc is surrounded by an infinite flange. This procedure enables the velocity potential at any point to be exactly expressed as a definite integral involving Bessel functions, so that pressure variations may be computed close to the oscillating disc as well as at a great distance. The analysis also makes it possible to take into account the viscosity of the medium and to estimate its influence on the transmission.

Section 2. Determination of the Velocity Potential in Cylindrical Co-ordinates

We consider a rigid circular disc of radius a caused to oscillate in a closely fitting circular aperture in a fixed rigid wall of infinite extent, constituting a "piston diaphragm" with an infinite flange, actuated by a suitably arranged piezo-electric (or other) mechanism.

For periodic motion of the diaphragm with frequency $f=\omega/2\pi$ we have to solve for the velocity potential ϕ from the wave equation

$$\nabla^2\phi + \kappa^2\phi = 0 \ , \tag{1}$$

where $\kappa=\omega/c$, and c is the velocity of sound in the medium.

[1] *Manuscript received May 29, 1934.*
Contribution from the Department of Physics, McGill University, Montreal, Quebec, Canada.

[2] *Macdonald Professor of Physics, McGill University.*

In terms of cylindrical co-ordinates (z, ρ) referred to the centre of the diaphragm as origin and the axis of z directed into the medium, it is easily seen that a solution of Equation (1) (2, §27, p. 73)* representing divergent waves is given by

$$\phi = \int_0^\infty e^{-\mu z} J_0(\lambda\rho) f(\lambda) \frac{\lambda}{\mu} d\lambda \ , \tag{2}$$

where $\mu = (\lambda^2 - \kappa^2)^{\frac{1}{2}}$, and $f(\lambda)$ is a function of the parameter λ to be determined by the boundary conditions over the plane $z=0$. If $\dot{x}$ is the velocity of the disc at any instant, we evidently have

$$-\left(\frac{\partial\phi}{\partial z}\right)_{z=0} = \int_0^\infty \lambda J_0(\lambda\rho) f(\lambda) d\lambda = \begin{cases} \dot{x} & (0 \leq \rho < a) \ . \\ 0 & (a < \rho < \infty) \ . \end{cases} \tag{3}$$

The solution of Equation (3) as an integral equation is at once furnished by Hankel's inversion theorem (7, 15, 16) which gives, if the velocity $\dot{x}$ is everywhere constant over the disc,

$$f(\lambda) = \dot{x} \int_0^a \rho J_0(\lambda\rho) d\rho = \frac{\dot{x}a}{\lambda} J_1(\lambda a) \ . \tag{4}$$

We now have by substitution in Equation (2) the exact and compact expression for the velocity potential

$$\phi = a\dot{x} \int_0^\infty e^{-\mu z} J_0(\lambda\rho) J_1(\lambda a) \frac{d\lambda}{\mu} \ , \tag{5}$$

valid at all points of the field.

Section 3. Calculation of Acoustic Impedance of Diaphragm

The wave not being plane, the pressure variation, or harmonic excess pressure, at any point on the diaphragm is given by

$$\delta p_0 = \rho_0 (\dot{\phi})_{z=0} = \rho_0 a \ddot{x} \int_0^\infty J_0(\lambda\rho) J_1(\lambda a) \frac{d\lambda}{\mu} \ ,$$

where ρ_0 is the density of the medium. It will be noticed that δp_0 is not constant, as would be the case for an infinite diaphragm transmitting plane waves, but is a function of ρ.

Integrating over the area of the disc, we easily find for the total pressure P_0

$$P_0 = \int_0^a \delta p_0 2\pi\rho d\rho = 2\pi\rho_0 a^2 \ddot{x} \int_0^\infty \frac{J_1^2(\lambda a) d\lambda}{\mu\lambda} \ . \tag{6}$$

It is at once evident that the integral of Equation (6) consists of a real and imaginary part. We write

$$M_1 - iM_2 = \int_0^\infty \frac{J_1^2(\lambda a)}{(\lambda^2 - \kappa^2)^{\frac{1}{2}}} \frac{d\lambda}{\lambda} = \int_\kappa^\infty \frac{J_1^2(\lambda a)}{(\lambda^2 - \kappa^2)^{\frac{1}{2}}} \frac{d\lambda}{\lambda} - i \int_0^\kappa \frac{J_1^2(\lambda a)}{(\kappa^2 - \lambda^2)^{\frac{1}{2}}} \frac{d\lambda}{\lambda} \ . \tag{7}$$

* *This type of cylindrical wave-function does not appear to have been used hitherto in acoustic problems, although such solutions of the wave equation are well known in electromagnetic theory, especially in connection with antenna radiation fields.*

The first integral is at once expressible in terms of Struve's function $H_1(2\kappa a)$ by writing $z=\kappa a$ and $u=\lambda a$ in the known integral (16; §13. 47(9); 7, p. 210),

$$M_1 = \int_z^\infty \frac{J_1^2(u)}{(u^2-z^2)^{\frac{1}{2}}} \frac{du}{u} = \frac{1}{2z^2} H_1(2z) \ . \tag{8}$$

This gives

$$M_1 = \int_\kappa^\infty \frac{J_1^2(\lambda a)}{(\lambda^2-\kappa^2)^{\frac{1}{2}}} \frac{d\lambda}{\lambda} = \frac{1}{2\kappa^2 a} H_1(2\kappa a) \ . \tag{9}$$

To calculate the second integral in Equation (7), write $\lambda=\kappa \sin\theta$. Then, writing $z=\kappa a$,

$$M_2 = \int_o^\kappa \frac{J_1^2(\lambda a)}{(\kappa^2-\lambda^2)^{\frac{1}{2}}} \frac{d\lambda}{\lambda} = \frac{1}{\kappa} \int_o^{\frac{1}{2}\pi} \frac{J_1^2(z\sin\theta)}{\sin\theta} \, d\theta \ . \tag{10}$$

Obviously

$$\frac{d}{dz}(\kappa M_2) = 2\int_o^{\frac{1}{2}\pi} J_1(z\sin\theta) \ . \ J'_1(z\sin\theta)d\theta = \int_o^{\frac{1}{2}\pi} J_1(z\sin\theta)\left(J_o(z\sin\theta)-J_2(z\sin\theta)\right)d\theta \ .$$

If we write $\zeta=2z\cos\phi$, we may express the products J_1J_o and J_1J_2 in the form (16: §5. 43(1) and (2)),

$$\left.\begin{aligned} J_1(z\sin\theta) \ . \ J_o(z\sin\theta) &= \frac{2}{\pi}\int_o^{\frac{1}{2}\pi} \cos\phi J_1(\zeta\sin\theta)d\phi \\ J_1(z\sin\theta) \ . \ J_2(z\sin\theta) &= -\frac{2}{\pi}\int_o^{\frac{1}{2}\pi} \cos 3\phi J_1(\zeta\sin\theta)d\phi \ . \end{aligned}\right\} \tag{11}$$

Interchanging the order of integration,

$$\frac{d}{dz}(\kappa M_2) = \frac{4}{\pi}\int_o^{\frac{1}{2}\pi} \cos\phi\cos 2\phi d\phi \int_o^{\frac{1}{2}\pi} J_1(\zeta\sin\theta)d\theta \ .$$

Since (16: §12. 11(2); §10. 42(3) and 7, p. 39),

$$\int_o^{\frac{1}{2}\pi} J_1(\zeta\sin\theta)d\theta = \left(\frac{\pi}{2\zeta}\right)^{\frac{1}{2}} H_{\frac{1}{2}}(\zeta) = \frac{1-\cos\zeta}{\zeta} \ , \tag{12}$$

we have

$$\frac{d}{dz}(\kappa M_2) = \frac{2}{\pi z}\int_o^{\frac{1}{2}\pi} \cos 2\phi\Big(1-\cos(2z\cos\phi)\Big)d\phi \ .$$

The first integral vanishes, while the second is

$$-J_2(2z) = \frac{2}{\pi}\int_o^{\frac{1}{2}\pi} \cos 2\phi \ \cos(2z\cos\phi)d\phi \ .$$

Thus

$$\frac{d}{dz}(\kappa M_2) = \frac{1}{z} J_2(2z) \ ,$$

which gives on integration

$$\kappa M_2 = \tfrac{1}{2}\left(1-\frac{J_1(2z)}{z}\right) \ ,$$

the constant of integration being chosen to make κM_2 vanish with z as it should according to Equations (9) and (10). We then have from Equations (7), (9) and (10)

$$M_1 - iM_2 = \int_0^\infty \frac{J_1^2(\lambda a)}{\mu} \frac{d\lambda}{\lambda} = \frac{H_1(2\kappa a)}{2\kappa^2 a} - \frac{i}{\kappa}\left(1 - \frac{J_1(2\kappa a)}{\kappa a}\right) . \tag{13}$$

If m_o is the mass of the diaphragm and μ_o is the natural restoring force, the equation of motion is

$$m_o\ddot{x} + \mu_o x = F - P_o ,$$

where F is the total pressure exerted by the piezo-electric drive.

Since $\ddot{x} = -\omega^2 x$ and $\dot{x} = i\omega x$, we have, introducing the value of P_o from Equations (6) and (13),

$$\ddot{x}\left(m_o + \frac{\pi\rho_o a}{\kappa^2} H_1(2\kappa a)\right) + \dot{x}\left(1 - \frac{J_1(2\kappa a)}{\kappa a}\right)\pi\rho_o a^2 c + \mu_o x = F , \tag{14}$$

as the equation of motion, in agreement with that deduced by Lord Rayleigh (12, v. 2, p. 169, Eq. 29). If we denote by m_a the *acoustic mass* and by k_a the *acoustic damping* or radiation constant, the equation of motion of the diaphragm is, in general, of the form

$$(m_o + m_a)\ddot{x} + k_a\dot{x} + \mu_o x = F , \tag{15}$$

and, in the present instance, we have for a piston diaphragm,

$$m_a = \frac{\pi\rho_o a}{\kappa^2} H_1(2\kappa a) \qquad \text{and} \qquad k_a = \pi\rho_o a^2 c\left(1 - \frac{J_1(2\kappa a)}{\kappa a}\right) . \tag{16}$$

In particular, we derive m_a and k_a for diaphragms of linear dimensions small and large compared to the wave-length λ :

Small diaphragms ($\kappa a = 2\pi a/\lambda \ll 1$).

From well known formulas (16: §10.4) we find,

$$H_1(2\kappa a) \sim \frac{2}{3}\frac{(2\kappa a)^2}{\pi} + \ldots , \qquad 1 - J_1(2\kappa a)/\kappa a \sim \tfrac{1}{2}\kappa^2 a^2 + \ldots .$$

so that

$$m_a \sim \tfrac{8}{3}\rho_o a^3 \qquad \text{and} \qquad k_a \sim \tfrac{1}{2}\rho_o \pi a^4 \omega^2/c . \tag{17}$$

Large diaphragms ($\kappa a = 2\pi a/\lambda \gg 1$).

For large values of $2\kappa a$ we make use of the asymptotic expansion (16; § 10.4),

$$H_1(2\kappa a) \sim 2/\pi + \ldots + Y_1(2\kappa a) ,$$

so that, neglecting terms of order $(2\kappa a)^{-\frac{1}{2}}$ and smaller, we have, approximately

$$\left.\begin{aligned} m_a &\sim 2a\rho_o/\kappa^2 = a\rho_o\lambda^2/(2\pi^2) . \\ k_a &\sim \pi a^2\rho_o c . \end{aligned}\right\} \tag{18}$$

Section 4. Calculation of Radiation Output

It follows from Equations (6) and (7) that we may write the total pressure P_o on the diaphragm in the form

$$P_o = 2\pi a^2\rho_o\ddot{x}(M_1 - iM_2) . \tag{19}$$

In terms of the velocity amplitude $|\dot{x}|$ of the diaphragm, we have

$$\dot{x} = |\dot{x}|e^{i\omega t} \qquad \text{and} \qquad \ddot{x} = i\omega|\dot{x}|e^{i\omega t} .$$

At any instant the rate at which the diaphragm is doing work by compressing the medium is, expressing both P_o and $\dot{x}$ as real quantities,

$$dW/dt = P_o\dot{x} = 2\pi a^2\rho_o\omega|\dot{x}|^2(M_1 \sin \omega t + M_2 \cos \omega t) \cos \omega t .$$

On taking the time average, we have for the rate of output of radiation

$$[dW/dt] = \pi a^2\rho_o\omega|\dot{x}|^2M_2 = \tfrac{1}{2}k_a|\dot{x}|^2 = \tfrac{1}{2}\pi a^2\rho_o c\,[1 - J_1(2\kappa a)/\kappa a] , \tag{20}$$

where k_a is the acoustic radiation constant defined by Equation (15).

Numerical Example.

To obtain a numerical estimate of the physical quantities involved in a piezo-electric oscillator in this and following sections, we consider a disc of radius $a = 30$ cm. to be radiating 50 watts on a wave-length of $\lambda = 3.77$ cm. in sea water of density $\rho_o = 1.025$, the velocity of sound being taken as $c = 1.490 \times 10^5$ cm. per sec., so that $\rho_o c = 1.53 \times 10^5$.

The area of the disc is $\pi a^2 = 2826$ cm^2., so that the sound is propagated at the rate of 0.0177 watts per cm^2.

Corresponding to the wave-length $\lambda = 3.77$ cm., we have the frequency $f = 4 \times 10^4$ and $\omega = 2\pi f = 2.50 \times 10^5$, while $\kappa a = 2\pi a/\lambda = 50$.

In these circumstances it is sufficiently accurate to employ the approximation from Equation (20),

$$[dW/dt] \sim \tfrac{1}{2}\pi a^2\rho_o c|\dot{x}|^2 = 50 \times 10^7 \text{ ergs/sec} . \tag{21}$$

Inserting numerical values we find for the velocity amplitude, $|\dot{x}| = 1.53$ cm./sec., while the corresponding displacement amplitude is 612×10^{-8} cm. $= 612$ Angstrom units, about one tenth the wave-length of sodium light, or roughly, 300 times the diameter of a hydrogen molecule.

Section 5. Discussion of the Radiation Field, General Theorems

The expression for the velocity potential deduced in Equation (5) of Section 2,

$$\phi = a\dot{x}\int_0^\infty e^{-\mu z}J_o(\lambda\rho)J_1(\lambda a)\frac{d\lambda}{\mu} \tag{22}$$

is, as far as the writer is aware, new. It is easily seen that we may write this in the form $\phi = a\dot{x}(P - iQ)$, where

$$\left.\begin{aligned} P &= \int_0^\infty J_o(\kappa\rho \cosh \phi) \cdot J_1(\kappa a \cosh \phi) \cdot e^{-\kappa z \sinh \phi}\, d\phi \\ Q &= \int_0^{\frac{1}{2}\pi} J_o(\kappa\rho \sin \theta) \cdot J_1(\kappa a \sin \theta) \cdot e^{-\kappa z \cos \theta}\, d\theta . \end{aligned}\right\} \tag{23}$$

The pressure amplitude is obviously given by,

$$|\delta p| = \rho_o|\dot{\phi}| = a\rho_o\kappa c|\dot{x}|\{P^2 + Q^2\}^{\frac{1}{2}} \tag{24}$$

Mapping of the radiation field is best carried out in cylindrical co-ordinates in terms of the integrals P and Q computed by graphical methods, or preferably by means of a mechanical integrator.

In general, the expression of integrals of the type of Equation (22) in terms of known functions of the polar co-ordinates (r, θ) is not a simple matter. It is, however, possible to obtain an asymptotic expression for the radiation field at distances great compared to the wave-length and linear dimensions of the wave source, corresponding to a velocity potential of the form

$$\phi = \int_0^\infty e^{-\mu z} J_0(\lambda\rho) f(\lambda) \frac{\lambda d\lambda}{\mu} . \tag{25}$$

We will suppose that $f(\lambda)$ is capable of expansion as a convergent power series in μ^2, *i.e.*,.

$$f(\lambda) = a_0 + a_2\mu^2 + a_4\mu^4 + \ldots + a_{2n}\mu^{2n} + \ldots = \sum_0^\infty a_{2n}\mu^{2n} .$$

Since

$$(d/dz)^{2n} e^{-\mu z} = \mu^{2n} e^{-\mu z} ,$$

we at once see that

$$\int_0^\infty e^{-\mu z} J_0(\lambda\rho) f(\lambda) \frac{\lambda d\lambda}{\mu} = \sum_{n=0}^\infty a_{2n} \left(\frac{\partial}{\partial z}\right)^{2n} \int_0^\infty e^{-\mu z} J_0(\lambda\rho) \frac{\lambda d\lambda}{\mu} = \sum_{n=0}^\infty a_{2n} \left(\frac{\partial}{\partial z}\right)^{2n} \frac{e^{-ikr}}{r} ,$$

where we have made use of the well known integral (16: §13.47 (4)),

$$\int_0^\infty e^{-\mu z} J_0(\lambda\rho) \frac{\lambda}{\mu} d\lambda = \frac{e^{-ikr}}{r} , \quad r^2 = (\rho^2 + z^2) \tag{26}$$

which, with the time factor $e^{i\omega t}$ represents a diverging wave.

Since

$$\partial/\partial z = \cos\theta \partial/\partial r - (\sin\theta/r)\partial/\partial\theta ,$$

we have the symbolic representation of the integral in the form

$$\int_0^\infty e^{-\mu z} J_0(\lambda\rho) f(\lambda) \frac{\lambda d\lambda}{\mu} = f\left(\kappa^2 + \cos^2\theta \left(\frac{\partial}{\partial r}\right)^2\right)^{\frac{1}{2}} \cdot \frac{e^{-ikr}}{r} . \tag{27}$$

Since

$$F\left(\frac{\partial}{\partial r}\right) \cdot \frac{e^{-ikr}}{r} = e^{-ikr} F\left(\frac{\partial}{\partial r} - i\kappa\right) \frac{1}{r} ,$$

we may write the right-hand side of Equation (27) in the expanded form

$$\int_0^\infty e^{-\mu z} J_0(\lambda\rho) f(\lambda) \frac{\lambda d\lambda}{\mu} = e^{-ikr} \left[\sum_n a_{2n} \left(\frac{\partial}{\partial r} - i\kappa\right)^{2n} \cos^{2n}\theta\right] \frac{1}{r} = \frac{e^{-ikr}}{r} \sum_n \frac{A_{2n}(\cos\theta)}{r^{2n}} , \tag{28}$$

where $A_{2n}(\cos\theta)$ are polynominals in $\cos^2\theta$.

We easily find

$$A_0 = \sum_n (-1)^n a_{2n} (\kappa \cos\theta)^{2n} = f(\kappa^2 - \kappa^2 \cos^2\theta) = f(\kappa \sin\theta) .$$

We thus have for the asymptotic expansion of the radiation field,

$$\phi = \int_0^\infty e^{-\mu z} J_0(\lambda\rho) f(\lambda) \frac{\lambda}{\mu} d\lambda \sim \frac{e^{-ikr}}{r} f(\kappa \sin\theta) . \tag{29}$$

This theorem is apparently new and is especially useful as it enables us to calculate the rate of radiation of energy in any particular direction. In general $f(\lambda)$ will be complex, so that writing $f(\kappa \sin\theta) = f_1(\theta) + if_2(\theta)$, we have taking the real part of Equation (29),

$$\phi \sim f_1(\theta)\frac{\cos(\omega t - \kappa r)}{r} - f_2(\theta)\frac{\sin(\omega t - \kappa r)}{r} ,$$

from which it follows, on taking a time average, that for unit spherical area in direction θ, the rate of radiation of energy, or the radiation intensity, $I(\theta)$, is

$$I(\theta) = \left[\frac{dw}{dt}\right]_\theta \sim \tfrac{1}{2}\frac{\kappa^2 c\rho_o}{r^2}\left[f_1^2(\theta) + f_2^2(\theta)\right] , \tag{30}$$

and therefore the rate of radiation in a cone of semi-vertical angle θ is,

$$\left[\frac{dW}{dt}\right]_o^\theta \sim \pi\kappa^2 c\rho_o \int_o^\theta \left[f_1^2(\theta) + f_2^2(\theta)\right]\sin\theta d\theta . \tag{31}$$

Section 6. Applications to Supersonic Oscillator

If we now apply the theorems of the last section to the integral expression of Equation (22) for the velocity potential of a supersonic oscillator, we at once obtain for the intensity in a direction θ the well known expression

$$I(\theta) \sim \tfrac{1}{2} c\rho_o |\dot{x}|^2 \frac{a^2}{r^2}\frac{J_1^2(\kappa a \sin\theta)}{\sin^2\theta} , \tag{32}$$

while, according to Equation (31),

$$\left[\frac{dW}{dt}\right]_o^\theta \sim \pi c\rho_o a^2 |\dot{x}|^2 \int_o^\theta \frac{J_1^2(\kappa a \sin\theta)}{\sin\theta}\, d\theta . \tag{33}$$

We notice that if we write $\theta = \frac{1}{2}\pi$ in Equation (33) we obtain the same result as that given in Equation (20) for the radiation output computed at the diaphragm.

We notice from Equation (32) that the polar curve for intensity shows a series of loops bounded by cones in which the intensity vanishes to the order a^2/r^2. These angles are given by $\kappa a \sin\theta_s = j_{1s}$, where j_{1s} is the s'th root of $J_1(x) = 0$.

The maxima are given by $\kappa a \sin\theta_s = j_{2s}$ where j_{2s} is the s'th root of $J_2(x) = 0$.

Applying these results to the numerical example of Section 4 for which $\kappa a = 50$, we find for the directions of minimum and maximum intensities:

θ_{min}		4°.9	8°.1	11°.7	etc.
θ_{max}	0°	5°.9	9°.7	12°.8	etc.

while

$I(\theta_{max})/I(o) = 1$	.0175	.00416	.00160	etc.

Of considerable interest is a numerical estimate of the relative proportion of energy radiated in the first loop. The integral of Equation (33) as it stands

is not easily exactly evaluated in finite terms. When θ is small, we notice that with an error of less than 1% for an angle of 4°.9 in the numerical example quoted,

$$\int_o^{\theta_1} \frac{J_1^2(\kappa a \sin\theta)}{\sin\theta}\, d\theta > \int_o^{\theta_1} \frac{J_1^2(\kappa a \sin\theta)}{\sin\theta} \cos\theta\, d\theta = \tfrac{1}{2}\,[1 - J_o^2(\kappa a \sin\theta_1) - J_1^2(\kappa a \sin\theta_1)] \ .$$

Since $J_1(\kappa a \sin\theta_1) = 0$ at the first maximum, we have for the proportion of power radiated in the first loop to the total the ratio,

$$\frac{[dW/dt]_o^{\theta_1}}{[dW/dt]_o^{\frac{1}{2}\pi}} > \frac{1 - J_o^2(\kappa a \sin\theta_1)}{1 - J_1(2\pi a)/(\kappa a)} \ . \tag{34}$$

This result shows that more than 84% of the radiant energy is contained in the primary beam for which $\theta_1 = 4°.9$.

Section 7. Distribution of Intensity on the Axis

If we write $\rho = 0$ in Equation (22), we obtain for the velocity potential on the axis the well known formula

$$\phi = a\dot{x} \int_o^{\infty} e^{-\mu z} J_1(\lambda a) \frac{d\lambda}{\mu} = \frac{\dot{x}}{i\kappa} \left[e^{-i\kappa z} - e^{-i\kappa(a^2+z^2)^{\frac{1}{2}}} \right] \ . \tag{35}$$

The integration is effected by multiplying each side of Equation (26) by ρ and integrating from 0 to a.

From Equation (35) we at once obtain for the pressure amplitude, writing $R^2 = a^2 + z^2$,

$$|\delta p|^2 = 4(c\rho_o)^2 |\dot{x}|^2 \sin^2 \tfrac{1}{2}\kappa(R - z) \ . \tag{36}$$

If, as usual, we define intensity as rate of transmission of energy across unit area we have for points on the axis

$$I(0) = (c\rho_o)^2 |\dot{x}|^2 [1 + z/R] \sin^2 \tfrac{1}{2}\kappa(R - z) \ . \tag{37}$$

The velocity-amplitude is given by

$$|Q|^2 = \left[\frac{\partial\phi}{\partial z}\right]^2 = |\dot{x}|^2 \left[\left(1 - \frac{z}{R}\right)^2 + \frac{4z}{R} \sin^2 \tfrac{1}{2}\kappa(R - z) \right] \ . \tag{38}$$

The experimental interpretation of a quasi-stationary field, such as that of a piezo-electric oscillator, is seen from the last three formulas to depend on the type of apparatus employed for measuring and detecting pressure and velocity variations in the medium. An optical method which responds to changes of refractive index arising from changes of density will give fluctuations of the measured quantity according to Equation (36). A small listening probe which absorbs all the energy incident on it will give rise to fluctuations represented by Equation (37), while a small Rayleigh disc will respond to Equation (38). In these three cases the position and amplitudes of the maxima and minima will be different.

These peculiar features of a quasi-stationary field, as contrasted with the plane progressive or stationary fields, indicate the precautions to be observed in interpreting such experiments as those of Boyle and his coworkers (6). The experimental results referred to are not strictly comparable with the

theoretical calculations of this paper owing to the absence of the infinite flange which makes a rigorous mathematical solution possible. Furthermore a practical disc shows variations of amplitude not contemplated by theory. The acoustic radiation pressure on a circular disc even of circumference small compared with the wave-length may be calculated, and it is found, again, that the variation of the readings is again different from any of the formulas quoted. Only when z/a is very large or very small, so that the waves are practically plane, are the results of observation by different methods easily comparable.

We notice that Equations (36) and (37) agree in giving rise to a finite number of points of zero pressure amplitude or intensity. These are given by the roots of $\sin \frac{1}{2}\kappa(R-z)=0$, *i.e.*, for $\frac{1}{2}\kappa(R-z)=s\pi$, where s takes integral values.

In terms of the wave-length, the position of these silent spots is given by

$$2z = \frac{a^2}{s\lambda} - s\lambda \ .$$

Since z must be positive, it is readily seen that the number of silent spots possible is equal to the number of integers less than a/λ.

In the numerical example already quoted for which $a=30$ cm. and $\lambda=3.77$ cm. ($\kappa a=50$), there are seven silent spots situated at the following distances from the plate: 3.9, 6.7, 14.5, 24.4, 35.3, 56.2 and 118 cm.

A theoretical investigation by the author (not yet published) shows that only with pressure discs of circumference very small compared to the wave-length can these silent spots be observed by this method. The writer is informed by Dr. Boyle, however, that by means of a "listener" of diameter of the same order as a wave-length the "silent spots" (or probably marked minima of intensity) can be detected (6: pp. 183-187).

Section 8. Calculation of Velocity Potential and Pressure over the Diaphragm

At the centre of the diaphragm we have, writing $z=0$ in Equation (35)

$$\phi_o = \dot{x}a \int_o^\infty J_1(\lambda a)\,\frac{d\lambda}{\mu} = \frac{\dot{x}}{i\kappa}(1-e^{-i\kappa a}) \ , \tag{39}$$

in agreement with the result obtained by N. W. McLachlan (11). From this we obtain for the pressure amplitude at the centre, due to the reaction of the medium,

$$|\delta p_o| = 2c\rho_o|\dot{x}| \sin \tfrac{1}{2}\kappa a \ . \tag{40}$$

Considering the numerical example of Section 4, we have

$$c\rho_o = 1.53 \times 10^6 \qquad \text{and} \qquad |\dot{x}| = 1.53 \text{ cm./sec.}$$

giving

$$|\delta p_o| = 0.47 \times 10^6 \sin \tfrac{1}{2}\kappa a \text{ dynes/cm}^2,$$

indicating that for an average emission of 0.0177 watts per cm². from a disc of 30 cm. radius the pressure amplitude may amount to nearly half an atmosphere.

At the edge of the diaphragm $\rho = a$, so that

$$\phi_0 = \dot{x}a\int_0^\infty J_0(\lambda a)J_1(\lambda a)\frac{d\lambda}{\mu} = \frac{\dot{x}}{2i\kappa}\left[\left(1-J_0(2\kappa a)\right) + iH_0(2\kappa a)\right] \quad , \tag{41}$$

also in agreement with the result obtained by McLachlan (11). The integral is easily obtained by noticing that

$$J_0(\lambda a)J_1(\lambda a) = \frac{2}{\pi}\int_0^{\frac{1}{2}\pi} J_1(2\lambda a\cos\theta)\cos\theta d\theta \quad , \tag{42}$$

and then utilizing Equation (39) with a replaced by $2a\cos\theta$.

The pressure amplitude at the edge is seen to be

$$|\delta p_0| = \tfrac{1}{2}\rho_0 c|x|\left[\left(1-J_0(2\kappa a)\right)^2 + H_0^2(2\kappa a)\right]^{\frac{1}{2}}.$$

In the numerical example just cited with $\kappa a = 50$, we have as a rough approximation $|\delta p_0| \backsim \frac{1}{2}\rho_0 c|\dot{x}|$, amounting to one-quarter of the maximum possible pressure at the centre of the diaphragm.

Of considerable interest is the variation of pressure over the diaphragm. The calculation is, however, a matter of some difficulty. We note that

$$J_1(\lambda\rho)J_1(\lambda a) = \frac{1}{\pi}\int_0^\pi \cos\theta\, J_0(\lambda R)d\theta \quad , \tag{43}$$

where

$$R^2 = a^2 + \rho^2 - 2a\rho\cos\theta \quad . \tag{44}$$

Utilizing the well known integral of Equation (26), we have

$$\int_0^\infty \frac{\lambda}{\mu} J_1(\lambda\rho)J_1(\lambda a)d\lambda = \frac{1}{\pi}\int_0^\pi \frac{e^{-i\kappa R}}{R}\cos\theta\, d\theta \quad . \tag{45}$$

In terms of the spherical wave-functions $\psi_n(x)$ and $f_n(x)$ defined in terms of Bessel functions by the relations (8, p. 504),

$$\left.\begin{aligned} x^n\psi_n(x) &= (\tfrac{1}{2}\pi/x)^{\frac{1}{2}} J_{n+\frac{1}{2}}(x) & x^n\phi_n(x) &= (-1)^n(\tfrac{1}{2}\pi/x)^{\frac{1}{2}} J_{-n-\frac{1}{2}}(x) \\ x^n f_n(x) &= -i(\tfrac{1}{2}\pi/x)^{\frac{1}{2}} H^{(2)}_{n+\frac{1}{2}}(x) & f_n(x) &= \phi_n(x) - i\psi_n(x) \end{aligned}\right\} \tag{46}$$

we have the well known expansion, valid for $0<\rho<a$ (8, p. 512),

$$\frac{e^{-i\kappa R}}{R} = \sum_{s=0}^\infty (2s+1)(\kappa a)^s f_s(\kappa a)(\kappa\rho)^s\psi_s(\kappa\rho)P_s(\cos\theta) \quad . \tag{47}$$

Denoting

$$A_s = \frac{1}{\pi}\int_0^\pi \cos\theta\, P_s(\cos\theta)d\theta = \frac{1}{\pi}\int_{-1}^{+1} \cot\theta\, P_s(\cos\theta)d(\cos\theta) \quad , \tag{48}$$

we easily deduce from the known expansion of $\cot\theta$ in spherical harmonics,

$$A_{2s} = 0 \text{ and } A_{2s+1} = \frac{2s+2}{2s+1}\left[\frac{1}{2}\cdot\frac{3}{4}\cdot\ \ldots\ \cdot\frac{2s+1}{2s+2}\right]^2 \tag{49}$$

If now we integrate both sides of Equation (45) with respect to ρ from 0 to a, we finally obtain after a few reductions,

$$\phi_{s-o} = \phi_0 - \frac{a\dot{x}}{\kappa}\sum_{s=0}^\infty (4s+3)A_{2s+1}(\kappa a)^{2s+1} f_{2s+1}(\kappa a)\int_0^{\kappa\rho} \zeta^{2s+1}\psi_{2s+1}(\zeta)d\zeta \quad , \qquad (\rho<a) \quad , \tag{50}$$

where ϕ_o is the potential at the centre given by Equation (39). We have for $s=o$,

$$\int_o^{\kappa\rho} \zeta\psi_o(\zeta)d\zeta = 1 - \psi_o(\kappa\rho) = 1 - \frac{\sin\kappa\rho}{\kappa\rho} \cdot \tag{51}$$

Denoting

$$I_n = \int \zeta^n\psi_n(\zeta)d\zeta \ , \tag{52}$$

it is a simple matter to derive the recurrence formula, useful in numerical computations,

$$(n+1)I_{n+1} = nI_{n-1} - (2n+1)\zeta^n\psi_n(\zeta) \ , \tag{53}$$

which is also valid when $\psi_n(\zeta)$ is replaced by $f_n(\zeta)$ or $\phi_n(\zeta)$ in Equations (52) and (53).

From Equation (50) we may easily obtain the pressure amplitude by resolving the series into real and imaginary parts.

When $a<\rho<\infty$, the appropriate expansion, Equation (47), is obtained by interchanging a and ρ. In this case we integrate both sides of Equation (45) between a and ∞, and finally obtain

$$\phi_{s=o} = -\frac{a\dot{x}}{\kappa}\sum_{s=o}^{\infty}(4s+3)A_{2s+1}(\kappa a)^{2s+1}\psi_{2s+1}(\kappa a)\int_{\infty}^{\kappa\rho}\zeta^{2s+1}f_{2s+1}(\zeta)d\zeta, \quad (\rho>a) \ . \tag{54}$$

For $s=o$, we have

$$\int_{\infty}^{\kappa\rho}\zeta f_1(\zeta)d\zeta = -f_o(\kappa\rho) = -e^{-ik\rho}/\rho \ , \tag{55}$$

while the integrals may, in general, be computed by a recurrence formula of the type of Equation (53).

It does not appear possible to express the velocity potential ϕ for any point of the radiation field in terms of spherical wave-functions, although an attempt to do so has recently been made by Backhaus (1) and Ruedy (13), based on the assumption that for $r>a$ an expansion of the type

$$\phi_o = \sum A_s(\kappa r)^s f_s(\kappa r)P_s(\cos\theta) \tag{56}$$

is valid as representing divergent waves. It is possible to determine the coefficients A_s to make the value of ϕ on the axis, for which $\theta=0$, agree with the known value, Equation (35). The writer has verified by a simple independent calculation the values of the coefficients A_s obtained by Backhaus (1). Since the velocity potential is everywhere finite within the hemisphere $r=a$, we may similarly represent the velocity potential within this radius by

$$\phi_i = \sum B_s(\kappa r)^s\psi_s(\kappa r)P_s(\cos\theta) \ . \tag{57}$$

The writer's method is equally adapted to the determination of the coefficients B_s to give the required value, Equation (35), on the axis. It is found, however, that at $r=a$ the values of ϕ_o and ϕ_i do not agree for a given value of θ. There is similarly a discontinuity in the values of $\partial\phi_o/\partial r$ and $\partial\phi_i/\partial r$ at $r=a$, while the values of ϕ_i and ϕ_o for $\theta=\frac{1}{2}\pi$ do not agree with the expansions of Equations (50) and (54).

In fact, continuity of pressure and velocity over the sphere $r=a$ would require, if expansions of the type of Equations (56) and (57) were valid,

$$\left.\begin{aligned} A_s f_s(\alpha) &= B_s \psi_s(\alpha) \ , \\ A_s \frac{d}{d\alpha}\left[\alpha^2 f_s(\alpha)\right] &= B_s \frac{d}{d\alpha}\left[\alpha^2 \psi_s(\alpha)\right] \end{aligned}\right\} , \tag{58}$$

where we have written $\alpha = \kappa a$.

Since $f_s'(\alpha) = -\alpha f_{s+1}(\alpha)$ and similarly for $\psi_s'(\alpha)$, we have on differentiating the second and utilizing the first,

$$A_s f_{s+1}(\alpha) = B_s \psi_{s+1}(\alpha) \ . \tag{59}$$

Remembering that

$$f_s(\alpha) = \phi_s(\alpha) - i\psi_s(\alpha) \ ,$$

we would have, on eliminating A_s and B_s ,

$$f_{s+1}(\alpha)\psi_s(\alpha) - f_s(\alpha)\psi_{s+1}(\alpha) = 0$$

or

$$\phi_{s+1}\psi_s - \psi_{s+1}\phi_s = 0 \ , \tag{60}$$

which is clearly impossible, since (8, p. 505),

$$\phi_{s+1}\psi_s - \psi_{s+1}\phi_s = \alpha^{-(2s+3)} \ . \tag{61}$$

We are thus obliged to conclude that the velocity potential due to a rigid circular disc oscillating within an infinite flange cannot rigorously be expressed as a series of the type of Equation (56). When $\alpha = \kappa a$ is large, the discrepancy between Equations (60) and (61) is at most of the order $(\kappa a)^{-3}$, so that Backhaus' (1) formulas, although not rigorous, are not seriously in error, since his computations for comparison with experimental results are carried out for $(\kappa a) = 5, 8, 17$.

Section 9. Distance of Audible Transmission in a Frictionless Medium

On the axis $\theta = 0$, Equations (32) and (34) agree in giving for the intensity, when κa is large,

$$I(0) = \tfrac{1}{8}\rho_0 c\, |\dot{x}|^2\, a^2 \frac{(\kappa a)^2}{r^2} = \frac{1}{4\pi}\frac{(\kappa a)^2}{r^2}\left[\frac{dW}{dt}\right] \ , \tag{62}$$

where $[dW/dt]$ is the total radiation output given by Equation (20).

If we estimate easily audible reception on the axis to be represented by a level of 30 decibels, this corresponds to $I(0) = I_0 \times 10^3$, where I_0 is the "threshold intensity", $I_0 = 10^{-16}$ watt per cm^2. We thus have, to estimate the distance of easily audible reception,

$$\frac{1}{4\pi}\frac{(\kappa a)^2}{r^2}\left[\frac{dW}{dt}\right] = 10^{-13} \text{ watts/cm}^2 \ . \tag{63}$$

If we utilize the numerical data already quoted for a piezo-electric 50-watt oscillator for which $\kappa a = 50$, we find for the distance of easily audible transmission about 3200 km. The range of piezo-electric transmitters which have been built and tested hardly exceeds 20 km. It is evident that under actual conditions of use in the sea, many factors operate to reduce this theoretical estimate. Among these we may mention the generation of elastic waves in

the oscillating disc and surrounding flange, the scattering and diffraction of the sound waves by the free surface of the sea and the inhomogeneities of temperature and density, the effect of turbulence due to surface waves, and finally the effect of viscosity, which we proceed to examine in the next section.

Section 10. On the Effect of Viscosity on the Radiation Field of a Supersonic Oscillator

We denote by μ the coefficient of viscosity and by ν the kinematic coefficient of viscosity given by

$$\nu = \mu/\rho_o \ . \tag{64}$$

It is well known that when viscosity is taken into account, the general equations of periodic sound waves are satisfied by the velocity components

$$u = -\frac{\partial \phi}{\partial x} \qquad v = -\frac{\partial \phi}{\partial y} \qquad w = -\frac{\partial \phi}{\partial z} \ , \tag{65}$$

where ϕ satisfies the modified wave equation (8, §361, p. 654),

$$(\nabla^2 + \kappa^2)\phi = 0 \ , \tag{66}$$

and κ is given by

$$\kappa^2 = \frac{\omega^2}{c^2 + \frac{4}{3} i\nu\omega} \ . \tag{67}$$

In all practical cases relating to supersonic waves in water, $\frac{4}{3}\nu\omega/c^2$ is of the order 10^{-6}, so that denoting $\kappa_o = \omega/c$ we may, with sufficient accuracy write

$$\kappa \sim \kappa_o - i\kappa', \qquad \text{where} \qquad \kappa' = \tfrac{2}{3}\nu\kappa_o^2/c \ . \tag{68}$$

In a perfect fluid, the solution we have obtained exhibits a tangential discontinuity of velocity, or slip, at the boundary of the flange and diaphragm communicating vibrations to the medium. In an actual fluid no such discontinuity can exist. The tangential motion close to the vibrating surface is modified, and may even be reversed in direction. It is well known, however (8, §361, p. 657), that this effect extends only to a stratum whose thickness is of the order

$$\beta^{-1} = (2\nu/\omega)^{\frac{1}{2}} \ . \tag{69}$$

For water, $\beta^{-1} = .055/f^{\frac{1}{2}}$ cm., where f is the frequency. The motion at a distance from the boundary which is a moderate multiple of β^{-1} will be practically irrational, with a velocity potential given by Equation (44).

It is evident that in the supersonic range of frequencies, at a distance of the order β^{-1} from the diaphragm or infinite flange, the motion conforms practically to the same boundary conditions as those obtaining in the ideal problem of the frictionless medium, as long as the diameter of the diaphragm is also very great compared to β^{-1}.

The fundamental solution, Equation (5), of the modified wave-equation (66) is also valid for complex values of κ, and care has been taken to make certain that all formulas derived from it are also valid for a complex κ. It follows that with the restrictions referred to above, we have available the characteristics of the supersonic radiation field as affected by the viscosity of the medium.

Section 11. On the Effect of Viscosity on the Axial Distribution of Intensity

If we write $\kappa=\kappa_o-i\kappa'$ in Equation (35), we easily obtain for the pressure amplitude on the axis

$$|\delta p|^2=\frac{4(\rho_o c)^2|\dot{x}|^2}{|\kappa/\kappa_o|^2}e^{-2\kappa'(R+z)}[\sinh^2\tfrac{1}{2}\kappa'(R-z)+\sin^2\tfrac{1}{2}\kappa_o(R-z)]\ . \tag{70}$$

We now see that theoretically, owing to the effect of viscosity, there are no absolutely silent spots on the axis. It is of some interest, however, to evaluate the minimum pressure amplitude in the practical example already quoted for which $\kappa_o a=50$, $a=30$ cm., $\lambda=3.77$ cm. and $|\dot{x}|=1.53$ cm./sec.

At 20° C. we may take for sea water $\mu_{20}=.0101$, while $\rho_o c=1.53\times 10^5$. We then find from Equation (68),

$$\kappa'=\tfrac{2}{3}\mu\kappa_o^2/(c\rho_o)=1.20\times 10^{-7}\ .$$

It is obvious that with this extremely small value of κ', minima of $|\delta p|^2$ occur very nearly at the same points as the "silent spots" of the ideal theory, *i.e.*, for $\frac{1}{2}\kappa_o(R-z)=s\pi$.

We see from Equation (70) that at these minima the pressure amplitude is, approximately,

$$|\delta p|_{min}\sim 2(\rho_o c)|\dot{x}|s\pi(\kappa'/\kappa_o)\ . \tag{71}$$

The minimum nearest to the diaphragm corresponds to $s=7$, at 3.9 cm. distance.

From Equation (71) we easily obtain $|\delta p|_{min}=0.74$ dynes/cm²., while the ratio

$$|\delta p_{min}|/|\delta p_{max}|\sim s\pi(\kappa'/\kappa_o)=1.6\times 10^{-6}\ .$$

A pressure amplitude of 0.74 dynes/cm². in a plane progressive wave corresponds to an intensity

$$I=\tfrac{1}{2}|\delta p|^2/(\rho_o c)=1.81\times 10^{-6}\ \text{ergs/cm}^2\ .$$

equivalent to 32.5 decibels, while the pressure maxima in the radiation field are easily seen from Equation (70) to be practically unaffected by viscosity and correspond in a plane wave to 148 decibels.

As already mentioned in Section 6, the interpretation of observations of the field characteristics on the axis depends on the type of receiver employed to give a measurable physical effect: notwithstanding this feature, the above calculation indicates that the effect of viscosity is sufficient to give a detectable minimum of pressure amplitude, instead of a zero minimum as required in the ideal problem of a frictionless fluid.

Section 12. On the Effect of Viscosity on the Radiation Output

The procedure of Section 4 is applicable to the problem, since the integrals M_1 and M_2 of Section 3 are valid for complex values of κ. If we confine ourselves to the case $|\kappa a|\gg 1$, we find

$$M_1-iM_2\sim\frac{1}{\pi\kappa^2 a}-\frac{i}{2\kappa}\ .$$

Writing $\kappa=\kappa_o-i\kappa'$, we obtain

$$M_2\sim\frac{1}{2\kappa_o}\left[1-\frac{4}{\pi}\left(\frac{\kappa'}{\kappa_o}\right)^2\right] ,$$

and finally as in Section 4,

$$\left[\frac{dW}{dt}\right]=\tfrac{1}{2}\pi\rho_o a^2 c|\dot{x}|^2\left[1-\frac{4}{\pi}\left(\frac{\kappa'}{\kappa_o}\right)\right] . \tag{72}$$

In most practical cases the ratio κ'/κ_o is so small that the effect of viscosity on the radiation output as calculated for a frictionless medium is negligible.

Section 13. On the Effect of Viscosity on the Distant Radiation Field

Corresponding to a radiation field represented by the velocity potential

$$\phi=\int_o^\infty e^{-\mu z}J_o(\lambda\rho)f(\lambda)\frac{\lambda}{\mu}d\lambda , \tag{73}$$

the asymptotic formula (Equation 29),

$$\phi\sim f(\kappa\sin\theta)e^{-ikr}/r \tag{74}$$

is easily seen to be valid for complex values of $\kappa=\kappa_o-i\kappa'$.

Writing $f(\kappa\sin\theta)=f_1(\theta)+if_2(\theta)$, we find, taking the real part of Equation (74), that

$$\phi\sim f_1(\theta)e^{-\kappa' r}\frac{\cos(\omega t-\kappa_o r)}{r}+f_2(\theta)e^{-\kappa' r}\frac{\sin(\omega t-\kappa_o r)}{r} , \tag{75}$$

from which we easily deduce that the intensity in a direction θ is given by

$$I(\theta)\sim\tfrac{1}{2}\rho_o c\kappa_o^2\frac{e^{-2\kappa' r}}{r^2}\left[f_1^2(\theta)+f_2^2(\theta)\right] . \tag{76}$$

In particular, for the supersonic oscillator with an infinite flange, we have

$$f(\lambda)=a|\dot{x}|\frac{J_1(\lambda a)}{\lambda}\quad\text{and}\quad f'(\lambda)=-|\dot{x}|\frac{a^2}{\lambda}J_2(\lambda a) .$$

Since κ'/κ_o is always extremely small, we have, approximately,

$$f(\kappa\sin\theta)=f_1(\theta)+if_2(\theta)\sim f(\kappa_o\sin\theta)-i\kappa'\sin\theta f'(\kappa_o\sin\theta) ,$$

and hence

$$I(\theta)\sim\tfrac{1}{2}\rho_o c a^2|\dot{x}|^2\frac{e^{-2\kappa' r}}{r^2}\left[\frac{J_1^2(a\kappa_o\sin\theta)}{\sin^2\theta}+(a\kappa')^2J_2^2(a\kappa_o\sin\theta)\right] , \tag{77}$$

a result which expresses the influence of viscosity on the radiation field.

Section 14. Numerical Applications. Effect of Temperature on Range of Transmission

From physical tables (14, p. 163), we find for the specific viscosity of a solution of sodium chloride of density 1.024 the value 1.0107. For pure water at 0° and 20° C. we have $\mu_o=.0179$ and $\mu_{20}=.0100$.

In the absence of direct numerical data on viscosity of sea water, we may take for the coefficients of viscosity at 0° and 20° C., $\mu_o=.0181$ and $\mu_{20}=.0101$.

For the oscillator of 30 cm. radius for which $\kappa a = 50$, we find for κ' given by

$$\kappa' = \tfrac{2}{3}\frac{\nu}{c}\kappa_0^2 = \tfrac{2}{3}\frac{\mu\kappa_0}{\rho_0 c}$$

at temperatures 0° and 20° C. ($\lambda = 3.77$ cm.),

$$\kappa_0' = 2.16 \times 10^{-7} \text{ and } \kappa'_{20} = 1.20 \times 10^{-7} . \tag{78}$$

We now notice that with these numerical values, the effect of viscosity is inappreciable in Equation (72). Furthermore, it is evident from Equation (77) that except for the exponential factor, important in cutting down transmission at extreme distances, the effect of viscosity is negligible on the angular distribution of intensity which, to less than one part in a million, is the same as that in a frictionless medium.

Of great practical importance, however, is the effect of viscosity in reducing the range of transmission. On the axis, utilizing Equation (72), we may with sufficient accuracy write Equation (77) in the form

$$I(0) \sim \frac{e^{-2\kappa' r}}{r^2}\,\frac{(\kappa_0 a)^2}{4\pi}\left[\frac{dW}{dt}\right] . \tag{79}$$

To obtain a numerical estimate of the effect of viscosity, and hence of temperature, on transmission, we assume a reception level of 30 decibels, so that $I(0) = 10^{-13}$ watts per cm^2. With an input of 50 watts, Equation (79) requires us to solve for r from the equation

$$re^{\kappa' r} = (\kappa_0 a) \times 6.3 \times 10^6 \text{ cm.}$$

It is a simple matter to compute the data shown in Table I.

TABLE I

CALCULATED EFFECT OF TEMPERATURE ON SUPERSONIC TRANSMISSION IN SEA WATER

λ, cm.	T = 0° C., $\mu_0 = .0181$			T = 20° C., $\mu_{20} = .0101$		
	$\kappa' \times 10^6$	$\kappa' r$	r. km.	$\kappa' \times 10^6$	$\kappa' r$	r. km.
0.24	55.2	12.2	2.2	30.7	9.68	3.1
.47	13.8	8.34	6.0	7.68	7.81	10.0
.94	3.45	6.51	19.0	1.92	6.00	31
1.89	.864	4.73	54.5	.48	4.26	89
3.77	.216	3.09	143	.12	2.65	221

NOTE: *Radius of transmitter, 30 cm.; input, 50 watts; reception, 30 decibels.*

These results are shown graphically in Fig. 1, and indicate clearly the very marked effect of temperature on transmission, making evident that the effect of temperature on viscosity is able to explain in large measure the marked difference between reception of supersonic signals actually observed in the sea in summer and winter (17, p. 335 and 10).

Observations by P. Biquard (4) seem to indicate for plane stationary waves in liquids a much higher coefficient of absorption at extremely high frequencies than can be accounted for by viscosity. Thus denoting by α the observed coefficient, Biquard's (4) observations give the data shown in Table II.

TABLE II

DATA COMPUTED FROM BIQUARD (4)

Temp., °C.	f	λ, cm.	α	κ' (calcd.)
14	7.55×10^6	0.0194	1.74×10^{-2}	0.55×10^{-2}
17	7.97×10^6	0.0184	2.0×10^{-2}	0.60×10^{-2}

The last column shows that the coefficient κ' computed from the theoretical expression, Equation (67), is much smaller for these extremely high frequencies than the value α actually observed. The effect of thermal conductivity can easily be shown to be negligible, as it increases κ' only by a quantity of the order of 1.13×10^{-6} (3).

In view of the practical importance of viscosity in transmission of supersonics, it is important that the effective viscosity of sea water over the range of wave-lengths 0.5 to 5 cm. be measured, if possible, for a divergent radiation field such as that of a supersonic sound oscillator. Until such data have been obtained the numerical results of this section and the next can be regarded as having only a provisional value indicating the order of magnitude of effects which can be attributed to viscosity.

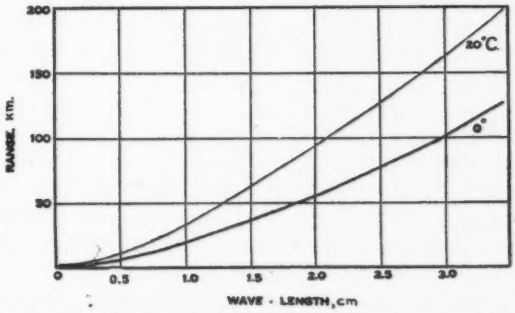

FIG. 1. *Calculated effect of temperature on supersonic transmission. Radius of transmitter, 30 cm. Input, 50 watts. Reception, 30 decibels. Viscosity of sea water: 0° C., $\mu_0 = 0.0181$; 20° C., $\mu_{20} = 0.0100$.*

In this connection it will be noticed that Equation (71) gives a possible means of determining κ' experimentally, should it be possible to measure the ratio of successive minima and maxima of the pressure amplitude on the axis. The effect would be best observed as acoustic radiation pressure on a small disc, for which an appropriate formula would have to be specially worked out. It must be remembered, however, that Equation (71) is valid only for an ideal piezo-electric oscillator surrounded by a theoretically infinite rigid flange.

Section 15. Conditions for Optimum Transmission and Reception*

On referring to Equation (79) for the intensity on the axis, we notice that for constant input the intensity at a distance r is a maximum for a certain

* *Since this paper was communicated, the writer has been informed by Dr. R. W. Boyle that he has been aware of the existence of an optimum wave-length, influenced by temperature, since 1918, having arrived at similar conclusions from theoretical considerations as well as from actual observations at sea.*

wave-length. It is evident that diminishing wave-lengths narrow the angle of the primary beam and increase the factor $(\kappa_o a)$, while through a corresponding increase of κ', the exponential factor in Equation (79) is diminished. Taking κ_o as the independent variable, we easily see that $I(0)$ is a maximum for $r\kappa_o \frac{d\kappa'}{d\kappa_o} = 1$, or, since $\kappa' = \frac{3}{4}\frac{\nu}{c}\kappa_o^2$, the condition of optimum reception is

$$\frac{4}{3}\frac{\nu}{c}\kappa_o^2 r = 1 , \qquad \text{giving} \qquad \lambda = 4\pi\left(\frac{\nu r}{3c}\right)^{\frac{1}{2}} . \tag{80}$$

Since the above condition also gives $2\kappa' r = 1$, the corresponding intensity on the axis is given by

$$I(0)_{max} = \frac{a^2}{4\pi e} \cdot \frac{3c}{4\nu} \cdot \frac{1}{r^3}\left[\frac{dW}{dt}\right] . \tag{81}$$

It is here assumed that the electrical system actuating the transmitter can be regulated to constant acoustic output. In general, however, $[dW/dt]$ will be a known function of the frequency or wave-length under specified conditions of electrical input, and the conditions for optimum reception will have to be modified accordingly.

Numerical Example

Utilizing numerical data pertaining to a disc of 30 cm. radius and 50 watts output, we have $a = 30$ cm., $c = 1.49 \times 10^5$ cm. per sec., $e = 2.72$, $[dW/dt] = 50$ watts. At 0° C., utilizing the usual value for the viscosity, we find $\nu_o = 0.0181$, and expressing the distance of transmission by R in kilometres, we find

$$I(0)_{max} = (8.13 \times 10^{-6})/R^3 . \quad (T = 0° C.) \tag{82}$$

If $\alpha(0)_{max}$ expresses the intensity on the *decibel scale*, we have

$$\alpha(0)_{max} = 10 \log_{10} [I_{o\,max} \times 10^{16}] = [109.1 - 30 \log_{10} R \text{ (km.)}] \text{ decibels, } (T = 0° C.) \tag{83}$$

while the corresponding wave-length is

$$\lambda(\text{cm.}) = 0.800\sqrt{R(\text{km.})} .$$

At 20° C. we take $\nu_{20} = 0.0101$, and the corresponding formulas are

$$\left.\begin{aligned} I(0)_{max} &= (14.57 \times 10^{-6})/R^3 \\ \alpha(0)_{max} &= [111.6 - 30 \log_{10} R(\text{km.})] \text{ decibels, } (T = 20° C.) \\ \lambda\,(\text{cm.}) &= 0.597\sqrt{R(\text{km.})} \end{aligned}\right\} \tag{84}$$

The above formulas are most conveniently expressed in the form of a graph plotted on semi-logarithmic paper, as shown in Fig. 2. The relations (83) and (84) connecting the level of reception in decibels with the range in kilometres give straight lines corresponding to sea water at 0° C. and 20° C., while the optimum wave-length for any given range is given by the corresponding curves and the scale on the right-hand side. For instance, at 20° C., 30 decibels reception is obtained at 550 km. for the optimum wave-length $\lambda = 13.6$ cm., whereas reference to Fig. 1 shows that the same level of

reception on a 2-cm. wave-length is only 95 km. At 0° C., 30 decibels reception is obtained at 440 km. for optimum wave-length $\lambda = 16.5$ cm., which may be compared to 55 km. on a 2-cm. wave.

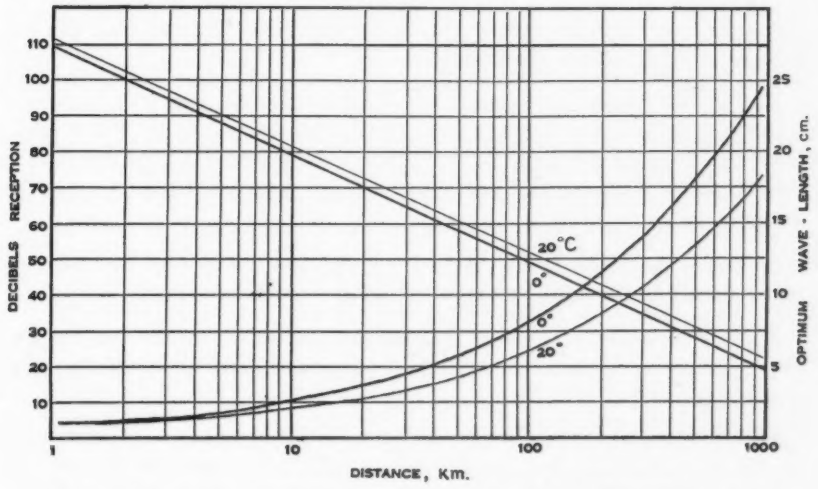

FIG. 2. *Chart for optimum reception. Input, 50 watts. Radius of transmitter, 30 cm.*

The numerical results of this section as well as the curves of Fig. 2 cannot be regarded as having more than a very rough accuracy in view of a considerable uncertainty as to viscosity of sea water at the frequencies considered, as well as to the existence of many factors affecting transmission not taken into account in the theory of the ideal transmitter.

Section 16. Summary and Conclusions

1. By the use of cylindrical wave-functions, it is possible by the application of Hankel's inversion formula to express the velocity potential due to a disc of radius a oscillating with uniform amplitude x in a closely fitting circular aperture surrounded by an infinite rigid flange in the form

$$\phi = a\dot{x}\int_0^\infty e^{-\mu z} J_0(\lambda\rho) J_1(\lambda a)\frac{d\lambda}{\mu} \ , \qquad \text{(i)}$$

where

$$\mu = (\lambda^2 - \kappa^2)^{\frac{1}{2}} \ .$$

2. The acoustic impedance of the disc as derived from the above formula agrees with the expression obtained by Lord Rayleigh's method.

3. The method of the present paper enables a large variety of radiation fields to be calculated corresponding to any given law of variation of amplitude of the disc with radius, provided always that it is surrounded by an infinite rigid flange.

4. The asymptotic expression for the distant field is shown to be

$$\phi = \int_0^\infty e^{-\mu z} J_0(\lambda\rho) f(\lambda) \frac{\lambda}{\mu} d\lambda \sim f(\kappa \sin\theta) \frac{e^{-i\sigma}}{r} , \qquad \text{(ii)}$$

where $f(\lambda)$ may be determined when the amplitude variation over the disc is given as a function of the radius.

5. The distribution of intensity on the axis for a disc vibrating with constant amplitude is easily obtained from the velocity potential (i) and agrees with the formula obtained by Lord Rayleigh's method. The position of "silent spots" is indicated and their position worked out in a numerical example.

6. The pressure amplitude over the disc and flange is worked out, and may be expressed as an infinite series of spherical wave-functions.

7. It is shown that it is not possible, in general, to expand the velocity potential (i) as a series of spherical wave-functions involving the polar co-ordinates (r,θ).

8. The effect of viscosity on the radiation field is to replace κ in Equation (i) by the complex value $\kappa = \kappa_0 - i\kappa'$, where $\kappa' = \frac{2}{3}\kappa_0^2(\nu/c)$, and ν is the kinematic coefficient of viscosity.

9. The effect of viscosity is to replace "silent spots" on the axis by minima at approximately the same positions. Numerical estimates are given of the pressure amplitude at these positions of minima in water.

10. With the usual coefficients of viscosity for water, it is shown that the effect on the radiation output and the angular distribution of the radiation field at a distance differs imperceptibly from the values for a perfect fluid.

11. Viscosity has, however, a marked effect on the range of distant transmission and, in consequence, the latter is markedly affected by temperature as illustrated by an appropriate graph.

12. Of considerable practical importance is the existence of an optimum wave-length for constant output and a given distance of transmission. By means of a simple chart it is possible to determine the optimum wave-length for a given transmitter when the level of reception (expressed in decibels) for a given range is stated.

13. It is probable in view of the results of Biquard (4) that, at supersonic frequencies, considerably higher values for the coefficient of viscosity must be taken. It is important that extended and accurate values be determined for sea water over the large range of frequencies used in practice.

14. Throughout the paper numerical estimates of various factors relating to the radiation field are calculated for a disc of 30 cm. radius having an output of 50 watts.

References

1. BACKHAUS, H. Ann. Physik, 5 : 1-35. 1930.
2. BATEMAN, H. Mathematical analysis of electrical and optical wave motion. Cambridge, University Press. 1915.
3. BIQUARD, P. Compt. rend. 193 : 226-229. 1931.
4. BIQUARD, P. Compt. rend. 197 : 309-311. 1933.
5. BOYLE, R. W. and LEHMANN, J. F. Can. J. Research, 3 : 491-509. 1930.
6. BOYLE, R. W., LEHMANN, J. F. and REID, C. D. Trans. Roy. Soc. Canada, 19, III : 167-196. 1925.
7. GRAY, A., MATHEWS, G. B. and MACROBERT, T. M. A treatise on Bessel functions and their application to physics. Macmillan and company. London. 1931.
8. LAMB, H. Hydrodynamics. 6th ed. Cambridge, University Press. 1932.
9. LANGEVIN, P. Hydrographic Review (Monaco), No. 3, 1924; No. 14, 1926.
10. LICHTE, H. Unterwasserschalltechnik. F. Aigner. Berlin. 1922.
11. MCLACHLAN, N. W. Phil. Mag. 14 : 747-758. 1932.
12. RAYLEIGH, Lord. Theory of sound. 2nd ed. Macmillan and company, London. 1896.
13. RUEDY, R. Can. J. Research, 5 : 297-301. 1931.
14. Smithsonian Physical Tables.
15. TITCHMARSH, E. C. Proc. Cambridge Phil. Soc. 21 : 463. 1923.
16. WATSON, G. N. A treatise on the theory of Bessel functions. Macmillan and company. London. 1931.
17. WOOD, A. B. A textbook of sound. Bell and Sons. London. 1930.

ON THE THEORY OF THE X-RAY DETERMINATION OF ELASTIC SCATTERING OF CATHODE RAYS[1]

By Darol K. Froman[2]

Abstract

This paper is a continuation of Bubb's (1) theoretical work which relates the energies and momenta of cathode rays to the properties of X-ray photons produced by them. Bubb's results are used to determine a scattering function for the cathode rays in a target in terms of the intensities of X-rays of minimum wave-length emergent from the target at various angles to the incident cathode-ray stream. It is shown that the self-consistency of Bubb's results can be tested by measurements of the intensities of two components of these X-rays polarized in mutually perpendicular planes. Mention is made of an experiment now in progress designed to test Bubb's theory by an absolute measurement using a gaseous instead of a solid target.

Introduction

Bubb (1) assumes that when an electron impinges on an atom and produces a quantum of white X-radiation, the energy and momentum are conserved, and the impulse given to the atom is in the direction of the electric vector of the electromagnetic wave associated with the X-ray photon. These assumptions, among others, lead to two results of interest here: (i) that if an electron gives up its entire energy to form an X-ray photon, that photon must emerge at a calculable angle to the momentum vector of the electron before collision; (ii) that the electric vector of the X-ray produced in this case must lie in the plane containing the emergent ray and the momentum vector of the electron before collision. A direct test of these results requires the use of a target so thin that the number of electrons scattered through appreciable angles in passing through it is negligible. In Section III, below, preliminary experiments with effectively thin vapor targets are described.

If, by means of the first-mentioned result, an angular distribution of the momenta of the electrons in a thick target which would produce any observed intensity function of the X-rays of minimum wave-length is found, the state of polarization of the X-rays can be predicted from the second result. An agreement between this prediction and experiment would constitute strong evidence for both the validity of Bubb's theory and the correctness of the scattering function.

I. The Scattering Function Determined from the X-Ray Intensities

In Fig. 1 let cathode rays moving in the positive direction of the x-axis be incident on a thick target whose face is parallel to the yz-plane. Let OB represent the direction of emission of an X-ray photon of minimum wave-length. In this Section, and in the next, only those cases in which the momentum of the electron is zero after emission, thus producing rays of

[1] *Manuscript received May 14, 1934.*
Contribution from the Faculty of Agriculture of McGill University, Macdonald College, Montreal, Quebec, Canada. Journal Series No. 47.
[2] *Lecturer, Department of Physics, Macdonald College.*

minimum wave-length, are to be considered. Let OB lie in the xy-plane making angle ϕ with the x-axis. Let OC represent the momentum of the electron producing this photon. Then by Bubb's result OC must make an angle ω with OB where ω is given by

$$\cos \omega = (1-\sqrt{1-\beta^2})/\beta \tag{1}$$

where βc is the velocity of the electron before collision and c is the velocity of light. Let Ψ be the angle through which this electron has been deflected, without loss of energy, from its original direction of motion. Let (x_1, y_1, z_1) be any point on OC and $(x_2, y_2, 0)$ be its projection on OB, and let r be the distance from 0 to (x_1, y_1, z_1). Let η be the angle between the lines joining $(x_2, y_2, 0)$ to $(x_1, y_1, 0)$ and to (x_1, y_1, z_1). Let $p(\Psi)$ be the probability that an electron incident along the x-axis be moving in a unit solid angle at an angle Ψ to the x-axis on emission of its total energy. Let $I(\phi)$ be the intensity of X-rays of wave-lengths between λ_0 and $\lambda_0+\delta\lambda$ (corresponding to electrons moving between ω and $\omega+\delta\omega$ to OB) emergent along OB. Then since the total radiation is incoherent,

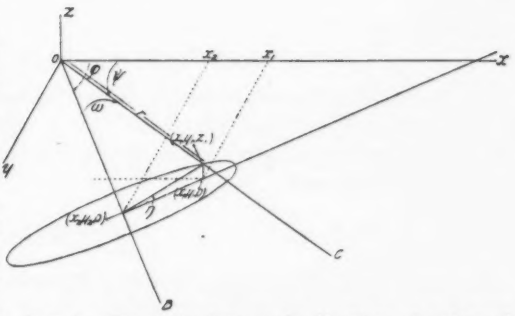

FIG. 1. *The angles between the directions of motion of electrons and X-ray photons.*

$$I_\phi = K_1 \sin \omega\delta\omega . 2 \int_0^\pi p(\Psi)d\eta \tag{2}$$

where K_1 is an unknown constant dependent on the number of incident electrons, etc. Since ω and $\delta\omega$ are independent of η and ϕ, let $K_2=2K_1 \sin \omega\delta\omega$. Then,

$$I_\phi = K_2 \int_0^\pi p(\Psi)d\eta \ . \tag{3}$$

From the geometry of Fig. 1,

$$x_1 = r \cos \Psi \ ,$$

$$x_2 = r \cos \omega \cos \phi \ ,$$

and

$$x_1 - x_2 = r \sin \omega \cos \eta \sin \phi \ ,$$

Hence

$$\cos \Psi - \cos \omega \cos \phi = \sin \omega \cos \eta \sin \phi$$

or

$$\cos \eta = (\cos \Psi - \cos \omega \cos \phi)/\sin \omega \sin \phi \ . \tag{4}$$

For brevity let:

$$b = \cos \omega \cos \phi \ , \quad a = \sin \omega \sin \phi \ , \text{ and } \xi = \cos \Psi \ . \tag{5}$$

Then

$$\cos \eta = (\xi - b)/a \tag{6}$$

$$\sin \eta = \sqrt{1-\cos^2\eta} = (1/a)\sqrt{a^2-b^2+2b\xi-\xi^2}\ , \tag{7}$$

and, from Equation (4),

$$-\sin \eta d\eta = -(1/a) \sin \Psi d\Psi = d\xi/a\ . \tag{8}$$

Therefore

$$d\eta = -d\xi/a \sin \eta = -d\xi/\sqrt{a^2-b^2+2b\xi-\xi^2}\ . \tag{8a}$$

If the target is homogeneous p will be symmetrical about the x-axis and can be expressed as a function of $\cos \Psi\ (=\xi)$. We assume it to be sufficiently general to assume a power series in ξ for p with the coefficients of all the negative powers zero. Then

$$p = \sum_{m=0}^{\infty} A_m \xi^m \tag{9}$$

where the A_m's are constant. Then by Equations (6), (8) and (9), Equation (3) becomes

$$I = -K_2 \sum_{m=0}^{\infty} A_m \int_{b+a}^{b-a} \frac{\xi^m d\xi}{\sqrt{a^2-b^2+2b\xi-\xi^2}} = -K_2 \sum_{m=0}^{\infty} A_m t_m \tag{10}$$

where (2, pp. 23-26)

$$t_m = \int_{b+a}^{b-a} \frac{\xi^m d\xi}{\sqrt{a^2-b^2+2b\xi-\xi^2}} = \left[\frac{\xi^{m-1}\sqrt{a^2-b^2+2b\xi-\xi^2}}{-m} + \frac{(2m-1)b}{m}\int \frac{\xi^{m-1}d\xi}{\sqrt{a^2-b^2+2b\xi-\xi^2}}\right.$$

$$\left. + \frac{(m-1)\,(a^2-b^2)}{m}\int \frac{\xi^{m-2}d\xi}{\sqrt{a^2-b^2+2b\xi-\xi^2}}\right]_{b+a}^{b-a} = \frac{(2m-1)b}{m}\, t_{m-1} + \frac{(m-1)\,(a^2-b^2)}{m}\, t_{m-2}\ . \tag{11}$$

Now

$$t_0 = \int_{b+a}^{b-a} \frac{d\xi}{\sqrt{a^2-b^2+2b\xi-\xi^2}} = \left[-\frac{1}{\sqrt{1}} \sin^{-1} \frac{2b-2\xi}{\sqrt{4b^2+4(a^2-b^2)}}\right]_{b+a}^{b-a} = \pm\pi = \text{a constant.} \tag{12}$$

Also,

$$t_1 = \int_{b+a}^{b-a} \frac{\xi d\xi}{\sqrt{a^2-b^2+2b\xi-\xi^2}} = \left[\frac{\sqrt{a^2-b^2+2b\xi-\xi^2}}{-1} + b\int \frac{d\xi}{\sqrt{a^2-b^2+2b\xi-\xi^2}}\right]_{b+a}^{b-a} = bt_0\ . \tag{13}$$

Hence t_0 is a constant factor in every term of the series for I. If we let $K = -K_2 t_0$ and $T_m = \frac{t_m}{t_0}$, Equation (10) becomes

$$I = K \sum_{m=0}^{\infty} A_m T_m$$

where

$$T_0 = 1, \quad t_1 = b = \cos \omega \cos \phi\ , \tag{14}$$

and

$$T_m = \frac{(2m-1)}{m} \cos \omega \cos \phi\ T_{m-1} + \frac{(m-1)}{m} (\sin^2\omega \sin^2\phi - \cos^2\omega \cos^2\phi)\ T_{m-2}\ .$$

We have also the normalizing condition expressing the existence of the electron:

$$1 = \int_0^{\pi} \rho 2\pi \sin \Psi d\Psi \ . \tag{15}$$

Substituting in Equation (15) from Equations (5), (8) and (9),

$$\begin{aligned} 1 &= -2\pi \int_1^{-1} \sum_{m=0}^{\infty} A_m \xi^m d\xi \\ &= 2\pi \sum_{m=0}^{\infty} \left[A_m \frac{\xi^{m+1}}{m+1} \right]_{-1}^{1} \\ &= 4\pi \sum_{n=0}^{\infty} \frac{A_{2n}}{2n+1} \quad \text{where } n \text{ is integral.} \end{aligned}$$

Therefore

$$K = 4\pi \sum_{n=0}^{\infty} \frac{KA_{2n}}{2n+1} \ . \tag{16}$$

Now if a sufficient number of the coefficients, KA_m, of T_m in Equation (14) be found by determinants to fit any experimentally determined $I(\phi)$, Equation (16) can be used to find K and thus to find A_m. Knowing A_m, $p(\Psi)$ can be computed directly from Equations (9) and (5). T_m decreases rapidly with increasing m, especially for high velocity cathode rays, and in view of the work of Wagner (3) and Webster (4) it is thought that $I(\phi)$ may be fitted within the limits of error of reasonably accurate intensity measurements using but the first few terms of the series, Equation (14).

This method may be used to compare the purely elastic scattering of electrons by different elements, and to determine the effect of tightly bound electrons on scattering, thus extending existing data obtained by scattering β-rays. It may be of interest to study the change in this scattering as the energy of the cathode rays is increased, so as to be able to eject more and more of the electrons in the atom. Also it might throw some light on the question of the efficiency of production of X-rays as a function of the material of the target.

II. The Polarization of the X-rays

Let $I(\phi)$ be resolved into its two components $H(\phi)$ and $V(\phi)$, polarized with the electric vectors in and perpendicular to the xy-plane respectively. Then

$$I(\phi) = H(\phi) + V(\phi)$$

and

$$H/V = I/V - 1 \ . \tag{17}$$

The intensity of the X-rays of minimum wave-length scattered at 90° to the ray perpendicular to the xy-plane can be determined experimentally. In the same way the intensity scattered at 90° to the ray but in the xy-plane may be measured. The ratio of these intensities is H/V.

We now use the second result from Bubb's theory to calculate V from the previously determined distribution of cathode rays in the target. By substituting this value of V and the experimental value of I in Equation (17) we obtain values of H/V, for all values of ϕ, which can be compared directly with the experimental values. Consequently the electric vector of any photon of minimum wave-length proceeding along OB in Fig. 1, and produced by an electron whose momentum before radiation was along OC, must lie in the plane defined by the points O, B and C. Hence the electric vector makes angle η with the xy-plane and the component of the intensity polarized with the electric vector perpendicular to the xy-plane is proportional to $\sin^2\eta$. On the directed quantum picture $\sin^2\eta$ is proportional to the probability that the photon be scattered at 90° to the ray in the xy-plane.

Then, using the notation of the previous section,

$$V(\phi) = K_1 \sin\omega\,\delta\omega \,.\, 2\int_0^{\pi} p(\psi)\sin^2\eta\, d\eta \tag{18}$$

and substituting from Equations (5), (7), (8) and (9), in Equation (18) we obtain

$$V(\phi) = -K_2 \sum_{m=0}^{\infty} A_m \frac{1}{a^2}\int_{b+a}^{b-a} \xi^m \sqrt{a^2-b^2+2b\xi-\xi^2}\; d\xi = -K_2 \sum_{m=0}^{\infty} \frac{A_m u_m}{a^2}\,, \tag{19}$$

where

$$u_m = \int_{b+a}^{b-a} \xi^m \sqrt{a^2-b^2+2b\xi-\xi^2}\; d\xi = \left[\frac{\xi^{m-1}(a^2-b^2+2b\xi-\xi^2)^{\frac{3}{2}}}{-(m+2)} + \int \xi^{m-1}\sqrt{a^2-b^2+2b\xi-\xi^2}\; d\xi \right.$$

$$\left. + \frac{(m-1)\,(a^2-b^2)}{m+2}\int \xi^{m-2}\sqrt{a^2-b^2+2b\xi-\xi^2}\, d\xi\right]_{b+a}^{b-a}$$

$$= \frac{(2m+1)b}{m+2}\,u_{m-1} + \frac{(m-1)\,(a^2-b^2)}{m+2}\,u_{m-2}\,. \tag{20}$$

Now

$$u_0 = \int_{b+a}^{b-a} \sqrt{a^2-b^2+2b\xi-\xi^2}\; d\xi = \frac{a^2}{2}\int_{b+a}^{b-a} \frac{d\xi}{\sqrt{a^2-b^2+2b\xi-\xi^2}} = \frac{a^2}{2}\,t_0\,. \tag{21}$$

Also

$$u_1 = \int_{b+a}^{b-a} \xi\sqrt{a^2-b^2+2b\xi-\xi^2}\; d\xi$$

$$= b\int_{b+a}^{b-a} \sqrt{a^2-b^2+2b\xi-\xi^2}\, d\xi = bu_0 = \frac{ba^2}{2}\,t_0\,. \tag{22}$$

Now Equation (19) becomes on substitution from Equation (21)

$$V = -K_2 \sum_{m=0}^{\infty} \frac{A_m}{a^2} u_m = \frac{-K_2 l_0}{2} \sum_{m=0}^{\infty} \frac{A_m u_m}{u_0}$$

or

$$V = \frac{K}{2} \sum_{m=0}^{\infty} A_m U_m \ ,$$

where

$$U_m = \frac{u_m}{u_0} = \frac{(2m+1)}{m+2} \cos\omega \cos\phi \ U_{m-1} + \frac{(m-1)}{m+2} (\sin^2\omega \sin^2\phi - \cos^2\omega \cos^2\phi) \ U_{m-2} \ .$$

$$U_0 = 1, \ U_1 = b = \cos\omega \cos\phi \text{ and, as before, } K = -K_2 l_0 \ . \qquad (23)$$

Here K and A_m have been determined from the intensity measurements and the values of U_m are defined. The value of V may be computed from Equation (23) and be substituted in the right-hand side of Equation (17) the check against H/V as determined by experiment.

III. The Use of a Vapor for an Effectively Thin Target

In addition to what has been mentioned, Bubb calculates from his assumptions the maximum frequency, ν_0, of X-rays which can be emitted in a direction making angle θ with the momentum vector of the cathode rays, *viz:*

$$\nu_0 = \frac{m\beta^2 c^2}{2h\sqrt{1-\beta^2}} \cdot \frac{\sin^2\theta}{1-\beta\cos\theta} \qquad (24)$$

where m is the mass of the electron. When $h\nu_0$ is equal to the total kinetic energy of an electron, $\theta = \omega$.

This relation between ν_0 and θ could be tested experimentally using a target so thin that few of the cathode rays would be scattered appreciably in passing through it. Metal foil targets are unsatisfactory for use with 30 or 40 kv. electrons, because of mechanical difficulties in their preparation, and the fact that extremely small tube currents must be used to prevent the formation of holes in them due to melting of the metal.

It was thought that the use of a mercury vapor target, whose thickness, measured in atoms, could be fixed easily at any desired value, might eliminate the difficulties. There is no limit to the tube current in this case as the target is already vaporized. An X-ray tube was built with a long, hollow anticathode cooled by water circulation. Cathode rays could pass through holes in the front and back of this anode into a chamber containing mercury, whose vapor could be kept at any desired temperature. The hollow anode served as a condenser for any mercury vapor diffusing into it, so that a high vacuum could be maintained in the fore part of the tube. The pressure of the vapor which will not cause scattering of more than any predetermined amount, can be computed or can be found experimentally, as the cathode rays excite mercury atoms, causing them to emit visible light in the beam.

The path of the cathode rays through the vapor was necessarily rather long (about 4 or 5 cm.) from the point at which the rays entered the vapor to the point from which X-rays were taken. This made necessary so low a pressure, to prevent excessive scattering, that the intensity of the X-rays was very weak. However, the X-rays could be detected quite easily photographically, but it was found impossible to keep the apparatus operating under constant conditions for a period long enough to obtain a spectrogram. It was estimated that an exposure time of 40 or 50 hr. would have been necessary to determine the minimum wave-length accurately.

A modification of the arrangement just described is contemplated in which the cathode rays will be allowed to pass through a molecular beam in which the density of atoms can be high when the cross section of the beam is small. It is hoped that the intensity of X-rays produced per unit volume (this factor governs exposure time) can be made high enough to give good spectrograms in practicable exposure times.

Acknowledgment

The writer wishes to acknowledge his indebtedness to Dr. W. W. Stewart for reading the manuscript and to Dr. R. Holcomb for suggesting the use of a molecular beam.

References

1. Bubb, F. W. Phys. Rev. 24 : 177-189. 1924.
2. Peirce, B. O. A short table of integrals. Ginn and Company, Boston. c1929.
3. Wagner, E. Jahr. Radioakt. und Elektronik. 16 : 212-213. 1920.
4. Webster, D. L. National Research Council, Washington. Bull. 7. 1920.

REFLECTIONS FROM THE IONOSPHERE[1]

By Sydney Sillitoe[2]

Abstract

Oscillograms showing unusually low layer reflections and exceptionally strong multiple reflections from the *F* layer, and oscillograms of the usual conditions for February, March and April, are presented. Some automatic continuous records of the heights of the reflecting layers are also shown.

The main features of the new design and technique, which were important factors in the elimination of all extraneous results, are clearly pointed out.

Introduction

The original intention of the author was to develop a system of continuous recording of the apparent heights of the reflecting layers in the ionosphere with both transmitter and receiver located in the same building. As the pulse method of Breit and Tuve was to be used it was felt that attention must be paid to stability (constancy of frequency of the transmitted pulse), and that therefore a stabilized master oscillator power-amplifier circuit should be used, with only short pulses of power emitted by keying in the antenna circuit. Furthermore, for economic reasons, the whole system had to be composed of a minimum of component parts, be as simple as possible, and yet be capable of delivering sufficient power to achieve the result in mind. The last consideration was achieved. Elaborate shielding precautions had to be taken, but despite these, it was found impossible, for any reasonable cost and effort, to build filters and install shielding sufficiently effective to allow the receiver to be located in such close proximity to the transmitter.

The transmitter, therefore, remained in the attic of the Macdonald Physics Building at McGill University, and the receiving apparatus was moved about two miles away to a location in Outremont just on the other side of Mount Royal. The location of the receiver was very fortunate, as the presence of the mountain probably reduced the intensity of the ground wave, leaving the receiver more sensitive to the reflection than it otherwise would have been. Both manual and continuous recording were successfully achieved in this location, and it is the purpose of this paper to describe fully the equipment, and to show and to discuss the results obtained.

The Transmitter

Most experimenters have employed transmitter circuits in which keying was effected either in the oscillator itself or in the power supply of one of the succeeding amplifier stages. Extra vacuum tubes of equal rating had to be used as keying devices in order to eliminate arcing, and this made the installation very costly. It is a well known fact that in any oscillator, the frequency, being dependent on the internal characteristics of the vacuum tube, which in turn vary with voltage fluctuation, cannot remain constant for the full

[1] *Original manuscript received April 26, 1934.*
Contribution from the Physical Laboratories, McGill University, Montreal, Canada.
[2] *Graduate student.*

duration of a short pulse obtained by interruption of the power supply. Actually, the frequency changes as the oscillations build up and die down in the tuned circuits. This effect is still present, but less pronounced, if the keying is done in succeeding amplifier stages. But, in both cases, the wave produced is unsymmetrical, owing to the flywheel effect of the tuned circuits, which do not cease oscillating for a short time after the keying operation is over.

For these reasons stability in the transmitter was recognized as being of primary importance, and the transmitter shown in Fig. 1 was designed and built. A stabilized Colpitts' master oscillator, as suggested by F. B. Llewellyn

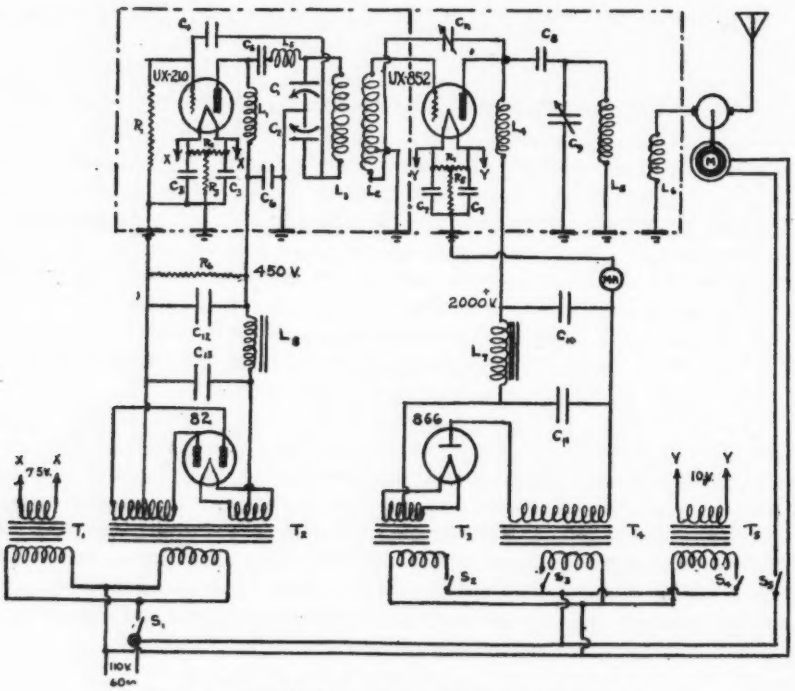

FIG. 1. *Simplified transmitter and power supply circuit.*

(7), employing a UX 210 tube to drive a UX 852—100 watt power amplifier was used. Full advantage of the oscillator stabilization was not taken, as neutralization of the UX 852 power amplifier was found necessary. Inductive coupling had therefore to be used. Self-biasing of both tubes, accomplished by resistors R_2 and R_5 in the cathode leads, was used to afford protection against overvoltage and interruption. The whole transmitter was completely shielded in a heavy copper case. By careful design a very low cost transmitter was thus produced, which operated at maximum possible efficiency and was sufficiently reliable to be left running without supervision.

Sharp, symmetrical wave pulses were radiated from the shielded transmitter by keying in the lead to the quarter-wave flat-top antenna. The commutator, driven by a synchronous motor, consisted of a fibre disk about eight inches in diameter, with three equally spaced brass segments imbedded in the surface. The width of the segments was such that it gave a pulse 0.0003 sec. long, but which could easily have been made less. Two phosphor bronze spring contacts, riding on the commutator, completed the antenna circuit for this short interval 90 times a second. This keying speed was adopted for two reasons: first, it made the framing of the picture on the oscillograph at the receiving station always possible and, second, the recurrence period of 1/90 of a second formed a convenient means of calibration, which eliminated the necessity of switching a calibration oscillator on the oscillograph in order to calculate equivalent heights. Anyone who has worked on this type of problem will appreciate the saving of time and the added convenience that this made possible. No telephone connection between stations was necessary, and it was possible for the author to operate the system alone.

In other words, keying at this speed and synchronizing the sweep with the 60 cycle power supply, made it possible to view in succession on the oscillograph screen the three transmitted pulses, corresponding to the three commutator segments. When the corresponding reflections following each transmitted pulse were identical in form and sequence, there could be no doubt that the reflections were genuine. This new technique and design were important factors in the elimination of extraneous results.

Receiving Apparatus

At the receiving station the apparatus was arranged as shown in Fig. 2. The radio receiving set used was a Silver Marshall 728 SW all wave model,

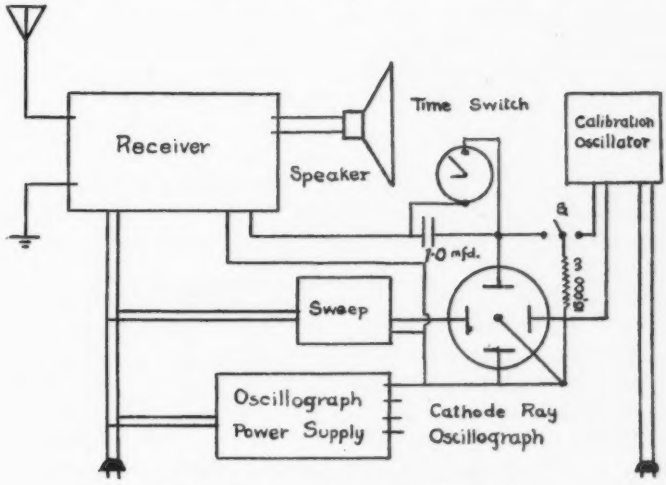

FIG. 2. *Receiver apparatus—block diagram.*

with a slight change in the output circuit. The oscillograph tube used was a Cossor type *C* fed from a General Radio cathode ray oscillograph power supply. A Cossor sweep circuit was used to supply a linear time axis.

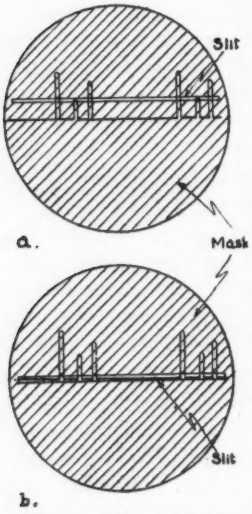

FIG. 3. *Two methods of placing the slit for continuous recording.*

The voltage developed across a 2000 ohm resistor in the plate circuit of the first audio tube of the receiver was applied through a blocking condenser (1.0 mfd.) to the ungrounded plate of the oscillograph. The ground connection to the oscillograph had to be made through the receiver which was solidly grounded. An alarm clock, with contacts placed upon the face, served as a time switch which shorted the stopping condenser and lifted up the beam for one and a half minutes at the hour points. The slit (Fig. 3), being photographed for continuous recording, was thus made blank for a long enough period each hour to make a distinct marking on the film, for the indication of the time of day at which the record was taken.

Photographs of the actual patterns on the oscillograph screen were made with a specially built box camera. Continuous records were made with a similar camera, the film being driven by a strong clockwork.

Methods of Continuous Recording

For continuous recording it is evident from Fig. 3 that there are two methods of placing the slit, depending on the type of record desired. In Fig. 3 *(a)* the slit is shown above the time line. The shutter in the camera is stopped down but left continuously open, and on the record either double or full black lines appear on a light background, depending on the intensities of the pulses. It is evident that this method records only those reflections which are above a certain intensity, and furthermore, interference conditions may completely destroy the record. When the lens is open all the time the slit cannot be placed as in Fig. 3 *(b)*, because there is a discrimination against the sustained conditions in the pattern. A transient condition, which often occurs, will bring the bright spot down to the slit and will quickly fog out a portion of the record which has almost, but not quite, completed the travel across the slit.

If the slit is placed as shown in Fig. 3 *(b)*, short exposures of one-half to one second in length must be made at intervals of one minute. This record has the advantage of being completely independent of interference conditions, as the breaks in the time line appear as white lines on a dark background, and the interference all goes into the background if the exposure is made sufficiently long. The mechanical set-up for this type of record is more elaborate. A cam arrangement is needed to actuate the shutter, and the power required for this is more than a clock can deliver.

A motor drive was used for both film and shutter, and this proved to be mechanically all that could be desired. Unfortunately the motor was the cause of a great deal of noise in the receiver and had to be discarded. A good induction motor might have served the purpose, but this was not available.

There was, however, another difficulty, in that the receiver had a recovery curve which originated in the coupling between the detector and audio stages, and this condition could not be easily eliminated. This over-swing after a strong pulse, clearly shown in Plate II, while of no particular disadvantage in a complete pattern photograph, proved nevertheless to be extremely inconvenient for continuous recording. The use of a horizontal, straight slit was impossible unless the slit was made very wide, and when this was done the record was poor. A crooked slit fitted to an average recovery curve was also useless, as this curve varied with the strength of the pulse. Other factors peculiar to the location made it impossible to obtain this type of record. Finally, it was decided to use the method shown in Fig. 3 *(a)*, as in general the reflections seemed to appear either intensely, or not at all. Moreover, the location was remarkably free from factors causing interference.

But again, when records were being made, two more difficulties arose. Changes in voltage of the power supply caused changes in the sensitivity of the oscillograph, and hence the linear amplitude of the time sweep varied; the vertical scale on the record fluctuated correspondingly. Phase changes in the power lines (which were used for synchronizing) between the transmitter and the receiver two miles away caused a creeping back and forth of the picture on the time axis—and therefore the ground level line did not appear straight as it should on the record.

Experimental Results

Most of the tests were made at a frequency of 3492 kc. A few oscillograms selected from over 500 taken are shown in Plates I and II, to represent conditions in the morning, at sunset and in the evening. Each division of the scale at the base represents 100 km. apparent height.

In Plate I the picture taken at 10:25 a.m. shows that the *E* layer and *F* layer reflections appear to come from heights of 80 km. and 207 km. respectively. The other pictures in the top row show *E* layer reflections from an average height of 105 km. In the morning, at this frequency, the *E* layer reflections were neither continuous nor strong, and, as shown, at 11:01 a.m. and 11:41 a.m., had died out completely. Strong, continuous *F* layer reflections from heights ranging from 207 to 233 km. appear, followed by weaker multiple reflections. Some synchronous interference causes the pulse located at 800 km. on the scale.

In the afternoon these same conditions prevail, but the *E* layer generally completely disappears except for very short intervals now and again.

Shortly after 5:10 p.m. in the months of February and March, a most interesting period for observation was almost always found. *Many transient conditions appear just before the sunset hour.* Suddenly, strong reflections

appear from the F layer, and the pattern on the screen of the oscillograph rolls like the waves on the ocean as the reflections and their many multiples appear and disappear. For short periods now and then, the E layer also reflects. Such conditions are clearly shown at the bottom of Plate I and the top of Plate II. Pictures such as those taken on March 15 are quite common and show the strong F layer reflection coming from an average height of 250 km. Many multiple reflections appear and disappear.

The two pictures taken on March 14 at 5:50$_{40}$ p.m. and 5:51 p.m. show an exceptional transient condition which was luckily photographed. These pictures, taken in rapid succession, show first the F layer and six multiple reflections, with F_5 and F_6 alternately dying out. Suddenly at 5:51 an intense E layer reflection appeared, which apparently was again reflected from the earth, to pierce the E layer and be subsequently reflected from the F layer producing all the multiple $E + F$ reflections shown. The duration of this condition was never more than half a minute. Note the intensity of the reflected sky waves in comparison with that of the ground wave. These are not the only photographs obtained of such conditions, but have been selected from a few pictures showing the same unusual condition.

In Plate II progressive stages of magneto-ionic splitting from the F region are shown for March 23. *These reflections are of a very transient nature and are rising and falling continually,* first on one side, and then on the other. Three and four pulses come in close together, and it is not strange that short wave messages are not clear under such conditions. At 9:45 p.m. on March 19, a very stormy night, the E (?) layer reflection was exceptionally strong and gave a multiple reflection also. Note that it is exceptionally low, 50 km. The condition shown existed, from time to time, for short intervals over a period lasting about three hours. Low layer reflections were also photographed on three other days, but the intensities were much less than in the example shown in Plate II.

In Fig. 4 the results obtained throughout the day in February and March have been plotted. The upper and lower boundaries of the regions from which reflections were obtained are shown. The F layer is closest to earth at noon, being as low as 160 km. The E layer reflections were relatively weak at this frequency (3492 kc). but the height of the layer is generally about 100 km. However, it should be noted that, at odd times in the afternoon and evening, reflections were returned from heights as low as 40 km.

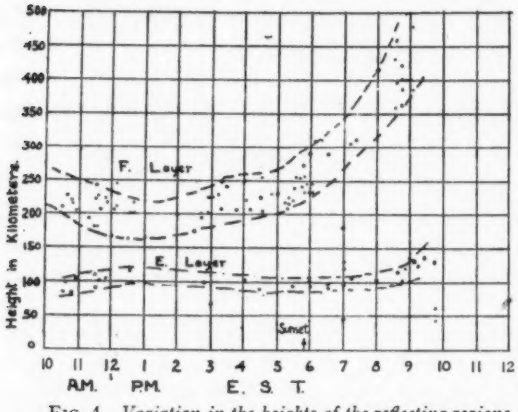

FIG. 4. *Variation in the heights of the reflecting regions with time of day. February and March, 1934. Frequency—3492 kc.*

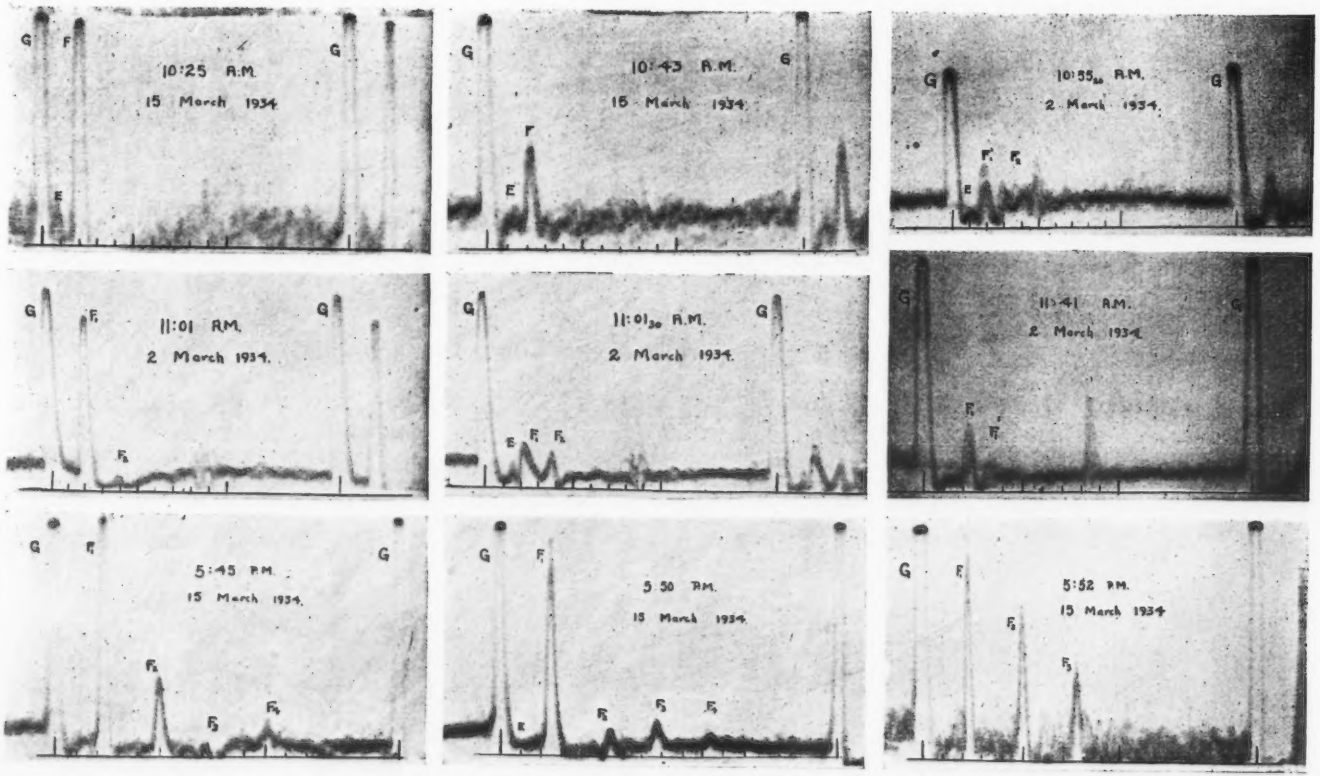

Oscillograms. Frequency—3492 kc.

PLATE I

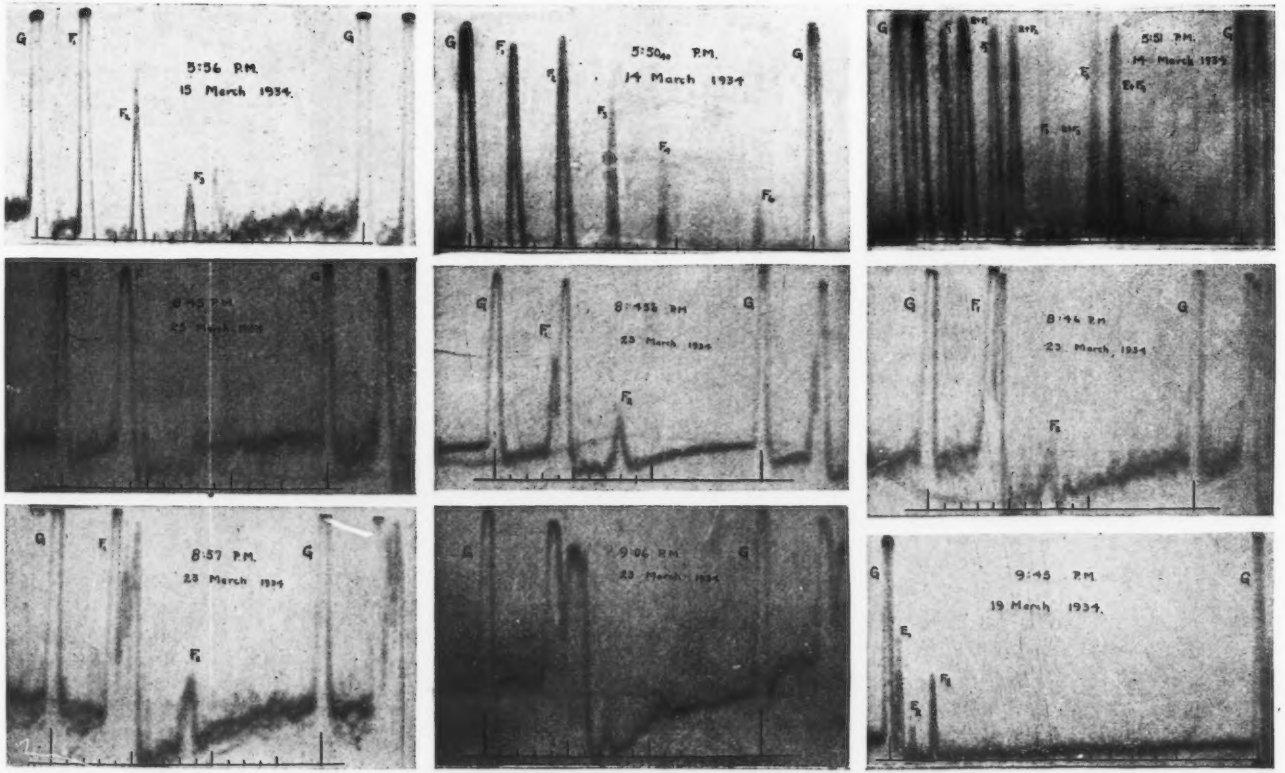

Oscillograms. Frequency—3492 kc.

PLATE II

PLATE III

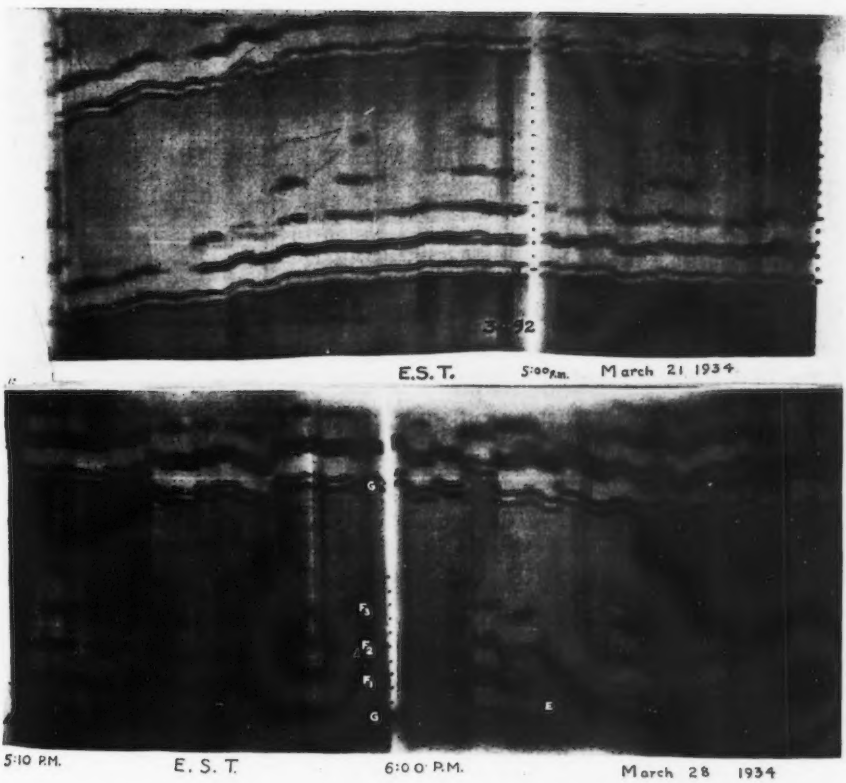

Continuous recordings of heights of reflecting layers. Frequency—3492 kc.

The results of a test run at a frequency of 2398 kc. are plotted in Fig. 5. In the morning the reflections were very weak, but at times the *E* layer seemed to be very low. The *E* layer appeared to rise from 100 km. at noon to 140 km. at 5 p.m. In the evening scattered reflections were obtained from as low as 70 km., and from as high as 160 km. The reflections from the *F* layer were very weak in the morning, but when they were present, the height was between 200 and 250 km. In the evening the reflections became much stronger and the height gradually increased. At 9:30 p.m., the interference became too great for successful photography.

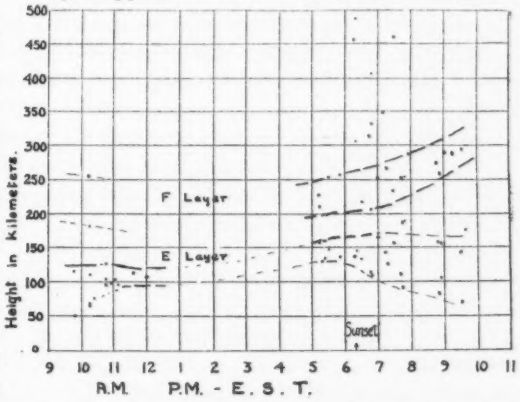

FIG. 5. *Variation in the heights of the reflecting regions with time of day. April 2 and 3, 1934. Frequency—2398 kc.*

In Plate III a section of a continuous record obtained on March 28 is reproduced. These records show directly the same type of information indicated in Figs. 4 and 5. The equivalent heights in 100 km. are shown on the hour lines. The difficulties encountered in obtaining this type of record, as already pointed out, are clearly apparent. Voltage and phase changes in the 60 cycle power lines were responsible for the fluctuations in the position and recurrence of the ground wave. Although, on this account it is in a somewhat inconvenient form, the information is nevertheless always available on these records. They do not give the same amount of information as the complete oscillogram, and at a frequency of 3492 kc. only unusually strong *E* reflections could be recorded. The recovery curve of the receiver also discriminated against the recording of the lower *E* layer echoes. When splitting occurred the echo lines were broadened out and less distinct.

Conclusions

In general, the results of these tests agree with those obtained by previous experimenters. However, on account of the short pulse and stability of the transmitter, it was possible to record reflections from the *E* (?) layer when apparently it was as low as 40 km. above the ground. In February, March and April, these reflections from an exceptionally low layer were observed on only four days. These were not continuous, but appeared from time to time, especially after sunset, and possibly in the early morning up to 10 a.m., and were generally weak when observed. The strength of the reflections and the unusual conditions shown in Plate II are quite interesting, and *indicate the quick changes that must take place in the ionosphere during certain periods.* The presence of a sixth multiple *F* reflection of good intensity shows the

efficiency of the reflecting or refracting layer and the relatively small absorption. It is curious to note that this wave actually travelled about 3000 km., but has progressed only two miles from the transmitter in so doing.

It is also a curious fact that an apparent multiple reflection may die out, while the two adjacent echoes remain. This effect was generally noticed near sunset and sometimes suggested, for short periods, another layer extremely high up, about 1100 km. The explanation of the fact that F_4, for example, has not returned to earth, while F_5 has successfully done so, may be that the reflection of F_4 took place from the top of a low E layer, which was sometimes observed, as already pointed out in the discussion of Fig. 4. Indeed, at other times, echoes were observed coming apparently from heights corresponding to $E + F$.

The results of tests at different frequencies indicate that the higher frequencies are more penetrating. In a short run at 4360 kc., made April 4, in the late afternoon, echoes from the F layer at a height of 360 km. were obtained, while at 3492 and 2398 kc. at corresponding times of day, the heights were found to be generally about 250 and 235 km. respectively. This is in accordance with the continuous observations over a wide frequency range made by Kirby, Berkner and Stuart.

Acknowledgments

The author wishes to express his sincere appreciation of the hospitality accorded him by Mr. and Mrs. J. T. Aikman and family, who so kindly gave space in their home for the location of the receiving equipment. He is greatly indebted to Mr. H. T. Pye and Mr. G. Tweeddale who assisted in building parts of the transmitter and camera, and to Mr. S. Amesse who photographed the plates shown in the paper. The helpful discussions with Dr. H. G. I. Watson and Dr. A. S. Eve were of definite value.

Bibliography

1. Appleton, E. V. J. Inst. Elec. Eng. London, 71 : 642-650. 1932.
2. Appleton, E. V. and Barnett, M. A. F. Proc. Roy. Soc. London, A, 109 : 621-641. 1925.
3. Appleton, E. V. and Builder, G. Proc. Phys. Soc. London, 45 : 208-220. 1933.
4. Breit, G. and Tuve, M. A. Phys. Rev. 28 : 554-575. 1926.
5. Breit, G., Tuve, M. A. and Dahl, O. Proc. Inst. Radio Eng. 16 : 1236-1239. 1928.
6. Kirby, S. S., Berkner, L. V. and Stuart, D. M. Bur. Standards J. Research, 12 : 15-51. 1934.
7. Llewellyn, F. B. Bell System Tech. J. 11 : 67-100. 1932.
8. Watt, R. A. Watson, Herd, J. F. and Bainbridge-Bell, L. H. Applications of the cathode ray oscillograph in radio research. H.M. Stationery Office, London. 1933.

TETRAPHENYLCYCLOPENTADIENONE IN THE DIENE SYNTHESIS[1]

By C. F. H. Allen[2] and L. J. Sheps[3]

Abstract

In continuation of the authors' earlier work on substances having a carbonyl bridge, it has been found that tetraphenylcyclopentadienone can be used as one of the components in the diene synthesis. Products are described resulting from the addition of maleic anhydride, maleic, fumaric, and acetylene dicarboxylic esters, and benzoyl phenylacetylene. In some instances the primary addition products containing a carbonyl bridge could be isolated. Tetraphenylbenzene derivatives result from secondary reactions. Benzalacetophenone, dibenzoylethylene and diphenylketene did not add to tetraphenylcyclopentadienone.

In the previously described reaction between maleic anhydride and anhydroacetonebenzil, certain intermediates have been isolated, confirming the mechanism suggested to account for the formation of a dianhydride.

It was recently shown in this laboratory that when cyclopentadienones dimerize the product is formed by a diene syntheses and has a carbonyl bridge across a six-membered ring (3, 4). On account of the ease of dimerization, a monomolecular form has never been isolated except in the case of tetraphenylcyclopentadienone (6, 14). In accordance with the assumption made in the previous paper, the latter would be expected to enter into the diene syntheses with some of the usual addends, and, as previously announced (3), it was found that it does.

When tetraphenylcyclopentadienone, I, and maleic anhydride are cautiously warmed together, an addition product, II, is formed.

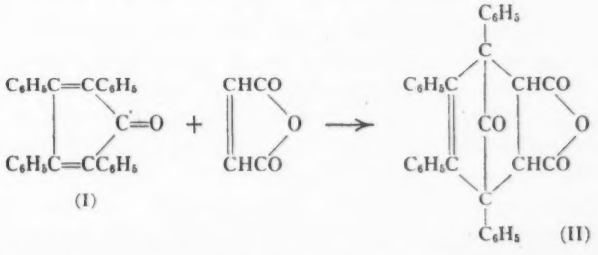

(I) (II)

When the reaction mixture is heated to a somewhat higher temperature, the bridge is lost as carbon monoxide, and a new anhydride, III, obtained. Finally, when the mixture is heated to 250° C. during the preparation, both carbon monoxide and hydrogen are lost, and tetraphenylphthalic acid, IV, is

[1] *Manuscript received June 22, 1934.*
Contribution from the Chemical Laboratory, McGill University, Montreal, Canada.
This paper was read at the meeting of the Royal Society of Canada at Quebec, May, 1934, and at the Toronto meeting of the Canadian Chemical Association, June, 1934.

[2] *Assistant Professor of Chemistry, McGill University.*
[3] *Graduate Assistant in Chemistry, McGill University.*

the substance actually isolated; this same product is also obtainable by heating II and III, with or without sulphur. Therefore, three series of products may be obtained, according to experimental conditions.

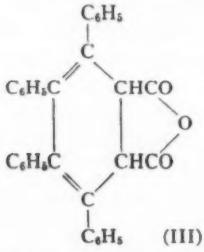

(III)

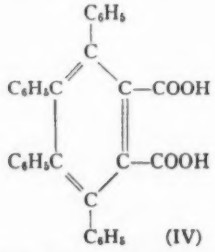

(IV)

The anhydrides and acid can be hydrolyzed and esterified; the esterification takes place slowly as with any hindered acid. When the anhydride II was treated with alcoholic hydrogen chloride it gave a mixture of mono and dimethyl esters; the diester was more conveniently prepared through the silver salt.

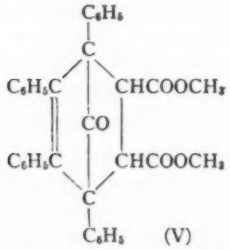

(V)

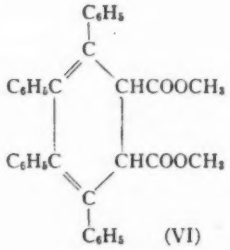

(VI)

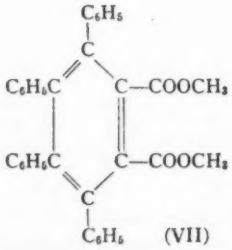

(VII)

The ester, V, being derived from maleic acid, would be expected to have the *cis* configuration; that it actually has is conveniently shown by the preparation of the *trans* ester, by the addition of methyl fumarate to tetraphenylcyclopentadienone. Ester VI is also *cis;* the *trans* isomer was obtained by conducting the addition of methyl fumarate at a high enough temperature to eliminate the bridge as carbon monoxide.

When methyl maleate is used as an addend, however, it is not possible to stop the reaction at any intermediate point, both carbon monoxide and hydrogen are lost, and the aromatic ester, VII, is formed. Whether the difference is due to the higher temperature of reaction required, or to some other reason, is uncertain.

Finally, to show that two atoms of hydrogen had been actually lost, and that VII is a benzene derivative, it was synthesized from tetraphenylcyclopentadienone and acetylene dicarboxylic (methyl) ester; the product was identical with the substance prepared in other ways. The ethyl ester was also prepared; in this case heating in a sealed tube was required. Owing to the higher temperature required to bring about the addition of these esters, the primary product containing a carbonyl bridge could not be isolated. All

efforts to secure the ethyl ester by esterification of the acid were unsuccessful, nor could it be hydrolyzed to this acid. It is a very stable substance, being recovered unchanged after heating with caustic potash at 360° C.

The relation between the various substances is much clearer, when summarized in a flowsheet.

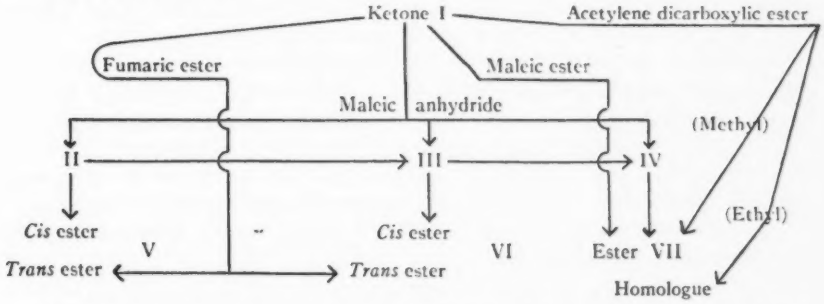

Neither benzalacetophenone nor dibenzoylethylene adds to tetraphenylcyclopentadienone, but benzoylphenylacetylene gives pentaphenylbenzophenone, VIII. As would be anticipated, this ketone has a very inactive carbonyl group.

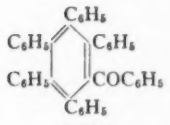
(VIII)

In the diphenylcyclopentadienone series, a dianhydride, XI, has previously been described (4); this may be accounted for as shown by the outline

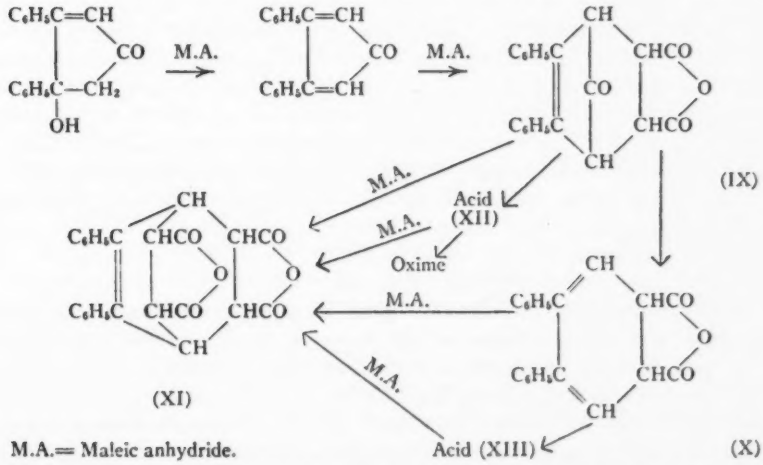

After the authors' preliminary notice on the di- and tetraphenyl series, and a paper on the diphenylcyclopentadienone series, had appeared, Dilthey (6, 8) published two short papers, almost devoid of experimental details, in which were described certain highly arylated benzene derivatives prepared from tetraphenylcyclopentadienone and several acetylenic compounds, and three anhydrides in the maleic anhydride series. It is of interest to note that in no single case, either in his or the authors' work, has a substance having a carbonyl bridge been obtained with acetylenic addends.

The intermediate anhydrides are oils, but the corresponding acids are solids. When the acid XII is heated, it loses carbon monoxide; the product XIII contains a conjugated linkage, to which maleic anhydride easily adds to form XI; the latter also results on heating IX and maleic anhydride. This behavior of these compounds is comparable to that of coumalin and maleic anhydride, in which case carbon dioxide was lost (5). Acid XII also forms an oxime, thus confirming the carbonyl group.

Staudinger found that ketenes and cyclopentadiene form addition products that might be represented as cyclobutane derivatives, or as endomethylene compounds, if a diene synthesis had taken place (10, pp. 23, 59; 11, 12, 13). If diphenylketene added to tetraphenylcyclopentadienone, this would offer evidence in favor of the latter possibility. However, the present authors have been unable to find any experimental conditions under which addition would take place, which, indirectly, favors the cyclobutane formulas. Phenyl azide, a reagent used to detect "active" ethylenic linkages (1, 2), does not add to any of the substances containing a carbonyl bridge in either series, possibly on account of the hindrance of the phenyl groups.

Experimental

A. Addition of Maleic Anhydride

(a) Anhydride (II) of 3,4,5,6-tetraphenyl-7-keto-1,2,3,6-tetrahydro-3,6-methanobenzene-1,2-dicarboxylic acid

A mixture of 5 gm. each of maleic anhydride and tetraphenylcyclopentadienone (hereafter referred to as the red ketone) was cautiously heated in an oil bath at 155–160° C., taking care not to exceed this temperature, until the red color had practically disappeared (five minutes). After cooling, the mass was readily removed if it was first loosened by addition of methanol and then gently warmed. After recrystallizing from acetic acid or benzene, 6 gm. (96%) of a pink product was obtained. The color disappeared after repeated treatments with a decolorizing carbon. It formed white plates, m.p. 220° C.* It is insoluble in the ethers and alcohols, moderately soluble in hot dioxane, acetic acid, benzene, and ethyl acetate, and very soluble in warm acetone and cyclohexanone. Calcd. for $C_{33}H_{22}O_4$: C, 82.1; H, 4.5%; mol. wt., 482. Found: C, 81.7; H, 4.7%; mol. wt., 486.

It was not possible to obtain an oxime or a phenylhydrazone. The results obtained with the Grignard machine were anomalous; until the behavior of other anhydrides is thoroughly investigated, their interpretation is impossible. Tetraphenylcyclopentadienone itself shows one addition, and tertiary alcohols have been prepared from it using phenyl and benzylmagnesium halides (9, 14).

The corresponding *cis* acid dissolves readily in the alcohols, ether, benzene, acetic acid, and decalin; the amorphous product melted at 190–191° C., with evolution of gas. Calcd. for $C_{33}H_{24}O_5$: mol. wt., 500. Found: mol. wt., 511. The silver salt shrivels and blackens at 185–190° C. Calcd. for $C_{33}H_{22}O_5Ag_2$: Ag, 30.2%. Found: Ag, 30.1%.

* *Melting points are corrected.*

The *cis* dimethyl ester, V, was obtained by refluxing 1 gm. of the silver salt with 5 cc. of methyl iodide for 0.5 hr., filtering and evaporating, and recrystallizing from dilute methanol, after treating with animal charcoal; yield, 0.65 gm. It forms a micro-crystalline powder which shrinks at 135° C., and gives off a gas at 155° C. Calcd. for $C_{35}H_{28}O_5$: OCH_3, 11.7%. Found: OCH_3, 11.3%.

The anhydride was dissolved in absolute methanol and saturated with hydrogen chloride for five hours at 0° C. After 24 hr. a solid, which melted at 120–122° C. with gas evolution, was obtained. Methoxyl values (8.4%) were intermediate between those of a half ester (6.0%) and the whole ester (11.7%,) but the solid could not be separated into its components. When 0.5 gm. was heated at 145–155° C. for a few minutes and worked up by appropriate manipulation, 0.3 gm. of the anhydride II resulted; the latter was presumably formed by loss of alcohol from the *cis* half ester. On the assumption that the conversion was quantitative, the calculated methoxyl value for the mixture is 8.2%.

(b) Anhydride (III) of 3,4,5,6-tetraphenyl-1,2-dihydro-o-phthalic acid

The anhydride II (1 gm.) was heated for 10 min. in an oil bath at 235–240° C., and the product crystallized from a chloroform-methanol mixture. It formed shining hexagonal plates, m.p. 255° C.; the yield was 1.4 gm. (82%). When acetic acid or benzene was used as solvent, a semi-gelatinous form was obtained. Calcd. for $C_{32}H_{22}O_3$: C, 84.6; H, 4.8%. Found: C, 84.2; H, 5.1%.

cis Methyl 3,4,5,6-tetraphenyl-1,2-dihydrobenzene-o-phthalate, VI. Dry hydrogen chloride was passed through a solution of 0.4 gm. of the anhydride in 40 cc. of absolute methanol at 0° C. for two hours. The solution was then refluxed for one hour. The next day the solvent was partially removed, and 0.3 gm. (68%) of the ester separated from the cold solution. It separated in shiny triangular plates from methanol, m.p. 149–150° C. Calcd. for $C_{34}H_{28}O_4$: OCH_3, 12.4%. Found: OCH_3, 12.2%.

(c) 3,4,5,6-Tetraphenyl-o-phthalic acid, IV

A mixture as in (*a*) was heated at 240–250° C. as long as gas was evolved, and treated with methanol, followed by recrystallization from acetic acid. Yellow rods were obtained, from which the color was removed with difficulty by repeated treatment with decolorizing carbon; m.p. 287° C. Calcd. for $C_{32}H_{22}O_4$: C, 81.7; H, 4.7%; mol. wt., 470. Found: C, 81.3; H, 4.6%; mol. wt., 468, 475. The acid is insoluble in the alcohols, and ether, but dissolves readily in hot ethyl acetate or benzene.

This acid also resulted in yields of 60–78% by heating either of the other anhydrides, II or III, alone or with sulphur at 260–270° C.

**Dilthey (8) gives the melting point 286° C., but analytical figures for the corresponding anhydride.*

The sodium salt separated as silky needles on cooling a hot solution of the acid in a 20% sodium hydroxide solution containing a little alcohol. The acid was regenerated by acidifying the hot solution.

Methyl 3,4,5,6-tetraphenyl-o-phthalate, VIII. Dry hydrogen chloride was passed through a suspension of 1 gm. of the acid in 40 cc. of dry methanol at 0° C. for three hours. After a week the ester had been formed in a yield of 90%; it crystallized in rosettes, m.p. 250–251° C. Calcd. for $C_{34}H_{26}O_4$: OCH_3, 12.4%. Found: OCH_3, 12.1, 12.2%.

It was impossible to secure the ethyl ester by esterification of the acid by any of the usual procedures, but it was obtained as described below.

B. Addition of Methyl Maleate

This same ester, VII, was obtained in a yield of 61% when the red ketone was heated with twice its weight of methyl maleate at 165° C.

C. Addition of Methyl Fumarate

(a) Trans methyl ester, V

Equal weights (2 gm. each) of the red ketone and methyl fumarate were well mixed and heated gently up to 170° C. by means of an oil bath. On cooling, the solid was boiled with 25 cc. of methanol and filtered hot. The residue was taken up in 35 cc. of hot dioxane, and an equal volume of methanol was added. On standing, 1.9 gm. (63%) of fine prisms separated; m.p., 214–215° C. with evolution of gas. Calcd. for $C_{35}H_{28}O_5$: C, 79.5; H, 5.3%. Found: C, 79.5; H, 5.0%.

(b) Trans methyl 3,4,5,6-tetraphenyl-1,2-dihydrobenzene-o-phthalate, VI

By heating the above mixture at 225° C. as long as gas was evolved, and recrystallizing from methanol, a 70% yield of this ester was obtained; it formed needles, m.p. 157° C. Calcd. for $C_{34}H_{28}O_4$: C, 81·6; H, 5.6%. Found: C, 81.3; H, 5.6%. It was also obtained on heating the ester,V; there was some reversal of the addition reaction, since some of the red ketone was also formed.

D. Addition of the Acetylene Dicarboxylic Esters

The methyl ester, VII, was prepared by cautiously heating a mixture of the red ketone and methyl acetylene dicarboxylate over a free flame. The mass was boiled with methanol, evaporated to dryness, and the gummy product washed free from oil with ether; the yield was 31%.

Ethyl 3,4,5,6-tetraphenyl-*o*-phthalate was formed in a 22% yield when 2 gm. of the red ketone and 4 gm. of the ethyl ester* were heated in a sealed tube for two hours at 300–310° C. The resulting mixture was boiled with alcohol, which left the unused ketone as a residue, decolorized with animal charcoal, and crystallized from a dioxane-alcohol mixture. It separated in

* *The acetylene dicarboxylic ethyl ester was kindly supplied by the National Aniline and Chemical Co.: their assistance is gratefully acknowledged.*

clusters of stubby rods, m.p. 187–188° C. Calcd. for $C_{36}H_{30}O_4$: C, 82.1; H, 5.7%. Found: C, 82.1; H, 5.4%. These components did not react at the boiling point of the ester.

This ester is very stable. It was recovered unchanged after being heated to 360° C. with molten potassium hydroxide, as well as after 27 hr. of refluxing with a 40% solution of aqueous alcoholic potash.

E. Addition of Benzoyl Phenylacetylene

2,3,4,5,6-Pentaphenylbenzophenone, VIII

A mixture of equal weights (0.5 gm. each) of benzoyl phenylacetylene and the red ketone was heated slowly to 195° C., in a closed system to measure the gas evolved, and kept at this point for five minutes; 29.8 cc. of gas was collected (calcd. 28.8 cc.). The pink reaction mixture was washed with methanol, leaving a 93% yield of a white product that, on recrystallizing from a dioxane-methanol mixture, formed diamond-shaped prisms, m.p. 340–341° C. It dissolved readily in the usual solvents except methanol. Calcd. for $C_{43}H_{30}O$; C, 91.8; H, 5.3%. Found: C, 91.4; H, 5.4%. It did not form an oxime, and it does not show any addition in the Grignard machine.

F. Miscellaneous

It was found impossible to add benzalacetophenone and *trans* dibenzoylethylene to the red ketone at the boiling point of the mixture, the components being recovered unchanged.

Diphenylketene

The operations were all conducted in an inert atmosphere. In no case was there an apparent reaction, the red ketone being entirely recovered. The conditions were varied widely, but prolonged contact at either low or high (250° C.) temperatures did not lead to the desired result.

G. Anhydracetonebenzil and Maleic Anhydride*

4,5-Diphenyl-7-keto-1,2,3,6-tetrahydro-3,6-methanobenzene-1,2-dicarboxylic Acid, XII

A mixture of 10 gm. each of anhydracetonebenzil and maleic anhyride was heated three to five hours in an ethylene bromide bath (b.p. 131° C.), and, while still hot, dissolved in 225–300 cc. of hot 7% potassium hydroxide solution. The solution was then allowed to cool and filtered. On addition of 80 cc. of concentrated hydrochloric acid an oil separated. The oil was taken up in ether and shaken with sodium carbonate solution. On acidifying the latter with concentrated hydrochloric acid a viscous oil was precipitated; after standing overnight the aqueous layer was decanted. The oil was taken up in alcohol, the solvent evaporated and the amorphous residue dissolved

* *Some of the preliminary experiments were performed by Dr. E. W. Spanagel.*

in chloroform; Skelly Solve C* was added until the solution became cloudy, and the whole allowed to evaporate spontaneously. The viscous mass was dissolved in hot benzene, cooled, and poured into Skelly Solve C with rapid stirring. The precipitate was collected and the process repeated 6–12 times, until an almost white amorphous product was obtained. It was then recrystallized from dilute alcohol until the melting point was 186–187° C. with gas evolution. The yield was 61–65%. The product formed shiny flakes, very soluble in the alcohols and ether, but less soluble in benzene and chloroform. When 10% hydrochloric acid was used in the acidification, the acid potassium salt separated. The silver salt, prepared in the usual manner, melted at 198–199° C. with decomposition. Calcd. for $C_{21}H_{16}O_5$: C, 72.4; H, 4.6%; mol. wt., 348; potassium salt, 9.2% potassium; silver salt, 38.4% silver. Found: C, 72.8, 72.6; H, 4.5, 4.8%; mol. wt., 347; K, 9.4; Ag, 38.5%.

The oxime was obtained by boiling for 27 hr. a mixture of 1 gm. of the acid and the filtered solution resulting from a mixture of 2 gm. of hydroxylamine hydrochloride, 3 gm. of potassium acetate, and 20 cc. of hot alcohol. After standing overnight, 0.65 gm. of prisms separated and was recrystallized from alcohol; m.p. 219–220° C. with decomposition. Calcd. for $C_{21}H_{17}O_5N$: N, 3.8%;—for $C_{21}H_{15}O_4N$: N, 4.1%. Found: N, 4.0%.

Attempted esterification by several methods, including the use of diazomethane, yielded oils that could not be purified. When a solution in absolute methanol was saturated with hydrogen chloride, a solid, m.p. 145° C. after recrystallization from methanol or benzene, was isolated. It was insoluble in sodium hydroxide solution and was recovered unchanged after shaking with concentrated ammonium hydroxide. Its structure was not determined; the analytical values are not far from those of a ketal-diester, XIV.

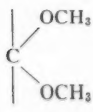

(XIV)

Calcd. for $C_{25}H_{26}O_6$: C, 71.1; H, 6.2; OCH_3, 29.4%. Found: C, 70.1, 70.5, 70.0; H, 5.3, 4.9, 5.2; OCH_3, 28.7, 30.0%.

4,5-Diphenyl-1,2-dihydro-o-phthalic acid, XIII

One gram of the acid XII was heated in an oil bath at 190° C. for one to two minutes, the glassy product taken up in hot benzene, and poured into an equal volume of Skelly Solve C with rapid stirring. The amorphous product was filtered and recrystallized from *p*-cymene. This gave a very fine powder, m.p. 235–243° C. with decomposition; yield, 1.1 gm. (65%). It dissolves readily in the usual organic solvents except petroleum ether. The silver salt had a melting point of 205° C. with decomposition. Calcd. for $C_{20}H_{16}O_4$: C, 75.0; H, 5.0%; silver in silver salt, 40.4%. Found: C, 74.7; H, 4.9; Ag, 40.2%. This acid also gave intractable oils on esterification.

Both acids, when heated with maleic anhydride at 200° C., gave the dianhydride XI. The behavior of these dianhydrides on heating, alone or admixed with an authentic sample, and that of the pure dianhydride, were the same.

* *Petroleum ether fraction, b.p. 90–100° C.: the Skelly Oil Co.*

H. Phenyl Azide

Mixtures of phenyl azide, a solvent, and all of the compounds with a carbonyl bridge, described in this and the previous paper, were kept in sealed tubes at room temperature for three to four months. In every instance, the substances were recovered unchanged.

References

1. ALDER, K. and STEIN, G. Ann. 485 : 211-222. 1931.
2. ALDER, K., STEIN, G. and FRIEDRICHSEN, W. Ann. 501 : 1-48. 1933.
3. ALLEN, C. F. H. and SPANAGEL, E. W. Can. J. Research, 8 : 414. 1933.
4. ALLEN, C. F. H. and SPANAGEL, E. W. J. Am. Chem. Soc. 55 : 3773-3780. 1933.
5. DIELS, O., ALDER, K. and MÜLLER, K. Ann. 490 : 257-266. 1931.
6. DILTHEY, W. and HURTIG, G. Ber. 67 : 495-496. 1934.
7. DILTHEY, W. and QUINT, F. J. prakt. Chem. 128 : 139-149. 1930.
8. DILTHEY, W., SCHOMMER, W. and TRÖSKEN, O. Ber. 66 : 1627-1628. 1933.
9. LÖWENBEIN, A. and ÜLICH, G. Ber. 58 : 2662-2667. 1925.
10. STAUDINGER, H. Die Ketene. F. Enke, Stuttgart. 1912.
11. STAUDINGER, H. and MEYER, P. J. Helv. Chim. Acta. 7 : 19-22. 1924.
12. STAUDINGER, H. and RHEINER, A. Helv. Chim. Acta. 7 : 8-18. 1924.
13. STAUDINGER, H. and SUTER, E. Ber. 53 : 1092-1105. 1920.
14. ZIEGLER, K. and SCHNELL, B. Ann. 445 : 266-282. 1925.

STUDIES ON HOMOGENEOUS FIRST ORDER GAS REACTIONS

V. THE DECOMPOSITION OF PARACETALDEHYDE AT HIGH PRESSURES[1]

By A. L. Geddes[2] and C. C. Coffin[3]

Abstract

The homogeneous first order gaseous decomposition of paraldehyde to acetaldehyde has been studied at temperatures from 230 to 254° C. up to pressures at which the liquid phase makes its appearance, *i.e.*, 12 atm. at 230° and 18 atm. at 254° C. Over-all velocity constants for the homogeneous reaction in the heterogeneous liquid-vapor system have been determined from these pressures up to the critical point. The data confirm results already published. It is found that in the purely gaseous system increase of pressure tends to diminish the reaction velocity. That the specific reaction velocity in the liquid phase is greater than that in the vapor phase is shown by the fact that the velocity constants of the heterogeneous systems increase progressively with the liquid-vapor ratio. Extrapolation to 100% of liquid gives velocity constants about five times as great as those characteristic of the vapor phase. Peculiarities in the behavior of the system at the critical point and preliminary measurements of the velocity of the trimolecular reverse reaction are described.

Introduction

Measurements of the rate of decomposition of paraldehyde to acetaldehyde at pressures up to, and beyond, the critical were undertaken for several reasons. In the first place it is of considerable importance to find a third order gas reaction suitable for study, and in this respect the reverse of the paraldehyde decomposition looked promising (1). It is also of interest to follow the rate and mechanism of such a simple clean-cut reaction through as large a concentration range as possible, as it is not clear from existing data to what pressures the limiting "high pressure rate" of a first order reaction may be extrapolated. The scarcity of data with regard to the rates of a first order reaction in the gaseous and liquid states, particularly in view of the catalytic effect associated in some types of reaction with the presence of the liquid phase (4, 9), was a further incentive to the undertaking of this work. Moreover, it was considered desirable to check the data already obtained for this decomposition (1) by an experimental procedure as different as possible from that previously employed. Such a check is particularly necessary in the case of a reaction as susceptible to traces of impurities as the paraldehyde decomposition appears to be.

It must be stated at once that the above objects are still far from being completely attained. The present paper is concerned only with reaction velocities in the vapor state up to pressures where the liquid phase appears, and with a preliminary exploration of the heterogeneous liquid-vapor system up to, and beyond, the critical point.

[1] *Manuscript received June 5, 1934.*
Contribution from the Laboratory of Physical Chemistry, Dalhousie University, Halifax, Nova Scotia, Canada.

[2] *Graduate Student in Chemistry, Dalhousie University.*
[3] *Associate Professor of Chemistry, Dalhousie University.*

Experimental

Purification of the Paraldehyde

Paraldehyde from three different sources was purified in several different ways. As no consistent difference in reaction velocity was evident among these samples, details of the methods employed need not be given. It is sufficient to state that the essential step in each case was one of the following:—recrystallization, fractional distillation at atmospheric pressue and *in vacuo*, treatment with metallic sodium and distilling, or freezing several times in a high vacuum and subsequently subliming at low pressures.

Rate Measurements at the Lower Pressures

Velocity constants were calculated from the changes in composition that occurred when bulbs containing paraldehyde were kept for a definite time in a thermostat. In the case of runs below about 20 atm. the reaction bulbs were made from wide (2–3 cm.) Pyrex tubing and were shaped as shown at *B* in Fig. 1. The thermostat, *H*, was an air bath consisting of a Pyrex Dewar flask (25 by 10 cm.) heavily lagged with shredded asbestos and connected to an electrically heated mercury boiler and a water cooled reflux condenser as shown in the diagram. The flask was lined with heavy sheet copper to increase its heat capacity and to protect it in case of an explosion. The pressure on the boiling mercury and in the 20-litre stabilizing volume (connected at *S*) was read on the manometer *M* and could be adjusted by manipulation of taps connected to a source of dry air or to an evacuating system. Temperatures were determined from the vapor pressure curve of mercury.*

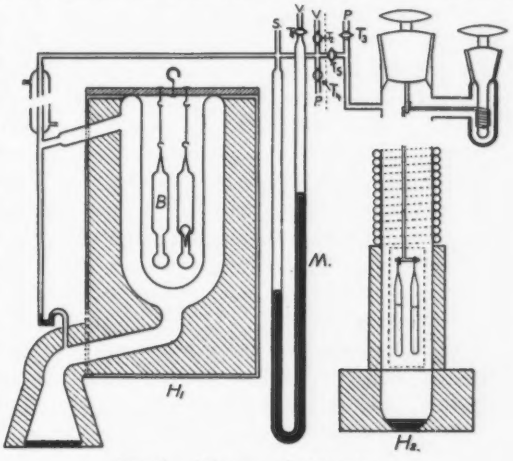

FIG. 1. *Diagram of apparatus.*

In the experiments at the lower pressures a sealed Pyrex capsule containing a weighed amount of paraldehyde was introduced into the open end of the reaction tube which was then drawn down, sealed to a manifold, thoroughly evacuated and sealed off. The capsule burst and the reactant vaporized when the bulb was lowered into the thermostat.

**This form of oven has been found to be very convenient for obtaining constant temperatures between 200 and 300° C. It has many obvious advantages over a liquid bath especially in this temperature range. The disadvantage that reaction bulbs do not reach the thermostat temperature as rapidly as when plunged into a liquid was eliminated here by working at temperatures low enough for the uncertainty about zero time to be negligible in comparison with the total time.*

Great pains were taken in cleaning and evacuating the reaction bulbs. In most cases the bulbs were cleaned with hot chromic acid mixture, thoroughly washed with distilled water and flamed *in vacuo* to a temperature near their softening point. In some instances all washing was avoided, the glass being simply wiped out with cotton plugs and flamed as before. As the treatment to which the bulbs were subjected, or the addition of broken glass, had no appreciable influence on the rate of decomposition, it is concluded that the reaction is homogeneous.

In the experiments at pressures greater than 10 atm. the empty reaction bulbs were sealed to a manifold and evacuated. They were then connected with a reservoir of carefully purified paraldehyde at room temperature and were kept at −78° C. until a suitable quantity had condensed in each bulb, which, after melting and freezing its contents several times *in vacuo*, was sealed off. The amount of paraldehyde in each bulb was determined at the end of the experiment by weighing the bulb before and after opening. Volumes were determined after opening by filling with water. Pressures were calculated from the gas laws.

After a definite time in the thermostat the reaction tubes were removed and the small bulbs at the bottom (see *B*, Fig. 1) were immersed as quickly as possible in a carbon dioxide-ether mixture to freeze out the contents. The bulbs were hung by hooks (shaped when sealing off after filling) from the heavy asbestos thermostat cover which could be raised or lowered from a distance by means of a system of strings and pulleys. The operator was thus out of range of the explosions which sometimes occurred as a result of the system cooling too rapidly. The bulbs were usually left in the thermostat for a length of time sufficient to allow the reaction to progress approximately to half-value. The extent to which the paraldehyde had decomposed was determined by one or both of two different methods.

1. The small bulb at the end of the reaction tube was cut off and dropped, while its contents was still frozen, into a stoppered flask containing 50 cc. of ice-cold sodium bisulphite solution of known iodine titre. The solution was titrated with standard iodine after it had stood for half an hour at 0° C. Preliminary experiments had shown that the method gave consistent and reliable results provided that the equilibrium between sodium bisulphite and acetaldehyde (8) was taken into account.

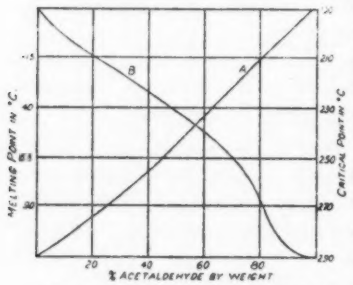

FIG. 2. *Curve A,—Critical temperatures of paraldehyde-acetaldehyde mixtures. Curve B,—Melting points of paraldehyde-acetaldehyde mixtures.*

2. The melting point of the bulb contents was determined and the composition of the mixture was interpolated from Hollmann's data (6) on the freezing points of paraldehyde–acetaldehyde mixtures (Curve B, Fig. 2). An alcohol-ether mixture vigorously stirred by means of a current of dry air and contained in a large transparent Dewar flask served as the melting point bath. The temperature

was regulated by the addition of "dry ice" or alcohol, and was measured on an alcohol thermometer graduated in $\frac{1}{5}$° C. and calibrated for total immersion over its whole range against a standardized thermocouple. Only the small bulbs at the bottom of the reaction tubes were immersed—the remainder of the tube being at room temperature. As the melting point was approached the temperature was allowed to rise very slowly and the contents of the bulbs was kept well mixed by vigorous shaking. The error due to vaporization of acetaldehyde was shown to be negligible for all temperatures and bulb volumes employed.

The extent to which the two analytical methods agree is shown in Table I, in which the velocity constants of some typical experiments at 230° C. are listed. As explained below the pressures given in Column 1 are the initial pressures that would have prevailed had all the paraldehyde vaporized. Actually, above 12 atm. liquid was present at this temperature during part of the time the bulbs were in the thermostat and the calculated pressure is simply taken as a measure of the over-all concentration. Columns 2 and 3 give the velocity constants determined by the titration method for reaction periods of three and six hours respectively. Constants as determined from the melting point after three and six hours in the thermostat are listed in Columns 4 and 5. In cases where both methods were used for the same bulb the melting point was of course determined before titrating.

TABLE I

TYPICAL FIRST ORDER VELOCITY CONSTANTS DETERMINED BY DIFFERENT METHODS AND FOR DIFFERENT TIMES OF REACTION. TEMPERATURE 230° C.

Initial press., atm.	$k \times 10^5$ by titration method		$k \times 10^5$ by melting point method		$k \times 10^5$ average	Initial press., atm.	$k \times 10^5$ by titration method		$k \times 10^5$ by melting point method		$k \times 10^5$ average
	Time, 3 hr.	Time, 6 hr.	Time, 3 hr.	Time, 6 hr.			Time, 3 hr.	Time, 6 hr.	Time, 3 hr.	Time, 6 hr.	
1.6	—	4.9	5.2	4.3	4.8	11.5	—	—	4.1	4.1	4.1
1.9	—	4.3	4.7	3.8	4.2	11.4	—	—	3.8	4.0	3.9
2.8	5.8	—	5.6	—	5.7	13.1	—	—	4.1	4.2	4.1
3.8	5.0	—	4.9	—	4.9	14.9	5.4	—	6.0	—	5.7
3.3	5.5	—	5.3	—	5.4	22.1	—	5.5	6.1	5.3	5.6
7.4	3.9	—	3.6	—	3.8	26.3	7.3	—	—	—	7.3
7.8	3.9	—	3.8	—	3.8	23.8	—	—	7.1	—	7.1
8.2	3.7	—	3.5	—	3.6	25.7	—	—	6.7	—	6.7
9.9	3.5	—	3.4	—	3.4	25.9	—	—	7.5	—	7.5
6.6	4.2	—	4.2	—	4.2	34.9	—	—	8.5	—	8.5
10.4	4.4	—	4.1	—	4.3	30.0	—	—	8.5	—	8.5
10.9	—	3.5	3.5	3.3	3.4	27.8	—	—	7.7	—	7.7
11.6	—	4.4	4.1	4.1	4.2						

It will be observed that for any one bulb the two methods agree as well as can be expected in work of this kind. In the later experiments the melting point method only was employed. After the experiments, in all cases, the contents of the bulbs were kept frozen until they could be analyzed.

The analytical methods described above were used in the case of bulbs in which the calculated initial pressures were less than about 15 atm.

If the volume of liquid in the bulb were less than a certain percentage of the total volume, the liquid disappeared on attaining the temperature of the thermostat and the reaction proceeded in the vapor phase. If the volume of the liquid were above this percentage, the liquid phase persisted until enough paraldehyde had decomposed to allow complete vaporization. These limiting volumes were determined by filling tubes to various levels and observing the time taken for the liquid to evaporate at the temperatures in question. The curves obtained were extrapolated to zero time and the corresponding initial percentage volumes were read from the graph. The results are shown in Table II. At these temperatures therefore bulbs containing volumes of liquid greater than these limiting percentages yielded "composite" velocity "constants"—part of the constant representing the velocity in the liquid phase, and part that in the vapor phase. These constants will be discussed later.

TABLE II

Temp., °C.	Initial % volume of liquid (at room temp.)	Calculated pressure of paraldehyde at temperature of thermostat, atm.
230	4	12.5
242	5	15.7
254	6	19.0

It was observed also that if a bulb more than 15% full of liquid at room temperature were placed in the thermostat, the critical composition of the system was reached before all the liquid had evaporated, *i.e.*, the liquid phase finally disappeared not by evaporation but by disappearance of the meniscus. If a bulb were more than about 50% full at room temperature it became filled with liquid before the critical composition was reached, and of course burst. In the case of bulbs between 15 and 50% full, therefore, over-all velocity constants were obtained by the following method which is based on the fact that the meniscus becomes invisible at any one temperature when a definite composition is reached.

Rate Measurements at the Higher Pressures

The bulbs were made of 2–3 mm. bore heavy walled Pyrex capillary tubing and were filled as before by distillation *in vacuo*. The reaction was carried out by immersing the bulbs directly in mercury vapor in the thermostat H_2 (Fig. 1), which consisted of a three-foot length of two-inch Pyrex tubing connected as shown to manometer, evacuating system, etc. The bulbs could be lowered quickly into, or removed from, the mercury vapor (below the copper cooling coil) by means of a hoist, the operation of which is obvious from the diagram. The entire length (10–15 cm.) of the bulbs was visible through the double window (dotted rectangle) cut in the asbestos insulation. During the reaction they were observed through a cathetometer behind a heavy plate glass shield. The time taken for the meniscus to disappear was noted and the composition of the mixture when this occurred was inter-

polated from Hollmann's (6) critical temperature curve (curve *A*, Fig. 2) for the two-component system. The total volume of the bulb and the initial volume of liquid paraldehyde at room temperature were estimated to a sufficient degree of accuracy with the cathetometer. First order velocity constants for the reaction in the heterogeneous system were calculated from the time taken to reach the critical composition.

These experiments exhibited some interesting features. During the reaction the position of the meniscus changed as shown in Fig. 3. The numbers on the curves of Fig. 3, *A*, (242° C.), and 3, *B*, (254° C.), are the percentages of the total bulb volume occupied by the liquid at room temperature. The ordinates give the change (in centimetres) in the height of the meniscus during the reaction and are calculated to a bulb length of 10 cm.; the zero is the position occupied by the meniscus at the temperature of the thermostat before any reaction has occurred. The abscissas represent the time; the end of each curve is the point at which the meniscus became invisible. All observations were made with a cathetometer.

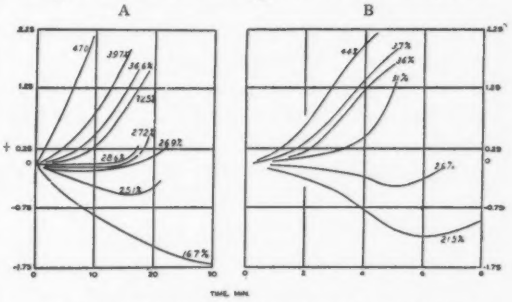

FIG. 3. *Change of position of meniscus with time at 242° C. (A) and at 254° C. (B).*

It will be observed that when a bulb more than about 27% full of liquid at room temperature is placed in the thermostat the meniscus steadily rises until it flattens out, becomes wider and less distinct, and finally disappears. If a bulb is less than 27% full the meniscus falls as the reaction proceeds until just before its disappearance, when it begins to rise. This rise does not occur until the surface has become mobile and hazy and is unmistakably a relatively broad density gradient. The same upward drift of the meniscus just before the critical point is reached occurs also in bulbs slightly more than 27% full and is the only movement of the meniscus during the reaction in bulbs just 27% full. It is noteworthy that Maass and coworkers (10) have observed that bulbs about 27% full of methyl ether, ethylene and propylene can be raised to the critical temperature without change in the position of the meniscus. This point is being considered more fully in another paper.

The appearance of the critical phenomenon differed somewhat from that usually observed in the case of one-component systems. In all bulbs, streams of bubbles much too small to appreciably affect the stability of the meniscus ascended continually throughout the reaction and became invisible when the meniscus did; no opalescence was visible as the critical composition was reached and passed. If, however, the bulbs were allowed to cool slowly and uniformly after the liquid phase had vanished, the phenomena associated with the reappearance of the meniscus were practically identical (except for

the bubbles) with those observed by Travers and Usher (11), for example, in their study of one-component systems. Thus if the meniscus had vanished near the top of the bulb the fog appeared in the space that had been occupied by the vapor; when it had disappeared near the bottom of the bulb the fog became visible in the space that had been occupied by the liquid. In the case of tubes 27% full the fog was uniformly distributed throughout the whole volume. Bulbs cooled so that a temperature gradient existed along their length frequently presented a very curious appearance for a few moments; *e.g.*, two and even three liquid surfaces were often present at the same time.

It should be pointed out that a polymerization reaction occurs to an appreciable extent if the liquid phase remains for a sufficient length of time. Thus at 230° C. the critical phenomena cannot be observed as the high boiling polymer has time to be formed in quantities sufficient to prevent the change of state. The polymer is dark red in color and according to Hollmann (6) its presence is readily detected by the yellow tinge it imparts to the liquid.

The Reverse Reaction

The critical point method described above is being used also to measure the velocity of the reverse reaction, *viz.*, the condensation of gaseous acetaldehyde to paraldehyde. Here the situation is more favorable for such a method, in that the system remains homogeneous until the composition is indicated by the appearance of the liquid phase and the experiment is completed. Preliminary experiments have given third order constants between 2 and 3 $\times$ 10^{-6} at 210.6° C. (nitrobenzene vapor).

Discussion of Results

The velocity constants obtained for the paraldehyde decomposition are plotted as ordinates in Figs. 4 (230° C.) and 5 (242 and 254° C.). The abscissas in Fig. 4 are the initial pressures that would have existed had all the paraldehyde vaporized. As already stated, when the calculated pressure is above about 12 atm. at 230° C. the liquid phase persists for a length of time which is proportional to the amount of paraldehyde present. A velocity constant above this calculated pressure therefore does not represent a true velocity in any one phase, but it may be regarded as a measure of the rate at which the heterogeneous system as a whole tends to reach equilibrium. The fact that these "constants" increase with the amount of liquid phase present indicates that the specific reaction velocity is greater in the liquid than in the vapor phase. It is to be noted that the minimum in the curve of Fig. 4 corresponds approximately to the point at which the systems become heterogeneous.

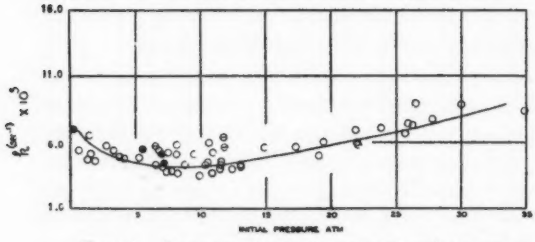

FIG. 4. *Variation of velocity constant with pressure at 230° C.*

In Fig. 5 the velocity constants at 242 and 254° C. are plotted against the initial percentage volume of paraldehyde in the bulbs at room temperature. The data below 15% volume were obtained by either melting points or titrations as already described. The contents of the bulbs more than 15% full were caused to react in the thermostat H_2, and were "analyzed" by observing the time taken for the meniscus to disappear. In these curves also the reaction velocity begins to increase after the liquid phase makes its appearance.

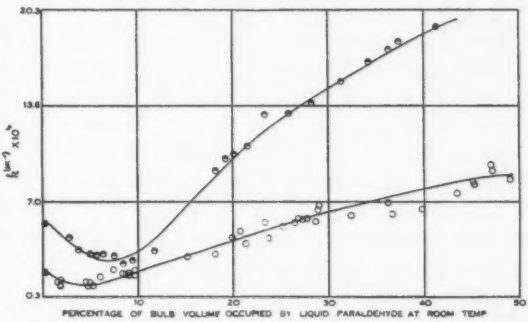

FIG. 5. *Velocity constants plotted against initial percentage volume of liquid. Upper curve,—254° C. Lower curve,—242° C.*

From the good agreement shown in Table I between the velocity constants determined for the same bulb after three hours' (approximately 50% reaction) and after six hours' (approximately 75% reaction) at 230° C., it is apparent that the decomposition remains first order for any one experiment over the pressure range in question. Table III which shows the velocity constants for different times of reaction at 242° C. is further evidence that this is the case. The time to half-value at 242° C. is roughly one hour.

TABLE III

FIRST ORDER CONSTANTS FOR DIFFERENT REACTION TIMES AT 242° C. COMPOSITIONS WERE CALCULATED FROM MELTING POINTS

% volume of paraldehyde at start (room temperature)	$k \times 10^4$ after 1 hr.	$k \times 10^4$ after 1.5 hr.	$k \times 10^4$ after 2 hr.	Mean $k \times 10^4$
1.6	1.4	1.3	—	1.4
1.8	1.2	1.0	—	1.1
1.9	1.5	1.3	—	1.4
8.3	1.9	—	1.7	1.8
8.7	2.0	—	1.7	1.8
9.0	1.9	—	1.6	1.7
9.4	2.2	—	1.9	2.0
9.7	2.4	—	2.3	2.3
9.7	1.8	—	1.7	1.7

The points ⊙ on the ordinates of Figs. 4 and 5 are the velocity constants calculated from the previously published (1) rate equation, *viz.*,

$$\ln k = 34.83 - \frac{44200}{RT}.$$

The good agreement between the results obtained by such widely different experimental methods is evidence that a true uncatalyzed reaction velocity is being measured. The points ● (Fig. 4) were obtained with bulbs containing a drop of mercury; the bulbs with which the points ⊖ were obtained were filled with finely broken glass. It is thus apparent that mercury vapor and glass surface are without appreciable effect on the rate of decomposition. Runs at 230° C. between 5 and 30 cm. pressure were made in an apparatus described elsewhere (2), with each of the six different preparations of paraldehyde used in obtaining the data of Fig. 4. As these experiments all gave constants between 6.5 and 6.9 $\times$ 10^{-5} it is probable that no catalytic impurity was present in any of the samples of paraldehyde used, and that the wide scattering of the points in Fig. 4 is due to errors in the rather difficult analyses.

The most striking feature common to the curves of Figs. 4 and 5 is the apparent drop in the velocity constant at any one temperature as the pressure is increased up to the point where the liquid appears. This decrease in velocity is so small that it is observable only over a large pressure range. It is however believed to be real and is being more carefully investigated. The scarcity of data with regard to clean-cut first order reactions at high pressures makes such a study particularly desirable. The authors have already suggested (3) that in the case of complex molecules, in which the energy distributions most probable on collision are not coincident with those most favorable to reaction, an increase in the number of collisions may mean a decrease in the rate of reaction. Kassel, however, has shown (7) that such a mechanism is unlikely. Experiments designed to reveal the cause of this effect and to discover to what extent it is characteristic of the decomposition of complex molecules are in progress.

From the curves of Figs. 4 and 5 it is evident that the specific reaction velocity is greater in the liquid than in the vapor phase. A rough idea of the velocity in the liquid phase may be obtained by extrapolating the curves for the heterogeneous systems to 100% liquid volume (66–69% volume at 20° C.). The results of the extrapolation are given in Table IV. The velocity constants in the vapor phase at pressures below one atmosphere (column 3) are calculated from the rate equation (1).

TABLE IV

FIRST ORDER VELOCITY CONSTANTS IN LIQUID AND VAPOR PHASES

Temp., ° C.	k (liquid phase)	k (vapor phase)
230	3×10^{-4}	6×10^{-5}
242	1×10^{-3}	2×10^{-4}
254	2.5×10^{-3}	5.5×10^{-4}

It will be observed that the specific reaction rates in the liquid state are about five times as large as those in the vapor state at the three different temperatures. It would thus appear that the temperature coefficients and hence the activation energies are the same in each phase, and that whatever may be the mechanism underlying the catalytic activity of the liquid state it is

not to be ascribed to a lowering of the activation energy. It must be remembered, however, that the uncertainties in the extrapolated values are so large that the figures of Table IV can be of significance only in so far as order of magnitude is concerned. Moreover, as a fall in E of 2000 calories would be more than sufficient to increase the reaction velocity by a factor of five, the necessity of more complete data in this connection is obvious.

References

1. COFFIN, C. C. Can. J. Research 7 : 75-80. 1932.
2. COFFIN, C. C. Can. J. Research 9 : 603-609. 1933.
3. COFFIN, C. C. and GEDDES, A. L. J. Chem. Phys. 2 : 47-48. 1934.
4. COFFIN, C. C. and MAASS, O. Can. J. Research 3 : 526-529. 1930.
5. COFFIN, C. C. and MAASS, O. Can. J. Research 3 : 540-542. 1930.
6. HOLLMANN, R. Z. physik. Chem. 43 : 129-159. 1903.
7. KASSEL, L. S. J. Chem. Phys. 2 : 106. 1934.
8. STEWART, A. W. J. Chem. Soc. 87, 185. 1905.
9. SUTHERLAND, H. S. and MAASS, O. Can. J. Research 5 : 48-63. 1931.
10. TAPP, J. S., STEACIE, E. W. R. and MAASS, O. Can. J. Research 9 : 217-239. 1933.
11. TRAVERS, M. W. and USHER, F. L. Proc. Roy. Soc. A. 78 : 247-261. 1906.

STUDIES ON THE OVERWINTERING OF CERTAIN FUNGI PARASITIC AND SAPROPHYTIC ON FRUIT TREES[1]

By L. W. Koch[2]

Abstract

Evidence is submitted that some conidia of the black knot fungus, *Dibotryon morbosum* (Sch.) T. and S., are capable of overwintering in a viable condition on *Prunus domestica*. *D. morbosum* has also been isolated on numerous occasions during the winter from definite chlamydospores on buds and bark of *P. domestica*. Pure cultures of *D. morbosum* produced chlamydospores only when grown in close proximity to certain other organisms, or when certain chemicals were introduced into the Petri dishes. Chlamydospore formation was also induced on twigs of *P. domestica* when conidia of *D. morbosum* germinated in intimate association with a strain of bacteria originally isolated from the same host. *Cladosporium carpophilum* was isolated in several instances from chlamydospores on the bark of *Prunus persica*. This organism also produced chlamydospores both on culture media and on peach twigs. A histological study revealed the presence of two types of twig lesion. Early infections produced primary lesions during the summer, and secondary lesions during the following winter as a result of the migration of the mycelium beyond the barriers of periderm delimiting the primary lesions. Late infections, on the other hand, rarely induced periderm formation and did not produce secondary lesions during the winter. *Taphrina deformans* was isolated during the winter from the surface of buds on *P. persica*. Proof is submitted that spores of *T. deformans* can remain viable throughout the winter on twigs of the above-mentioned host. Other fungi, presumably saprophytes, representing the genera *Coniothyrium*, *Cladosporium*, *Hormodendrum*, *Fumago* and a fungus impossible to identify because it produced chlamydospores only, all developed from chlamydospores occurring on various hosts. The latter fungi all produced chlamydospores in culture. The evidence obtained indicates the probability that many more fungi overwinter as chlamydospores than have been reported to do so. Certain misapplications of the term chlamydospore in the various groups of fungi are dealt with. Owing to their unsatisfactory mycological status the importance of chlamydospores has hitherto been incompletely appreciated. The results of these investigations emphasize the importance of the application of a dormant spray on fruit trees.

Introduction

The mode of overwintering of fungi parasitic on fruit trees is an unusually interesting problem, especially in view of the fact that certain of them have not been shown to produce a perfect stage. In the case of those organisms which do produce a perfect stage during the winter the ascospores are generally accepted as the only viable winter spore form and the possibility of the overwintering of other spore forms remote in time and place from the parent mycelium has not been investigated.

The present investigation was undertaken primarily to discover whether any of the fungi causing diseases of fruit trees overwinter by any method or methods other than those already reported. These investigations, conducted over the four-year period 1930-1934, evolved from a study of black knot, the causal organism of which was demonstrated in 1930 to be capable of overwintering in a form hitherto unreported. The studies were then extended to include not only *Dibotryon morbosum* (Sch.) T. and S., but also *Cladosporium*

[1] *Manuscript received May 23, 1934.*
Contribution (No. 403) from the Division of Botany, Experimental Farms Branch, Department of Agriculture, Ottawa, Canada.
[2] *Assistant Plant Pathologist, Dominion Laboratory of Plant Pathology, St. Catharines, Ontario.*

carpophilum Thüm., and *Taphrina deformans* (Fcl.) Tul., as well as certain saprophytic members of the Fungi Imperfecti. The latter were included because their method of overwintering was found to be similar to that of the pathogenes. For the purpose of clarity each organism has, for the most part, been dealt with separately in the present article.

Materials and Methods

Since in the investigations outlined below both the choice of materials and technique employed were the same for the different organisms concerned, a general outline of the methods and materials involved will suffice.

For purposes of isolation, buds and bark from branches of all ages were removed from *Prunus domestica*, *P. cerasus*, *P. americana*, *P. persica*, *Pyrus communis* and *Pyrus malus*. Earlier in the investigations various methods for freeing the fungous populations from the surfaces of buds and bark were attempted. These consisted of soaking in water overnight, centrifuging, etc., but the method finally adopted as most successful involved the moistening of the surfaces of buds or bark with sterile water for a period varying from 15 to 30 min. The moistened surface was then scraped lightly with a sterile scalpel and the cuticular and epidermal tissues thus removed were suspended in a drop of sterile water on a sterile slide and macerated thoroughly. The latter process was most necessary for the separation of the various organisms that were present. Loopfuls of the suspension were streaked on the surface of potato-dextrose agar in Petri dishes, the medium having been centrifuged prior to pouring to remove the larger opaque particles. By using dilutions of appropriate concentrations it was usually not difficult to remove separately the fungi which developed on the plates. Careful exploratory work with the microscope at frequent intervals during the subsequent few days revealed the presence of fungi in the form of (i) fragments of mycelium, and (ii) dark, thick-walled spores probably in the resting condition. Certain of these germinated quickly, others more slowly. This necessitated their removal at successive intervals to prevent one from overrunning the other. All were removed by the method employed by Keitt (9).

Dibotryon morbosum (Sch.) Sacc.

Since 1821 when Schweinitz (16) described the perithecial stage of the organism causing black knot, the fungus, since named *D. morbosum*, has been assumed to overwinter only in the form of mycelium perennial in those infected branches of *Prunus* spp. on which perithecia develop in the winter. The only other method which to date has received consideration by other investigators has been the possible overwintering of conidia produced the previous summer. The consensus of opinion in this regard, as expressed by Selby (17), has been that the conidia are incapable of remaining viable through the winter.

In the present study the possibility of the overwintering of conidia has been reinvestigated and other means have also been sought by which the fungus might perpetuate itself throughout the dormant season.

Conidia

To test the viability of conidia after exposure to winter conditions, tube cultures of the conidial stage as well as masses of dry conidia of *D. morbosum* in Petri dishes were placed outdoors about October 1 for three successive years. At the same time, suspensions of conidia were painted on buds and on surface-sterilized twigs, particularly at nodes. In these experiments only the most easily recognized strain of *D. morbosum* was used. Re-isolations from all of the above-mentioned materials were made at intervals of three weeks throughout the winter.

Particular care was taken to identify the pathogene on the twigs because another closely related fungus was frequently isolated from apparently normal twigs of *P. domestica*.

Periodic platings of materials lightly scraped both from the roughened surface of knots and from that of the bark adjacent to knots, consistently yielded isolants of *D. morbosum*, thus lending confirmatory evidence as to the ability of some conidia, at least, to remain viable throughout the entire winter.

In parallel experiments it was found also that conidia of *D. morbosum* placed in dry, sterile Petri dishes remained viable at room temperatures for 388 days, and in a refrigerator at −6° C., for at least 420 days.

To investigate the possibility of *D. morbosum* overwintering on buds or bark of *Prunus* spp. series of isolations were made at intervals during four consecutive winters. In the case of *P. domestica* isolations were made from check trees in the laboratory orchard (11) which were severely infected with black knot. Isolations from *P. cerasus* were made from buds and bark of specimens obtained from severely infected trees in unsprayed orchards in the Georgian Bay district. The results of these isolations are summarized in Table I.

TABLE I

SUMMARY OF RESULTS OF ISOLATIONS OF *D. morbosum* FROM *P. domestica* AND *P. cerasus*

Time of isolation	Source of isolations	Frequency of occurrence of organism	
		From monochlamydospores*	From undetermined sources
October to April	Scrapings from bark of *P. domestica*	42	115
October to April	Scrapings from buds of *P. domestica*	20	60
October, December and April	Scrapings from bark 6–10 in. from knots on *P. cerasus*	12	23

**The term "chlamydospore" as used in this article in connection with the fungi under investigation may be defined as a single or many-celled, thick-walled body, frequently with dense contents, sometimes highly vacuolated, borne on non-specialized, vegetative mycelium either in a terminal or intercalary position, and germinating by a germ tube.*

It will be observed in Table I that *D. morbosum* appeared 272 times in isolations made during four successive winters from the surface of buds and bark of *P. domestica* and *P. cerasus*. In 74 cases this organism developed from single chlamydospores and while the origin of the other 198 was not definitely determined, undoubtedly many of these also were of similar origin.

It is interesting to note in the above experiments: (i) that a fungus, identified as the conidial stage of *D. morbosum*, remained viable throughout the winter on buds and bark, and (ii) that in many instances the organism was perpetuated by chlamydospores, a spore form hitherto unreported for this fungus.

It should be pointed out here that in connection with all isolations involving chlamydospores, extreme care was taken to select single chlamydospores. In some instances, however, it was impossible to distinguish single compound chlamydospores from small groups possibly consisting of single-celled chlamydospores. In the case of intercalary chlamydospores difficulty was also experienced in separating the latter from mycelial fragments.

Artificially Induced Production of Chlamydospores by D. morbosum

In the face of the fact that *D. morbosum* developed from chlamydospores on buds and bark of *P. domestica*, although chlamydospores have never been reported in connection with the life history of this fungus, it was essential to demonstrate the capability of the organism to produce chlamydospores in culture.

The subjection of pure cultures of the organism growing on different media to a wide range of environmental conditions, particularly of temperature and moisture, failed to induce chlamydospore production. It was finally discovered, however, that an abundance of chlamydospores invariably developed in cultures to which certain organisms or chemicals were introduced.

(a) Production of Chlamydospores in the Presence of Certain Organisms

Petri dishes containing potato-dextrose agar were streaked on one half with conidia of *D. morbosum* and on the opposite half at some distance away, either (i) with suspensions of certain bacteria isolated from bark of *P. domestica* or (ii) with conidia of *Cephalothecium roseum* isolated from the surface of black knots (11). Both organisms grew normally for a few days, after which time, however, the growth of the mycelium of *D. morbosum* nearest to the bacteria or to *C. roseum* was arrested. This phenomenon was observed even when the organisms were separated by the distance of one inch, when there was less than 10 cc. of medium in the Petri dish in which the organisms were growing. Shortly after the arrest of growth an abundance of chlamydospores both intercalary and terminal (Plate I, Figs. 1–7) appeared on the mycelium of *D. morbosum* in closest proximity to the antagonistic bacteria, or to *C. roseum*.

A series of experiments in which suspensions of conidia of *D. morbosum* and of the antagonistic bacteria were intimately mixed and streaked on the surface of potato-dextrose agar resulted in similar but more marked results.

In these cases the conidia germinated slowly, but instead of normal germination, the majority formed typical, large, chlamydospore-like bodies either in direct association with the conidia or at the distal end of a short germ tube (Plate II, Figs. 6, 8, 9). These bodies were thick-walled and highly vacuolated, and became gradually darker in color with age. At intervals up to three weeks they were transferred to fresh acidified agar where a proportion of them always germinated and developed normal colonies of *D. morbosum*.

In another series of experiments small squares of agar were removed from just beyond the periphery of (i) colonies of the antagonistic bacteria and (ii) colonies of *D. morbosum*. The former were then transferred to the spaces previously occupied by the latter. It was observed that the cubes of agar removed from the proximity of the bacteria exerted the same inhibiting influence and induced chlamydospore formation as effectively as the bacteria themselves. Filtrates from the bacterial cultures also produced a similar though less marked effect.

(b) Production of Chlamydospores by the Introduction of Chemicals into Petri Dish Cultures of D. morbosum

Certain chemicals including sulphuric, nitric and hydrochloric acids, copper sulphate crystals, potassium and sodium nitrate and paradichlorobenzol were introduced into Petri dishes containing colonies of *D. morbosum*. Two of these chemicals, namely, sulphuric acid and copper sulphate, more particularly the former, induced chlamydospore formation.

When one drop of 75% sulphuric acid was introduced at the edge of a Petri dish in the centre of which was growing a young colony of *D. morbosum* the growth of the hyphae on the side of the colony nearest the acid was arrested. Twelve hours afterwards the beginning of chlamydospore formation was observed. The growth of the hyphae on the opposite side of the colony, on the other hand, appeared to be quite normal. Chlamydospore formation in these cultures, in some cases after a week or more, was followed by the formation of sclerotium-like bodies (Plate II, Fig. 10). In some instances where sulphuric acid was introduced into plates containing large amounts of media (about 15 cc.) extraordinarily large chlamydospore-like bodies developed. These bodies, much larger than either those observed outdoors or those more commonly observed in cultures, were almost spherical in shape, dark brown and usually thick-walled and vacuolated (Plate II, Figs. 1 and 4), and germinated by germ tubes in the same manner as those previously described (Plate II, Figs. 2, 3 and 5).

(c) Outdoor Experiments

To determine whether or not chlamydospore formation in *D. morbosum* could be induced outdoors on branches of *P. domestica*, water suspensions of conidia of the former mixed with antagonistic bacteria were painted on surface-sterilized, current-season twigs in September and October. As controls, other twigs, some of which were surface-sterilized and others not, were painted with pure suspensions of conidia of *D. morbosum*. The spore-

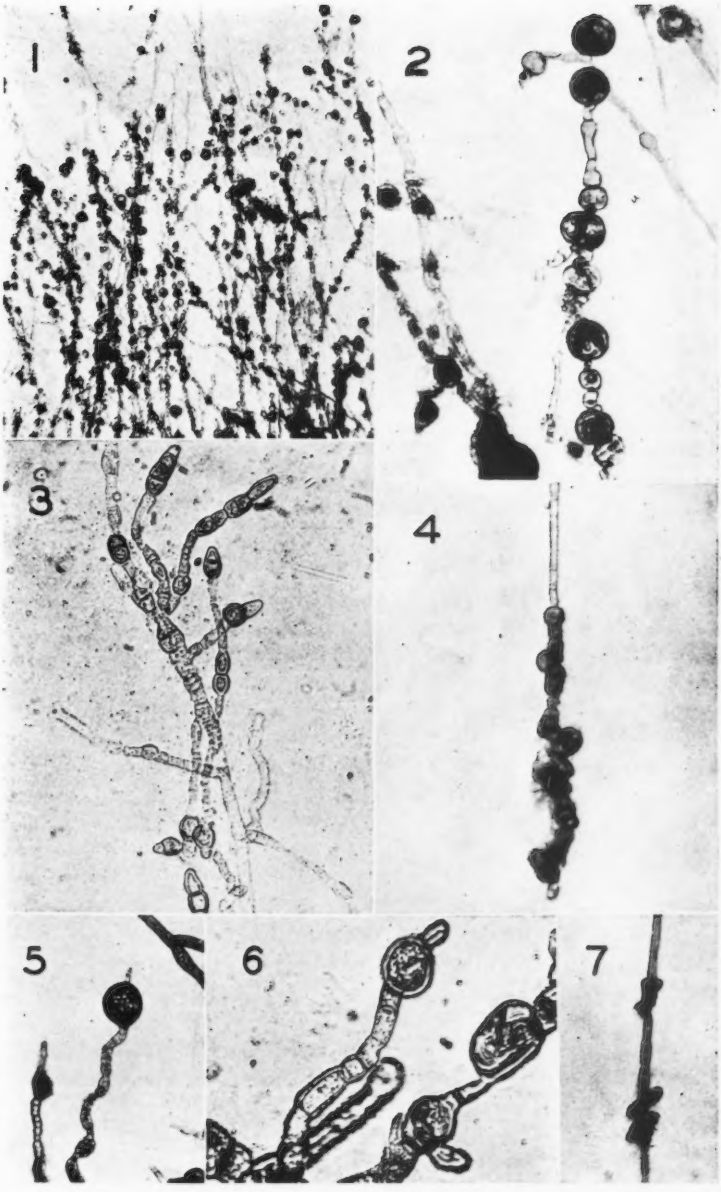

Photomicrographs of D. morbosum. Fig. 1, × 70: other Figs. × 340.

FIG. 1. *Typical chlamydospore production in Petri dish colony, induced by the close proximity of antagonistic bacteria.* FIG. 2. *Detailed structure of 1.* FIG. 3. *A distinctive type of chlamydospore, produced as in 1.* FIG. 4. *An approach to a sclerotial condition.* FIGS. 5 and 6. *As in 2.* FIG. 7. *Early stage of 4.*

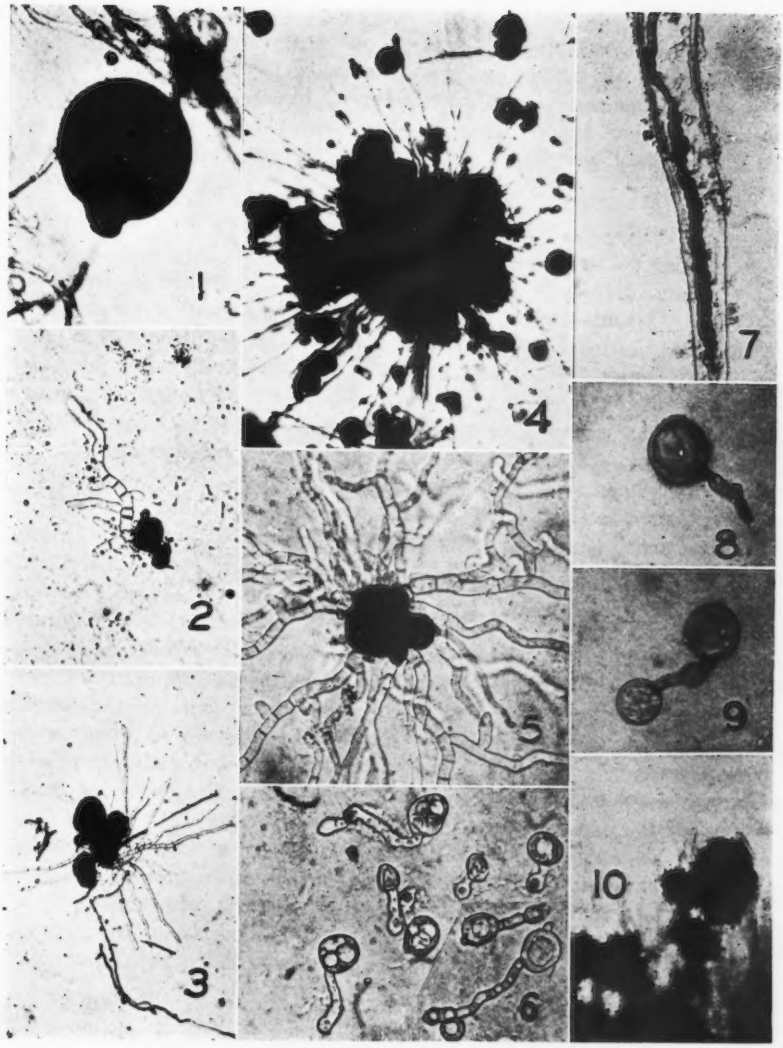

Figs. 1–6 and 8–10, photomicrographs of D. morbosum. Figs. 3, 4 and 10, × 110: other Figs., × 340.

FIG. 4. *Colony in Petri dish showing large chlamydospore-like bodies induced by introduction of sulphuric acid.* FIG. 1. *Enlargement of 4.* FIGS. 2 3 and 5. *Germination of chlamydospore-like bodies shown in 1 and 4.* FIGS. 6, 8 and 9. *Spherical chlamydospores developing either directly from conidia or at distal end of short germ tube.* FIG. 7. *Trichome of bud of peach infected by unidentified organism producing chain of chlamydospores on vegetative mycelium.* FIG. 10. *Sclerotium-like bodies in Petri dish colony, induced as in 4.*

covered surfaces of some of each set of twigs were wrapped, first with moist blotting paper and then with wax paper, to ensure moist conditions for germination while others were allowed to remain under natural conditions.

On all twigs painted with the mixtures of conidia and bacteria the germinating conidia developed chlamydospores similar to those observed in cultures. On the exposed twigs chlamydospores developed later and were fewer in numbers. On twigs painted with conidia only, chlamydospores were observed in small numbers on non-sterilized twigs but to a much lesser extent on sterilized ones.

Discussion

In summarizing the results of the experiments outlined above, conclusive evidence is adduced that some conidia of *D. morbosum* remain viable all winter on the buds and bark of *Prunus* spp.; also that *D. morbosum* can and does overwinter in some instances in a spore form hitherto unreported, namely, the chlamydospore. Not only was this organism isolated on numerous occasions from a random selection of single chlamydospores removed from the surface of buds and bark of *Prunus domestica* and *P. cerasus*, but it was also induced to form chlamydospores by (i) association with certain other organisms, and (ii) the introduction of certain chemicals.

The fact that either filtrates of antagonistic bacteria or portions of medium from just beyond the periphery of the bacterial colonies themselves induced a similar, though less marked effect, suggests the formation of a metabolic product by the bacteria, capable of stimulating the production of chlamydospores in *D. morbosum*.

When sown in direct contact with antagonistic bacteria, both in culture and outdoors on the surface of twigs and buds, conidia of *D. morbosum* in many cases produced chlamydospores immediately after germinating. On the other hand, pure suspensions of conidia of *D. morbosum*, treated in a manner similar to that described above for the mixed organisms, resulted in the formation of no chlamydospores in culture and only small numbers outdoors.

The evidence pointed out in the above paragraphs suggests the strong possibility that when a conidium of *D. morbosum* germinates on the surface of a twig in close proximity to an antagonistic organism the former soon develops a chlamydospore. It is also quite conceivable that upon the removal of the antagonistic organism the chlamydospore may germinate in the normal way provided other conditions are favorable.

Cladosporium carpophilum Thüm

Keitt (10), who has made important contributions to our knowledge of peach scab, observed that the causal organism, *C. carpophilum*, overwinters for the most part in the form of mycelium in lesions on living twigs. He suggests that mycelium of the fungus may also survive winter conditions saprophytically, for he states "the mycelium of this fungus may quite probably survive the winter under orchard conditions upon fallen fruits, twigs or leaves".

With these possibilities in mind an investigation of the overwintering of *C. carpophilum* was undertaken. Sections of twig and leaf pustules were examined critically at frequent intervals during all seasons, isolations were made from various host organs and the organism was studied in culture.

Isolations of C. carpophilum from the Surface of Peach Twigs

During the winter of 1931 numerous isolations were made from the surface of twigs of *Prunus persica*, variety Late Crawford. The twigs were chosen from two trees which had been very severely infected with scab and which, except for a single application of spray in 1933 to control leaf curl, had not been sprayed during the three-year period of the investigations. In the first series of isolations, four isolants of *C. carpophilum* developed in plates inoculated with material scraped from the surface of twigs. During the following two years, 16 isolants of the scab organism were obtained in a similar manner and seven of these were definitely determined as originating from single chlamydospores. In the latter instances, germination of the chlamydospores was so tardy and the growth of the resultant colonies so slow that their identity could not be established until 18 to 24 days after they were planted on the medium.

In December 1932, groups of chlamydospores and conidia of *C. carpophilum* were observed in macerations of material scraped from the axillary region of buds on twigs heavily infected with scab. Individual chlamydospores and conidia were isolated from suspensions of the macerated material, streaked on plates of solid medium and transferred to tubes. Eight isolants of *C. carpophilum* appeared in culture, six of them developing from chlamydospores, the other two from conidia. A large number of both types of spores did not germinate.

Production of Chlamydospores by C. carpophilum

(a) In cultures.—On potato-dextrose agar (dextrose, 3%) it was observed that *C. carpophilum* produced an abundance of chlamydospores, while on sterilized peach twigs microsclerotia were produced in equal abundance, in accordance with the observations of Keitt (10).

(b) On twigs.—To determine whether or not *C. carpophilum* could be induced to form chlamydospores on its host, heavy suspensions of conidia were painted in September of two successive years, on the surface of peach twigs, some of which had been surface-sterilized and others of which had been left untreated. Some of the spore-painted surfaces were wrapped with moist blotting paper enclosed by an outer wrapping of wax paper, while others were left exposed. Examinations of these twigs ten days to one month later showed that of the conidia which had germinated, some had produced chlamydospores soon afterwards. From the latter *C. carpophilum* was re-isolated in a few cases.

Pathological Histology of Lesions on Twigs and Leaves

To study the relation of *C. carpophilum* to its host, numerous sections of both twig and leaf lesions were made at close intervals throughout their developmental period. Fresh materials were utilized in all cases. Sections of twigs were cut with a sliding microtome while those of leaves were cut by the freehand method, and all were stained with cotton blue.

Examination of sections of infected twig material showed that: (i) in earlier stages of infection a mycelial mat of varying thickness occupied a position between the cuticle and the epidermis over the whole area of the lesion, with occasional hyphal strands ramifying between the epidermal cells (Fig. 1, *A*); (ii) in later stages of early current-season infection, the production of an abundance of conidia resulted in the rupture of the cuticle, and mycelium was present in abundance only at the periphery of the lesions where it still occupied the same relative position between the cuticle and the epidermis; (iii) except in very young lesions the superficial diseased tissue was completely delimited from the underlying, healthy cortical tissue by a periderm of varying thickness, which developed just in advance of the mycelium of the fungus.

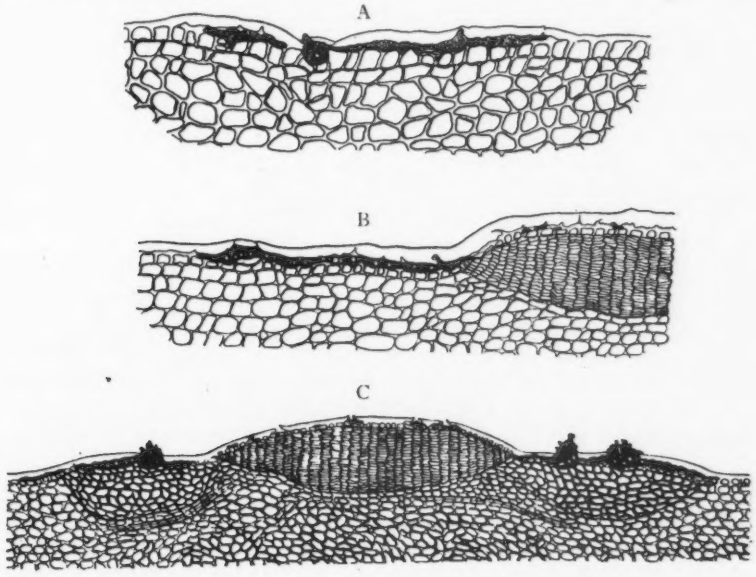

FIG. 1.

Diagrammatic representations of longitudinal sections of lesions caused by Cladosporium carpophilum on twigs of Prunus persica.

A. *Early stage of infection. Note position between cuticle and epidermis, occupied by mycelium.* × *45. Section cut 14.7.32.* B. *Later stage of infection. Note that mycelium has migrated beyond primary lesion delimited by periderm.* × *45. Section cut 17.11.33.* C. *Lesion approximately one year old showing primary and secondary lesions. Note position occupied by mycelium, and beginning of periderm formation beneath both primary and secondary lesions.* × *25. Section cut 20.6.33.*

In late season infections the lesion does not progress much beyond the initial stage, rarely induces periderm formation, and produces few or no conidia during the first season.

Examination of a large number of sections indicated that until the end of the growing season the fungus does not appear beyond the limits of the periderm induced by the action of the organism. Early in the dormant season, however, tissue development in the host ceases altogether or proceeds very slowly, while on the other hand, the fungus continues to advance between the cuticle and the epidermis, into which region periderm formation does not extend. Consequently by October the mycelium of the fungus has usually passed beyond the primary lesion, which may be identified by the underlying periderm (Fig. 1, B). During the winter and the following spring, the fungus advances slowly and produces in the newly invaded tissues what may be termed a secondary lesion (Fig. 1, C). The latter can be distinguished macroscopically as an irregular ring of tissue which is of a darker red color than the surrounding tissues and which gradually becomes elevated as the winter progresses. The walls of the host cells beneath the mycelium in the young secondary lesion become thickened but it is not until the following spring that a true periderm is laid down, delimiting the secondary lesion which is now clearly distinguishable from the primary lesion. During the second summer the fungus fruits most abundantly and in most cases only within the limits of the secondary lesions. Early in the second growing season the tissues underlying the primary lesions resulting from late summer infection closely resemble those below the secondary lesions described above. At the same time conidia are produced over the whole surface of the infected area, in marked contrast to the early season infections.

Examinations of sections of leaves showed a condition approximating that on twigs. During the summer definite lesions result from infection. The mycelium of *C. carpophilum* occupies a subcuticular position and is frequently delimited from the surrounding healthy tissues in much the same manner as on twigs. By fall, however, the mycelium has frequently advanced beyond the boundaries of the primary lesion where in many cases it fruits abundantly.

Discussion

These observations supply evidence that *Cladosporium carpophilum* may overwinter on the surface of peach twigs in the form of chlamydospores in addition to the well recognized and undoubtedly more important method of overwintering as mycelium in lesions on twigs.

When it is considered that *C. carpophilum* produces an abundance of chlamydospores in culture it is not surprising that the same spore form has been found outdoors; nor is it surprising that the chlamydospores of this fungus are capable of overwintering, since it has been observed by Keitt (10) that chlamydospores of this organism are highly resistant to desiccation. He cites one instance of chlamydospores in a gradually dried culture remaining viable for more than three years.

A critical examination of lesions on twigs has revealed certain interesting information. Twig lesions can be roughly divided into two classes: (i) early infections which produce conidia during the season of infection, and (ii) later infections which produce few or no conidia until the second season. Lesions of the first type produce secondary lesions during the winter as a result of the advance of the fungous mycelium beyond the primary lesion. During the whole course of infection the organism occupies a position between the cuticle and the epidermis.

Taphrina deformans (Fcl.) Tul.

Among numerous other fungi appearing in isolations from buds and bark of *Prunus persica*, an organism resembling *Taphrina deformans* appeared on five occasions, occurring first during the winter of 1930. As the actual method by which *T. deformans* overwinters was in doubt and as this organism is somewhat difficult to distinguish in culture from certain "budding" saprophytic fungi, many of which appear consistently in isolations from the bark of peach trees, it was necessary to prove the identity of the organism by inoculation. For this purpose two trees were chosen, both of which had been sprayed in the fall of 1930.

Before inoculation, branches were surface sterilized, and washed with sterile water. Three inoculated branches developed a total of 78 infected leaves. Unfortunately, however, check branches developed 17 infected leaves, though the latter occupied a position in most cases in close proximity to inoculated branches, thus indicating a spread of infection from the inoculated branches to the checks.

In the summer of 1931, tags were placed on 50 buds on branches which had showed 100% leaf curl infection earlier in the season. During the following winter isolations were made from these buds at intervals of one month, from October until May.

Among other organisms, *T. deformans** appeared in varying frequency in each series of isolations except those made in February. In the May series, when the organism appeared most frequently, as many as 17 colonies developed in isolations from a single bud.

Infection experiments were again conducted in the spring of 1932 with results essentially similar to those obtained during the previous year.

In September of two successive years suspensions of conidia and atypical spores of *T. deformans* were painted on surface sterilized buds and bark of twigs on sprayed Elberta trees to test the capability of the spores to overwinter on the exposed surfaces. Isolations were made from these twigs at intervals of one month until the following May. *T. deformans* appeared in every series of isolations during both winters.

Various attempts were made in the course of the above experiments to find out whether the conidia, or the atypical spores (resting spores, according

**This organism was compared microscopically with pure cultures of T. deformans obtained from other investigators, and proved similar in every respect.*

to Mix (13)), or both, were overwintering. This was done by making drawings of the spores when they were transferred singly from Petri dishes to tubes where their further development was followed.

Some evidence was obtained to the effect that so far as these experiments were concerned both conidia and atypical spores were overwintering. Many of both types of spores were observed to turn slightly brown in color after remaining on the bark for several weeks.

The evidence obtained in the above experiments on *T. deformans* agrees in general with that obtained by Fitzpatrick (7) who conducted intensive investigations on leaf curl concurrently with the overwintering studies outlined above, and strongly indicates that *T. deformans* overwinters in the form of spores on the surface of buds and bark of *P. persica*.

Coniothyrium sp.

A *Coniothyrium* sp. appeared as a frequent isolant from the surface of buds and bark of *Prunus domestica*, *P. persica*, *P. cerasus*, *P. pennsylvanica*, *Pyrus malus* and *P. communis*. As this organism has been dealt with in a previous article (11) it will not be discussed in detail here. It should be pointed out, however, that in numerous instances this *Coniothyrium* sp. was proved by isolation to overwinter on the above-mentioned hosts in the form of chlamydospores.

Two Members of the Fungi Imperfecti

Two fungi belonging in the Fungi Imperfecti were isolated consistently and frequently each winter from the surface of branches and buds of *P. domestica* in particular, and in some cases from *P. cerasus*. These fungi presumably were saprophytes but were particularly interesting because of their method of overwintering.

One of these fungi was *Torula*-like in character and was referred to that group, but owing to the unsatisfactory situation existing in the taxonomy of this group at the present time, it was impossible to identify it further.

On potato-dextrose agar this organism produced scarcely any mycelium, colonies consisting entirely of elevated, black, compact but not hard, somewhat sclerotium-like and irregularly shaped bodies (Plate III, Fig. 4). Colonies increased rapidly in size both outwards and upwards, frequently reaching the top of the Petri dish or test tube within two weeks. The black masses which composed the colonies consisted almost entirely of groups of dark colored spores, many of which were thick-walled and two-celled. The latter were always borne irregularly in groups on short strands of mycelium which varied considerably both in appearance and length. Groups of spores similar in every respect to those produced in culture were observed on numerous occasions in suspensions of materials removed from the surface of buds and bark of *P. domestica* during the winter.

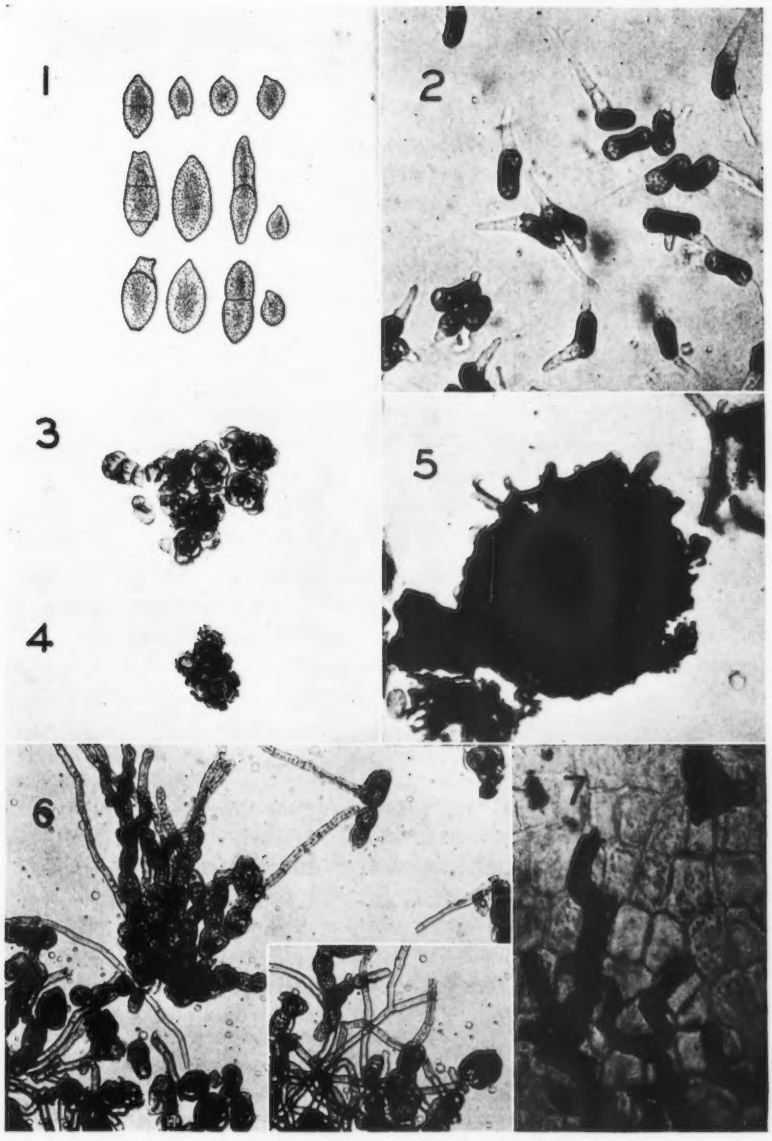

Fig. 1, drawing: Fig. 4, photograph: Figs. 2, 3, 5, 6 and 7, photomicrographs. Fig. 1, × 450: Fig. 3, × 3/4: other Figs., × 340.

FIG. 1. *Conidia of Cladosporium sp. isolated from bark of fruit trees. Note verrucose markings.* FIG. 2. *Germinating conidia of 1.* FIG. 3. *Spores of Torula-like fungus occurring on fruit trees.* FIG. 4. *Petri dish colony of 3.* FIG. 5. *Sclerotium-like body which commonly developed in cultures of 1.* FIG. 6. *Chlamydospore-producing fungus occurring on fruit trees.* FIG. 7. *Bit of epidermis removed from peach twig, showing one type of chlamydospore-like body present.*

It should be mentioned in this connection that owing to the sparse development of mycelium and also to the mycological situation referred to above, it was impossible to determine whether the spores produced by this organism should be termed conidia or chlamydospores.

Another fungus, also a member of the Imperfecti, was consistently isolated from sources similar to those from which the *Torula*-like fungus was obtained. It was impossible to identify this organism (which was isolated on 32 occasions from definite monochlamydospores) either on the host or in culture, because on both types of substratum the chlamydospore was the only type of spore produced. On malt agar, potato-dextrose agar and on sterilized cereals of various kinds the organism always produced an abundance of chlamydospores. On potato-dextrose agar the organism developed a dark green, elevated colony, the surface of which was covered with a mat of short, straight hyphae, pointing outwards. The organism grew very slowly in culture, attaining a diameter of approximately 20 mm. in 33 days. In order to isolate it during the winter it was always found necessary to transfer the chlamydospores to other media soon after plating, otherwise they became completely overrun with more rapidly growing organisms.

In older cultures the chlamydospores of this fungus readily separated from the parent mycelium. The chlamydospores were darker in color than the mycelium, had extremely thick walls, occupied either an intercalary or terminal position on the mycelium, contained numerous oil globules, and were usually two-celled in older cultures (Plate III, Fig. 6).

Cladosporium and *Hormodendrum*

Members of both the genera *Cladosporium* and *Hormodendrum* appeared consistently and frequently in isolations from numerous hosts. As distinguished by their morphological characters on potato-dextrose agar, three strains of the former and at least two of the latter were isolated consistently. Presumably all were saprophytes. An examination of the literature dealing with the description and occurrence of members of both of the above-mentioned genera would allow all strains of *Cladosporium* isolated to be called *Cladosporium herbarum* and similarly, all strains of *Hormodendrum* to be called *Hormodendrum cladosporioides*. However, since both of the above species names have been applied to most of the saprophytic members of their respective genera, dangerously wide limits have been set up for both species, as is evident in the opinion (1) that one of these species is merely a stage of the other. It was thought preferable, therefore, to refer to them only generically.

As they are of special interest in the present article only because of their method of overwintering, their occurrence is listed in Table II.

TABLE II

SUMMARY OF ISOLATIONS OF *Cladosporium* AND *Hormodendrum* FROM VARIOUS SUBSTRATA

Date	Hosts	Source of isolation	Number of isolants	
			Cladosporium	*Hormodendrum*
Nov.–Mar. (1929-33)	*Prunus domestica*	Monochlamydospores from surface of buds and twigs	15	8
"	*P. cerasus*	"	7	6
"	*P. virginiana*	"	5	9
"	*P. pennsylvanica*	"	12	7
"	*P. persica*	"	7	12
"	*Pyrus malus*	"	3	3
"	Various *Prunus* spp.	Undetermined	64	181

It will be observed from an examination of Table II that both *Cladosporium* and *Hormodendrum* appeared frequently in isolations from the buds and bark of numerous hosts. It will also be noted that *Cladosporium* appeared in all, 49 times, and *Hormodendrum* 45 times in isolations from monochlamydospores.

All strains of *Cladosporium* produced chlamydospores in pure cultures on potato-dextrose agar, and one strain, designated *A*, which was readily distinguished from others by its large verrucose spores, usually developed sclerotium-like bodies as well (Plate III, Figs. 1 and 5).

The evidence outlined above strongly suggests that at least certain members of the genera *Cladosporium* and *Hormodendrum* overwinter on the bud and bark surfaces of many fruit trees in the form of chlamydospores.

Fumago sp.

A species of *Fumago*, similar in many respects to *Fumago vagans* investigated by Fant (5), in 1928, appeared consistently and frequently in isolations from *Prunus domestica*, *P. persica*, *P. cerasus*, *P. americana*, *P. virginiana*, *P. pennsylvanica*, *Pyrus malus* and *P. communis*. The source of these isolations was proved in numerous instances to be chlamydospores. On moist filter paper and on potato-dextrose agar in Petri dish cultures which were either gradually desiccated or which contained numerous other organisms, an abundance of chlamydospores was frequently produced by the *Fumago* sp.

Other Fungi

Numerous other fungi, many of the budding type, were frequently isolated from the hosts already mentioned, but as they were all presumed to be saprophytes no investigation of them was undertaken.

Chlamydospores in Fungi

From the standpoint of etymology the term chlamydospore (chlamyd— combining forms from Greek χλαμύς , χλαμύος , mantle, chlamys) signifies a spore surrounded by a mantle. Since the earlier days of mycology the term has been employed by Van Tieghem and Le Monnier (19), de Bary (4), and others, in referring to bodies which they regard as accessory

conidia. However, definitions of chlamydospores have been many and varied, and until recent years, the term has been applied to almost any spore which has thick walls and functions as a resting spore, with no consideration of the morphology of the spores concerned. Instances of the occurrence of chlamydospores throughout almost the complete taxonomic range of fungi have been reported.

In the Phycomycetes, Fitzpatrick (6) points out that chlamydospores occur chiefly on old thalli and are not homologous with the sporangia. He also states that they function as resting spores, germinate by germ tubes, are non-deciduous, and may occupy a terminal or intercalary position on the mycelium.

Some confusion has apparently arisen through the application of the term chlamydospore to the azygospores formed by certain members of the Mucorales. But until an intensive investigation of the morphology of bodies commonly referred to as chlamydospores in the various fungi is undertaken, it will be impossible to definitely determine the status of bodies such as azygospores. However, the bodies in certain of the Mucorales designated gemmae by Gaümann (8) and chlamydospores by Fitzpatrick (6) are similar in every respect to those bodies in the Ascomycetes and Fungi Imperfecti which are conceded to be chlamydospores. Therefore, in the case of these Mucorales, it would seem preferable to restrict the use of the term chlamydospore to the thick-walled spore formed within the vegetative coenocytic mycelium, and to exclude azygospores, which are borne on specialized hyphae.

Among the Ascomycetes and Fungi Imperfecti chlamydospores have been reported for most genera. From the standpoint of the present investigations, chlamydospores are of interest chiefly in connection with these two groups of fungi, where the conception of a chlamydospore, at least during recent years, has been fairly well restricted to the limits already defined in this article. However, this definition is not satisfactory for the chlamydospores occurring in certain members of the above groups, not included in the present investigation. For instance, it would exclude chlamydospores formed either endogenously in the conidia of certain species of *Fusarium* and *Ramularia*, or on special lateral branches in certain species of *Fusarium* (18) or in *Thielavia basicola* (3). The use of the term chlamydospore has been confused in certain members of the the Taphrinales (*e.g. T. deformans*) when it has been applied (8) to the sub-epidermal layer of thick-walled cells from which the asci arise. This confusion has arisen, no doubt, because these fungi have been considered by certain mycologists to be closely related to the Protomycetaceae.

Even in recent years the resting spores of the Ustilaginales have frequently been referred to as chlamydospores, but of late there appears to be a tendency on the part of many investigators to avoid the use of the term in connection with the smut fungi. If chlamydospores were considered in the light of function only, to the entire disregard of their morphology, it would then be correct to term a smut spore a chlamydospore. It would also be

equally correct to apply the term to an aeciospore, a urediniospore or a teliospore of a rust fungus as Brefeld (2) and others have in the past considered them. A similar argument would hold even for the zygospore of a Zygomycete. In recent years, however, the restriction of the occurrence of chlamydospores to the vegetative phase and their consequent asexual nature, have been considered to be just as significant regarding their designation as the function which they perform. Chlamydospores have also been reported in certain other Basidiomycetes, but their occurrence in this group will not be discussed in detail.

In the case of certain fungi, members of the Fungi Imperfecti in particular, it may be difficult to distinguish a chlamydospore from a conidium. Such difficulty has been experienced, as pointed out previously, in connection with the *Torula*-like fungus isolated frequently during the present investigations. It is quite true that chlamydospores may tend in one extreme towards sclerotia and in the opposite towards conidia or, more often, towards ordinary vegetative mycelium.

In conclusion it should be mentioned that the secondary importance usually attached to chlamydospores can be traced largely to their lack of diagnostic value from the mycological standpoint. Chlamydospores produced by a single organism vary so greatly both in shape and size that it has in most cases proved impossible to diagnose species by the morphological characters of their chlamydospores.

Sherbakoff (18) however, discovered that the genus *Fusarium* could be delimited into sections on the basis of the presence or absence of chlamydospores; in one case he even distinguished two species of *Fusarium* by their position on the hyphae. Undoubtedly similar situations will be found to exist within other genera as they become more intensively investigated.

The above paragraphs point out the almost universal occurrence of chlamydospores in fungi, as well as a certain confusion regarding the use of the term. The importance of the chlamydospore from the pathological standpoint, which has hitherto been incompletely appreciated, because of its unsatisfactory mycological status, has been emphatically demonstrated by the present, somewhat limited investigations. Future work along similar lines will undoubtedly disclose a similar degree of importance for chlamydospores in numerous other fungi.

Discussion

The present investigations on the overwintering of certain fungi have revealed several new and important features in the life histories of the organisms concerned.

In the case of *Dibotryon morbosum*, the cause of black knot, not only have conidia been found to remain viable on the host throughout the winter, but also a new overwintering stage in the form of chlamydospores has been definitely proved. In cultural studies the interesting discovery was made that *D. morbosum* produced chlamydospores *only* when grown in close prox-

imity to certain other organisms or when chemicals were introduced into the culture medium. Chlamydospore formation was also induced on twigs of *Prunus domestica* when conidia of *D. morbosum* germinated in intimate association with antagonistic bacteria originally isolated from the same host. Though a survey of the literature relevant to the occurrence of chlamydospores in fungi has not revealed data similar to those outlined in the present investigation regarding *D. morbosum*, Porter (14) reports a somewhat similar phenomenon in his investigations on association of organisms.

This phenomenon of chlamydospore formation as observed for the black knot organism may be significant from the standpoint of biologic control. Sanford and Broadfoot (15) discovered that certain fungi and bacteria "suppressed" the pathogenicity of *Ophiobolus graminis*. Numerous other instances of a similar nature have also been reported during recent years, particularly in connection with soil fungi. No investigations are reported, however, which were undertaken primarily to determine the actual fate of the organism, the pathogenicity of which was inhibited by the antagonistic organism(s). It has been shown in the present investigations that the continued presence of the antagonistic organism inhibits the vegetative growth of *D. morbosum* and induces profuse chlamydospore formation on the part of the latter organism. On the removal of the antagonistic organism however, the chlamydospores germinate and the fungus resumes vegetative growth. It is quite possible that similar phenomena may occur in the case of other fungi, particularly soil fungi, because of the continually changing flora consequent upon variations in environmental conditions.

The present investigations, confirming those of Keitt (10) in 1917, demonstrate that the chief method of overwintering of *C. carpophilum* is in the form of mycelium occurring in lesions on the superficial tissues of twigs. Histological studies of these lesions have indicated that certain of them resemble lesions on apple twigs caused by *Venturia inaequalis* (described in detail recently by Marsh and Walker (12)). *C. carpophilum*, as in the case of the latter organism, develops secondary lesions during the winter as a result of the migration of the mycelium between the cuticle and the epidermis, into which region the periderm barriers underlying and delimiting the primary lesion do not extend. It was interesting to note that in cases of infection where both primary and secondary lesions developed, the mycelium of *C. carpophilum* overwinters most frequently only in the secondary lesions where it fruits the following summer. The facts, first, that *C. carpophilum* produces an abundance of chlamydospores in culture, and second, that the organism was isolated from chlamydospores removed from the surface of the host during the dormant season, indicate that the fungus also overwinters in nature in the form of chlamydospores.

The isolation of *Taphrina deformans* from the surface of buds and twigs of *Prunus persica*, and the proof that spores of *T. deformans* can overwinter on the above-mentioned organs, confirms Fitzpatrick's (7) recent findings in regard to this organism and is of particular interest in view of the fact that the method of overwintering of this fungus has heretofore remained in doubt.

It is interesting to note that other fungi, presumably saprophytes, representing six different genera, developed from chlamydospores removed from the surface of many hosts during the winter. Since all of these fungi also produced chlamydospores in artificial culture it is reasonable to assume that they do so in nature. The results of these investigations strongly suggest that many more fungi overwinter in the form of chlamydospores than the literature to date indicates. This is not surprising in consideration of the fact that, from the standpoint of taxonomy, plant pathologists and mycologists have regarded the chlamydospore as possessing relatively little value. This situation, as pointed out above, has been largely responsible for the misapplication of the term chlamydospore.

From the economic standpoint the present investigations emphasize the importance of the application of the dormant spray on fruit trees, since it has been demonstrated that both conidia and chlamydospores of several of the important plant pathogenes can overwinter on the exposed bud and bark surfaces.

Acknowledgment

Thanks are gratefully extended to Dr. G. H. Berkeley for many helpful suggestions offered during the course of this investigation.

References

1. BANCROFT, C. K. Researches on the life-history of parasitic fungi. Ann. Botany, 24 : 359-373. 1910.
2. BREFELD, O. Botanische Untersuchungen. Heft. VII, 178 pp. 1888.
3. BRIERLEY, W. B. The "Endoconidia" of *Thielavia basicola*, Zopf. Ann. Botany, 29 : 483-493. 1915.
4. DE BARY, A. Vergleichende Morphologie und Biologie der Pilze, Mycetozoen und Bacterien. 585 pp. 1884.
5. FANT, G. W. The development of peach sooty mold at normal and low temperatures. J. Elisha Mitchell Sci. Soc. 43 : 217-220. 1928.
6. FITZPATRICK, H. M. The lower fungi. Phycomycetes. McGraw-Hill Book Co. Inc., New York. 331 pp. 1930.
7. FITZPATRICK, R. E. The life history and parasitism of *Taphrina deformans*. Sci. Agr. 14 : 305-336. 1934.
8. GAÜMANN, E. Vergleichende Morphologie der Pilze, 626 pp. Jena. 1926.
9. KEITT, G. W. Simple technique for isolating single spore strains of certain types of fungi. Phytopathology, 5 : 266-269. 1915.
10. KEITT, G. W. Peach scab and its control. U.S.D.A. Bull. 395. 1917.
11. KOCH, L. W. Investigations on black knot of plums and cherries, II. The occurrence and significance of certain fungi found in association with *D. morbosum* (Sch.) T. and S. In press.
12. MARSH, R. W. and WALKER, MARY W. The scab fungus (*Venturia inaequalis*) on apple shoots. J. Pomology Hort. Sci. 10 : 71-90. 1932.
13. MIX, A. J. Biological and cultural studies of *Exoascus deformans*. Phytopathology, 14 : 217-233. 1924.
14. PORTER, C. L. Concerning the characters of certain fungi as exhibited by their growth in the presence of other fungi. Am. J. Botany, 11 : 168-188. 1924.
15. SANFORD, G. B. and BROADFOOT, W. C. Studies of the effects of other soil-inhabiting micro-organisms on the virulence of *Ophiobolus graminis* Sacc. Sci. Agr. 11: 512-528. 1931.
16. SCHWEINITZ, A. *Sphaeria morbosa*. Synopsis Fungorum Carolinae superioris. 134. 1821.
17. SELBY, A. D. Peach yellows, black knot and San Jose scale. Ohio Agr. Exp. Sta. Bull. 72 : 206-209. 1896.
18. SHERBAKOFF, C. D. Fusaria of potatoes. Cornell Agr. Exp. Sta. Memoir 6. 1915.
19. VAN TEIGHEM, P. and LE MONNIER, G. Recherches sur les Mucorinees. Ann. Sci. Nat. ser. 6. 1875.

THE RELATION BETWEEN AWNS AND YIELD IN SPRING WHEAT[1]

By O. S. Aamodt[2] and J. H. Torrie[3]

Abstract

Considerable interest has been aroused over the possible relationships existing between the presence of awns and the grain yield of wheat. The general consensus of opinion is that awned varieties tend to outyield awnletted or awnless varieties. A number of investigations with barley and wheat have shown that the awns play an important role in transpiration, and that their removal results in reduced yields. Genetic studies dealing with the relation between awns and grain yield of wheat have given contradictory evidence. Certain workers have reported positive, others negative, and still others no relationship, existing between the presence of awns and grain yield.

In the present investigation, the problem was studied with a number of F_3 lines of Reward × Caesium, and also with a number of awned and awnletted strains of Marquillo × Marquis-Kanred. In neither case were any significant relationships found to exist between awns and grain yield. The apparently contradictory results obtained by the different investigators suggest that the relation between the two characters differs, depending both upon the material used and the environmental conditions under which it is grown.

Introduction

Considerable interest has been aroused over the possible relationships existing between the presence of awns and the grain yield of wheat, the general consensus of opinion being that awned varieties tend to outyield awnletted or awnless varieties. As a result most wheat breeding programs are stressing the presence of awns as one of the factors contributing to higher yield. If such an association exists, the reason for increase in yield may be due to several factors. It may be that the awns play an important physiologic role in the metabolism of kernel development, or it may be that the factors governing awns are linked with some of the factors influencing grain yield. Ceres, introduced recently by Waldron (16), is an example of a high-yielding awned variety. On the other hand, there are the various awnless Red Bobs selections (Red Bobs No. 222, Early Triumph and Supreme), which are commonly grown in western Canada, and which have been found to possess high-yielding abilities (1, 2, 7, 15).

A review of the investigations on the relation between awns and grain yield shows that certain workers found awnedness to be associated with increased yield (3, 4, 9, 10, 12), others found no association (6, 13), while still others report a decrease in yield with an increase in awnedness (5). The present investigation deals with the relation between awns and grain yield, in the F_3 of Reward × Caesium, and in a number of awned and awnletted Marquillo × Marquis-Kanred strains.

[1] *Manuscript received June 1, 1934.*
Contribution from the Department of Field Crops, University of Alberta, Edmonton, Canada.

[2] *Professor of Genetics and Plant Breeding, University of Alberta.*
[3] *Graduate Assistant, University of Alberta.*

Materials and Experimental Methods

Materials

The F_3 only, of Reward × Caesium was used in the present study. Reward, C.A.N. 1509*, is a hard red spring wheat, originating from a Marquis × Prelude cross made at the Central Experimental Farm, Ottawa. It is awnletted and of fair yielding ability. Caesium 0.111, C.A.N. 1256, was obtained from Dr. Talanov of the West Siberian Experimental Station in 1928. It is fully awned and high in yielding ability.

The hybrid strains of Marquillo × Marquis-Kanred were introduced from the University of Minnesota in 1928, and selected at the University of Alberta. Certain of these strains are awnletted, while others are fully awned.

Experimental Methods

The F_3 lines of Reward × Caesium were grown at Edmonton in 1933 in 10-ft. rows, 1 ft. apart, with approximately 50 seeds per row. The plant yield of grain in grams was determined on 57 F_3 lines of Reward × Caesium and five rows of each parent. The plants in each row were pulled separately and the heads wrapped in cheesecloth to prevent loss in handling. The border plants at the ends of each row were noted and were not used for yield studies. Each plant was threshed separately and the yield recorded in grams. The average grain yield per plant for each row was calculated.

Rod row trials consisting of quadruplicated three-row plots were conducted on 34 hybrid strains of Marquillo × Marquis-Kanred on stubble in 1930, and on 28 strains on fallow in 1931.

The method used in measuring the independence and association of awns and yield was by contingency tables, in which the two characters are compared. The relationship between the two characters was obtained by calculating χ^2 and determining the P value from Fisher's χ^2 tables (8). In determining P from the tables, Fisher's suggestion for degrees of freedom was used. For example, a 4 × 3-fold table has six degrees of freedom. A P value of 0.05, or less, is necessary before it can be concluded that an association exists. A P value of 0.05 means that any association that exists between the distribution of the two characters might occur by chance in 1 out of 20 cases.

Literature Review

Zoebl and Mikosch, and later Schmid, cited by Hayes (12), stress the importance of awns as organs of transpiration in cereals. Perlitius, also cited by Hayes (12), conducted transpiration studies with awnless and awned varieties of spring and winter wheat, and with barley. His results were in agreement with those of the previous workers mentioned. He reports that the awned wheats tended to be plumper and to possess a higher starch content than the awnless wheats.

*C.A.N. = Canadian Accession Number.

Grantham (10) studied the yield of a number of awnless and awned winter wheats over a period of years. His results show that the average yield of the awned varieties was 3.1 bu. greater than that of the awnless varieties.

Harlan and Anthony (11) found that the removal of the awns in the case of Hannchen and Manchuria barley resulted in lower yields. This reduction in yield, they state, could not be attributed to any injury to the plant. The awned plants showed a greater activity during the period of starch infiltration. The differences in the ultimate weight of the kernels produced were primarily due to differences in the quantity of starch produced. Whether or not the reduction of transpiration, as the result of the removal of the awns, is sufficient to account for a lower rate of starch formation is a question. However, they conclude that the loss of the awn definitely results in lower yield.

Hayes (12) with Marquis × Preston hybrids found that in each of the generations from the F_3 to the F_5, the bearded families gave a higher average yield than the awnless families. During the favorable seasons of 1918 and 1920, the bearded families yielded between 7 and 8% more than the awnless families, while in the unfavorable season of 1919, the difference in yield was 17% in favor of the bearded families.

Clark (3) studied the effect of awns on yield in the F_2 of Kota × Hard Federation hybrids, grown at St. Paul, Minnesota, and Mandan, North Dakota. At both stations the awned plants outyielded the awnless plants by 11 to 15%, the odds being 9:1. Although these results are not significant, Clark states that they indicate that awns probably have some effect on yield under dry as well as humid conditions. In the F_3 a similar relationship was shown between awns and yield. In this case, however, the results were significant.

Clark, Florell and Hooker (4) studied the relation between awns and yield in the F_2 and F_3 of Bobs × Propo and Hard Federation × Propo crosses at Davis, California. In the F_2 of both crosses there was a decrease in yield with increase in the length and number of awns. This may be due largely to greater shattering in the case of the awned plants. In the F_3, in which shattering did not occur, the average yield tended to increase with awnedness. The authors concluded that when shattering was not a factor, there was a tendency toward increased yields with increased awnedness, under the conditions prevailing at Davis.

Goulden and Neatby (9) studied the association between awning and grain yield in rod row trials of awned and awnless strains of H–44–24 × Marquis. They obtained a P value of 0.0004, which indicates a very high probability of association between the presence of awns and high grain yield.

Moskalenko (13) studied the dependence between awnedness and the "elements of productivity" with winter wheat hybrids. He concluded that during the years of 1922, 1925, 1926 and 1927, there was no genetic relationship between awnedness and the "elements of productivity", under the conditions of the Ukranian steppe.

Clark and Quisenberry (5) report on the relation of awnedness to yield in the F_2 and F_3 of Kota × Marquis, grown at Bozeman, Montana. In both the generations studied, significant differences were obtained, showing that the awnletted plants and strains outyielded the awned plants and strains, in spite of the greater extent of shattering in the awned plants.

Clark, Quisenberry and Powers (6), working with Hope × Hard Federation crosses, found no relationship existing between awnedness and grain yield.

Parker (14) reported an experiment on the effect of awn removal on the yield of Kanred wheat. The awns were removed at the blossoming stage, one week later, and four days before harvest. He concludes that mechanical removal of the awns results in lower yields, the reduction in yield being less as the crop approaches maturity.

Experimental Results

The average grain yield per plant was determined on 57 F_3 lines of Reward × Caesium. The data in Table I give the frequency distribution and the average grain yield for the awnletted, segregating and awned F_3 lines and parental rows.

TABLE I

FREQUENCY DISTRIBUTION OF REWARD × CAESIUM F_3 AWNLETTED, SEGREGATING AND AWNED LINES AND PARENTAL ROWS, FOR AVERAGE GRAIN YIELD, GROWN AT EDMONTON IN 1933

Class	Grain yield, gm.										Average yield, gm.
	5.8	6.3	6.8	7.3	7.8	8.3	8.8	9.3	9.8	10.3	
Awnletted				5	2	3			1		7.9 ± 0.15
Segregating	1	1	5	6	4	5	4	3			7.7 ± 0.13
Awned			1	2	5	3	2	2	1	1	8.3 ± 0.15
Reward		2	2	1							6.7 ± 0.07
Caesium								1	1	3	10.5 ± 0.10

NOTE: $\chi^2 = 17.20$, $P = 0.50$.

The data in Table I show that Caesium, the awned parent, gave significantly higher yields than Reward, the awnletted parent. Although the average grain yield of the awned hybrid lines was 0.4 gm. more than that of the awnletted hybrid lines, the difference is not significant in the light of a P value of 0.5. Tests of association and independence were also made on the individual plants for each of the segregating F_3 lines. No significant relationship was found between awns and yield in any of the 29 segregating lines. The results of this experiment indicate that the presence of awns does not significantly increase the yielding capacity of the plants in F_3 lines of Reward × Caesium crosses.

Tests of association and independence were calculated to determine whether or not any relationship existed between awns and yield for the strains of Marquillo × Marquis-Kanred for the two years 1930 and 1931.

The data in Table II show that the average yield of the awnletted strains was 1.9 and 0.5 bu. higher than that of the awned strains in 1930 and 1931 respectively. These differences, in the light of their *P* values of 0.34 and 0.96 respectively, are not significant. The results of this experiment support those obtained from the F_3 of Reward × Caesium.

TABLE II

AVERAGE YIELD AND *P* VALUE OF AWNLETTED AND AWNED STRAINS OF MARQUILLO × MARQUIS-KANRED, GROWN ON STUBBLE IN 1930 AND ON FALLOW IN 1931, AT EDMONTON

Class	1930		1931	
	Average yield, gm.	*P* value	Average yield, gm.	*P* value
Awnletted	25.1 ± 0.54	0.34	51.7 ± 0.95	0.96
Awned	23.2 ± 0.31		51.2 ± 0.63	

Discussion and Conclusions

The results reported in this paper showing that there is no relation between grain yield and the presence of awns are in agreement with the work of Moskalenko (13) and Clark, Quisenberry and Powers (6). Grantham (10), Hayes (12), Clark (3), Clark, Florell and Hooker (4) and Goulden and Neatby (9) report that the presence of awns is associated with an increase in grain yield. Clark and Quisenberry (5) report a negative relation between the presence of awns and grain yield. These apparently contradictory conclusions of the different investigators indicate that the relation between awns and grain yield differs, depending both upon the varieties used and the environmental conditions under which the material is grown.

From the data reported in this paper, it may be concluded that, under Edmonton conditions, and for the material studied, there is no significant relation between the presence of awns and grain yield.

References

1. AAMODT, O. S. The Press Bulletin. Dept. of Extension, Univ. of Alberta, Edmonton, Canada 2 (19) : 3. 1933.
2. ALBRIGHT, W. D. Report of the Superintendent for the year 1929. Experimental Sub-station, Beaverlodge, Alberta, 69 pp., 1931.
3. CLARK, J. A. Segregation and correlated inheritance in crosses between Kota and Hard Federation wheats for rust and drought resistance. J. Agr. Research, 29 (1) : 1-47. 1924.
4. CLARK, J. A, FLORELL, V. H. and HOOKER, J. R. Inheritance of awnedness, yield and quality in crosses between Bobs, Hard Federation, and Propo wheats at Davis, California. U.S. Dept. of Agr. Tech. Bull. 39. 40 pp., 1928.
5. CLARK, J. A. and QUISENBERRY, K. S. Inheritance of yield and protein content in crosses of Marquis and Kota spring wheats grown in Montana. J. Agr. Research, 34 (4) : 205-217. 1929.
6. CLARK, J. A., QUISENBERRY, K. S. and POWERS, L. Inheritance of bunt reaction and other characters in Hope wheat crosses. J. Agr. Research, 46 (5) : 413-25. 1933.
7. FAIRFIELD, W. H. Report of the Superintendent for the year 1928. Experimental Station, Lethbridge, Alberta, 66 pp., 1929.
8. FISHER, R. A. Statistical methods for research workers. Oliver and Boyd. Edinburgh and London. 269 pp., 1928.

9. GOULDEN, C. H. and NEATBY, K. W. A study of disease resistance and other varietal characters of wheat. Application of the analysis of variance and correlation. Sci. Agr. 9 (9) : 575-586. 1929.

10. GRANTHAM, A. E. Wheat investigations—varieties. Del. Agr. Exp. Sta. Ext. Bull. 6. 1919.

11. HARLAN, H. V. and ANTHONY, S. Development of barley kernels in normal and clipped spikes and the limitations of awnless and hooded varieties. J. Agr. Research, 19 : 431-472. 1920.

12. HAYES, H. K. Inheritance of kernel and spike characters in crosses between varieties of *Triticum vulgare*. Univ. of Minn. Studies in Biol. Sci. 4 : 163-183. 1923.

13. MOSKALENKO, G. L. Investigations on the dependence between awnedness and the elements of productivity on hybrids of winter wheat. Abs. Proc. of the U.S.S.R. Congress of Genetics, Plant and Animal Breeding. Leningrad. Jan. 10-16. 1929. p. 240-241. 1929.

14. PARKER, J. H. Relation of the awn to yield in Kansas wheat. Northwestern Miller, April 18. p. 180. 1934.

15. REED, F. H. Report of the Superintendent for the year 1930. Experimental Station, Lacombe, Alberta. 59 pp. 1931.

16. WALDRON, L. R. Hybrid selections of Marquis and Kota. North Dakota Agr. Exp. Sta. Bull. 200, 64 pp. 1926.

A KARYOSYSTEMATIC INVESTIGATION IN THE GRAMINEAE[1]

By A. W. S. Hunter[2]

Abstract

The history and the present state of the classification of the Gramineae are briefly reviewed and a number of the different characteristics on which phylogenetic systems have been based are considered. The subjects of chromosome morphology and the application of idiograms and karyotypes to taxonomic studies are discussed. Avdulov's recently reported findings on the phylogeny of the grasses are summarized and compared with the results of other workers and those obtained in the present investigation. Three species of bamboos were studied for the first time and evidence secured to indicate that the basic number of the tribe is probably not 12 as has been elsewhere reported. In the Festuceae the chromosome number of *Phragmites communis* Trin. was definitely ascertained, confirming Avdulov's supposition that the basic number for the genus is 12. The other three species investigated agreed with the arrangement as proposed by Avdulov. The tribe Chlorideae, with the exception of the genus *Beckmannia*, has been reported to be almost entirely Panicoid with respect to chromosome morphology. This was confirmed in the four species examined. Avdulov's rearrangement of the tribe Hordeae was somewhat altered and a confusion in the nomenclature of the genus *Lepturus* was corrected. An anomalous situation was cleared up in the tribe Agrostideae by the establishment of the chromosome number of *Sporobolus tennuissimus* Kuntz as 40. The specimen of *Anthoxanthum odoratum* L. (tribe Phalarideae) examined provided a very interesting example of secondary splitting in somatic chromosomes. One species was examined in the tribe Melinideae and six in the tribe Paniceae. In the latter tribe no difference could be detected between the several subdivisions of the genus *Panicum*. The same condition held for the large genus *Andropogon* in the tribe Andropogoneae. In the tribe Maydeae the chromosome number of *Tripsacum dactyloides* L. was found to be 9, and the suggestion was made that it may be a link, along with the genus *Coix*, between the Andropogoneae and the Maydeae. The other four species examined all had a basic number of 10.

Introduction

The classification of the family Gramineae has long presented many difficulties to the systematist. Numerous workers have attempted to divide the family in a natural manner, but so far they have failed to reach agreement even on the division into the main groups—subfamilies and tribes.

Brown (7) was the first to recognize the two main subfamilies, which he called "tribes," the Panicoideae and Pooideae. Following him, Kunth (26), Endlicher (14) and Steudel (47) proposed classifications differing from one another only in details and in the number of genera included. They did not, however, recognize the division of the family into subfamilies as proposed by Brown (7), and it was not until the work of Bentham and Hooker (5) that this distinction was revived. Bentham and Hooker called the subfamilies Paniceae and Poaceae respectively. The system of Hackel (16) differed very little from that of Bentham and Hooker (5). He replaced the names of the subfamilies by the terms "Series A" and "Series B" and changed the order of some of the tribes. However, inasmuch as the arrangement of the tribes

[1] *Manuscript received May 22, 1934.*
Contribution from the Department of Genetics, McGill University, Montreal, Quebec, Canada.

[2] *Graduate Student, Department of Genetics, McGill University.*

in any linear phylogenetic series is impossible, this difference is not very important. The system is still followed more or less closely by most modern workers. It has been added to and modified mostly by Stapf (quoted by Bews (6)) who has elevated many subtribes to the rank of tribes, and has also split up some of Hackel's larger genera, such as *Andropogon*, changing many sub-genera of earlier authors following Hackel to genera, and creating many new ones. The same has been done for other genera such as *Panicum*, by Hitchcock and Chase (21). Apart from this, Hitchcock and the other American botanists generally follow Hackel in their delimitation of the tribes, though not in their order of arrangement. Bews (6), whose system is followed in this study, draws upon the work of all these authors. He divides the Gramineae into two subfamilies—the Pooideae and the Panicoideae. The Pooideae are in turn divided into the tribes Bambuseae, Phareae, Festuceae, Aveneae, Chlorideae, Hordeae, Agrostideae, Zoysieae, Phalarideae, Arundinelleae and Oryzeae. The Panicoideae are divided into the Melinideae, Paniceae, Andropogoneae and Maydeae.

The earliest classifications were based on external morphology alone. In 1858, however, Trecul (50) noted the organization of the starch grains in plants and classified them as simple and compound. In 1881-82 Harz (17) used these data for building up a phylogenetic scheme for the family. It has since been shown, however, that the type of starch grain in a plant cannot be determined from an examination of its structure in mature seeds but only by a study of its ontogeny. The taxonomic value of this characteristic must therefore be somewhat limited until such time as careful studies shall have been made.

Duval-Jouve (12, 13), Grob (Prat (41)) and Pée-Laby (39) studied the anatomy of the leaves and arrangement of cell types in the epidermis. Pée-Laby (39) was able to distinguish between two anatomically distinct groups of grasses by the arrangement of the chlorenchyma tissue. One group has the chlorenchyma localized in two layers of cells around the vascular bundles. Avdulov (1) calls this arrangement "type 1." The other group has the chlorenchyma uniformly distributed throughout the leaf and is referred to as "type 2." Prat (41) extended the work of Duval-Jouve and Grob. He based his classification not on any one or a few separate characteristics, but on a complete analysis of the size, shape, structure distribution and maturity of the various cell types on all parts of the plant, stem, leaves, glumes, etc. He found that certain characteristics serve to distinguish large groups; others define more restricted groups, and still others the simple forms caused by variation in environment, etc. By this method Prat was particularly successful in studying and amending the classification of the tribe Hordeae, and in indicating its relationship with the rest of the Gramineae.

S. Nawaschin was probably a pioneer in the study of chromosome morphology, but since he published his results in Russian they were available only to a very limited circle of investigators and it was not until 1924, when he published in German (37) that his results became generally known. Lewitsky (30) quotes Nawaschin as saying in 1910 that according to his observations "the chromosomes of *Fritillaria tenella* are distinctly double and distinctly divided in the place where the bundles of the spindle fibers are attached." A year later he distinguished between three types of bivalent chromosomes according to the position of the attachment constriction: (i) U-shaped, almost equal-armed; (ii) U-shaped, distinctly unequal armed and (iii) hook-shaped, one arm being very small. In 1912 he reported "on the dimorphism of the nuclei in somatic cells of *Galtonia candicans*," showing the presence of special, minute but perfectly constant appendages attached by means of a thread to two (out of four) medium sized chromosomes characteristic of this plant. He called these appendages "satellites," or in German "trabanten" (the latter term is now more widely used), and noted that during the division of the nucleus they split along with the remaining body of the chromosome. Here, for the first time, was the possibility of distinguishing between chromosomes by the peculiarities of their structure. In 1915 Delaunay (Lewitsky (30)) definitely proved the existence of tri-articulate chromosomes. Delaunay claimed that the number of segments and degree of differentiation were characteristic of definite chromosome types of definite species. This character represents the second type of secondary differentiation of the chromosomes.

In the same year that Nawaschin's German paper (37) appeared, Newton (38) and Taylor (48) published results of investigations from which it was evident that they had arrived at similar conclusions.

Sakamura (45) made extensive use of artificial methods to intensify the morphological differentiation of the chromosomes. He came to the conclusion that the presence of constant constrictions in the chromosomes is a general phenomenon in plants and animals, and that at the point of attachment of the spindle fibres the chromosomes always show a constriction or a rudiment of one.

Early observation convinced the investigators that there existed a more or less definite constancy of chromosome number. Further work, however, resulted in an appreciation of the fundamental constancy of the morphological composition of the nucleus. This later became expressed in the form of the "idiogram." Changes of the idiogram in a series of successive species afforded material for drawing up particular phylogenetic lines as well as for establishing some facts in connection with the evolution of the species.

Lewitsky (31) discusses fully this question of the use of karyotypic characters in systematics. He defines an idiogram as the graphic representation of a chromosome set with all the diversity of its structure. Separate species of a genus are characterized by quite definite and constant idiograms. These idiograms, although varying somewhat from one species to another usually maintain the same general type throughout the genus. On the contrary, when passing from one genus to another, the type of idiogram undergoes a complete transformation and appears as a new "karyotype." It would seem, therefore, that in classifying plants all that would have to be done would be to group those species having similar idiograms into the same genus, and into different genera when the karyotype changed. The question, however, is not quite as simple as this, for we are immediately faced with the difficulty of deciding when a difference in idiogram is great enough to justify the establishment of a new karyotype. This is a very difficult point, especially so when it is known that there exists a uniformity in the number and main characteristics of chromosomes through whole groups of genera which, though allied, are yet unquestionably different. Instances of a real coincidence of idiogram for whole large families have been known. On the other hand there may be a clear divergence of idiograms in adjacent species, which are then characterized by different karyotypes.

Lewitsky (31), in his analysis of the differences to be found in idiograms, notes that in general, chromosomes with equal arms indicate a more primitive stage of development, both morphologically and cytologically, than those with sharply unequal arms. Exceptions to this rule occur sometimes in the case of the formation of heads on chromosome fragments in X-rayed plants (32). It should be noticed, however, that the extent to which the constrictions so formed are functional has not yet been finally settled.

Distinction must be made, in the comparison of idiograms, between chromosome sets which have been differentiated through a process of gradual shortening and those which have undergone more complicated processes such as translocation, fragmentation, constriction-shifting, etc. Lewitsky and Araratian (32) conclude that the sharp differences sometimes observed in the idiograms of closely related species may be due to fragmentation and subsequent loss of portions of the chromosomes, while close similarity of idiograms in morphologically dissimilar genera indicates that the differences between the genera are chiefly genic. Another explanation for the wide difference in idiograms sometimes noticed in related species is afforded by the translocation of parts of chromosomes following fragmentation. Lewitsky and Araratian (32) cite an instance of such a change in a triploid *Crepis*. Similar transformations have been produced by the action of X-rays.

Thus, though the taxonomic significance of one or another of the karyotypic peculiarities is, generally speaking, variable, nevertheless some of them characterize large systematic units and others small ones. In this respect the first place is taken by the basic number and the size of the chromosomes.

A basic number for a polyploid series is usually of great systematic importance, characterizing whole families and tribes. The size of the chromosome is used to separate, for example, subfamilies in the Gramineae and tribes in the Leguminosae, as well as many genera, species and varieties. Next in order of importance come idiogram types, characterized by changes of greater or lesser degree in the length and structure of the arms of the individual chromosomes. Of least importance is the polyploid multiplication of whole chromosome sets.

In conclusion, Lewitsky and Araratian (32) state that "the idea of the karyotype as a karyological characteristic especially and exclusively applied to generic definitions or to any other definite systematic unit does not hold. One cannot state what extent of similarity of idiogram involves their subordination to the same karyotype. On the ground of larger or lesser community of characters, one may distinguish in one and the same complex of forms karyotypes of families, genera, species and races. Therefore, the karyotype is a karyological characteristic of a group of allied forms which may be applied to any systematic unit."

Smith (46) has furnished a striking example of the significance of chromosome morphology in relation to systematics. His arrangement of the Anchuseae on this basis alone accords perfectly with the revision of the group made by Johnston (Smith (46)) from a general taxonomic study.

Early attempts to classify the Gramineae on a karyological basis met with little success, however, on account of the lack of a sufficiently broad collection of material and the use of meiotic instead of mitotic chromosomes, together with limited concepts of chromosome morphology. Meiotic chromosomes rarely retain their individuality and they are of very limited value for the purpose of karyo-systematics.

Avdulov (1) was the first to realize and correct these faults and in consequence was able to propose a system of classification which is, in the main, in accordance with recent findings from other fields of study.

Materials and Methods

The material used was collected by Dr. C. L. Huskins in 1930 while at the John Innes Horticultural Institution, Merton, England. In 1931 Avdulov's (1) important and extensive study on the karyo-systematics of the Gramineae was published. This research has resolved itself into a scrutiny and extension of his work. The figures are from root-tip preparations fixed in LaCour's (28) 2BE or 2BD fixatives. Sections were cut 14μ thick and stained by LaCour's chromic acid modification of Newton's gentian violet method. Drawings were made with the aid of a camera lucida, 30 $\times$ ocular and Zeiss objective 1.5 mm., N.A. 1.3, giving a magnification at table level of approximately 6,900$\times$. This has been reduced in reproduction to approximately 3,450$\times$.

Table I shows a summary of the classification and somatic chromosome numbers of the species examined in the present investigation. The classification, as mentioned, is based on Bews' (6) system.

TABLE I

LIST OF SPECIES EXAMINED AND THEIR SOMATIC CHROMOSOME NUMBER

Subfamily Pooideae	Chromosome number	Subfamily Panicoideae	Chromosome number
Bambuseae		Melinideae	
Arundinaria fortunei Fenzl.	48	*Melinis minutiflora* Beauv.	36
Arundaria pygmaea Kurz.	54	Paniceae	
Phyllostachys flexuosa .	54	*Digitaria exilis* Stapf.	54
Festuceae		*Echinochloa frumentacea* (Roxb.) Link.	36
Arundo donax L.	110	*Oplismenus burmanii* (Retz.) Beauv.	72
Phragmites communis Trin.	48	*Brachiaria mutica* Stapf.	36
Gynerium argentea (Nees) Stapf.	76	*Pennisetum clandestinum* Hochst.	36
Melica altissima L.	18	*Cenchrus tribuloides* L.	34
Chlorideae		Andropogoneae	
Eleusine coracana Gaertn.	36	*Miscanthus saccharifera* Benth.	64
Chloris gayana Kunth	20	*Miscanthus sinensis* Anderss.	42
Eustachys sp.	40	*Andropogon eliottii* Chapm.	20
Cynodon dactylon Pers.	30	*Andropogon scoparius* Michx.	40
Hordeae		*Apluda mutica* L.	20
Lepturus cylindricus Trin.	52	Maydeae	
Agrostideae		*Tripsacum dactyloides* L.	36
Sporobolus tennuissimus Kuntze.	40	*Coix lachryma-jobi* L.	20
Phleum phleoides L.	14	*Euchlaena mexicana* Schrad.	20
Phalarideae		*Euchlaena perennis* Hitch.	40
Anthoxanthum odoratum L.	20	*Zea mays* L. subsp. *indentata*	20
Phalaris arundinacea L.	28		

Observations

Subfamily Pooideae

Bews (6) describes the subfamily Pooideae as follows: "Spikelets two to many flowered or reduced from above downward to a one flowered condition, with or without one or more empty lemmas, or a prolongation of the rachilla above the single fertile floret. Sometimes there may be empty lemmas below the fertile floret, usually two in number. The mature spikelets break up, leaving the glumes behind, or if they fall off entire with the glumes, then they do not consist of two heteromorphous florets as in the Panicoideae. The spikelets are usually more or less laterally compressed. The basic chromosome number in a great many is seven."

Tribe Bambuseae

This tribe is characterized by an extraordinary variety in the reproductive organs, yet despite this diversity it forms throughout a natural group which is more readily separated from its neighbors than any of the other tribes. The connecting character is chiefly a vegetative one, the culm being lignified either throughout its entire length or only at the base. The sessile leaves are also a general characteristic.

The internal anatomy has not been investigated to any very great extent. Prat (41) maintains that the epidermis of such members of the Bambuseae as he has analysed resembles more closely the epidermis of the Panicoideae than it does the epidermis of the Pooideae. Certain anatomical and morphological peculiarities, however, separate them from the former and he considers it better to create a new subfamily, the Bambusoideae, for the tribe Bambuseae.

Cytological data are scarce. Avdulov (1) examined an undetermined species from each of the genera *Bambusa*, *Arundinaria* and *Phyllostachys*. In each case he found the chromosome number to be somewhere between 68 and 74. More recently, Yamaura (51) reported 48 as the diploid number for *Sasa kozasa* Nakai, *Sasa kurilensis* var. *cernua* Nakai, and var. *Uchidai* Makino, *Sasa paniculata* var. *paniculata* Nakai, *Sasamorpha borealis* Nakai and *Pleioblastus maximowiczii* Nakai, and 72 as the diploid number for *Bambusa nana* Roxb. The present investigation included three species. Their chromosome numbers were as follows: *Arundinaria fortunei* Fenzi, $2n=48$ (Fig. 1); *Arundinaria pygmaea* Kurz., $2n=54$ (Fig. 2); *Phyllostachys flexuosa*, $2n=54$ (Fig. 3).

Yamaura (51) considers the basic number of the Bambuseae to be 12, but this is rendered doubtful by results here published unless great differentiation of chromosome number has occurred within the tribe. This question of basic number is associated with that of the primitiveness of the tribe. Certain features of the flower of the bamboos have led systematists to believe that they are not far removed from the original ancestors of the grasses. Lamb (29) placed the tribe at the tip of the phylogenetic tree of the family, but Schellenberg and also Hayek (Avdulov (1)) considered it as a side branch of development, that is, as derived from the same ancestor as the rest of the grasses. Prat (41) notes that the flowers of the Bambuseae approach closer to the typical monocotyledon flower than any of the other grasses, and that certain peculiar characteristics of the epidermis are found also in the Cyperaceae. Evolution in the epidermis of the Gramineae seems to have been in the direction of a progressive simplification, and it is interesting to note that in epidermal elements the Bambuseae are the most variable and the most complex of all the grasses.

Avdulov (1) considers that the basic number in the Gramineae has undergone a progressive diminution, probably from some such number as 12 to the 7, 6 and even 5, as found in the Pooideae and that this reduction in the basic number was preceded by an increase in size of the chromosomes. Lewitsky (30) maintains that in general, small chromosomes with equal arms indicate a more primitive stage of development, both morphologically and cytologically, than those with sharply unequal arms. This primitive morphological condition is well indicated in the chromosomes of the species here illustrated and also in those reproduced by Avdulov (1) and Yamaura (51).

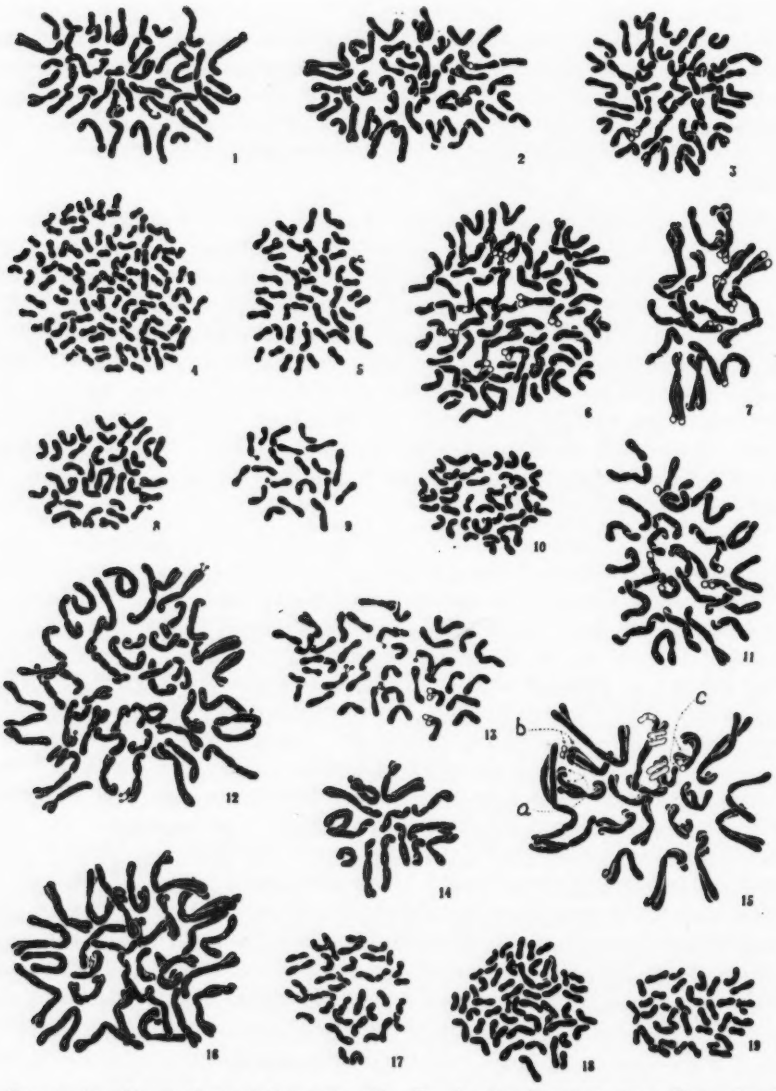

FIG. 1. *Arundinaria fortunei Fenzi, 2n=48.* FIG. 2. *Arundinaria pygmaea Kurz., 2n=54.* FIG. 3. *Phyllostachys flexuosa, 2n=54.* FIG. 4. *Arundo donax L., 2n=110.* FIG. 5. *Phragmites communis Trin., 2n=48.* FIG. 6. *Gynerium argentea (Nees) Stapf., 2n=76.* FIG. 7. *Melica altissima L., 2n=18.* FIG. 8. *Eleusine coracana Gaertn., 2n=36.* FIG. 9. *Chloris gayana Kunth, 2n=20.* FIG. 10. *Eustachys sp., 2n=40.* FIG. 11. *Cynodon dactylon Pers., 2n=30.* FIG. 12. *Lepturus cylindricus Trin., 2n=52.* FIG. 13. *Sporobolus tennuissimus Kuntze, 2n=40.* FIG. 14. *Phleum phleoides L., 2n=14.* FIG. 15. *Anthoxanthum odoratum L., 2n=20.* FIG. 16. *Phalaris arundinacea L., 2n=28.* FIG. 17. *Melinis minutiflora Beauv., 2n=36.* FIG. 18. *Digitaria exilis Stapf., 2n=54.* FIG. 19. *Echinochloa frumentacea (Roxb.) Link., 2n=36.*

Tribe Festuceae

Kunth (26) originally set up three tribes instead of the one tribe *Festuceae*, out of which the Bambuseae were later divided off. Bentham and Hooker (5) combined the three main tribes into one and allowed the fourth, Bambuseae, to stand. Hackel (16) adhered to this classification and later, along with Bentham and Hooker (5), divided the tribe into a whole series of subtribes. Much confusion followed as the individual constituents of the tribe were interpolated here and there throughout the system. Finally the view was taken that the whole multiplicity of several-flowered Gramineae, with the exception of certain specially differentiated tribes, the Aveneae and Hordeae, should be classed together as the Festuceae.

Bews (6) considers the Festuceae to be the most primitive of the *common* grasses. This claim to primitiveness is based chiefly on their many-flowered spikelets and short glumes. The tribe is divided into seven subtribes of which the first two, Centothecinae and Arundinae are the most primitive. The main line of evolutionary differentiation commences in the Festucinae and is followed through in the Dactylidinae-Seslerinae group, the Melicinae, the Eragrostinae and the Pappophorinae. The last subtribe is in some respects the most advanced of all the Festuceae though on the whole it is still rather specialized.

Cytologically the tribe may be divided into three groups which by no means agree with the established subtribes. The majority of genera which Avdulov (1) investigated belong to the temperate zones and are marked by large chromosomes having the basic number 7, type 2 leaf anatomy and clumped starch grains. In this first group belong the genera *Glyceria*, *Puccinellia*, *Poa*, *Festuca*, *Sclerochloa*, *Scleropoa*, *Briza*, *Dactylis*, *Desmazeria*, *Lamarckia*, *Sesleria*, *Koeleria*, *Echinaria*, *Melica*, *Catabrosa*, *Bromus*, *Boissiera* and *Schismus*. Polyploidy is observed in the genera *Poa*, *Glyceria* and *Puccinellia*, and a probable instance of the loss of a chromosome pair from a tetraploid form of a series with the basic number 7 is afforded by *Koeleria phleoides* which has 26 chromosomes in comparison with the multiples of seven of the other species investigated.

In the genera *Echinaria*, *Melica* and *Catabrosa* the basic number deviates from the typical 7 of this group, being 9 in the first two and 10 in the last. The specimen of *Melica altissima* here examined (Fig. 7) agrees with Avdulov's (1) material in number and morphology of chromosomes. In *Schismus calicinus* the chromosomes are considerably smaller than usual and the basic number is 6. Inasmuch as none of these differences are bound up with any sharp phenotypic or karyotypic difference, Avdulov does not object to their inclusion in this group.

The second karyo-systematic group contains, so far, only the genera *Diplachne* and *Eragrostis*. The basic number is 10 and the chromosomes are small. These characters of the karyotypic structure are connected with a series of morphological characters. In its cytology, the group is reminiscent of the Panicoideae and the Chlorideae. The resemblance extends to the

epidermis. Prat (41) analyzed the epidermis of *Eragrostis pilosa* and *E. minor* and remarked that even though there is considerable similarity between the epidermal characteristics of this genus and those of the Panicoideae, yet, owing to the complexity and heterogeneity of the Festuceae he does not consider it necessary to remove the genus from that tribe, but merely to give it a special position within the tribe.

Bews (6) notes that Stapf elevated the subtribe Eragrostinae to the rank of a tribe and placed it close to the Panicoideae and also that he removed the genus *Diplachne* to the Chlorideae. As will be seen later this latter tribe is itself very Panicoid in character and there thus exists a remarkable unanimity among three methods of classification; morphological, anatomical and cytological.

The third group has small chromosomes, a basic number 12 and type 2 leaf anatomy. The genera *Centotheca*, *Uniola*, *Phragmites* and *Arundo* fall into this class. The characteristic of small chromosomes in multiples of 12 is common to the groups to which *Oryza* (Oryzeae) and *Erharta* (Phalarideae) belong, and which they also resemble in structure of starch grains, leaf anatomy and geographical distribution.

In the present investigation, *Phragmites communis* (Fig. 5) was found to have 48 chromosomes, agreeing with Avdulov's (1) belief that the basic number for the genus is 12. The genus *Arundo* is closely allied to *Phragmites* and *A. donax* (Fig. 4) was found to have 110 chromosomes.

The genus *Gynerium* is morphologically closely related to *Centotheca*, *Arundo* and *Phragmites* and the chromosomes of *Gynerium argentea* (Fig. 6) though different in number, $2n=76$, are very similar to those of the species of *Centotheca* and *Uniola* which Avdulov (1) described. Recently, Avdulov (3) published 72 as the somatic number of an undetermined species of *Gynerium*. In the light of this it is possible that some of the extremely small bodies considered as chromosomes in the present material may be only fragments and the basic number of the genus be actually 12 as in the rest of the group.

Tribe Aveneae

In the tribe Aveneae "the glumes are lengthened, and, with rare exceptions, exceed the nearest lemma, often exceeding the whole spikelet, which is thus enclosed and protected by the enveloping glumes. The lemmas remain primitive in being usually 5 to many nerved, and are often awned from the back or sometimes from the tip, or between teeth or lobes, or more rarely are awnless. The spikelets, as in the Festuceae, are two or more flowered, very rarely they are single flowered." (Bews (6).)

The tribe has been regarded by most authors as one of the most natural, yet there are very marked differences within it which may interfere with this naturalness. The position of the awn on the lemma divides the tribe into two groups which correspond very closely with their geographical distribution. Those genera which have the awn springing from the back of the lemma, or which in a very few cases lack awns, belong to the northern group, native to

the north temperate and cold zones. The remaining awn types are almost exclusively in the southern group, and are found in the northern hemisphere only in tropical regions. In the northern group are the genera *Holcus*, *Aira*, *Antinaria*, *Molineria*, *Deschampsia*, *Corynephorus*, *Ventenata*, *Trisetum*, *Arrhenatherum*, *Avena*, *Gaudinia* and *Airopsis*, while the southern group includes *Prionachne*, *Eriachne*, *Zenkeria*, *Coelachne*, *Micrairia*, *Achneria*, *Anisopogon*, *Danthonia* and *Amphibromus*. This southern group is very heterogeneous.

Avdulov's (1) investigation covers only genera from the northern group, *Corynephorus*, *Holcus*, *Trisetum*, *Deschampsia*, *Arrhenatherum*, and *Avena*, and he finds the size and number of the chromosomes to be quite uniform. The basic number, with one or two unimportant exceptions, is 7. The southern group has not yet been studied cytologically.

There is no doubt that the northern members of the Aveneae are very closely related to the Festuceae and Hordeae. Prat (41) considers the Aveneae and Hordeae as subordinate groups of the tribe Festuceae, the Hordeae being those Festuceae with sessile spikelets and the Aveneae those with dorsally articulated awns. This close relationship is amply supported by such karyological data as are available at present. Whether or not an investigation of the southern group of the Aveneae, those not characterized by dorsal articulation of the awn, will suggest their removal from this large Festuceae group remains to be seen.

Tribe Chlorideae

The Chlorideae are distinguished from other tribes by the presence of two series of closely touching spikelets which form a one sided spike. The differences within the tribe, however, are large.

Bews (6) subdivides the tribe into three groups based on the reduction of the number of flowers in the spikelet. The first group contains those with two to several perfect florets in each spikelet, among which are *Eleusine*, *Dactyloctenium*, *Beckmannia* and *Leptochloa*. Some of the genera in this group are hardly distinguishable from the Festuceae.

The members of the second group have only one perfect floret and one or more imperfect florets in each spikelet. *Bouteloua*, *Gymnopogon*, *Chloris*, *Eustachys* and *Munroa* are some of the genera which fall in this class.

The most advanced group contains those genera with the spikelets having definitely one floret, with or without a prolongation of the rachilla. The most important representatives are *Cynodon* and *Spartina*.

The anatomy of the leaves of the Chlorideae differs from that of most of the Pooideae in being type 1. Guntz (1886), quoted by Avdulov (1) placed *Spartina* in type 1, while Duval-Jouve (13) put it in type 2. Avdulov unhesitatingly classifies it as type 1 after inspection of a colleague's material. The single exception to the rule seems to be the genus *Beckmannia* which definitely has type 2 chlorophyll arrangement.

All the genera, with the possible exception of *Gymnopogon*, have clumped starch grains. Grob. (1896; Avdulov (1)) demonstrated the presence of two-celled hairs, "Winkelhaaren," on the epidermis of the Panicoideae and also in a few species of the Pooideae. It is interesting to note that all the Chlorideae with the exception of the genus *Beckmannia* possess these two-celled hairs and that Prat (41) considers the genera *Dactyloctenium*, *Eleusine*, *Spartina*, and *Bouteloua* to resemble more closely the Paniciodeae than they do the Pooideae. The tribe shows the same relationship in geographical distribution, *Beckmannia* being a native of temperate regions while the rest of the tribe is more or less tropical or subtropical as is the majority of the Panicoideae.

Avdulov (1) divides the tribe into two karyo-systematic groups. The first is characterized by small chromosomes and the basic numbers 9, 10 and rarely 12. Into this group fall the majority of genera investigated including *Spartina*, *Cynodon*, *Trichloris*, *Dinebra*, *Eleusine*, *Dactyloctenium*, *Leptochloa*, *Buchloe* and *Bouteloua*. In the present study *Chloris gayana* (Fig. 9) was found to have 20 chromosomes, and an undetermined species of *Eustachys* (Fig. 10) had 40 chromosomes. Hackel considers the genus *Eustachys* Desv. to be a subgenus of *Chloris* Sw. Nash (36) points out, however, that most of the points of resemblance of the two genera are common to the tribe Chlorideae as a whole. The details of the spikelet and geographical distribution, at least in North America, are so different that Nash concludes that they should be considered as separate genera. Bews (6) also treats them in this manner and cytological results appear to favour this system. The two genera have similar types of chromosomes but they are present in very different proportions. This might indicate a close relationship and at the same time a difference, which when coupled with large enough morphological changes, would justify their separation.

The present examination of *Eleusine corcarana* (Fig. 8) gave the same number ($2n=36$) as reported by Avdulov (1). *Cynodon dactylon* (Fig. 11) however was found to have 30 instead of 36 chromosomes. Avdulov considered the basic number of the genus to be 12 but in the light of the above results this appears to be doubtful. The basic number appears rather to be 10 as in most species of this group.

In the genus *Spartina* Avdulov (1) examined *S. cynosuroides* Willd. and *S. schreberi* J. F. Gmel. In the former he counted from 80 to 88 chromosomal bodies and in the latter 40 to 43. He noticed, however, that if any more than 80 or 40 bodies, respectively, were present then there was a corresponding number of chromosomes without attachment constrictions. He therefore assumes that those chromosomal bodies above 80 or 40 are merely fragments and that the basic number for the genus is 10. Church (10), however, reported 14 as the haploid number for *S. michauxiana* Hitch which Saint-Yves (44) says is synonymous with *S. cynosuroides* Willd. and Huskins (22) in his investigation of the origin of *S. townsendii* found it to have 126 chromosomes,

S. alterniflora to have 70 and *S. stricta* to have 56. Church (10) had reported 14 bivalents and 14 univalents in *S. alterniflora*. There is evidently considerable variation and polyploidy within the species of this genus but multiples of 7 seem most common. Avdulov's (1) *S. cynosuroides*, therefore, probably had 84 chromosomes and his *S. schreberi* 42. All the species so far examined are very similar in regard to the morphology of their somatic chromosomes. They are also similar to the rest of Avdulov's first group in this respect. The similarity is strengthened by a series of morphological and anatomical characteristics and there is therefore no need to remove the genus from this group.

The second group contains as yet only the genus *Beckmannia*. Avdulov (1) examined *B. erucaeformis* Host var. *ramosa* Paczosky and *B. erucaeformis* Host var. *baicalensis* W. Kusnezow, and counted 14 chromosomes in each. The chromosomes are large and altogether resemble those of the northern grasses of the Phalarideae, Aveneae, Festuceae and Agrostideae. Therefore, in addition to leaf anatomy, epidermal hairs and geographical distribution, the genus *Beckmannia* differs from the rest of the tribe in its cytology. These characteristics plus a whole series of morphological characters indicate that the genus would be more properly placed with the tribe Festuceae.

Tribe Hordeae

The Hordeae are still more advanced than the Chlorideae in having the spikelets always definitely sessile and usually more or less sunk in the notches on opposite sides of a spike. With the exception of one isolated genus, *Pariana*, they are more or less confined to the temperate regions. The tribe as a whole is extremely uniform, both from the morphological and from the anatomical point of view. Prat (41, 42) made an exhaustive study of the epidermal characters of a number of the genera and came to the conclusion that with the exception of *Nardus* and *Jouvea*, and two other small genera, the tribe was remarkably homogeneous.

There are several differences within the tribe, however, which serve to break it up into sub-tribes. Harz., 1880–1882, and Hayek, 1925 (quoted by Avdulov (1)), divided the tribe into the Triticeae or Hordeae with simple starch grains, and the Lolieae with compound starch grains. Hackel (16) divided the tribe into six sub-tribes, the Nardeae, Lolieae, Leptureae, Triticeae, Elymeae, and Parianeae. Bews (6) combined some of these and proposed the following classification:—

(i) Parianinae (=Parianeae Hackel) containing the isolated genus *Pariana*.

(ii) Elyminae (=Elymeae Hackel) containing the genera *Elymus*, *Sitanion*, *Hystrix*, *Hordeum* and *Asprella*.

(iii) *Triticinae* (=Lolieae, Leptureae and Triticeae Hackel) containing the genera *Agropyron*, *Haynaldia*, *Heteranthelium*, *Triticum*, *Secale*, *Lolium*, *Kerinozoma*, *Jouvea*, *Scribneria*, *Psilurus*, *Ischnurus*, *Lepturus* and *Pholiurus*.

(iv) Nardinae (=Nardeae, Hackel) containing only the genus *Nardus*.

Prat (42) considers the following subdivision of the tribe to be more natural:—

(i) Triticae (2 glumes; spikelets transverse and solitary): *Agropyron*, *Aegilops*, *Triticum*, *Secale*, and *Haynaldia*.

(ii) Hordinae (2 glumes; spikelets transverse and 2–6 at each node): *Hordeum*, *Elymus* and probably *Hystrix* and *Sitanion*.

(iii) Loliae (1 glume; spikelets longitudinal): *Lolium*, *Lepturus*, *Monerma* and *Psilurus*.

(iv) Pholiureae (2 glumes; transverse spikelets but with deeply excavated rachis and epidermis of paleas very little differentiated): *Pholiurus* and *Scribneria*.

There are two genera now generally included in the Hordeae which have given taxonomists considerable trouble; these are *Nardus* and *Jouvea*. The retention of the genus *Nardus* within the Hordeae is morphologically dependent on the fact that the inflorescence is a simple spike. Numerous anatomical features clearly separate it from that tribe, however, and to these Prat (41) has added a series of epidermal observations. The retention of the genus within the Hordeae destroys the admirable unity of that tribe and the only alternative seems to be to create for it a special tribe. This tribe has been called the Nardoideae. Further investigation reveals that this new tribe does not properly belong in the subfamily Pooideae at all, but in the Panicoideae. Prat (42) also transfers the genus *Jouvea* to the Panicoideae and suggests that the genera *Kralikia* Coss and *Kerinozoma* Stend., likewise belong in that subfamily.

With the exception of *Zea mays*, the common cereals, of which three occur in this tribe, are probably the best known, both cytologically and genetically, of all the grasses. The genus *Triticum* forms a definite polyploid series with 7 as its basic number, and is an important example of the use of chromosome numbers alone in classification. The cytological grouping agrees exactly with the classification based on morphological and serological grounds, as well as on the basis of size of pollen grain, rust resistance and mutual fertility or sterility.

Aegilops, *Hordeum* and *Agropyron* likewise form polyploid series within the genus; *Aegilops* with 7 and 14 and *Hordeum* with 7, 14 and 21 chromosomes. Peto (40) reported an almost complete series from diploid to decaploid in *Agropyron*. He also obtained considerable evidence of hybridity. This would help to explain the intergradation of forms frequently observed in the genus.

Avdulov (1) found three different types of chromosome set within the genus *Agropyron*. The first type of set is composed exclusively of *V*-shaped chromosomes (*A. caninum*, *A. cristatum*, etc.); the second type has every chromosome with one arm reduced to a head (*A. prostratum*), and the third type is an equal mixture of the first two types (*A. orientale*). He suggests that *A. orientale* may be the result of a cross between a member of the *V*-chromosome group and a species with only headed chromosomes.

Avdulov studied three species of *Lepturus* and one of *Monerma* and observed the following chromosome numbers:—*Lepturus incurvatus* (L.) Trin. ($2n=36$); *Lepturus filiformis* (Roth.) Trin. ($2n=14$); *Lepturus pannonicus* Kunth ($2n=14$); *Monerma cylindrica* Coss and Dur. ($2n=26$). The specimen corresponding to *M. cylindrica* which was examined in the present investigation (Fig. 12) had 52 chromosomes and is a tetraploid. Camus (8) notes that the name *Lepturus* has priority over *Monerma*, and that therefore *Monerma cylindrica* Coss and Dur. should be called *Lepturus cylindricus* Trin. She also places the three species considered by Avdulov as *Lepturus* in the genus *Pholiurus*. These three species she considers should be named *P. incurvus* A. Camus, *P. filiformis* A. Camus and *P. pannonicus* Trin., respectively.

It is evident from Avdulov's (1) illustrations that the four species mentioned above have chromosomes of similar types but that they have them in different proportions. Their close relationship is therefore reflected cytologically. We appear to have an instance of redistribution of chromatin; such loss or change as has occurred has not had any striking effect on the phenotype.

Avdulov (1) removes these four species to his tribe Festucaceae which is a member of his series Festuciformes and contains most of the Festuceae and Aveneae. He also examined *Nardus stricta* (26 chromosomes), *Lolium italicum* (28 chromosomes) and *Psilurus nardoides* (28 chromosomes) and included them in his Festucaceae. Prat (41) found considerable similarity between the epidermis of the Hordeae, Festuceae and Aveneae, but the inclusion of *Nardus* in this group is absolutely contrary to practically all existing morphological, anatomical and epidermal evidence. As has already been pointed out, this genus is very different from the rest of the tribe and approaches the Chlorideae in its resemblance to the Panicoideae. In spite of the almost entire lack of Panicoid characters (more or less small chromosomes in multiples of 9 or 10) in its karyotype, it nevertheless seems to belong naturally to that subfamily. This is a case where more or less definite karyological evidence must be subordinated to an overwhelming weight of evidence of another nature.

Unfortunately, the genera *Jouvea*, *Kralikia* and *Kerinozoma* have not so far been cytologically examined. The remaining genera fall in Bews' (6) subtribes Elyminae and Triticinae or into Prat's (42) subtribes Triticae and Hordinae. Avdulov (1) finds this to be a very uniform group with chromosomes all more or less the same in size and characterized by the basic number 7. He leaves these genera in their original position in what he calls the tribe Frumentaceae which contains also the genera *Bromus* and *Boissiera* of the Festuceae. Thus, with the exception of the genus *Nardus* his classification agrees exactly with that of Prat (42) and shows the artificiality of grouping the subtribes Lolieae-Leptureae and Triticeae. Such correspondence between classifications based on two so entirely different characters is good evidence of correctness.

Tribe Agrostideae

According to Bews (6), "in the Agrostideae the spikelets are definitely one-flowered, without sterile lemmas or male flowers, so that the usual evolutionary trend seen in the tribes so far dealt with, namely, the reduction of the number of flowers in the spikelet, does not apply to this tribe." Other important evolutionary trends are well illustrated, however, and are used as a basis for subdivision into subtribes. "The most advanced subtribe, the Stipinae, have the lemma indurated, or at least much harder than the glumes at maturity, and closely enveloping the fruit. The others have a hyaline or membranaceous lemma, more delicate than the glumes. These are further subdivided into two other subtribes, the Phleinae with the stigmas having short branches all round and projecting from the apex of the lemmas, and the Agrostinae with the stigmas plumose, projecting from the side of the spikelet."

The Phleinae are a distinct, but not important, subtribe. *Phleum*, *Heleochloa* and *Alopecurus* are the only genera of importance. The genus *Sporobolus* is rather distinct from either the Agrostinae or Phleinae, but is included in the former by Hackel. Stapf (Bews (6)) separates it as a distinct tribe, the Sporoboleae, and places it next the Eragrosteae which he removed from the Festuceae. The subtribe Stipinae is the most advanced of the three as is evident from their more efficient means of seed dispersal and adaptation to a more or less xerophytic habitat.

Cytologically the tribe may be divided into three fundamental groups. The first is represented by the genera *Muhlenbergia* and *Lycurus* on the one hand and *Heleochloa* and *Sporobolus* on the other. It is characterized by small chromosomes and a basic number of 10 for the first part and 9 for the second. Avdulov (1) bases his conclusion as to the basic number of the second part on *Heleochloa schoenoides* which has 36 chromosomes and on two forms of *Sporobolus indicus*, one of which has 18 and the other 36 chromosomes. *S. tennuissimus* (Fig. 13) was examined in the present investigation and found to have 40 chromosomes which gives it the basic number 10 and makes it conform with the first part of the group. The group as a whole resembles the subfamily Panicoideae of Bews, in regard to its leaf anatomy, geographical distribution and structure of the ligule as well as in its cytology. Krause, according to Avdulov (1), demonstrated the morphological connection of *Heleochloa* with *Sporobolus* and of both with the Chlorideae and the genus *Tragus* of the Zoysieae. Both these tribes are similar to this group in cytology, structure of starch grains and leaf anatomy and, as Prat (41) points out, in certain epidermal characteristics also.

The second cytological group contains the genera *Calamagrostis*, *Agrostis*, *Mibora*, *Cornucopiae*, *Phleum*, *Alopecurus* and *Milium*. It is characterized by large chromosomes and the basic number 7, with the exception of *Milium vernale* which has 18 chromosomes. *Milium effusum*, however, has 28 chromosomes. *Phleum phleoides* (Fig. 14) was the only representative of this group examined in the present investigation. It had 14 chromosomes. Avdulov

(1) studied four species and Gregor and Sansome (15) studied two strains each of two species of *Phleum*. The basic number 7 was constant throughout.

Three genera of this group, *viz.*, *Phleum*, *Mibora* and *Alopecurus* are connected morphologically with the genera *Hierochloa*, *Anthoxanthum* and *Phalaris* in the tribe Phalarideae by reason of the fact that the awn springs from the tip of the glume. In *Apera*, however, it arises from the back of the glume as in the Aveneae. The group agrees with the above members of the Phalarideae and with the Aveneae in having clumped starch grains, type 2 leaf anatomy, parallel epidermal organization (Prat (41)), and in being distributed mostly in the northern hemisphere. The similarity extends also to their cytology. All have large chromosomes, and the basic number 7 is characteristic of the Aveneae and two of the three genera of Phalarideae.

The third group, represented by the genera *Stipa* and *Oryzopsis*, is characterized by small chromosomes with a basic number 12. Of the eight species of *Stipa* investigated by Avdulov (1), one, *S. sibirica*, has 24 chromosomes and the rest have 44. These species are presumably tetraploids derived from a diploid form with a basic number 12, which had lost one pair of chromosomes. The two species of *Oryzopsis*, *O. miliacea* and *O. virescens*, both have 24 chromosomes.

Cytologically this group approaches *Oryza* (Oryzeae), where the basic number is also 12 and where the chromosomes are also small. These genera are likewise similar floristically, all approaching a more or less primitive, hexameric type of flower structure. There thus seems to be a linkage between small chromosomes with the basic number 12 and this flower type.

Tribe Phalarideae

This is a small tribe containing only six genera. It is divided naturally into two groups. The first contains *Ehrharta*, *Microlaena* and *Tetrarrhena* and is characterized by the third and fourth outer glumes being larger than the first and second. The second group, comprising the genera *Phalaris*, *Anthoxanthum* and *Hierochloa* has the third and fourth glumes smaller than the first and second. The two groups are also different in geographical distribution. The first is confined to the southern hemisphere while the second, with the exception of one species of *Anthoxanthum* grows entirely in the northern hemisphere. Both groups have compound starch grains and type 2 leaf anatomy.

Cytologically the tribe is divided into two groups corresponding, as far as present investigations indicate, to the above mentioned taxonomic groups. Avdulov (1) finds that the chromosomes of the first group, represented in his work by *Ehrharta panicea*, are small and in multiples of 12. They therefore resemble the genus *Oryza*. The structure of the starch grains, anatomy of the leaves and geographical distribution are also the same as in the Oryzeae.

The second group is characterized by large chromosomes in multiples of 7 or less. In the genus *Phalaris* the chromosomes are at least three times as large as those of *Ehrharta panicea* and the basic number is 7. *Phalaris canariensis* formed an apparent exception since both Avdulov (1) and Church (10)

reported 12 as its diploid number. Recently, however, Nakajima (35) has established its haploid number as 14 and its diploid number as 28. The only species of this genus examined in the present investigation was *P. arundinacea* (Fig. 16). The diploid number of 28 coincides with that of Avdulov's material.

Anthoxanthum also has large chromosomes. Marchal (1920) (Avdulov (1)) counted 8 chromosomes in the meiotic first metaphase of *A. odoratum*, but Avdulov (1) reported no deviation from 20 chromosomes in somatic tissue; the material examined in the present study also had 20 chromosomes (Fig. 15). *A. aristatum* has 10 chromosomes and therefore the basic number for the genus is probably 5. Two interesting features were observed in the material examined. In one cell it could be seen very clearly that the ends of three of the chromosomes (a, b, and c, Fig. 15) were four-partite instead of bi-partite as is commonly the case. The other feature was the presence, in all the cells examined, of two pairs of large "fragments" and one pair of small, almost spherical, ones (shown in outline in Fig. 15). These "fragments" do not stain as deeply as the rest of the chromosomes, they always lie in definite pairs as shown, and no attachment constriction is visible. They appear to be a constant component of the nucleus, however, as they were found in more than the one root-tip. It seems, therefore, that they may be analogous either to the "chromosomal bodies" reported by Avdulov (2) in *Zea mays* or the "additional chromosomes" reported by Avdulov and Titova (4) in *Paspalum stoloniferum*.

Thus we have two basic numbers in this second group; 7 for the genera *Phalaris* and *Hierochloa* and 5 for the genus *Anthoxanthum*. Avdulov (1) thinks that this difference between the basic numbers may be due to an evolutionary deviation of *Anthoxanthum* away from the more primitive number 7, characteristic of the other members of the group and, indeed, of the majority of the Pooideae.

There seems to be some relationship between the second group and the Aveneae. In *Anthoxanthum* the lower lemmas sometimes bear male flowers and are awned from the back as in the Aveneae. In *Hierochloa* the lower lemmas, or at least one of them, always bear male flowers. The chromosomes of the two groups are also very similar, both in basic number and in morphology. There is also a marked correspondence in their geographical distribution.

On the other hand, the first group of the Phalarideae, of which *Ehrharta panicea* is so far the only representative to be examined cytologically, bears a close similarity to the Oryzeae.

Prat (41) examined the epidermis of *Phalaris paradoxa*, *Phalaris minor*, *Phalaris arundinacea* and *Anthoxanthum odoratum* and considers them to have well marked affinities with the Oryzeae. In the face of this evident disagreement between the two methods of classification it is advisable that further and more detailed study be made, both of their karyology and "dermatology" (Prat), before any definite placing be given to either

of the groups of genera. At present, however, the cytological data seem more conclusive, at least in so far as the second group is concerned. It appears to be fairly certain therefore, that this second group and the Aveneae are quite closely related. Avdulov (1) considers that this resemblance may be taken to represent a side-line development by the genera *Phalaris*, *Anthoxanthum* and *Hierochloa* that has not become differentiated to any great extent.

Tribe Oryzeae

According to Bews (6) "the Oryzeae, or Rice tribe, are particularly interesting for many reasons. They are an isolated group, without any very obviously close connections; in some ways they are rather primitive, as, for instance, in the prevalence of six stamens among them; in other respects they are advanced, the spikelets being reduced to the one-flowered condition, and the glumes often being entirely suppressed or replaced by two minute empty lemmas, or rarely both glumes and empty lemmas may be present as in *Oryza* itself. One whole section (which Hitchcock elevates to the rank of a distinct tribe, the Zizaneae) has the spikelets unisexual and the plants monoecious. In some respects the Oryzeae suggest the Paniceae, particularly in the suppression of the glumes, and Hackel placed them in the Panicoideae. But they differ from the rest of the Panicoideae in having the spikelets laterally compressed, and they are now always included in the Pooideae.

Not only are they somewhat isolated floristically, but they are also very distinct ecologically, for they have responded to a different environment from the majority of the grasses. With the exception of *Lygeum spartum*, all the genera have become adapted to hygrophilous or purely aquatic modes of life. The aquatic forms are the most advanced."

It is evident from morphological and anatomical studies, that the Oryzeae as a tribe do not belong to the Panicoideae. The Oryzeae have clumped starch grains and type 2 leaf anatomy, whereas the Panicoideae have simple starch grains and type 1 leaf anatomy. There is a variation in epidermis within the tribe, however. Grob (1896) (Avdulov (1)) found that the genera *Oryza*, *Zizania* and *Lygeum* possessed the two-celled hair characteristic of the Panicoideae and that the genera *Pharus*, *Luziola*, *Zizaniopsis* and *Hygroryza* lacked them. Prat (41) prefers to group the Oryzeae with the Panicoideae, but his investigations were confined to the genera *Oryza* and *Lygeum*, both of which belong to Grob's Panicoid group.

Similarly, cytological study has been made of only one species, *Oryza sativa* (1). In this case, however, the evidence is against classifying the genus with either of the existing subtribes. Its chromosomes are small like those of the Panicoideae but its basic number is 12. It resembles a number of genera scattered throughout the Pooideae in this respect and, while evidence based on only one genus is naturally rather inconclusive, yet Avdulov (1) prefers to create a special section of the subtribe, Poateae (Hitchcock) Avdulov, for those forms with small chromosomes in multiples of 12.

Subfamily Panicoideae

Bews' (6) description of this subfamily is as follows: "Except in unisexual and neuter spikelets, the spikelets have one terminal perfect floret, with a male floret or empty lemma below it. One glume, or rarely both glumes, may be wanting. The rachilla is not continued above the upper floret. The spikelets fall entire from their pedicels, singly or in groups, or together with the joints of the rachis. The spikelets are usually more or less compressed.

The Panicoid series seems to have had a distinct origin from the Pooideae but may connect somewhat remotely with ancestral forms which resemble the Bamboos. It is obvious that the whole of the Panicoideae are rather highly developed in so far as reduction in the number of flowers in the spikelet is concerned. But, as we have seen, this reduction occurs in primitive tribes of the Pooideae as well. Though a very important evolutionary trend, it is, after all, only one among many. It has taken place within all the separate circles of affinity." Bews (6) considers that there are really only two main tribes of the Panicoideae, for the Maydeae are little more than a subtribe of the Andropogoneae and the Melinideae an unimportant transitional tribe which might be included in the Paniceae.

Tribe Melinideae

This tribe is of little importance. It is rather a heterogeneous collection of genera in which the spikelets have the two heteromorphous florets, the upper perfect, the lower male or barren, characteristic of the whole Panicoid series. The glumes and lemmas are both membranaceous, the latter not harder than the glumes, as in the Paniceae, and the former not much harder either, or at least not closing round the spikelet as in the Andropogoneae. Bews (6) says that Stapf includes the genera *Rhynchelytrum*, *Tricholaena* and *Melinis* in the Paniceae, and *Beckera* in the Oryzeae. Unfortunately, only one of these genera has been examined cytologically.

Avdulov (1) examined the genera *Arundinella*, *Melinis* and *Phaenosperma*. Hackel (16) maintained that *Arundinella* was the genus from which the tribe Andropogoneae originated. Avdulov (1) believes their morphological similarity to be confirmed cytologically through *A. anomala* and *Miscanthus japonicus*. According to his study they have the basic number 9. Two species of *Miscanthus* examined in the present investigation were found to have the basic number 7 and 8 respectively. This may not signify lack of correctness in Hackel's (16) surmise however, since, as has already been noted, it is possible for such a change to occur without producing any great effect on the expression of the phenotype. Avdulov doubts that all the Andropogoneae were derived from the genus *Arundinella*, but rather considers it more probable that *Arundinella* and *Miscanthus* form a connecting link between the Andropogoneae and the Melinideae.

Hackel (16) believed the genus *Melinis* to have sprung from the Paniceae and, as mentioned, Stapf includes it in that tribe. Avdulov (1) examined *M. minutiflora* and found its chromosome number to be 36; this was confirmed (Fig. 17). Since the basic number of most of the Paniceae is 9, and

since most of them have small chromosomes, as has *M. minutiflora*, Avdulov considers it quite logical to regard the genus as a member of the Paniceae.

The third genus which Avdulov investigated was the monotypic *Phaenosperma*, represented by *P. globosa*. It is cytologically very different from the other members of the tribe in that it has the basic number 12. This change in basic number is accompanied by parallel morphological differences which, along with the size of its chromosomes, place it in close relationship with *Oryza*, *Ehrharta* and the group within the Agrostideae represented by *Stipa* and *Oryzopsis*. Hackel (16), Bews (6), and other systematists seem to have erred, therefore, in including this genus in the Panicoideae.

Tribe Paniceae

The Paniceae are less advanced than the Andropogoneae floristically, and this is reflected very clearly in their distribution and ecological behavior. According to Bews: "They are grasses of the great tropical and subtropical regions of the world, where they are abundant. They do not enter very much into the composition of subtropical mesophytic grassland, a type of vegetation which, on the other hand, is completely dominated by the Andropogoneae." It is true that the Paniceae have produced some rather highly evolved ecological types, but the large majority belong to the primitive hygrophilous situations of the tropics. The more advanced types occupy drier situations in the warm regions, and a few, *e.g.* a species of *Paspalum* in South America, occur in grasslands, mixed with the Andropogoneae.

The Paniceae form a very large tribe having, according to Bews (6), about 60 genera and nearly 1400 species. Yet, as is to be expected from the uniformity of their habitat, many of the genera are very closely related, and the tribe as a whole forms one of the most natural groups within the family. Bews (6) follows Stapf in dividing up some of Hackel's (16) genera, chief among which is *Panicum*. Bews' nomenclature is followed in the present discussion of the tribe.

Hackel's section *Digitaria* of the genus *Panicum* becomes Bews' genus *Digitaria*. Avdulov (1) examined two forms of the species *Digitaria sanguinalis* Scop.; *viz.*, *f. australis* Mez. and subsp. *horisontalis* Mez. In both he found 36 chromosomes. *D. exilis* (Fig. 18) was found in the present study to have 54 chromosomes.

The section *Echinochloa* is also raised to the rank of a genus. According to Kihara *et al.* (25), *Panicum crusgalli* L. var. *frumentaceum* Hook. = *Echinochloa crusgalli* Beauv. = *Echinochloa frumentacea* (Roxb.) Link. Hitchcock (20) gives *Echinochloa frumentacea* Link. as synonymous with *Echinochloa crusgalli edulis* Hitchc. Avdulov (1) reports 54 chromosomes in *Panicum crusgalli* L. var. *frumentaceum* (Roxb.) Frimen. Church (11) gave 21 as the haploid number for *Panicum crusgalli* L. var. *frumentaceum* Hook. *Echinochloa frumentacea* (Roxb.) Link. (Fig. 19) examined in the present study had 36 chromosomes. The basic number is the same as in Avdulov's material, and it appears that Church (11) may have been mistaken in his observations.

The section *Brachiaria* becomes Bews' (6) genus of the same name. The genus is based on *Panicum eruciformis* Sibth. (Hitchcock and Chase (21)). Hitchcock (19) gives this species as synonymous with *B. erucaeformis* (J. E. Smith) Griseb. Avdulov (1) reported 18 chromosomes in it. *B. mutica* Stapf has 36 chromosomes (Fig. 21).

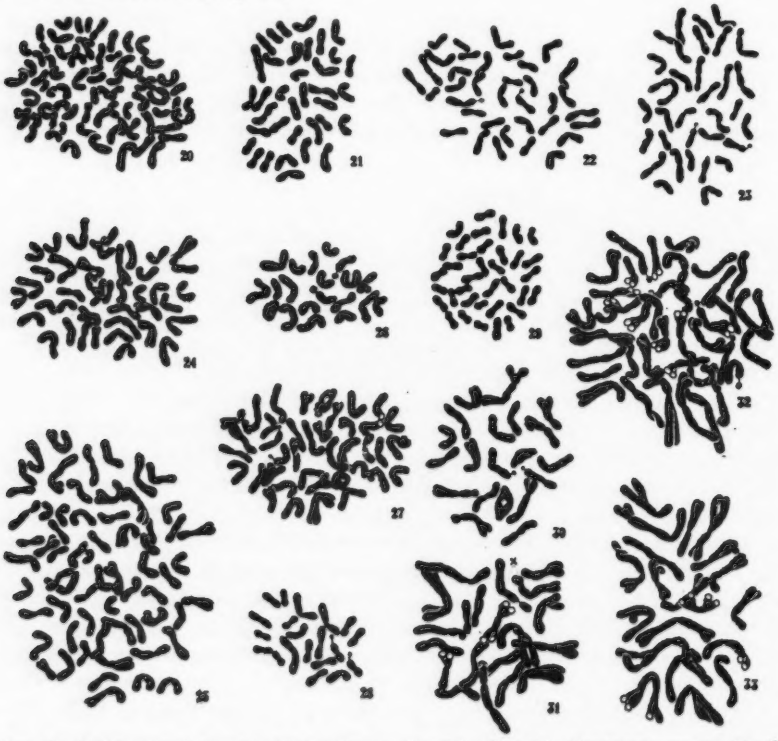

FIG. 20. *Oplismenus burmanii (Retz.) Beauv., 2n=72.* FIG. 21. *Brachiaria mutica Stapf., 2n=36.* FIG. 22. *Pennisetum clandestinum Hochst., 2n=36.* FIG. 23. *Cenchrus tribuloides L., 2n=34.* FIG. 24. *Miscanthus sinensis Anderss., 2n=42.* FIG. 25. *Miscanthus saccharifera Benth., 2n=64.* FIG. 26. *Andropogon eliottii Chapm., 2n=20.* FIG. 27. *Andropogon scoparius Michx., 2n=40.* FIG. 28. *Apluda mutica L., 2n=20.* FIG. 29. *Tripsacum dactyloides L., 2n=36.* FIG. 30. *Coix lachryma-jobi L., 2n=20.* FIG. 31. *Euchlaena mexicana Schrad., 2n=20.* FIG. 32. *Euchlaena perennis Hitch., 2n=40.* FIG. 33. *Zea mays L. subsp. indentata, 2n=20.*

Hitchcock (20) makes the section *Ptychophyllum* of the genus *Panicum* a section of the genus *Chaetochloa* Scribn. This latter genus is synonymous with *Setaria* Beauv. Hackel's (16) *P. plicatum* Lam., in which Avdulov counted 36 chromosomes, falls in this group. Of the other species of *Setaria* which Avdulov examined, two have 18 chromosomes and two 36, making a polyploid series with 9 as the basic number.

The remaining section which Avdulov examined, Hackel's *Eupanicum*, Bews retains in his genus *Panicum*. All species investigated have multiples of 9 chromosomes.

Throughout the whole of Hackel's genus *Panicum* there is, then, no divergence from the basic number 9, with one very doubtful exception. All the species are so similar in their chromosome morphology that it is impossible as yet to subdivide them on that score. A very careful comparison of their karyotypes may bring out definite generic differences, but until then their classification must be based on other than cytological grounds.

Avdulov found a characteristic case of polyploidy in the genus *Pennisetum*. Of the species so far investigated, one is a diploid ($2n=18$), one is a triploid ($2n=27$), two are tetraploids ($2n=36$), two are pentaploids ($2n=45$), and two are hexaploids ($2n=54$). To this list has been added the species *P. clandestinum* (Fig. 22) with 36 chromosomes, a tetraploid.

The genus *Pennicillaria* Willd. is included by Bews and Hackel in the genus *Pennisetum* Pers. Avdulov examined *Pennicillaria spicata* Willd. and found that it had 14 large chromosomes, larger than those of any other member of the tribe. In view of its peculiar karyotype, it seems better to retain it in a separate genus, as does Willdenow (quoted by Chase (9)), rather than to group it with *Pennisetum*.

Of the three species of *Oplismenus* which Avdulov examined, one had 54 chromosomes and the other two had 72. In the present investigation *O. burmanii* (Fig. 20) was found to have 72 chromosomes, giving the basic number 9.

In the genus *Cenchrus*, Avdulov finds three species with the basic number 17 and one with 35. *C. tribuloides* (Fig. 23) which was examined in the present study has 34 chromosomes. Avdulov believes that the number 34 must have originated from a tetraploid form of a series with the basic number 9 through the loss of one pair. The 70-chromosome form, in his opinion, might have arisen through the backcross of a 34-chromosome form with a 36-chromosome form followed by chromosome doubling.

An interesting case is disclosed in the genus *Paspalum*. All the species so far examined have their chromosomes in multiples of 10. This basic number is characteristic of most of the Andropogoneae. In point of chromosome size there is also a decided similarity between the two groups. This evidence along with the fact already noted, that the genus is one of a few that desert the typical habitat of the Paniceae and is found growing mixed with the Andropogoneae, points to the possibility that it should be included with the latter tribe rather than with the Paniceae.

Tribe Andropogoneae

The Andropogoneae are marked by an extreme specialization in the inflorescence. This specialization marks an advance and applies, with variations, to the whole tribe. "Within the tribe, however, are further degrees of advance and specialization, and the genera fall into two series, the one with the joints and pedicels relatively slender and not approximate or fused together—relatively primitive in this respect—and the other more advanced, with the joints and pedicels more or less stout and approximate or fused

together, forming a receptacle of the sessile spikelet." The first series consists of the subtribes Saccharinae and Andropogoninae, and the second of the subtribes Ischaeminae and Rottboellinae.

The Saccharinae are probably the most primitive and its members include *Saccharum* and its allies *Imperata*, *Miscanthus* and *Erianthus*, as well as *Eulalia*, *Polytrias* and several others. They are all relatively primitive ecologically as well as floristically.

The Andropogoninae is a much larger and more progressive subtribe. It includes only seven genera in Hackel's (16) arrangement, for he grouped a large number into the single genus *Andropogon*. Other authorities, however, gave generic rank to the numerous subgenera of *Andropogon*. Stapf has retained most of them and also established several more, so that the subtribe now contains about thirty genera. Some of these are *Andropogon*, *Cymbopogon*, *Sorghum*, and *Amphilophis*, subdivisions of Hackel's *Andropogon*, as well as *Themeda*, *Arthraxon*, and so on. Bews (6) follows this system.

Under the subtribe Ischaeminae come *Apluda*, *Jardinea* and *Elyonurus*, and under the Rottboellinae the most important is *Rottboellia*.

Avdulov (1) examined representatives of a number of genera and found that in most cases the basic number was 10, but that in *Miscanthus*, *Arthraxon* and *Rottboellia* it was 9. In the present investigation two species of *Miscanthus*, *M. sinensis* (Fig. 24) and *M. sacchariferа* (Fig. 25), were examined and found to have 42 and 64 chromosomes respectively. Avdulov (1) examined only *M. japonicus* and found 36 chromosomes. We have here an instance of a change in the basic number within the genus. As was mentioned in the general discussion on the use of the karyotype in systematics, it is possible for such a change to occur without producing any great effect on the expression of the phenotype and, since the three species are closely related, they are most likely derivatives of one another.

Avdulov (1) follows Hackel's (16) system of classifying the genus *Andropogon* and finds all the species investigated to have the basic number 10. The species *A. eliottii* (Fig. 26) and *A. scoparius* (Fig. 27) have 20 and 40 chromosomes respectively. Huskins and Smith (23) reported 40 as the somatic chromosome number of *Sorghum halepense* and 20 for twenty-one other species and varieties of *Sorghum*. They found also a number of tetraploid segments and one octoploid segment in root-tips of diploid plants. *S. dimidiatum* Stapf, *S. versicolor* Anders. and *S. purpurea sericeum* Ascher and Schweinf. have since been found to have only 10 chromosomes (18). The chromosomes are much larger than those of the 20-chromosome group, and of very different shapes. The suggestion is made by Huskins (18), that the 10-chromosome sorghums constitute a closely interrelated group very distinct cytologically from the remainder of the genus.

The similarity between the chromosomes in all the species so far investigated, with the exception of the above small group of sorghums, is so great that it is impossible to subdivide the genus *Andropogon* as constituted by Hackel (16) on purely cytological grounds.

In the subtribe Ischaeminae the only genera which have been examined are *Ischaemum* and *Apluda*. Avdulov (1) doubts Kuwada's (1915) (Avdulov (1)) count of 68 in *I. anthephoroides* and gives 20 as the count in *I. timorense*. For *Apluda mutica* he reports 40 chromosomes. The present material (Fig. 28) had only 20 chromosomes, so that it is probably a diploid and Avdulov's a tetraploid.

The whole tribe, then, is characterized by a remarkable regularity in basic number and size of chromosomes. It thus becomes interesting to speculate on the course taken by evolution in the development of the tribe. Avdulov (1) considers that the genus *Miscanthus*, which he postulates as a link between the Andropogoneae and Melinideae, constitutes the point of origin for the whole tribe. From this point development has proceeded in two directions, towards *Imperata* and towards *Erianthus*, in both cases with an increase in basic number from 9 to 10. Further variation in *Erianthus* follows a course through *Pollinia* to *Ischaemum* and *Andropogon* without a change in basic number. From *Ischaemum* it goes in one direction to *Apluda* and in the other direction, with a decrease in the basic number to 9, to *Rottboellia*. *Andropogon* likewise proceeds to *Themeda* without change and to *Arthraxon* with a drop to 9. In addition there is a decrease in basic number from 9 to 8 to 7 within the genus *Miscanthus*.

Tribe Maydeae

There are only seven genera included in this small tribe. Bews (6) considers it as little more than a subtribe of the Andropogoneae. All the members are monoecious, the male and female flowers being in the same inflorescence in some, such as *Tripsacum* and *Coix*, while in *Euchlaena* and *Zea* the male spikes are terminal in a panicle and the female in the leaf axils. The whole tribe is obviously advanced and specialized to a supreme degree, in many ways the most specialized of all the grasses. Within the tribe the genera *Euchlaena* and *Zea* are the most advanced.

The basic chromosome number for most of the genera has been established as 10. Longley (33) reported 35 as the haploid number for *Tripsacum*. Avdulov (1) examined *T. dactyloides* and maintained that it had not less than 72 and probably as many as 80 chromosomes. The material examined in the present study (Fig. 29) definitely had 36 chromosomes. This rather destroys Avdulov's contention that the basic number is probably 10 as is the case with the rest of the tribe. This fact, together with the extreme difference in chromosome size, fits in well however with the acknowledged morphological isolation of the genus.

Avdulov (1) reported 40 as the chromosome number of *Polytoca macrophylla*. This gave it also the basic number 10.

Kuwada (from Avdulov (1)) gave 10 as the haploid number for *Coix lachryma-jobi*. Taylor (49) agreed with him. Avdulov counted 20 chromosomes in the somatic cells. This was substantiated in the present study (Fig. 30). This genus, as well as *Tripsacum*, occupies an isolated position in the tribe, and here again morphological dissimilarity is reflected in the karyo-

type. Its chromosomes, though larger than those of *Tripsacum*, are on the whole considerably smaller than those of the other genera of Maydeae investigated.

The genus *Euchlaena* is *Zea's* closest relative. Kuwada in 1915 (Avdulov (1)) reported 20 as the chromosome number of *E. mexicana*, and Longley (33) counted 40 in *E. perennis*. The present investigations agree with both of these (Figs. 31 and 32). An interesting observation in *E. mexicana* was the discovery of a heteromorphic pair of chromosomes. These are indicated in the figure by an X. This condition was constant in all the cells examined. The material was grown from seed supplied by Dr. G. W. Beadle, who noted on the seed packet that it "might have been contaminated by maize pollen in comparatively recent generations." Only one plant has so far been examined.

In his survey of chromosome numbers in *Zea mays*, Randolph (43) notes that Kuwada (1911, 1915 and 1919) reported the haploid number as varying from 9 to 12, sugary varieties usually having higher numbers than starchy varieties. Longley (33) examined four varieties and found no deviation from 10, but later (34) he found more than 10 in two starchy and two sugary strains. Fisk in 1925 (Randolph (43)) investigated different strains and "found no clear evidence of numbers other than 20 (diploid) except in the sugary variety Black Mexican." Here he found, as did Kuwada, inconstancy of number both in different individuals and in different cells of the same individual. Kiesselbach and Petersen (24) made a large number of counts. No deviations from 10 as the haploid number were discovered. The suggestion was made that the extreme variation reported by Kuwada was perhaps due to errors of counting. Kuwada (27) re-examined the preparations on which his former accounts had been based and found additional evidence in support of his earlier observations. Recent investigations by Avdulov (2) confirm Kuwada's earlier observations. The exact nature of these supernumerary chromosomes, however, is not yet definitely settled. In the present study a variety of Dent corn, *Zea mays indentata* (Fig. 33), was examined and no deviation from 20 chromosomes was found.

A comparison of the Andropogoneae and Maydeae with regard to basic number and chromosome size shows that while the basic number 10 is typical of both, the chromosomes of the latter are very much larger. *Tripsacum* and *Coix* are exceptions and may be said to form a connecting link, cytologically, between the two tribes. Because of this almost general extreme difference in chromosome size it seems more logical to consider the Maydeae as a distinct tribe rather than merely as a subtribe of the Andropogoneae.

Conclusions

On the basis of his investigations Avdulov (1) divided the grasses into three groups. The first group is characterized by (i) type 1 leaf anatomy, (ii) chromosomes in multiples of 9 or 10, rarely more or less, (iii) elliptical or lanceolate first leaf, growing horizontally, (iv) usually a row of small hairs in

place of the ligule, (v) tendency of the main shoot to tiller, (vi) peculiar shape of the silicated cells and the presence of two-celled hairs on the epidermis of the leaf, (vii) alternation in the leaf of one primary with several or many secondary vascular bundles and (viii) limitation almost entirely to tropical or subtropical regions. The group of genera possessing this complex of characters, which includes the Panicoideae, Chlorideae and a number of genera from other tribes, constitutes, therefore, a very natural group. Avdulov thus defines a new subfamily Sacchariferae (Harz) Avdulov.

The second group differs from the first in having (i) its chromosomes in multiples of 7 or less, rarely 9, together with (ii) a linear first leaf growing vertically, (iii) type 2 of chlorophyll arrangement, (iv) the primary vascular bundles of the leaf alternating with one, two, or, at the most, four secondary ones, (v) two-celled hairs entirely absent, (vi) starch grains compound, except a small group in the Hōrdeae, together with *Bromus* and *Boissiera*, where the starch grains are still different from those of the *Sacchariferae*, and (vii) limitation to the temperate or cold zones.

The third group, *Oryza*, etc., lacks uniformity in many respects. Avdulov (1) has examined only isolated genera of this group, but believes it to constitute a tropical or subtropical group with small chromosomes in multiples of 12 but with a different type of leaf structure from that of the Sacchariferae.

The second and third groups are placed together in the second subfamily Poateae (Hitchcock) Avdulov, the second as the Festuciformes Avdulov, and the third as the Phragmitiformes (Harz) Avdulov. The group Festuciformes is subdivided into two tribes, the Frumentaceae (Harz) Avdulov, and the Festucaceae (Kunth) Avdulov, the first with simple and the second with compound starch grains.

The present investigation with a few minor exceptions supports Avdulov's conclusions. It is evident that parts of the family have not yet received sufficient attention and that more work must be done on them before any really valid conclusions can be reached. This applies in particular to Avdulov's third group which at present comprises a more or less heterogeneous collection of genera bound together only by rather superficial resemblances. The tribe Bambuseae is also deserving of more attention. Many investigators claim that it forms a subfamily of its own which is probably intermediate in position between the other two subfamilies or from which they have developed. Some smaller groups seem incapable of further development along cytological lines. In such a case all that cytology can do is indicate the existence of a more or less close relationship between its members. An examination of such groups confirms the important fact that was brought out in the introduction, *viz.*, a karyotype cannot be exclusively applied to any particular systematic unit. We are thus brought to a recognition of the fact that cytology can no more be used as the sole basis of classification than can any single form of anatomical or morphological study. It can, however, when properly used and correctly interpreted, form a very powerful tool in the hand of the system-

atist who is willing to correlate its facts with those derived from other branches of study. When two or more unrelated lines of investigation point to the same conclusion, the probability of that conclusion being correct is, naturally, very greatly enhanced.

Acknowledgment

The writer wishes to express his appreciation to Dr. C. L. Huskins, under whose direction the work was carried out, for his assistance in supplying the material on which this investigation was based and for his help throughout the study, and to Dr. H. Prat, of the University of Montreal, for his kindly interest and suggestions.

References

1. AVDULOV, N. P. Karyo-systematische Untersuchung der Familie *Gramineen*. (Russian with German summary). Bull. Appl. Bot., Suppt. 44. 1931.
2. AVDULOV, N. P. On the additional chromosomes in maize. (Russian with English summary). Bull. Appl. Bot. 2 (2) : 101-130. 1933.
3. AVDULOV, N. P. Karyologische Ergänzungsdaten zur Systematik der *Gramineen*. (Russian with German summary) Bull. Appl. Bot. 2 (2) : 131-136. 1933.
4. AVDULOV, N. P. and TITOVA, N. Additional chromosomes in *Paspalum stoloniferum* Bosco. (Russian with English summary). Bull. Appl. Bot. 2 (2) : 165-172. 1933.
5. BENTHAM, G. and HOOKER, J. D. Genera Plantarum. Vol. III, Part 2 : 1074-1215. 1883.
6. BEWS, J. W. The world's grasses. Longmans, Green and Co., London. 1929.
7. BROWN, R. Prodromus Florae Novae Hollandiae. (Quoted by Avdulov, 1931.)
8. CAMUS, A. Note sur les genres *Lepturus* R. Br. et *Pholiurus* Trinius. Ann. Soc. Lin. Lyon, 69 : 86-90. 1922.
9. CHASE, AGNES. The North American species of *Pennisetum*. Contr. U.S. Nat. Herb. 22 : 209-234. 1921.
10. CHURCH, G. L. Meiotic phenomena in certain *Gramineae*. I. *Festuceae, Aveneae, Agrostideae, Chlorideae* and *Phalarideae*. Botan. Gaz. 87 : 608-628. 1929.
11. CHURCH, G. L. Meiotic phenomena in certain *Gramineae*. II. *Paniceae* and *Andropogoneae*. Botan. Gaz. 88 : 63-84. 1929.
12. DUVAL-JOUVE, M. J. 1870. (Quoted by Duval-Jouve, 1875.)
13. DUVAL-JOUVE, M. J. Histotaxie des feuilles de *Graminées*. Ann. Sci. Nat., Ser. 6, Bot. 1 : 294-371. 1875.
14. ENDLICHER, S. L. Genera Plantarum. 1836-1840.
15. GREGOR, J. W. and SANSOME, F. W. Experiments on the genetics of wild populations. II. *Phleum pratense* L. and the hybrid *P. pratense* × *P. alpinum*. J. Genetics, 22 : 373-387. 1930.
16. HACKEL, E. "Gramineae" in Engler and Prantl's "Die Näturlichen Phflanzenfamilien." II Teil, 2 Abteilung. 1887.
17. HARZ. Beitrage zur Systematik der Gramineen. Linaea 43 : 1-30. 1880-1882. (Quoted by Avdulov, 1931.)
18. HILL, A. W. Hooker's Icones Plantarum. In press. 1934.
19. HITCHCOCK, A. S. The genera of grasses in the United States, with special reference to the economic species. U.S. Dept. Agr. Bull. 772. 1920.
20. HITCHCOCK, A. S. Revision of North American grasses: *Isachne Oplismenus, Echinochloa* and *Chaetochloa*. Contr. U.S. Nat. Herb. 22 : 115-208. 1920.
21. HITCHCOCK, A. S. and CHASE, AGNES. The North American species of *Panicum*. Contr. U.S. Nat. Herb. 15 : 1-387. 1910.
22. HUSKINS, C. L. The origin of *Spartina Townsendii*. Genetica, 12 : 531-538. 1931.
23. HUSKINS, C. L. and SMITH, S. G. A cytological study of the genus *Sorghum* Pers. I. The somatic chromosomes. J. Genetics, 25 : 241-250. 1932.
24. KIESSELBACH, T. A. and PETERSEN, N. F. The chromosome numbers of maize. Genetics, 10 : 80-85. 1925.

25. KIHARA, H., YAMAMOTO, Y. and HOSONE, S. A list of chromosome numbers of plants cultivated in Japan. Yokendo, Tokyo. Reprinted from "Shokubutsu senshokû-taisû nokenyu" (Studies on chromosome numbers in plants). 1931.
26. KUNTH, C. S. Enumeratio Plantarum. Vol. I. 1833. (Quoted by Avdulov, 1931).
27. KUWADA, Y. On the number of chromosomes in maize. Botan. Mag. Tokyo. 39 : 227-234. 1925.
28. LACOUR, L. F. Improvements in the everyday technique in plant cytology. J. Roy. Micros. Soc. 51 : 119-126. 1931.
29. LAMB, W. H. The phylogeny of grasses. Plant World, 15 : 264-269. 1912.
30. LEWITSKY, G. A. The morphology of chromosomes. (Russian with English summary). Bull. Appl. Bot. 27 : 19-174. 1931.
31. LEWITSKY, G. A. The karyotype in systematics. (Russian with English summary). Bull. Appl. Bot. 27 : 187-240. 1931.
32. LEWITSKY, G. A. and ARARATIAN, G. A. The transformations of chromosomes under the influence of X-rays. (Russian with English summary). Bull. Appl. Bot. 27 : 265-303. 1931.
33. LONGLEY, A. E. Chromosomes in maize and maize relatives. J. Agr. Research, 28 : 673-682. 1924.
34. LONGLEY, A. E. Segregation of carbohydrates in maize pollen. Science, 61 : 542-543. 1925.
35. NAKAJIMA, G. Chromosome number in some angiosperms. Japan J. Genetics, 9 : 1-5. 1933.
36. NASH, G. V. Revision of the genera *Chloris* and *Eustachys* in North America. Bull. Torrey Club, 25 : 432-450. 1898.
37. NAWASCHIN, S. (Summary of work reported by Lewitsky, 1931. (30).)
38. NEWTON, W. C. F. Studies on somatic chromosomes. I. Pairing and segmentation in *Galtonia*. Ann. Botany, 38 : 197-206. 1924.
39. PÉE-LABY, M. E. Étude anatomique de la feuille des *Graminées* de la France. Ann. Sci. Nat., Ser. 8, Bot., 8 : 227-346. 1898.
40. PETO, F. H. Cytological studies in the genus *Agropyron*. Can. J. Research, 3 : 428-448. 1930.
41. PRAT, H. L'épiderme des *Graminées*. Étude anatomique et systématique. Ann. Sci. Nat., Ser. 10, Bot., 14 : 117-324. 1932.
42. PRAT, H. Remarques sur la position systématique de genre *Jouvea* Fourn. et sur les limites de la tribu des *Hordées*. Bull. Soc. Bot. France, 80 : 357-367. 1933.
43. RANDOLPH, L. F. Chromosome numbers in *Zea mays* L. Cornell Univ. Agr. Exp. Sta. Memoir 117. 1928.
44. SAINT-YVES, A. Monographia Spartinarum, Candollea, 5 : 19-100. 1932.
45. SAKAMURA, T. Experimentelle Studien über die Zell- und Kernteilung mit besonderer Rücksicht auf Form, Grösse und Zahl der Chromosomen. J. Coll. Sci. Imp. Univ. Tokyo, 39 : Art. 11. 1920.
46. SMITH, S. G. Cytology of *Anchusa* and its relation to the taxonomy of the genus. Botan. Gaz. 94 : 394-403. 1932.
47. STEUDEL, E. G. Synopsis Plantarum Graminearum. 1855. (Quoted by Avdulov, 1931.)
48. TAYLOR, W. R. Cytological studies on *Gasteria* L. Chromosome shape and individuality. Am. J..Botany, 11 : 51-59. 1924.
49. TAYLOR, W. R. Chromosome constrictions as distinguishing characteristics in plants. Am. J. Botany, 12 : 238-244. 1925.
50. TRECUL, A. Des formations vésiculaires dans les cellules végétales. Ann. Sci. Nat., Ser. 4, Bot., 10 : 205-382. (Quoted by Avdulov, 1931.)
51. YAMAURA, A. Karyologische und embryologische Studien über einige Bambus-arten. (Vorläufige Mitteilung). (Japanese with German summary). Botan. Mag. Tokyo, 47 : 551-555. 1933.

A NEW *OPHIOBOLUS* ON EELGRASS[1]

By Irene Mounce[2] and Wm. W. Diehl[3]

Abstract

Ophiobolus halimus Diehl and Mounce n. sp. is reported on *Zostera marina* L. from St. Andrews, N.B. It was collected on rhizomes and fertile shoots, and developed in leaves kept in sea water in the laboratory. The fungus is described and illustrated and it is compared with related species.

Introduction

The almost complete disappearance of eelgrass, *Zostera marina* L., during the seasons 1930-1933 from the western Atlantic coast and the development of a similar condition in Europe have excited considerable interest not only among botanists, but among the public generally. Since the cause of these phenomena has lacked adequate explanation, any organisms found growing on or in the eelgrass plants are of possible significance. It seems desirable, therefore, to record a hitherto unknown fungus on *Zostera* which has been under observation in the field and in culture, and to distinguish it from related species with which it may be confused.

Field Observations and Cultures

In co-operation with the Biological Board of Canada, a preliminary investigation of the conditions affecting eelgrass was begun last autumn near their station at St. Andrews, N.B., by the senior author.

Most of the observations on *Zostera* were made at Tidal Cove and Birch Cove, two closely adjacent inlets of Passamaquoddy Bay. A dam was built across the upper end of Tidal Cove some years ago and in the tidal pools behind it the supply of *Zostera* was fairly abundant, whereas at Birch Cove only a few scattered young plants remained.

Perithecia of an ascomycetous fungus occurred in great numbers on the lower parts of most of the fertile shoots which remained at Tidal Cove in late August and September. At that time, few spores were present but they were sufficiently abundant that the fungus could be characterized by their size, shape, and hyaline tips.

Mature perithecia have been found in the rhizomes of a few sickly plants at both Birch Cove and Tidal Cove (Figs. 7, 9). In such rhizomes the cells are filled with septate hyphae (Figs. 8, 9).

Perithecia developed, too, on the rhizome of one plant of *Zostera* which had been kept in a jar of sea water in the laboratory at room temperature,

[1] *Manuscript received July 7, 1934.*
Contribution from the Dominion of Canada Department of Agriculture, Ottawa, Canada and the United States Department of Agriculture, Washington, D.C., U.S.A.

[2] *Assistant Plant Pathologist, Dominion of Canada Department of Agriculture, Ottawa, Canada.*

[3] *Associate Pathologist, United States Department of Agriculture, Washington, D.C., U.S.A.*
The senior author is responsible for all field and culture work with this fungus and the junior author for the taxonomic considerations.

but the greatest numbers of mature perithecia were obtained from leaves (Figs. 1, 3). Tips of apparently healthy leaves were placed in test tubes or flasks, which had been partially filled with sea water and plugged with cotton wool, and kept either at room temperature or partially immersed in a tank of running sea water where the temperature ranged from 13.5°–15° C. At the end of six weeks to two months development was complete.

Perithecia have matured on leaves collected in September and October, and on some which were sent to Ottawa from St. Andrews early in January. Because of the larger amount of this latter material it has been used as the basis for taxonomic consideration.

Taxonomic Relations

This fungus is readily identified as belonging to the genus *Ophiobolus*, but it appears to differ from any described species of that genus as outlined below:

Ophiobolus medusa

A little-known species, *O. medusa* Ell. and Ev., (1, p. 150) which was found in 1884 in New Jersey growing upon sand-buried leaf sheaths of *Spartina* sp.; in reality *S. cynosuroides* (L.) Roth., does bear a certain remarkable resemblance* due to a character which is not noted, however, in the original description. This feature common to *O. medusa* and the fungus on *Zostera* is the hyaline tips or apiculi of the ascospores. No attempt is made here to determine the nature of this apiculus other than to note that it seems not to be an evaculated cell but a solid hyaline cap. In *O. medusa* the tip of this cap or apiculus tends to be inflated and flattened somewhat (Fig. 6*D*), a character that is readily overlooked unless examined with an oil-immersion lens. In the fungus on *Zostera* the ascospore apiculus terminates normally as a rounded cone (Fig. 6*B*).

In *O. medusa* the asci are described as more than 400μ long, being larger than those of the fungus on *Zostera* where the equivalent dimensions are usually 270-300μ. In the microscopic preparation from the type of *O. medusa* the asci and spores are somewhat smaller than in the description owing doubtless to the fact that they are slightly immature. The ascospores of *O. medusa* have a densely staining central cell (Fig. 6*C*) which is less evident in the fungus on *Zostera*, and in the latter there is a spring-like turgidity lacking in *O. medusa* (Figs. 5; 6*A*). It is, of course, always difficult to make fair comparisons of spores from dried specimens with those from fresh material.

The texture of the perithecial walls and of the ostiolar beak of *O. medusa* is heavier and less membranous than in the fungus on *Zostera*. The perithecia of *O. medusa* are surrounded by attached brown hyphae (hairs) which are not evident in the fungus on *Zostera*. In *O. medusa* the ostiolar beak does not protrude (Fig. 2) from the tissues of the host while in the fungus on *Zostera* they are decidedly exsurgent (Fig. 3).

**Dr. John Dearness in a communication to the senior author suggested that if the fungus on Zostera were not a form of O. medusa it was probably a new species.*

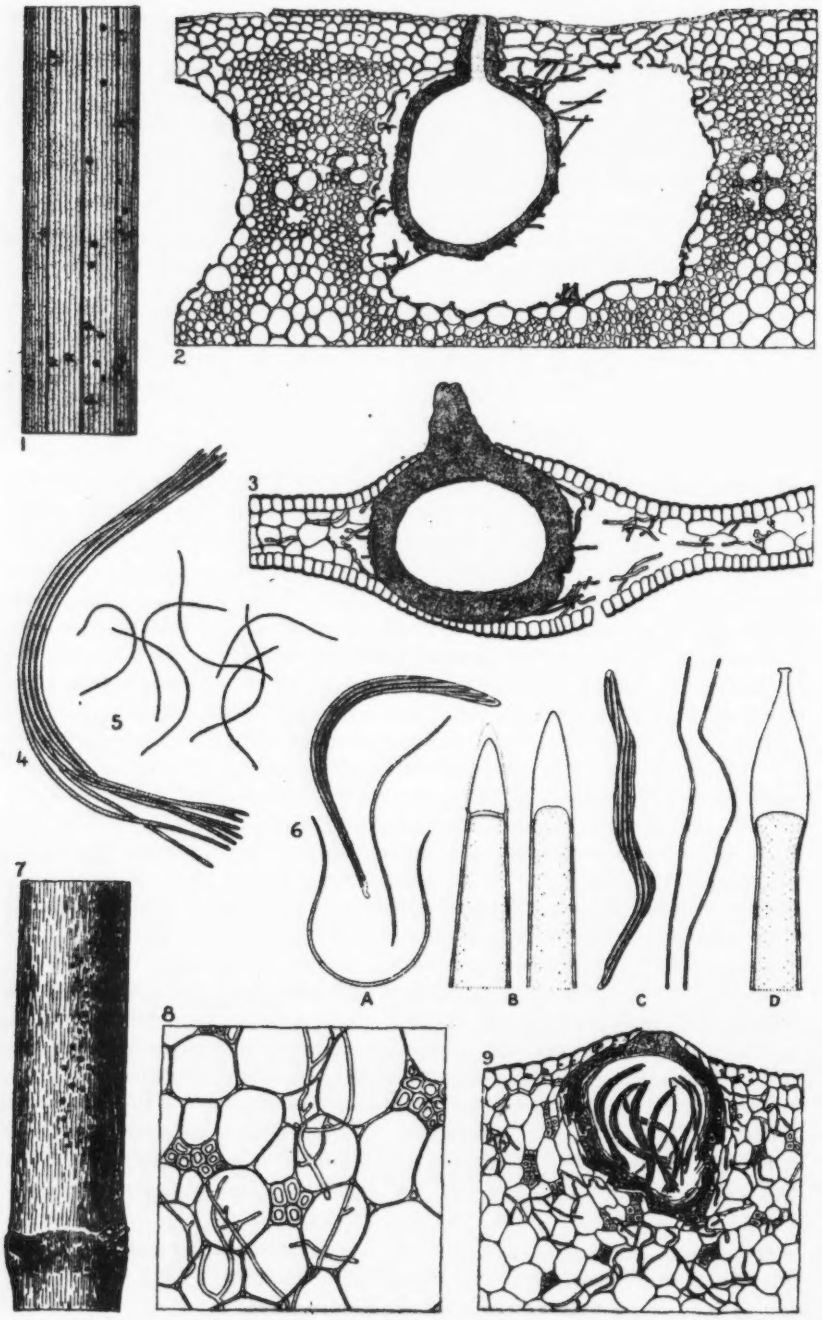
1
2
3
4
5
6
A
B
C
D
7
8
9

These features in *O. medusa* have been observed in slides made from the fragmentary type specimen in the Ellis Collection of types of the Farlow Herbarium at Harvard University. Another duplicate type (syntype), that is in the Ellis Herbarium of the New York Botanical Garden, was examined, but no ascospores were found. No other specimen of *O. medusa* has been available thus far although the junior writer has searched for it on buried *Spartina cynosuroides* during the spring of 1934 in the Chesapeake Bay region.

Ophiobolus medusa var. *minor*

A supposedly related fungus, *O. medusae* var. *minor* Ell. and Ev. (2, p. 239) described from *Andropogon muricatus* at St. Martinville, La. in 1889 by A. B. Langlois, as attested by the type specimen in the Langlois Herbarium (A.B.L. 1771), in the Mycological Collections of the U.S. Bureau of Plant Industry, has small asci 110 – 120 × 7–8μ and spores 90 – 110 × 2.5μ, which lack the peculiar appendages referred to above, and is characterized by an erumpent ostiolar beak. A proper disposition of this fungus from Louisiana would be elsewhere than with *O. medusa* and it can have no bearing upon the taxonomy of the fungus on *Zostera*.

Ophiobolus maritimus

A discussion of *Ophiobolus* on *Zostera* cannot ignore the record of *O. maritimus* Sacc. (3, p. 350) described from Europe as growing in the North Sea on *Z. marina*. Although no specimens of this fungus are available for comparison, it also would seem different from the fungus on *Zostera* from New Brunswick, since it is described with much smaller asci, 140–150 × 10–12μ, and 15–18 septate spores which break up into uniseptate segments 15–20 × 2μ in dimensions.

Since this fungus on *Zostera* cannot be identified with either of those with which for various reasons it might have been confused, it is proposed as new:

Ophiobolus halimus Diehl and Mounce, sp. nov.

Perithecia sparse and somewhat equally arranged in groups, intramatrical, sphaeroid, 240–435μ in diameter, with rostrate ostioles emerging amphigenously, sometimes with more than one ostiole to the perithecium; rostra conoid, acute, blackish, up to 278μ in length by 260μ in basal diameter;

EXPLANATION OF FIGURES

FIG. 1. *Ophiobolus halimus. Perithecia in leaf of Zostera marina.* × 6. FIG. 2. *Ophiobolus medusa. Drawing of a freehand section of a perithecium from type specimen, showing the perithecium within an air space of the host and the intramatrical ostiolar neck.* ×103. *Section made by Dr. G. D. Darker and preserved in Amann's solution.* FIG. 3. *O. halimus. Drawing from a freehand section of a perithecium in a leaf of Z. marina.* ×103. FIGS. 4–5. *O. halimus. Spores.* ×273 *and* ×103 *respectively.* FIG. 6. *A. O. halimus. Ascus and spores.* ×182. *B. O. halimus. Ascospore tips showing appendage.* ×910. *C. O. medusa. Ascus and spores.* ×182. *D. O. medusa. Ascospore tips showing appendage.* ×910. FIG. 7. *O. halimus. Distribution of perithecia on rhizome of Z. marina.* ×6. FIG. 8. *O. halimus. Septate hyphae in cells of rhizome.* ×273. FIG. 9. *O. halimus. Perithecium and spores in a rhizome of Z. marina* ×103.

perithecial walls 9–15μ in thickness, context blackish brown, fleshy pseudoparenchyma of thin-walled cells laterally compressed; asci arcuate-fusoid, slightly attenuate at the base, subsessile, apically somewhat truncate, 270–300 × 12–15μ, eight-spored, ascospores parallel but slightly spirally arranged and filling the ascus, aparaphysate; ascospores filiform, acicular arcuate to spring-like spiral when free, gradually tapering from the thicker centre to the tips, 260–308 × 2–4μ, spores terminated by a peculiar hyaline appendix which reached a length of 3μ and a diameter of 1.3μ.

Parasitic in leaves of *Zostera marina* in culture in 1934, I. Mounce, Herb. Div. Bot. Ottawa 3584, (type); and naturally on rhizomes and bases of fertile shoots of *Z. marina*, St. Andrews, N.B., August-October, 1933, I. Mounce.

Ophiobolus halimus Diehl and Mounce, sp. nov.

Peritheciis sparsis et equaliter gregariis, intra matricem immersis, atris, sphaeroideis, 240–435μ diam. ostiolis rostratis amphigenis emergentibus, rostris ostiolorum conoideis acutis, atris 278μ altis, 260μ latis; muris perithecorum 9–15μ crassis, contextu atro-fuliginoso, carnoso pseudoparenchymatico, e cellulis subregularibus, lateraliter subcompressis et muris tenuibus praeditis efformato; ascis arcuato-fusoideis, basi obtuse attenuatis, subsessilibus, apice tenuiter truncatis, 270–300 × 12–15μ, octosporis; aparaphysatis; ascosporis parallelis vel paulo subspiraliter in asco dispositis, acicularibus arcuatis, in medio crassiusculis, hyalinis, pseudoseptatis, appendiculis terminalibus hyalinis, 260–308 × 2–4μ.

In foliis *Zosterae marinae* parasitans in cultura I. Mounce 1934 (typus); et naturaliter in sinu maris prope St. Andrews, in Nova Brunsvigia, 10 Septembris 1933. I. Mounce.

Type material of this species has been deposited in the following herbaria: Division of Botany, Ottawa; the Mycological Collection of the United States, Bureau of Plant Industry; the Royal Botanic Gardens, Kew; the New York Botanic Garden; and the Farlow Herbarium of Harvard University.

Acknowledgments

The authors are much indebted to Miss Ruth Macrae for most of the drawings, to the Biological Board of Canada for additional collections of *Zostera marina*, to Dr. G. D. Darker for sectioning and preparing slides from the type of *Ophiobolus medusa* at the Farlow Herbarium, and to Dr. F. J. Seaver for permission to examine the type specimen of the same species at the New York Botanical Garden.

References

1. Ellis, J. B. and Everhart, B.M. J. Myc. 1 : 148-154. 1885.
2. Ellis, J. B. and Everhart, B.M. Proc. Acad. Nat. Sci. Phila. 42 : 219-249. (1890). 1891.
3. Saccardo, P. A. Syll. Fung. 2. 1883.

REVIEWS AND NOTES

NOTE SUR LES ÉMULSIONS DE LA TRIÉTHANOLAMINE AVEC LE KÉROSÈNE ET DES HUILES LUBRIFIANTES MINÉRALES[1]

PAR J. RISI[2] ET H. BERNARD[3]

La triéthanolamine (4, 5) donne avec les acides gras des savons (1, 3, 8), lesquels forment avec diverses substances minérales et végétales des émulsions aqueuses plus ou moins stables. Nous avons eu l'occasion d'étudier des émulsions de la triéthanolamine avec le kérosène et des huiles lubrifiantes minérales, et nous voudrions signaler quelques propriétés autres que celles déjà données dans la littérature (7).

Emulsions de kérosène

La stabilité et l'homogénéité des émulsions dépendent beaucoup de la méthode de préparation, ainsi que des variations même très minimes de la viscosité, de l'acidité et du poids spécifique des produits de départ. Les meilleurs résultats au point de vue de la stabilité ont été obtenus par émulsification de 87 g. de kérosène, 9 g. d'acide oléique, 4 g. de triéthanolamine, 50 g. d'eau distillée, d'après les méthodes connues (1, 3, 8). Cette émulsion concentrée à 66% d'huile forme une crème visqueuse, blanche, stable pendant plusieurs mois et miscible à l'eau. Elle possède les propriétés suivantes:—poids spécifique; 0.878 à 15.56° C.: point de liquéfaction; —1° C.: point d'inflammabilité; 97° C.: point de combustion; 95° C. après avoir brisé l'émulsion par ébullition prolongée: essai de corrosion; négatif pour le cuivre et pour les tissus végétaux: propriétés détersives; aussi prononcées que celles d'une solution de savon neutre ordinaire.

Emulsions d'huile minérale

Dans le but d'obtenir une huile lubrifiante soluble, nous avons émulsifié le savon oléique de la triéthanolamine avec une huile minérale raffinée de P.E. 300–327° C. ne contenant aucune addition d'huile animale ou végétale. Les meilleurs résultats ont été obtenus avec 89 g. d'huile, 3.9 g. de triéthanolamine, 7.1 g. d'acide oléique et 50 g. d'eau distillée. Cette émulsion concentrée, à 66% d'huile, est une crème assez visqueuse, presque blanche, parfaitement neutre et qui s'émulsifie très facilement en ajoutant graduellement de l'eau avec agitation modérée. Ses propriétées sont les suivantes:—poids spécifique; 0.763 à 15.56° C.: point de liquéfaction; — 4° C.: point

[1] *Manuscrit reçu le 4 mai, 1934.*
Contribution de l'Ecole Supérieure de Chimie, Université Laval, Québec, Canada. Note basée sur une thèse présentée par Hervé Bernard pour l'obtention du degré de M.Sc. de l'Université Laval.

[2] *Professeur de chimie organique, Université Laval.*
[3] *Etudiant gradué, Université Laval.*

d'inflammabilité; 105° C.: point de combustion; 114° C.: essai de corrosion; négatif: stabilité; la couche supérieure se solidifie après 24 heures, lorsque l'émulsion est exposée à l'air, grâce à une inversion par l'anhydride carbonique (2, 6).

Le tableau I donne les coefficients de friction, μ, des émulsions à 60, 40 et 30% d'huile déterminés dans l'appareil de Thurston. Les coefficients de friction de l'huile à moteur "Marvelube Twenty" de viscosité 315 sec. à 100° F. sont donnés pour comparaison.

TABLEAU I

COEFFICIENTS DE FRICTION DE QUELQUES ÉMULSIONS À BASE DE TRIÉTHANOLAMINE ET D'UNE HUILE À MOTEUR

Minutes	Emulsions			"Marvelube Twenty" μ	Minutes	Emulsions			"Marvelube Twenty," μ
	66% d'huile, μ	40% d huile, μ	30% d'huile, μ			66% d'huile, μ	40% d'huile, μ	30% d'huile, μ	
0	0.067	0.060	0.060	0.060	7	0.026	0.058	0.053	0.060
1	0.067	0.011	0.017	0.035	8	0.026	0.043	0.059	0.060
2	0.067	0.011	0.017	0.035	9	0.026	0.043	0.066	0.060
3	0.038	0.011	0.023	0.035	10	0.026	0.043	0.071	0.060
4	0.033	0.040	0.047	0.035	11	0.026	0.058	0.071	0.060
5	0.029	0.058	0.047	0.035	12	0.026	0.070	0.071	0.060
6	0.026	0.058	0.047	0.060	13	0.026	0.085	0.071	0.060
					14	0.026		0.085	0.076

Références

1. Carbide and Carbon Chemicals Corporation. Emulsions. 1930 et 1932.
2. DAVEY, W. P. Phys. Rev. 11 : 138-139. 1918.
3. HOCKENYOS, G. L. J. Ind. Eng. Chem. 21 : 647-648. 1929.
4. I. G. FARBENINDUSTRIE A. G. E. P. 309,842. 1927.
5. I. G. FARBENINDUSTRIE A. G. F. P. 650,574. 1928.
6. MEAD, B. and MCCOY, J. T. Colloid Symposium Monograph. 4 : 44-57. 1926.
7. TROTMAN, S. R. Textile Recorder, 48 : No. 567, 59-61. 1930.
8. WILSON, A. L. J. Ind. Eng. Chem. 22 : 143-146. 1930.